Online Supplement

Genetic Architecture of 11 Major Psychiatric Disorders at Biobehavioral, Functional Genomic, and Molecular Genetic Levels of Analysis

Table of Contents

Supplementary Note

Psychiatric Phenotypes. We curated the largest and most recent GWAS summary data from individuals of European ancestry for eleven major psychiatric disorders (Supplementary Table 1). We refer the reader to the original articles for the corresponding univariate GWAS for details about sample ascertainment, quality control, and related procedures. For PTSD, MDD, ADHD, ANX, and ALCH, phenotype-specific meta-analyses of GWAS summary data derived from two different contributing sources per disorder were conducted in Genomic SEM so as to account for potentially unknown degrees of participant overlap across contributing samples. Models were specified to be equivalent to a fixed-effects meta-analysis, with both variables loading on the latent variable with an unstandardized loading fixed to 1.0, and both residual variances fixed to 0. LDSC-estimated genetic correlations within-phenotype-across-data-source were all ≥ .6 (Supplementary Table 45). These GWAS meta-analyses in Genomic SEM were highly genetically correlated (≥ .94 as estimated with LDSC) with those estimated in METAL,[1] which does not take sample overlap into account. Consistent with the differences in whether sample overlap is considered, Genomic SEM and METAL yielded univariate LDSC intercepts slightly below and slight above 1, respectively.

For the five meta-analyzed traits we provide Manhattan plots, tables of independent loci, and tables of hits that are in LD with hits previously identified in the GWAS catalogue (Supplementary Figure 42; Supplementary Tables 46-53). We find that many of the identified loci have been previously reported for the same or overlapping traits. As expected, the results for MDD and ADHD also overlap strongly with findings from the most recent MDD[2] and ADHD[3] papers that use highly similar samples to those that contributed summary data analyzed here. The observed differences are attributable to different analytic pipelines and partially non-overlapping contributing cohorts; for example, results reported from the published GWAS of ADHD[3] include non-European samples, and hold some cohorts out for independent follow-up analyses.

The current analyses included GWAS summary statistics produced using self-report items not directly assessed by a clinician for MDD, ANX, ALCH, and ADHD. The inclusion of these cohorts was based on the large genetic correlations between the clinically diagnosed and self-report GWAS, the increased mean chi-square when meta-analyzing self-report and clinical diagnosis GWAS (Supplementary Table 45), and a general trend in psychiatric genomics to include self-report cohorts in the primary GWAS studies being published. In some cases, multiple self-report options were available, in which case phenotypes were chosen based on the field standard and prior findings. For example, the choice to use the broad depression phenotype from UK Biobank and self-report 23andMe MDD phenotype was based on the inclusion of both phenotypes in the most recent GWAS of MDD[4] and of the latter phenotype in the prior PGC GWAS of MDD.[5] In addition, Wray et al.[5] find that polygenic scores constructed from MDD 23andMe summary statistics predict equal, or greater, amounts of out-of-sample variance in MDD phenotypes than PGS constructed from PGC case/control summary statistics. Moreover, they find that the meta-analyzed summary statistics across both 23andMe and PGC cohorts predicted the greatest amount of variance. We note also that the meta-analysis between PGC Alcohol Use Disorder and UKB self-reported alcohol use is limited to self-reported problematic alcohol use (as assessed by the AUDIT-P) and not alcohol consumption (as assessed by the AUDIT-C). This is based on prior work indicating stronger genetic correlations between self-reported problematic alcohol use and alcohol dependence relative to self-reported alcohol consumption.[6]

While conducting this project the more recent PGC Freeze 2 release of PTSD became available.[7] However, the GWAS *z* statistics and heritability estimates for PTSD Freeze 2 were lower than were observed for PTSD Freeze 1. As a result, our attempts to incorporate the PTSD Freeze 2 summary data produced a variety of technical problems (e.g. out of bounds genetic correlations and small heritability estimates). We therefore report results based on PTSD Freeze 1 summary data.

Investigation of Genome-Wide Factor Structure. In order to explore the full-scope of factors solutions, EFAs were conducted using the *factanal* R package for two to five factor solutions using both oblique rotations, which allow for correlations among the latent factors, and orthogonal rotations, which assumes factors are independent (i.e., uncorrelated). Orthogonal rotations were examined as we, in part, sought to identify maximally separable dimensions with distinct sets of psychiatric indicators. EFAs were conducted for the genetic correlation structure derived from odd autosomes only. Confirmatory factor analyses (CFAs) specified on the basis of these EFAs were subsequently fit to a genetic correlation matrix estimated using only even autosomes. Using odd and even autosome covariance matrices for the exploratory and confirmatory models, respectively, provided a form of cross-validation to guard against model overfitting. For comparative purposes, we also consider model fit and final factor solutions for CFAs fit to the S-LDSC matrix (Supplementary Figure 42).

For the CFAs, factors were assigned to traits when their standardized loading exceeded .35 in the corresponding EFAs, with two exceptions. First, for all EFAs with > 3 factors, a factor was identified with TS as its only indicator with standardized loading >.35. In the context of the CFAs, assigning TS to all factors at once, or to one factor at a time, resulted in issues with model convergence. Consequently, this final factor was removed in the CFA and TS was specified to always load on the factor with the largest EFA loading (excluding the factor defined only by TS) and models were compared where TS loaded onto one of the remaining factors. Among these combinations of TS models, a final model was selected using model fit indices (i.e., AIC, SRMR, and CFI). Second, for certain EFA solutions, there were traits that did not meet the standardized loading criteria of .35 for any factor. For these traits, we assigned factors to them in the CFA when their standardized loading exceeded a more lenient threshold of 0.2. We then inspected model fit indices for the follow-up CFA model to confirm that including those factor loadings provided better fit to the data.

All CFAs were fit using the Weighted Least Squares (WLS) estimator in the *GenomicSEM* R package described above, which uses the inverse of the diagonal of the sampling covariance (*V*) matrix to weight the discrepancy function. This works to prioritize reducing model misfit for those cells in the genetic covariance matrix that are estimated with greater precision, with the desirable result of generally decreasing the sampling variance of parameter estimates in Genomic SEM. It should be noted that WLS estimation does not necessarily produce a solution whereby the better powered GWAS have larger factor loadings. In instances where traits with better-powered GWAS estimates evince lower genetic correlations with other included traits, WLS estimation will produce a solution that prioritizes lower factor loadings for these traits and consequently minimize their downstream influence on multivariate GWAS estimates.

CFAs based on orthogonal EFA results allowed for freely correlated factors, as pruning factor loadings has the potential to reintroduce factor correlations. In the context of the CFAs, we also considered a common factor model in which all 11 traits loaded onto a single factor. CFAs with 4 correlated factors were similar in both factor structure and fit to the data (Supplementary Table 53). In addition, the CFAs with 4 correlated factors provided far superior fit to the data (Supplementary Figures 42-43), relative to the other models, with a number of the other CFAs failing to converge. Moreover, as indicated by model fit statistics, and observed directly in genetic correlation heatmaps, the correlation structure implied by the model estimates was much closer to the observed genetic correlations for these CFA solutions (Supplementary Figure 44). The final model was chosen as a four correlated factor CFA (Supplementary Table 55) as this ultimately provided the best fit to the data (χ^2[33] = 126.85, AIC = 192.85, CFI = .955, SRMR = .078; Supplementary Table 48 for fit statistics of all models). Importantly, the model identified using a split of even and odd autosomes also fit the data well when applied to the genome-wide matrix estimated using autosomes 1-22 for LDSC (Figure 1b; χ^2[33] = 161.66, AIC = 227.66, CFI = .975, SRMR = .072) and S-LDSC (Supplementary Figure 42; χ^2[33] = 89.63, AIC = 155.63, CFI = .976, SRMR = .086).

The moderate factor correlations in this final model were also suggestive of a hierarchical structure (Supplementary Figure 43). This provided relatively comparable fit to the data for the LDSC genome-wide matrix (Figure 1c; χ^2[35] = 171.37, AIC = 233.37, CFI = .974, SRMR = .079) and S-LDSC genome-wide matrix (Supplementary Figure 42; χ^2[35] = 91.83, AIC = 153.83, CFI = .976, SRMR = .087). The absence of improved fit for the hierarchical model may reflect the fact that there was observable bias when comparing the factor correlations from the non-hierarchical model against the model implied correlations within the hierarchical model (Supplementary Figure 44). In this model, the *p*-factor explained the greatest proportion of variance in the Internalizing disorders factor (55%) and relatively similar proportions of variance in the remaining three factors (30%-34%).

As the hierarchical model reflects a constrained version of the bifactor model, the bifactor model is always able to approximate the empirical genetic covariance as well as, or better than, the hierarchical model.[8] Indeed, the bifactor model fit the data very well (χ^2[28] = 120.35, AIC = 196.35, CFI = .982, SRMR = .062).

Genomic SEM Estimates Excluding Self-Report GWAS. In a sensitivity analysis, we re-examined the Genomic SEM factor solutions when excluding GWAS summary statistics that included cohorts for which the psychiatric phenotypes were based primarily on self-report items not directly assessed by a clinician. This involved excluding the UK Biobank samples from MDD, ANX, and ALCH, and the 23andMe cohorts from MDD and ADHD. This reflected an 81% reduction in effective sample size for MDD, an 82% reduction for ANX, a 24% reduction for ADHD, and an 84% reduction for ALCH. To begin, we examined the heatmap of genetic correlations among the 11 traits, along with the difference in genetic correlations relative to genetic correlations estimated using all cohorts. We observe similar patterns of clustering among the traits (Supplementary Figure 1). Relative to using all cohorts, these analyses produced slightly larger genetic correlations for MDD and slightly smaller correlations for ANX.

We conducted a new EFA excluding the self-report cohorts using the same procedure of fitting the EFA in odd chromosomes and the CFA in even chromosomes. These analyses revealed a correlated factors model with four factors to be the best fitting model, with this model fitting the data well in both even chromosomes, $\chi^2[35] = 135.70$, AIC = 197.70, CFI = .907, SRMR = .104; and all chromosomes, $\chi^2[35] = 209.54$, AIC = 271.54, CFI = .936, SRMR = .078 (Supplementary Figure 1c; Supplementary Table 51). This factor structure was highly similar to that identified using all cohorts, with the factors again best characterized as reflecting compulsive, psychotic, neurodevelopmental and internalizing disorders. The one notable exception was cross-loadings of both MDD and ANX on the Compulsive disorders factor. A hierarchical model fit overtop this factor structure fit the data relatively worse in both even chromosomes, $\chi^2[37] = 170.30$, AIC = 228.30, CFI = .878, SRMR = .147; and all chromosomes, $\chi^2[37] = 231.59$, AIC = 289.59, CFI = .929, SRMR = .103.

We went on to estimate the parameters from the final confirmatory correlated factor model represented in Figure 1 using this more restricted dataset. Overall, both factor loadings and factor correlations from this restricted dataset were highly similar to those for the full dataset, and fit the data well, $\chi^2[33] = 189.48$, AIC = 255.48, CFI = .942, SRMR = .098; albeit with a lower loading of ANX on the Internalizing disorders factor (Supplementary Figure 1). We additionally used the restricted dataset to estimate a five-factor orthogonal EFA model, which was the model that served as the basis for the final confirmatory factor model in the main set of analyses. To quantify the similarity of EFA solutions across the full and restricted datasets, we computed factor congruence coefficients using the R *psych* package. Congruence coefficients index the similarity between factor solutions, with possible values ranging between -1.0 and +1.0. A congruence coefficient greater than .90 indicates an extremely high level of similarity of the factors, and values above .84 are considered reasonably similar. The congruence coefficients were .92 for the Compulsive disorders factor, 1.0 for the Psychotic disorders factor, .93 for the Neurodevelopmental disorders factor, and .85 for the Internalizing disorders factor. Of note, the factor solution identified using all cohorts provided better fit to the data excluding self-report cohorts than the factor solution identified using an EFA in self-report cohorts only reported above. In order to provide a more direct comparison to results using the full dataset, and owing to the better model fit, the correlated factor model identified using the full dataset was carried forward to examine GWAS hits in the restricted dataset.

As a final set of sensitivity analyses, we reexamined the SNP effects for the 154 hits identified from the correlated factors model estimated in the restricted dataset. All hits for the Compulsive and Psychotic disorders factor were also identified as hits using the restricted dataset, 8 out of 9 hits were genome-wide significant for the Neurodevelopmental disorders factor, and none of the 44 hits were estimated as genome-wide significant for the Internalizing disorders factor (Supplementary Table 3). However, plotting the distribution of effects indicate clear signal for these 44 loci in the restricted dataset relative to the estimated SNP effects for a random subset of 500 SNPs. Moreover, there was extremely high concordance for this subset of SNPs for the estimated factor betas across the full and restricted datasets ($r \geq .94$ Supplementary Figure 2). In addition, the hits identified in the full dataset were neither Q_{SNP} hits nor characterized by robust Q_{SNP} signal in the restricted dataset (Supplementary Table 3). Finally, we note that there were only 2 independent loci for MDD and 1 independent locus for ANX in the restricted sample for the listwise deleted set of SNPs present across the 11 psychiatric disorders. The absence of

Internalizing factor hits in the restricted dataset, therefore, appears to largely reflect an attenuated signal as a result of a substantial reduction in sample size.

Genetic Correlations with External Traits. For biobehavioral traits, summary statistics for 49 phenotypes broadly related to various domains of human health and well-being were downloaded from various online sources, primarily sourced from GWAS Atlas.[21] For brain morphology, 101 summary statistics were downloaded from the GitHub page that corresponds to the summary data produced by Zhao et al. (2019).[22] For accelerometer data, 24 summary statistics for each hour of movement across the day in UK Biobank were downloaded from the GCTA website.[23] All summary statistics were cleaned and processed using the munge function of Genomic SEM, retaining all HapMap3 SNPs outside of the major histocompatibility complex (MHC) regions with minor allele frequencies (MAFs) ≥ .01. To evaluate potential associations between the psychiatric genetic factors and external traits, we used Genomic SEM to estimate genetic correlations between each of the four psychiatric factors, the hierarchical *p*-factor, and all of the relevant traits.

Brain Morphology. Genetic correlations were examined between both the four correlated factors and the hierarchical factor with 101 metrics of brain morphology. We also used model χ^2 difference tests to determine whether the genetic correlations were likely to operate through the psychiatric factor, or were heterogenous across the factor indicators. For the second-order factor from the hierarchical structure, these model comparisons indexed heterogeneity at the level of the psychiatric factors. These results should be treated as preliminary as no correlations survived Bonferroni correction for 101 tests ($p < 4.95e\text{-}4$). However, it is of note that the rank ordering of genetic correlations with brain regions was largely specific to the four psychiatric factors (Supplementary Table 4). With respect to overlap across factors, there was an association between the Psychotic, Neurodevelopmental and *p*-factor and the right caudal middle frontal region, an area within the dorsolateral prefrontal cortex (dlPFC). This is consistent with previous findings that have identified dlPFC alterations for schizophrenia,[9] bipolar disorder,[10] and ADHD.[11] Unique to the Psychotic disorders factor was an association with another dlPFC region, the left rostral middle frontal gyrus, which has previously been associated with schizophrenia.[12] However, this was significantly heterogeneous and showed a unique association with BIP in our dataset (Supplementary Figure 4). In addition, the Psychotic disorders factor was genetically correlated with the pars opercularis, a central region of Broca's area that has been associated with both bipolar disorder and schizophrenia.[13]

The Compulsive disorders factor was most significantly correlated with the left and right caudate and putamen, regions that have been implicated for both OCD and TS.[14-16] Notably, the left and right putamen were also strongly associated with the hierarchical *p*-factor. The Neurodevelopmental disorders factor was correlated with the right putamen and the left and right pericalcarine region, both of which have been associated with autism.[17,18] Both the left and right pericalcarine were also significantly heterogenous, evincing a more robust association with PTSD and AUT relative to ADHD and MDD. The Internalizing disorders factor was particularly genetically correlated with the left medial orbitofrontal region, which has been associated with both trait anxiety[19] and the comorbid presentation of MDD and GAD relative to controls or MDD alone.[20]

Genetic Correlations with Biobehavioral Traits. As expected, all factors were positively, genetically associated with psychiatric phenotypes from outside studies, including the cross-disorder iPSYCH results, and negatively genetically correlated with indices of positive mental health (*e.g.*, subjective well-being, family relationship satisfaction; Supplementary Figure 6). In the remainder of this section, we generally describe patterns of genetic correlations with external biobehavioral traits outside of the psychiatric domain.

The Compulsive disorders factor was negatively genetically correlated with anthropomorphic traits (BMI, waist-to-hip ratio) and risk-taking behaviors (e.g., automobile speeding, Figure 3). Educational attainment (EA) and childhood intelligence evinced particular patterns of genetic associations with the individual compulsive disorders that were inconsistent with their operation via the Compulsive disorders factor, where AN and OCD were positively associated and TS negatively associated (Supplementary Figure 7).

The Psychotic disorders factor was negatively associated with BMI and positively associated with neuroticism. Phenotypes whose patterns of genetic associations with the individual disorders were inconsistent with their operation via the Psychotic disorders factor were largely cognitive, for which BIP was associated with more positive outcomes relative to SCZ.

The Neurodevelopmental disorders factor was genetically associated with earlier age at menopause. All other external correlates outside of the psychiatric domain that survived Bonferroni-correction exhibited patterns of associations with the individual neurodevelopmental disorders that were inconsistent with their operation via the factor. Cognitive (*e.g.*, educational attainment, intelligence) and economic outcomes (*e.g.*, own housing outright) had the strongest disorder-specific associations, with positive associations observed for AUT, and negative associations for PTSD and ADHD. In a few instances, PTSD stood apart from the remaining indicators. This included a stronger, negative genetic correlation between PTSD and agreeableness and a stronger, positive genetic correlation with suicide attempts relative to AUT and ADHD.

The Internalizing disorders factor exhibited negative genetic associations with age at menopause, EA, and positive associations with various adverse health outcomes (e.g., asthma, back pain, coronary artery disease). Phenotypes with disorder-specific associations included socioeconomic phenotypes (*e.g.*, owning a house outright), which tended to exhibit slightly stronger negative genetic associations with MDD than with ANX. In addition, we observed a disorder-specific association with neuroticism, where ANX was estimated to have a stronger, positive genetic correlation relative to MDD.

The *p*-factor exhibited a homogenous genetic correlation with automobile speeding propensity only. All other external non-psychiatric correlates that survived Bonferroni-correction exhibited patterns of associations with the first order psychiatric genetic factors that were inconsistent with their operation via the *p*-factor. The genetic associations with EA deviated most strongly from the hierarchical factor structure. These patterns of widespread heterogeneity in genetic correlations with external phenotypes undermine the utility of the *p*-factor.

Consistent with phenotypic findings[24] and conceptualizations[25] that posit cognitive deficits as a central distinguishing factor across SCZ and BIP, we observe distinct genetic associations with

cognitive outcomes, with BIP associated with better outcomes relative to SCZ. Within the personality domain, neuroticism—a construct commonly observed to be both phenotypically[26] and genetically[27] associated across internalizing disorders—showed a stronger association with ANX over MDD. As many of these external traits and the disorders are multi-faceted in nature, it will be important for future work to obtain finer-grained phenotypes to better define the boundaries of these findings. Indeed, recent work using Genomic SEM found that ANX and MDD may share unique genetic associations with specific facets of neuroticism.[28]

Estimation of Q Metrics. We compute heterogeneity statistics for both associations with external traits (Q_{Trait}) and individual SNPs (Q_{SNP}). These index violation of the null hypothesis that a given trait or SNP acts through a given factor. Put another way, it quantifies whether the external trait or SNP is more likely to operate through the common pathways of the psychiatric factors, or the independent pathways of individual disorders. These Q metrics thereby identify instances when associations with a trait or SNP do not plausibly operate on the individual phenotypes exclusively by way of associations with common factor(s), and may be highly specific to the individual disorder. Four separate, follow-up models were estimated in which the SNP or trait predicted three of the overarching factors *and* the indicators of the remaining fourth factor (see Supplementary Figure 5 for Q_{Trait} path diagrams; Supplementary Figure 45 for Q_{SNP} path diagrams). Computing the nested χ^2 difference test between the common pathways model, in which the SNP or trait predicted all four factors, to one of these four, follow-up, independent pathways models produces a factor-specific Q metric. We note that it has been previously demonstrated that common and independent pathways models are nested and, therefore, appropriate for comparison via the nested χ^2 difference tests[29] used to compute Q metrics here.

We calculate model χ^2 for both the common and independent pathways models using the two-step procedure described in Grotzinger et al. (2019).[30] In Step 1 of this procedure a proposed model is estimated. In Step 2, the Step 1 estimates are fixed and the residual covariances and variance of the indicators are freely estimated. The estimates in Step 2 capture both the discrepancy between the model implied and observed covariance matrices, and the corresponding sampling covariance matrix (V_R) of R. The V_R matrix has the eigendecomposition:

$$V_R = (\mathrm{P}_1\ \mathrm{P}_0)\begin{pmatrix} E & 0 \\ 0 & 0 \end{pmatrix}\begin{pmatrix} P_1' \\ P_o' \end{pmatrix}$$

with P_1 reflecting a matrix of principal components (eigenvectors) of V_R, E a corresponding diagonal matrix consisting of non-zero eigenvalues, and P_0 the null space of V_R. Projecting R_i, the vector of residual covariances estimated in Step 2, onto P_1 and adjusting for corresponding eigenvalues produces:

$$E^{\frac{-1}{2}} P_1' R_i N(0, I_r)$$

Therefore,

$$R_i'\mathrm{P}_1 E^{-1}\mathrm{P}_1' R_i \sim \chi^2(r)$$

It has been previously confirmed via simulation that this equation produces a χ^2 distributed test statistic.[30] This method of computing χ^2 difference tests across a common pathways model and an independent pathways model to arrive at a Q metric is mathematically equivalent to the procedure outlined for calculating Q_{SNP} in Grotzinger et al. (2019).[30]

We note a number of important points to keep in mind with respect to interpreting Q (see de la Fuente et al. [2020][31] for additional explication). First, Q will be most significant for a factor when the vector of observed effects with an external trait or SNP is not proportional to the unstandardized loadings of the disorders on the factor. Consequently, Q is not necessarily significant when the vector of observed external SNP/trait effects is unequal across the disorders as, in many cases, the disorders will also have unequal unstandardized factor loadings. For example, in cases where a particular disorder has a low unstandardized loading relative to the other disorders, we would expect Q to be *high* for SNPs or external traits that show comparable associations across all disorders. As Q is calculated based on observed beta coefficients, and not *z*-statistics, this has the desirable property that Q will not increase simply due to differences in power across the univariate GWAS. As an interpretive caveat, we note also that Q will not be significant in instances when the effect of an external trait or SNP has similar, but mechanistically independent, effects on the disorders that define the factor. In this sense, Q is most appropriately viewed in the same light as many other statistical hypothesis tests: as a means of rejecting the null (i.e., that the trait or SNP acts solely via the factor) but not as a means of directly confirming the null. Indeed, patterns of external associations are generally not expected to conform exactly to the factor model, just as population effects are never expected to be exactly 0. However, by setting stringent significance thresholds we seek to identify via Q those SNPs and external traits that strongly deviate from the factor structure, thereby offering insight into underpinnings of genetic divergence across even highly correlated disorders.

For the hierarchical factor structure, we computed the χ^2 difference test for a model in which the SNP or trait predicted only the second-order *p*-factor, to the model χ^2 for a model in which the SNP or trait predicted only the four, first-order psychiatric factors. For the bifactor model, we compared a model in which the SNP predicted only the *p*-factor to a model in which the SNP predicted both the *p*-factor and the remaining four orthogonal factors. For both the hierarchical and bifactor model, Q indexes heterogeneity at the level of the psychiatric factors (i.e., deviation from the null that the SNP or trait operates through the *p*-factor). Therefore, a significant Q statistic for the hierarchical or bifactor model is likely to identify patterns of external associations that are specific to a subset of the psychiatric factor(s). This is distinct from the interpretation of Q in the context of the correlated factors model, as a significant hierarchical or bifactor Q may still conform to the local structure of one of the correlated factors.

Identification of Top Hits (Clumping) and Overlapping Hits. Lead SNPs for meta-analyzed univariate indicators and the latent genetic factors were identified using the clumping and pruning algorithm in FUMA.[33] Independent significant SNPs were defined as crossing the genome-wide significance threshold of $p < 5e\text{-}8$ that were independent from other SNPs at $r^2 < 0.1$. We used pre-calculated LD from European 1000 Genomes Phase 3 reference panel to identify independent SNPs. Top loci were subsequently identified by merging any SNPs in close proximity (< 250 kb) into a single genomic locus such that an individual locus could include multiple independent SNPs at $r^2 < 0.1$. We depict only the significant loci (referred to as hits throughout the paper) in the Miami plots, but report independent significant SNPs in supplementary tables. This same pipeline was used for the full set of univariate summary statistics (i.e., not listwise deleted across all 11 traits) in order to produce a comparable set of loci for the univariate disorder GWAS. To determine overlap with hits across the factors and disorders, we identified all independent SNPs for the psychiatric factors that were in LD ($r^2 > 0.6$) with independent SNPs for the individual disorders.

We report univariate hits and consider overlap with identified factor hits using the European ancestry summary statistics used as input to Genomic SEM. Therefore, the total number of univariate hits will differ from prior reports utilizing transethnic analyses. As LD structure can vary across different cohorts, we also considered hits to be overlapping (in LD) if loci from the univariate disorder GWAS were within a 250 kb window (125 kb on either side of the index variant) of loci identified for the psychiatric factors or omnibus test.

Comparison of Results to CDG2. The factor analytic results, with additional disorders and larger GWAS sample sizes, largely replicate findings from PGC Cross-Disorder Group 2 (PGC-CDG2).[32] More specifically, PGC-CDG2 reported factors representing compulsive, psychotic, and neurodevelopmental disorders, which correspond closely to our first three factors. Our identification of an Internalizing factor can largely be attributed to the inclusion of ANX, and to a lesser extent PTSD, in addition to MDD in the current analysis. It is of note that both TS and ALCH evinced the lowest factor loadings, indicating the most distinct genetic etiology among the 11 disorders in this model.

We next consider overlap with respect to GWAS results, comparing our findings to the 109 pleiotropic (i.e., associated with more than one disorder irrespective of directionality) and 146 total hits from PGC-CDG2.[32] The unstructured multivariate GWAS recaptures 69 of the 109 (63.3%) pleotropic loci and 97 of the 146 (66.4%) total loci from PGC-CDG2. For the structured, factor model GWAS, of the 109 pleiotropic hits from PGC-CDG2, none were in LD with hits for the Compulsive disorder factors, 52 hits were in LD with hits for the Psychotic disorders factor, 4 hits were in LD with hits for the Neurodevelopmental disorders factor, and 14 hits were in LD with hits for the Internalizing disorders factor. As 5 of these overlapping hits were redundant across the factors, the correlated factors model indicates that 65 of the 109 (59.6%) PGC-CDG2 hits may be interpreted as acting pleiotropically via the factors identified here.

Multivariate GWAS Simulations

Simulation Procedure. In order to examine the calibration of Genomic SEM for multivariate GWAS, we began by estimating the model implied genetic covariance matrix for a model in which rs9314056—a hit for the Internalizing disorders factor and a univariate hit for MDD and ANX—was specified to predict the four factors from the correlated factors model. Nine different versions of this genetic covariance matrix were used to form population generating covariance matrices from which individual covariance matrices were simulated using the *rmvrnorm* function in the *rockchalk* R package. The observed sampling covariance matrix (*V*) was used for sampling from the population matrices, and was subsequently paired with each simulated genetic covariance matrix when estimating the model in Genomic SEM. As the *V* matrix includes squared *SEs* on the diagonal, simulated parameters (e.g., the genetic covariance between MDD and ANX; the association between the SNP and PTSD, etc.) were therefore specified to have the same precision as in the observed data. This has the intended consequence that the simulations reflect the empirical data scenario wherein certain associations are estimated with greater precision, as will often be the case when the contributing univariate GWAS was estimated using a larger participant sample. We have therefore endeavored to conduct a series of simulations that are both directly relevant to the current analyses and more broadly reflect the realistic scenario of differentially powered GWAS entered into the same multivariate framework.

Genetic covariance matrices were sampled 250 times for nine different population generating scenarios, for a total of 2,250 simulations. These nine scenarios consisted of: Scenario 1 in which the model implied matrix was unchanged; Scenario 2 in which the covariance between the SNP and ALCH was set to 0; Scenario 3 in which the covariance between the SNP and PTSD was set to 0; Scenario 4 in which the covariance between the SNP and ANX was set to 0; Scenario 5 in which the covariance between the SNP and MDD was set to 0; Scenario 6 in which the covariance between the SNP and PTSD, ALCH, and ANX was set to 0; Scenario 7 in which the covariance between the SNP and MDD, PTSD, ALCH, and ANX was set to 0; Scenario 8 in which the covariance between the SNP and all 11 psychiatric traits was set to 0; and Scenario 9 in which the direction of the covariance between the SNP and ANX and ALCH was reversed (i.e., multiplied by -1). These nine scenarios were chosen to reflect varying degrees of conformity to the Internalizing disorders factor structure, with Scenario 1 exactly matching the model and Scenario 9 reflecting the most extreme deviation from the model wherein the SNP has directionally opposing effects on ALCH and ANX. We include Scenario 8 in addition to Scenario 7 as the estimated SNP effects for the Internalizing disorders factor may include some minimal genetic signal from the broader correlated factors model. Note that none of the subsequent models estimated in Genomic SEM fixed the relationship between a psychiatric trait/factor and SNP to 0, nor were the simulated covariance matrices likely to produce a SNP-trait relationship at exactly 0. Rather, SNP-trait associations were *only* set at 0 in the generating population.

In the sections below, we first compare results across the nine different population generating scenarios for a factor model multivariate GWAS in Genomic SEM in which the SNP effect was specified to predict the four factors from the correlated factors model. We subsequently compare these results to those from an unstructured GWAS (discussed further below) in Genomic SEM that seeks to provide an exhaustive list of SNPs relevant to the traits of interest. This is in contrast to the factor model results that estimates SNP effects specified to operate via the structure of the factors. We additionally consider results across three, separate multivariate GWAS methods: MTAG,[34] N-GWAMA,[35] and MA-GWAMA,[35] also discussed further below.

Factor Model. We first examined the distribution of estimated SNP effects and Q_{SNP} specific estimates for the Internalizing disorders factor in Genomic SEM across the nine scenarios. As expected, the distribution of estimated SNP effects revealed the strongest signal for Scenario 1 in which the population exactly matched the factor model (Supplementary Figure 25), with all 250 runs producing genome-wide significant hits for the Internalizing disorders factor (i.e., no false negatives) and an average *p*-value for the estimated SNP effect on the factor of 2.51E-10 (Supplementary Table 11). The signal was also comparable for Scenarios 2 and 3 where the SNP association with the two disorders with the smallest factor loadings, ALCH and PTSD, was 0 in the population (Supplementary Figures 1 and 3). This was followed by reduced signal when the SNP with ANX association was 0 (Scenario 4), the SNP association with PTSD, ANX and ALCH was set to 0 (Scenario 6), and the SNP association with MDD was set to 0 (Scenario 5).

A particular concern for the Internalizing disorders factor may be that the larger sample size for MDD relative to the other three disorders that load on this factor results in estimated factor SNP effects that merely recapitulate the signal for MDD. Scenario 6 was designed to test this concern. As can be seen in the distribution of effects (Supplementary Figures 25 and 27) there is a marked

downshift in the signal for this scenario when all SNP associations with Internalizing indicators *except* MDD were set to 0 in the population. This demonstrates that while SNP associations with a factor will certainly be more influenced by a better powered factor indicator that also has a larger factor loading, that the signal is not strictly dominated by this indicator. As would also be expected, the signal was particularly attenuated for Scenario 9 when the direction of the SNP association with ALCH and ANX was reversed, and was the weakest for Scenarios 7 and 8 in which the SNP association with the four Internalizing factor disorders and all 11 disorders were set to 0 in the population. Moreover, there were no factor hits (i.e., no false positives) in the latter two scenarios, and all SNPs in Scenario 9 were estimated as hits for Q_{SNP}.

The trends for Q_{SNP} were also in the expected directions. More specifically, there was a clear null signal for Q_{SNP} for Scenario 1 for which the model matched the population (Supplementary Figure 28), no Q_{SNP} hits (i.e., no false positives) and an average Q_{SNP} *p*-value of .560. There was a similar absence of signal for Scenarios 2 and 3, also with no Q_{SNP} hits and no deviation from the expected *p*-values in the QQ-plot. In addition, there was very little signal for Scenarios 7 and 8 where trait and SNP associations were at 0. This is also expected, as estimated SNP associations that are consistently near 0 across indicators that load on the same factor are, in fact, not hugely discrepant from the factor model. Q_{SNP} signal increased for the scenarios that more strongly deviated from the structure, in which ANX, MDD, or PTSD, ALCH and ANX were 0 in the generating population. The signal was by far the largest for Scenario 9 (Supplementary Figure 28) in which the directionality of the SNP effect was reversed for ANX and ALCH, with 100% of the 250 runs estimated as genome-wide significant Q_{SNP} hits. This is the scenario that deviated strongest from the factor model and, in line with observation, is expected to pick up on the largest Q_{SNP} signal.

Comparing Genomic SEM to Other Multivariate Methods. In the absence of other summary statistics based SEM methods, we sought to perform a comparison of Genomic SEM to three of the most closely related multivariate methods: MTAG,[34] N-GWAMA,[35] and MA-GWAMA.[35] These methods were considered most similar to Genomic SEM in that they also account for unknown degrees of sample overlap via the bivariate LDSC intercept and produce results by statistically incorporating the estimated genetic covariance across included traits. We additionally compare results to an unstructured model in Genomic SEM that seeks to identify an exhaustive set of SNPs relevant to the traits of interest, irrespective of directionality. MTAG, N-GWAMA, and MA-GWAMA, utilized only the four internalizing disorder indicators (ANX, PTSD, ALCH, MDD) to mirror the factor model simulation results presented above for the Internalizing disorders factor. Before comparing simulation results across methods, we first provide a brief overview of each method and how results were produced using our simulation procedure. We refer to the reader to the original articles for further details on estimation procedures and statistical properties for each method.

Unstructured Model. We estimate SNP effects via an unstructured model in Genomic SEM by calculating a model χ^2 difference test for a model in which the SNP is allowed to have direct regression relations with each of the 11 disorders (i.e., a fully saturated model) against a null model in which the SNP is associated with none of the disorders. This omnibus test is χ^2 distributed with 11 *df,* and quantifies evidence for an overall effect of the SNP on any subset of the disorders, irrespective of the patterning or directionality of the effects. These models do not include any higher order factors and are meant to provide an exhaustive list of SNPs associated with included

traits. All 11 disorders were included for the unstructured models, despite choosing simulation parameters for a SNP that is specifically relevant to the Internalizing disorder factor and indicators. By including all 11 disorders, the simulations mirror the real data analyses conducted and provide a more conservative test of the unstructured GWAS approach. That is, if the goal is to identify a comprehensive set of associated SNPs, it is most informative to examine the performance of the unstructured models for scenarios in which the SNP affects only a subset of the included traits.

Multi-trait Analysis of GWAS (MTAG).[34] MTAG works by leveraging the shared genetic information across traits, as indexed by the LDSC genetic covariance, to increase power for a particular trait. The MTAG model was specified in Genomic SEM in order to directly use the simulated genetic covariance matrices for analyses. We have shown previously that MTAG specified in Genomic SEM produces estimates that are correlated at > .99 with summary statistics produced from the original MTAG software.[30] We specified MDD to be the MTAG "target" and PTSD, ADHD, and ANX as the secondary traits used to boost signal; a schematic of the MTAG model for MDD as estimated in Genomic SEM is depicted in Supplementary Figure 29.

Model Averaging GWAMA (MA-GWAMA).[35] MA-GWAMA functions by first estimating a manifold of models that specify the simple regression relationship between the SNP and a set of traits using distinct design matrices, X. Mirroring the original MA-GWAMA approach, X is composed of two vectors: a unit vector, and a dichotomously coded (0, 1) vector in which the coding varies across the models, such that each model allows for the existence of two distinct genetic effects across subsets of traits. The estimates from these models are then aggregated using weights derived from the fit of the model, as indexed using AIC_C. In order to mirror the format of results expected by the software, all simulated SNP-phenotype covariances and corresponding standard errors were transformed into SNP-phenotype regressions using the simulated SNP variance. As with MTAG, we report MA-GWAMA results for MDD from models that additionally included PTSD, ADHD, and ANX.

N-Weighted Multivariate GWAMA (N-GWAMA).[35] N-GWAMA produces a single multivariate test statistic that is computed as the weighted sum of test-statistics taking into account both sample overlap and the genetic covariance across included traits. Reported simulation results then reflect a weighted aggregate across MDD, PTSD, ADHD, and ANX, as opposed to an updated test statistic for MDD as in the case of MA-GWAMA and MTAG. The SNP-phenotype covariances were also transformed to SNP-phenotype regressions to mirror the expected format of results for the N-GWAMA software.

We highlight results for a few key scenarios here. For Scenario 1, in which the generating population matched the specified model, the factor model in Genomic SEM was slightly better powered than the other methods (Supplementary Figures 30-31; Supplementary Table 11). For Scenario 5, in which the population generating SNP and MDD association was 0, the unstructured and factor models were generally better powered than the remaining three methods. Conversely, for Scenario 6 in which the population generating SNP association was 0 for all Internalizing traits *except* MDD, the signal was the most reduced for the factor model. This pattern of results is consistent with the analytic goals of each individual method. For Scenarios 7 and 8, in which the population generating SNP associations were zero, results revealed similarly null signals across all methods. Finally, in Scenario 9 in which the SNP association with ANX and ALCH was

directionally reversed, the factor model and unstructured model showed the weakest and strongest signal, respectively, compared to the other three methods.

These results collectively speak to the fact that, relative to other multivariate methods, the multivariate GWAS signal for the factor model is not dominated by any single trait and is particularly sensitive to distinct patterns of SNP associations across traits. In addition, an unstructured model was especially well-suited for identifying a comprehensive set of SNPs associated with the traits. This does not indicate that Genomic SEM should be universally preferred over other multivariate genomic methods, as many approaches seek to increase signal for a particular target trait. Indeed, consistent with this particular analytic goal the signal was more deflated for the MTAG model and MA-GWAMA relative to Genomic SEM when the population SNP effect was 0 for the target trait, MDD. For the current investigation, the analytic goals reflect identifying SNPs generally associated with psychiatric risk and characterizing the genetic underpinnings of convergence and divergence across clusters of psychiatric disorders. The current simulations indicate that unstructured and factor models are particularly well-suited for these purposes in both an absolute sense and relative to existing alternatives.

Comparing GWAS Results to Prior Findings. Of the 39 unstructured model novel hits, nine have not been described for independent studies of psychiatric traits/symptoms and were largely characterized by hits previously found for cognitive (e.g., intelligence) or anthropometric traits (e.g., BMI; Supplementary Table 13). Moreover, 7 hits were entirely novel in that they were not in LD with any previously discovered hits in the GWAS catalogue.

Of the 12 unique psychotic disorders factor hits, Of 8 have been reported as hits in independent (or semi-independent) external GWAS of psychiatric traits, 2 were novel for psychiatric traits, and 2 were entirely novel (Supplementary Table 18). The two novel Neurodevelopmental disorder factor hits were in LD with hits previously described for GWAS of psychiatric traits (Supplementary Table 21). Among these 6 novel loci, 3 were identified in outside studies of psychiatric traits, one has been identified for smoking initiation, and two have yet to be described for any trait (Supplementary Table 24). Three of the bifactor p-factor hits were novel for psychiatric traits more generally (Supplementary Table 30).

Multivariate Mendelian Randomization Identifies Causal Effects of Alcohol Use. We incorporated Mendelian randomization (MR) into a Genomic SEM framework, in order to consider models in which the relationships between disorders may partially reflect direct causal effects of ALCH on risk for either the individual disorders themselves or the more general factors.

We began by running a single variant MR model using the rs4699743 index variant in the alcohol dehydrogenase (ADH1B) gene. The alcohol dehydrogenase variants on chromosome 4q23 are arguably the most well-described for any alcohol use phenotype. They are consistently identified in ALCH GWAS,[36-39] are highly expressed in the liver, and are directly involved in the major human ethanol metabolic pathway.[40] Moreover, this variant was identified as significant for Q_{SNP} across all four factors in the correlated factor model. Using the ADH1B SNP as an instrument for ALCH, we examined causal effects of ALCH at both the level of the individual disorders and the psychiatric factors. For the individual disorders model, the ADH1B variant was specified to directly predict ALCH, and ALCH to directly predict the 7 disorders from the Psychotic (BIP;

SCZ), Neurodevelopmental (PTSD; ADHD; AUT), and Internalizing disorders (MDD; ANX) factors on which ALCH also loaded. A separate model that examined the causal effects of ALCH on the psychiatric factors, also specified ADH1B to predict ALCH, but specified ALCH to directly predict the Psychotic, Neurodevelopmental, and Psychotic disorders factors.

The model for individual disorders fit the data well (χ^2[36] = 151.90, AIC = 235.90, CFI = .978, SRMR = .064). This model indicated causal effects of ALCH on BIP (p = .028) and MDD (p = .024), but not the remaining disorders (Figure S28A). The model for the factors also fit the data well (χ^2[40] = 156.70, AIC = 232.70, CFI = .978, SRMR = .064), and indicated a causal effect of ALCH on the Internalizing disorders factor (p = .031), but not the Psychotic or Neurodevelopmental disorders factors (Supplementary Figure 39). We went on to examine whether these causal estimates would persist when using multiple instruments for ALCH identified through external GWAS.

For multi-variant MR, we began by selecting instruments for ALCH using the 10 loci identified in an independent discovery GWAS of ALCH conducted in the Million Veterans Project.[41] We removed two SNPs (rs1421085; rs4936277) based on weak SNP associations for the ALCH PGC GWAS , UKB GWAS, and meta-analysis GWAS of the two cohorts. Among the remaining 8 SNPs, 3 SNPs (rs5860563, rs1229984, rs61902812) were not present in the current set of summary statistics across the 11 disorders. For these 3 SNPs, we used LD proxies that were within the same gene region and confirmed that these proxy SNPs showed strong associations with ALCH.

Multi-variant MR allows us to relax a core assumption of univariate MR by modeling potential pleiotropy wherein a subset of the SNPs that act on ALCH are also allowed to directly affect the downstream disorders or factors. To this end, we adopted methods for Multiple Indicator Multiple Cause (MIMIC) modeling[42] to iteratively identify direct paths from the SNP to the disorders or factors. This was done in two phases. In Phase 1, a baseline model was estimated in which no pleiotropic paths were allowed. In Phase 2, all of the Phase 1 estimates were fixed, and the residual variances and covariances between all SNPs and disorders or factors was estimated. The Phase 2 model produces point estimates and standard errors that are equivalent to the difference between the observed genetic covariance matrix and the Phase 1 model-implied genetic covariance matrix. A direct path corresponding to the most significant residual effect was then added to the model to create a new baseline model. These paths between the SNPs and the disorders or factors were added one by one until they no longer reached a significance threshold of $p < .01$. We chose the threshold of $p < .01$ in our test for pleiotropy so as to maintain consistency with other multivariant MR approaches.[43]

For the individual disorders, we began with a baseline model in which the 8 SNPs selected as instruments predicted ALCH, and ALCH predicted the 7 disorders from the Psychotic, Neurodevelopmental, and Internalizing disorders factors on which ALCH also loaded. We note that these models directly accounted for LD across the 8 near-independent variants by directly modeling their correlation structure. LD across the variants was obtained from the 1000 Genomes European Phase 3 sample. Our iterative two-phase procedure identified 7 additional direct (pleiotropic) paths from individual SNPs to disorders. This final model (Supplementary Figure 40) provided better fit to the data (χ^2[99] = 240.47, AIC = 422.47, CFI = .976, SRMR = .043) than the original baseline model (χ^2[106] = 453.17, AIC = 621.17, CFI = .942, SRMR = .044). In line with

results for ADH1B alone, results indicated causal effects of ALCH on MDD (p = .037) and BIP (p = .046), but not the remaining disorders.

Using the same general procedure, we examined causal effects of ALCH at the level of the psychiatric factors. The baseline model included the 8 SNPs predicting ALCH, along with ALCH predicting the Psychotic, Neurodevelopmental, and Internalizing disorders factors. Our iterative two-phase procedure identified 6 additional direct paths from SNPs to factors for the same SNPs identified with pleiotropic pathways for the individual traits. This model (Supplementary Figure 40) provided better fit (χ^2[104] = 249.33, AIC = 421.33, CFI = .976, SRMR = .043) relative to the baseline model (χ^2[110] = 456.92, AIC = 616.92, CFI = .942, SRMR = .044). Results indicated no significant causal effects of ALCH on the factors. Collectively, these results suggest causal effects of ALCH on MDD and BIP.

Comparison of LDSC and S-LDSC. For psychiatric traits, the mean ratio of non-redundant elements in the genetic covariance matrix, calculated as LDSC over S-LDSC, was 1.029 and 1.268 for heritabilities and genetic covariances, respectively. That is, generally larger estimates were obtained for LDSC, though the difference was fairly minimal. The unstandardized regressions of S-LDSC predicting LDSC summary statistics from the correlated factors multivariate GWAS also indicated close correspondence between the two methods: compulsive disorders, *beta* = .84, *intercept* = .07; psychotic disorders, *beta* = .98, *intercept* = -.006; neurodevelopmental disorders, *beta* = .96, *intercept* = .005; and internalizing disorders, *beta* = .96, *intercept* = .006. These results indicate a trend of closer correspondence between LDSC and S-LDSC multivariate GWAS estimates for factors defined by higher powered univariate indicators.

Multivariate GWAS using S-LDSC. For the unstructured multivariate GWAS, S-LDSC—based analyses produced 151 hits, 123 of which were in LD with univariate hits. Of the 109 pleiotropic CDG2 hits, 63 were identified for the omnibus test.

We did not identify any hits for the Compulsive disorders factor or its Q_{SNP} statistic. 89 independent loci were genome-wide significant ($p < 5 \times 10^{-8}$) for the Psychotic disorders factor. Of the 89 loci, 12 were not previously identified in any of the contributing univariate GWASs, and 7 of these 12 were not identified as either genome-wide significant or suggestive of significance ($p < 1 \times 10^{-5}$) in a separate, previously published GWAS of psychiatric traits. The majority of these 7 novel loci were previously found to be associated with some aspect of cognitive performance (e.g., math ability; Supplementary Table 34). Q_{SNP} results for the Psychotic disorders factor produced 10 independent loci, including two that were only genome-wide significant univariate hits for SCZ (rs28637922; rs1150711).

For the neurodevelopmental disorders factor, S-LDSC—based analyses produced identified 8 significant loci, 3 of which were not significant for any of the univariate traits. These 3 loci have previously been described in outside studies of the same trait, or were near genome-wide significant for summary statistics included in the present analyses (Supplementary Table 38). Neurodevelopmental Q_{SNP} results revealed 7 independent loci, one of which was significant for only AUT (rs7844805).

Finally, for the Internalizing disorders factor we identified 29 genome-wide significant loci, 2 of which were not in LD with any of the univariate hits. Of these two, a single locus (rs1994375) has not been previously described for any outside traits (Supplementary Table 41). Internalizing Q_{SNP} results revealed 6 independent loci, two of which were also identified as significant for the Neurodevelopmental and Psychotic disorders Q_{SNP} metric. These two Q_{SNP} loci consisted of one locus that was significant for ALCH (rs28712821) and one locus that was significant for both ALCH and SCZ (rs71621626). An additional Internalizing Q_{SNP} locus was also significant for the Neurodevelopmental Q_{SNP} statistic and a univariate hit for ALCH (rs3114045).

Of the 109 pleiotropic hits from CDG2, 49 Psychotic disorders factor hits were in LD, 4 Neurodevelopmental hits were in LD, and 10 Internalizing hits were in LD. As 4 of these CDG2 hits were redundant across the factors S-LDSC-based analyses indicate that a total of 60 of the 146 (55%) of the CDG2 hits may be interpreted as acting pleiotropically via the factors identified here. Five hits from the correlated factors were in LD were across the factors, and 2 hits were in LD with a Q_{SNP} hit. In total, we therefore discover 119 independent loci that are likely to operate through pleiotropic mechanisms, 14 of which were novel relative to the univariate traits. Furthermore, accounting for LD across factor-specific Q_{SNP} hits, we identify 14 independent Q hits that do not conform to the identified factor structure, many of which appeared to operate through pathways unique to ALCH.

Quality Control Procedures

LD-Score Regression. Quality control (QC) procedures for producing the genetic covariance (S) and sampling covariance (V_S) matrix followed the defaults in LDSC. This included removing SNPs with an MAF < 1%, information scores (INFO) < .9, SNPs from the MHC region, and filtering SNPs to HapMap3. The LD scores used for the analyses presented were estimated from the European sample of 1000 Genomes, but restricted to HapMap3 SNPs as these tend to be well-imputed and produce accurate estimates of heritability. EFA and CFA analyses using odd and even chromosomes, respectively, utilized M—reflecting the number of SNPs in the original LDSC equation[9]—for just the odd or even chromosomes.

Multivariate GWAS. To obtain summary statistics for multivariate GWAS, we used the default QC procedures in Genomic SEM of removing SNPs with an MAF < .005 in the 1000 Genomes Phase 3 reference panel and SNPs with an INFO score < 0.6 in the univariate GWAS summary statistics. These are currently the default QC procedures for the *GenomicSEM* R package. Using these QC steps, there were 4,775,763 SNPs present across all eleven sets of European ancestry summary statistics. Prior to running any multivariate GWAS, all summary statistics were standardized with respect to the total variance in the outcome using the *sumstats* function in *GenomicSEM* and corrected for genomic inflation using the conservative approach of multiplying the standard errors by the univariate LDSC intercept when the intercept was above 1.

Extended Limitations. It is important to note a number of limitations of the current analytic framework. Stratified Genomic SEM inherits the assumptions and limitations of traditional S-LDSC.[44] This includes using an additive model of gene action that does not consider the role of epistatic effects, and only modelling the covariance among relatively common variant SNPs for which LD information is available. In future work, larger univariate GWAS coupled with Stratified

Genomic SEM would allow for fitting qualitatively distinct structural models for individual annotations. It is conceivable, for example, that a simpler two-factor model may best describe genetic covariance in evolutionarily conserved regions, whereas a five-factor model may reflect the underlying architecture in genes that are intolerant to protein truncation. The statistical tools developed here would allow for testing such hypotheses in future work by relaxing the assumption that a single structural model characterizes the genetic relationships across psychiatric disorders. Moreover, our results may have been influenced by the phenotyping and case-ascertainment methods used. Cai *et al*. (2020)[45] have specifically reported that psychiatric phenotypes derived using minimal phenotyping (defined as "individuals' self-reported symptoms, help seeking, diagnoses or medication") may produce GWAS signals of low specificity. Although our sensitivity analyses suggested minimal differences when excluding GWAS that used self-report cohorts this issue should continue to be explored in future work. The current findings at all levels of analysis (biobehavioral, functional, SNP) should also be interpreted with respect to the power of the individual disorders used to define the factors. In particular, the paucity of GWAS hits and significant enrichment findings for the Compulsive disorders factor should be considered in the context of the relatively low power for the disorders that define this factor. The current findings at all levels of analysis (biobehavioral, functional, SNP) should also be interpreted with respect to the power of the individual disorders used to define the factors. In particular, the paucity of GWAS hits and significant enrichment findings for the Compulsive disorders factor should be considered in the context of the relatively low power for the disorders that define this factor. Future analyses may also benefit from evaluating these findings using a set of traits that is balanced with respect to statistical power. Additionally, it was not possible to validate our findings in independent datasets owing to the fact that secondary datasets of sufficient sample size do not yet exist for many of the included disorders. The replicability of these findings will of course be critical to examine in future analyses. It will also be informative for future research to examine further the effect of heterogeneity in how samples are ascertained and disorders are assessed on cross- and within-disorder relationships.[46] Application of detailed and standardized assessment protocols to large, representative samples would of course be ideal. More pragmatically, future work may apply multivariate genetic approaches, such as those showcased here, at the level of individual symptoms.[47]

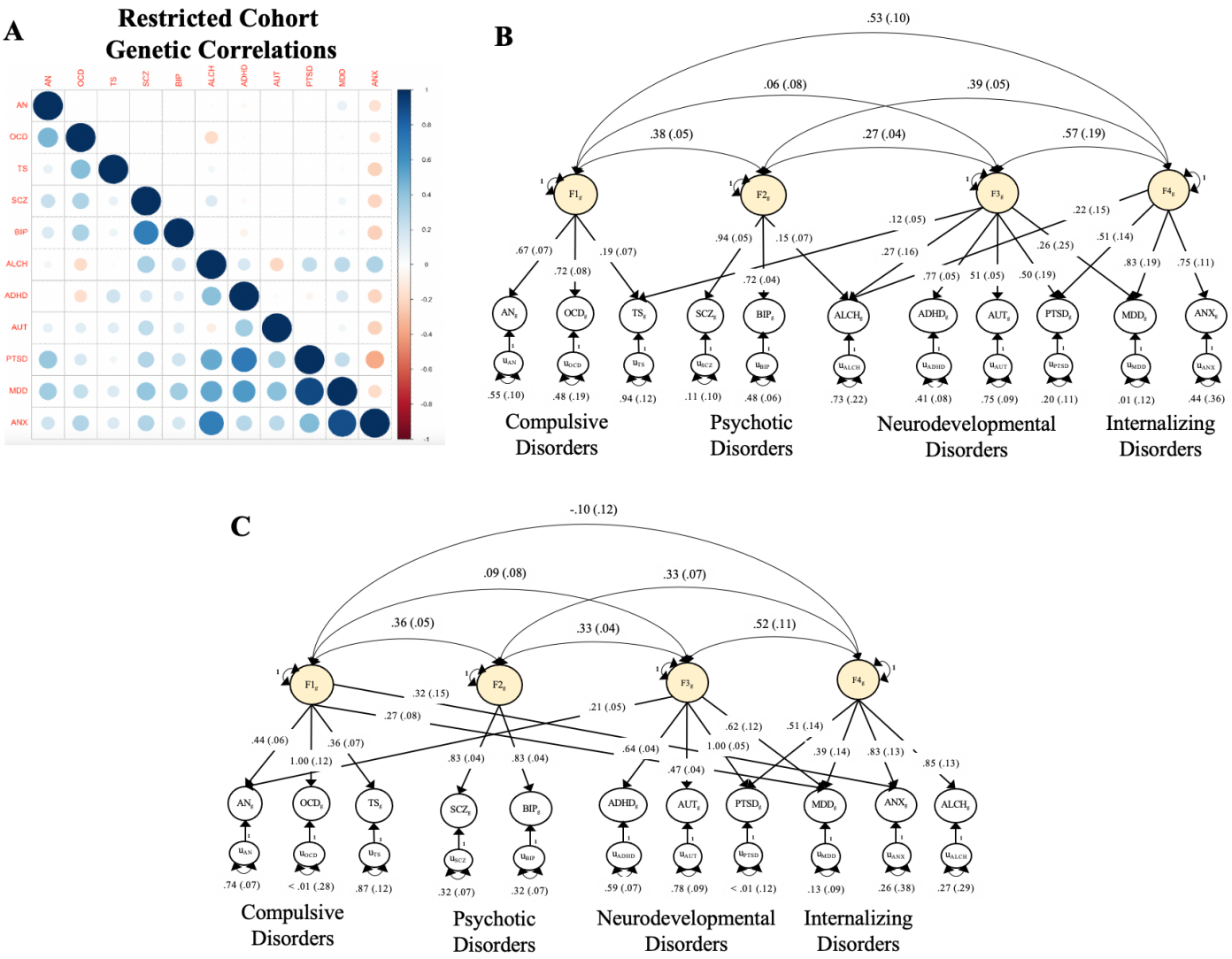

Supplementary Figure 1. Sensitivity Analysis Excluding GWAS Utilizing Self-report Cohorts. Panel A**:** Values below the diagonal depict genetic correlations estimated using LDSC excluding GWAS that included cohorts for which the psychiatric phenotypes were based primarily on self-report items not directly assessed by a clinician. We excluded the UK Biobank samples from MDD, ANX, and ALCH, and the 23andMe cohorts from MDD and ADHD. Values above the diagonal reflect genetic correlations estimated using all cohorts subtracted from the restricted cohort genetic correlations. Therefore, negative values for ANX above the diagonal indicate that genetic correlations between ANX and the remaining traits were generally estimated as larger when using all cohorts. **Panel B:** Figure presents standardized results for the correlated factors model fit to the restricted cohorts genome-wide LDSC genetic covariance matrix. **Panel C:** Figure presents standardized results for the correlated factors model identified using EFA in the restricted cohort fit to the restricted cohort genome-wide LDSC genetic covariance matrix. ADHD = attention-deficit/hyperactivity disorder; OCD = obsessive-compulsive disorder; TS = Tourette syndrome; PTSD = post-traumatic stress disorder; AN = anorexia nervosa; AUT = autism spectrum disorder; ALCH = problematic alcohol use; ANX = anxiety; MDD = major depressive disorder; BIP = bipolar disorder; SCZ = schizophrenia.

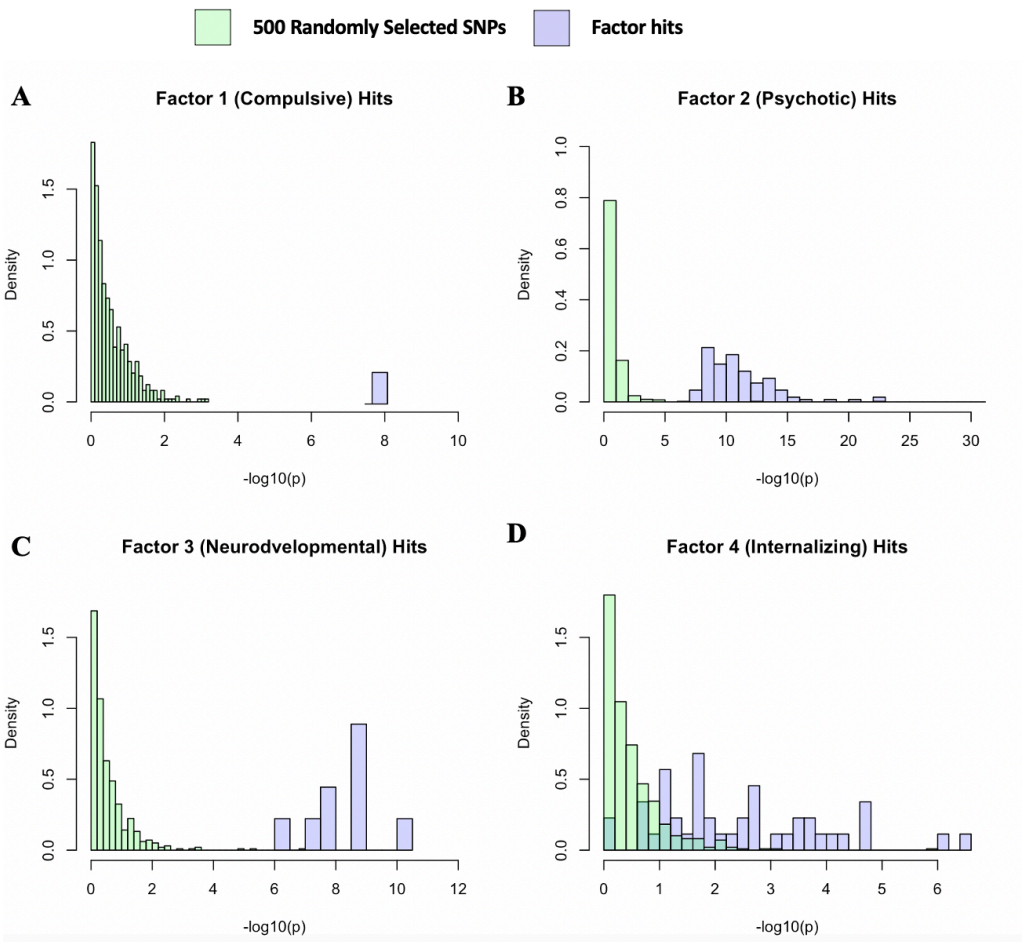

Supplementary Figure 2a. Histogram of Hits Excluding Self-report Cohorts. Panels depict the hits identified using the full dataset when analyzed using the restricted dataset for the Compulsive (panel A), Psychotic (panel B), Neurodevelopmental (panel C), and Internalizing disorders (panel D) factors. Blue bars depict the factor hits, while green bars depict 500 randomly selected SNPs. In all panels, there is clear signal maintained in the restricted dataset for the factor hits identified using the unrestricted datasets relative to the 500 randomly selected SNPs.

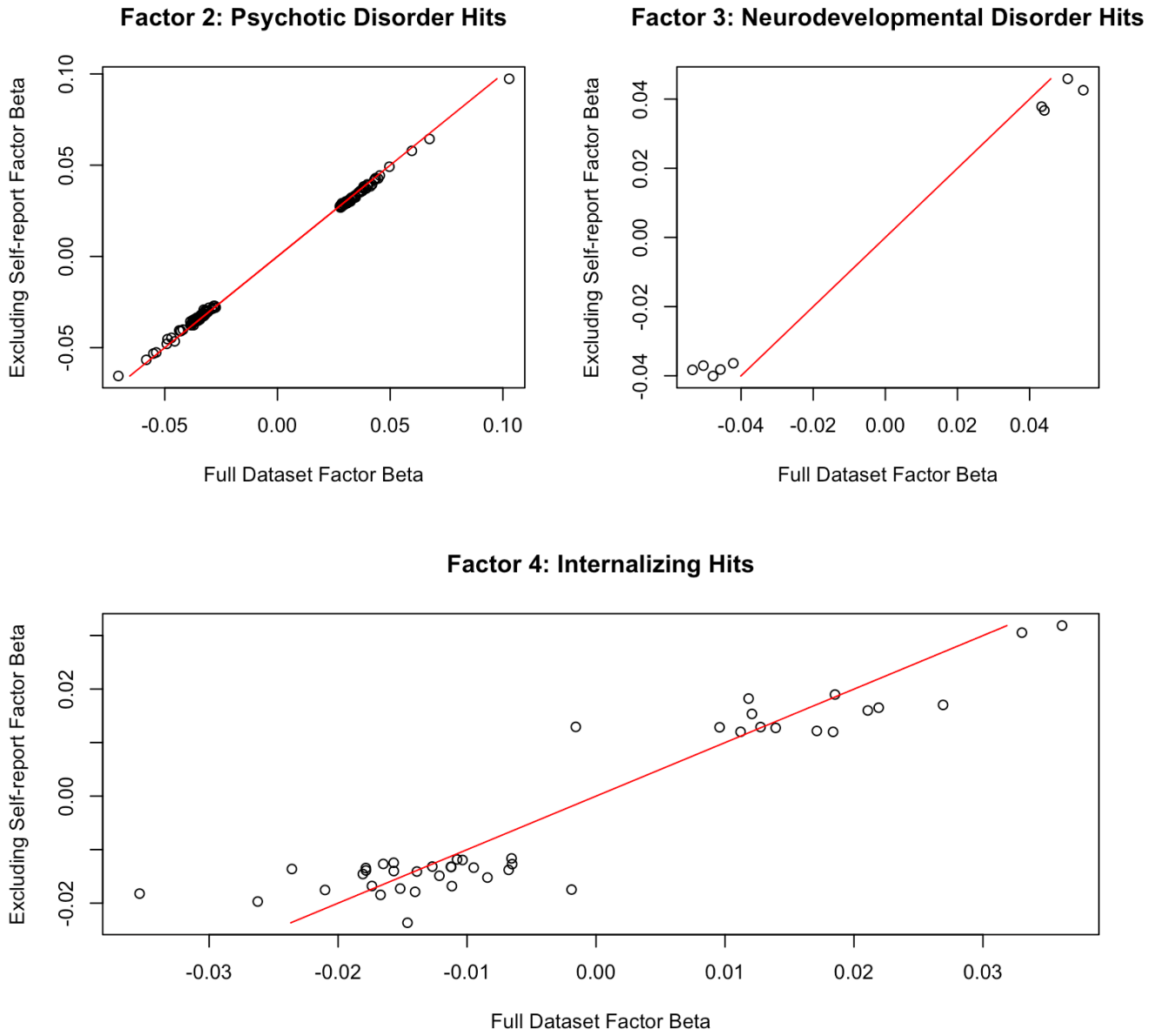

Supplementary Figure 2b. Scatterplot of Betas for Full and Restricted Dataset. Panels depict the hits identified using the full dataset for the estimated factor betas for the full dataset on the x-axis and the estimated factor betas for the datasets excluding self-report cohorts on the y-axis. Results are shown for the Psychotic (panel A), Neurodevelopmental (panel B), and Internalizing disorders (panel C) factors. Results are not depicted for the Compulsive disorders factor as there was only 1 hit identified for this factor. Red lines indicate the full dataset predicting itself, with values above the line estimated as larger in the full dataset. The scatterplots show strong concordance in estimated effects across the full and restricted dataset, with high correlations across the estimates for the full and restricted dataset for the Psychotic ($r > .99$), Neurodevelopmental ($r > .99$), and Internalizing disorders factors ($r = .94$).

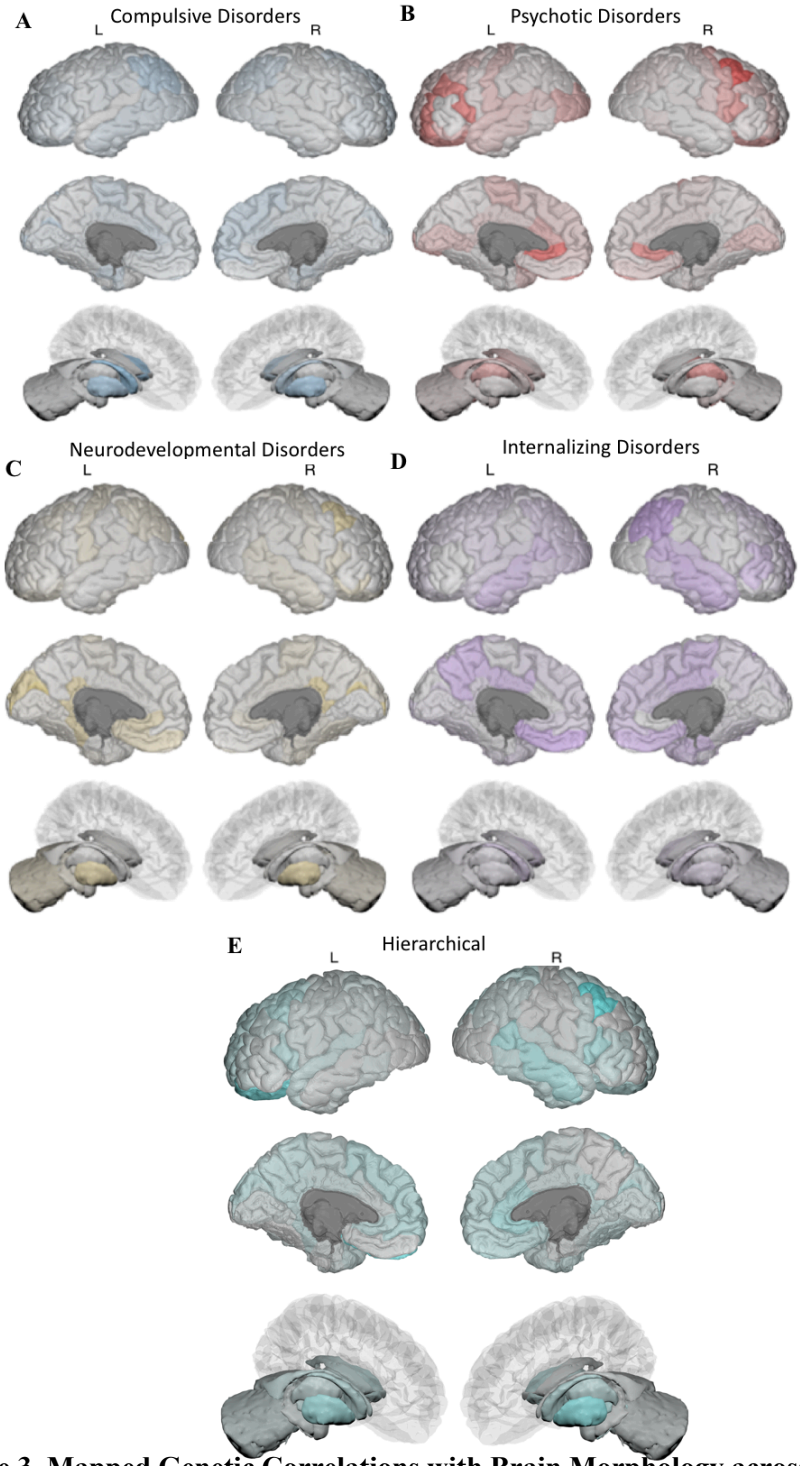

Supplementary Figure 3. Mapped Genetic Correlations with Brain Morphology across Psychiatric Factors. Panels depict the significance of genetic correlations between the psychiatric factors and brain volume for compulsive disorders (panel A), psychotic disorders (panel B), neurodevelopmental disorders (panel C), and the internalizing disorders (panel D) factor from the correlated factors model. Panel E depicts genetic correlations with the second-order, hierarchical p-factor. For all panels, darker shading indicates more significant effects. Cortical and sub-cortical regions of interest are plotted according to the Desikan-Killiany-Tourville atlas, shown on a single manually-edited surface.[48]

Supplementary Figure 4a. Genetic Correlations with Brain Morphology across Psychiatric Factors. Panels depict the genetic correlation point estimates in bar plots, with error bars depicting +/- 1.96 *SE*s, for associations with 9 of the 101 brain morphology metrics and the 11 psychiatric traits. The 11 psychiatric traits are grouped according to the correlated factor structure, with compulsive disorders depicted in light blue, psychotic disorders in red, neurodevelopmental disorders in golden yellow, and internalizing disorders in purple. For psychiatric traits that loaded on multiple latent factors (e.g., ALCH), the traits are colored to be grouped with the factor that they loaded on the strongest. Genetic correlations depicted with a dashed outline were significant at a Bonferroni corrected threshold for model comparisons indicating heterogeneity (i.e., significant Q_{Trait}) across the factor indicators in their genetic correlations with the brain morphology metric. The sample size for all brain morphology metrics was *N*= 19,629. The sample size for the psychiatric traits was: AN (*N*= 16,992 cases and 55,525 controls), OCD (*N*= 2,688 cases and 7,037 controls), TS (*N*= 4,819 cases and 9,488 controls), SCZ (*N*= 53,386 cases and 77,258 controls), BIP (*N*= 20,352 cases and 31,358 controls), ALCH (*N*= 176,024 observations), ADHD (*N*= 24,116 cases and 91,557 controls), AUT (*N*= 18,382 cases and 27,969 controls), PTSD (*N*= 12,255 cases and 26,338 controls), MDD (*N*= 249,227 cases and 553,712 controls), and ANX (*N*= 30,992 cases and 69,883 controls).

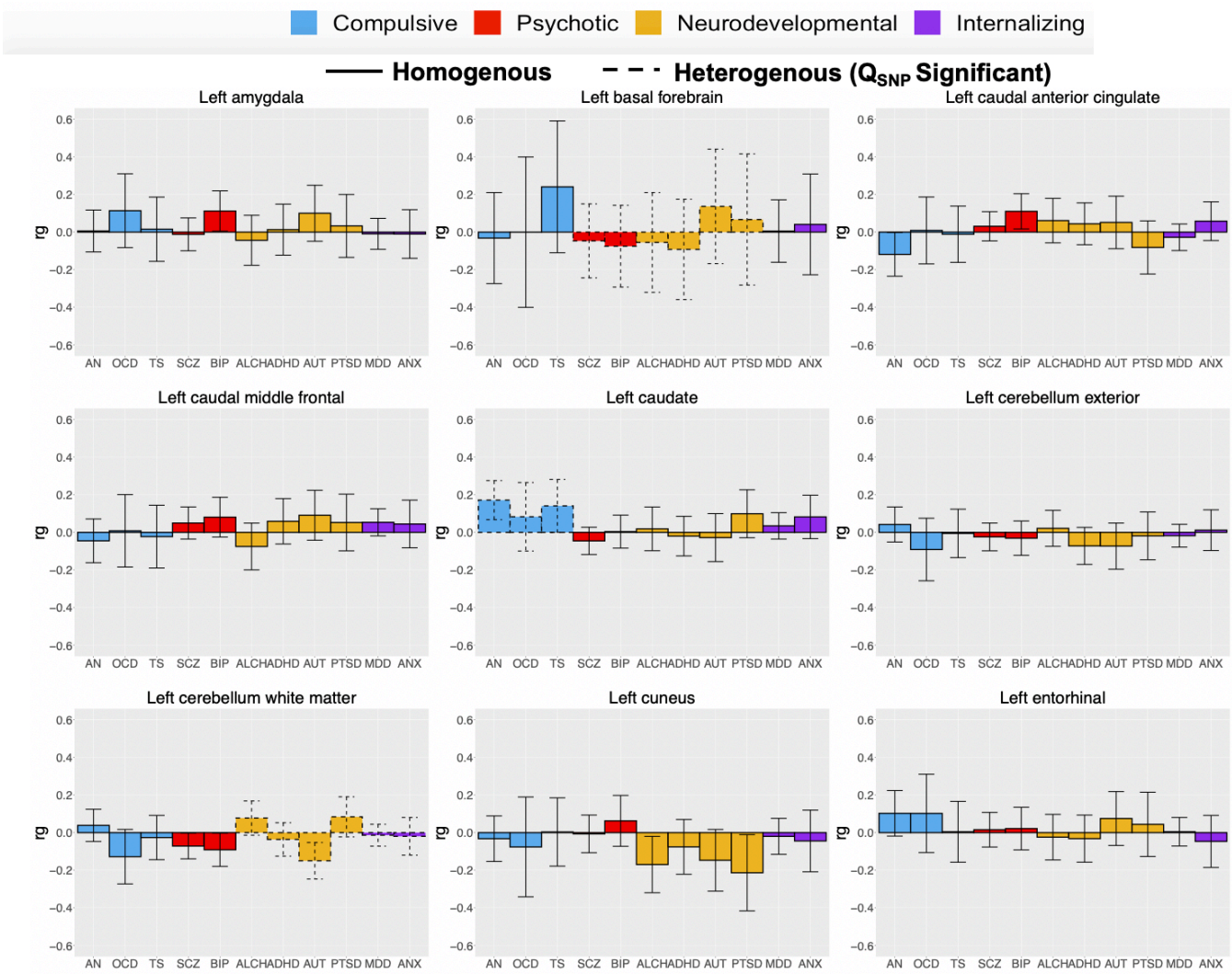

Supplementary Figure 4b. Genetic Correlations with Brain Morphology across Psychiatric Factors. Panels depict the genetic correlation point estimates in bar plots, with error bars depicting +/- 1.96 *SE*s, for associations with 9 of the 101 brain morphology metrics and the 11 psychiatric traits. The 11 psychiatric traits are grouped according to the correlated factor structure, with compulsive disorders depicted in light blue, psychotic disorders in red, neurodevelopmental disorders in golden yellow, and internalizing disorders in purple. For psychiatric traits that loaded on multiple latent factors (e.g., ALCH), the traits are colored to be grouped with the factor that they loaded on the strongest. Genetic correlations depicted with a dashed outline were significant at a Bonferroni corrected threshold for model comparisons indicating heterogeneity (i.e., significant Q_{Trait}) across the factor indicators in their genetic correlations with the brain morphology metric. The sample size for all brain morphology metrics was *N*= 19,629. The sample size for the psychiatric traits was: AN (*N*= 16,992 cases and 55,525 controls), OCD (*N*= 2,688 cases and 7,037 controls), TS (*N*= 4,819 cases and 9,488 controls), SCZ (*N*= 53,386 cases and 77,258 controls), BIP (*N*= 20,352 cases and 31,358 controls), ALCH (*N*= 176,024 observations), ADHD (*N*= 24,116 cases and 91,557 controls), AUT (*N*= 18,382 cases and 27,969 controls), PTSD (*N*= 12,255 cases and 26,338 controls), MDD (*N*= 249,227 cases and 553,712 controls), and ANX (*N*= 30,992 cases and 69,883 controls).

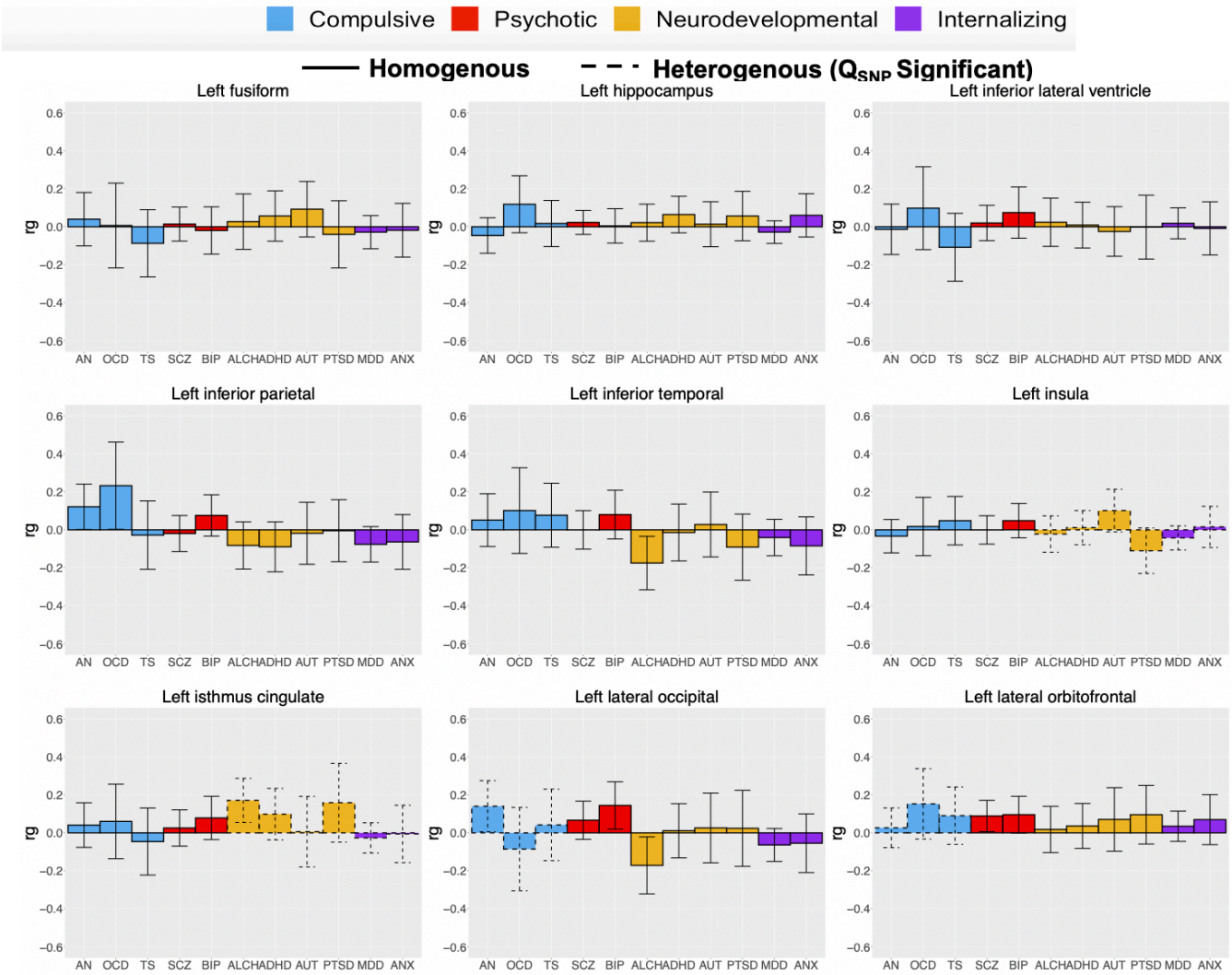

Supplementary Figure 4c. Genetic Correlations with Brain Morphology across Psychiatric Factors. Panels depict the genetic correlation point estimates in bar plots, with error bars depicting +/- 1.96 *SE*s, for associations with 9 of the 101 brain morphology metrics and the 11 psychiatric traits. The 11 psychiatric traits are grouped according to the correlated factor structure, with compulsive disorders depicted in light blue, psychotic disorders in red, neurodevelopmental disorders in golden yellow, and internalizing disorders in purple. For psychiatric traits that loaded on multiple latent factors (e.g., ALCH), the traits are colored to be grouped with the factor that they loaded on the strongest. Genetic correlations depicted with a dashed outline were significant at a Bonferroni corrected threshold for model comparisons indicating heterogeneity (i.e., significant Q_{Trait}) across the factor indicators in their genetic correlations with the brain morphology metric. The sample size for all brain morphology metrics was *N*= 19,629. The sample size for the psychiatric traits was: AN (*N*= 16,992 cases and 55,525 controls), OCD (*N*= 2,688 cases and 7,037 controls), TS (*N*= 4,819 cases and 9,488 controls), SCZ (*N*= 53,386 cases and 77,258 controls), BIP (*N*= 20,352 cases and 31,358 controls), ALCH (*N*= 176,024 observations), ADHD (*N*= 24,116 cases and 91,557 controls), AUT (*N*= 18,382 cases and 27,969 controls), PTSD (*N*= 12,255 cases and 26,338 controls), MDD (*N*= 249,227 cases and 553,712 controls), and ANX (*N*= 30,992 cases and 69,883 controls).

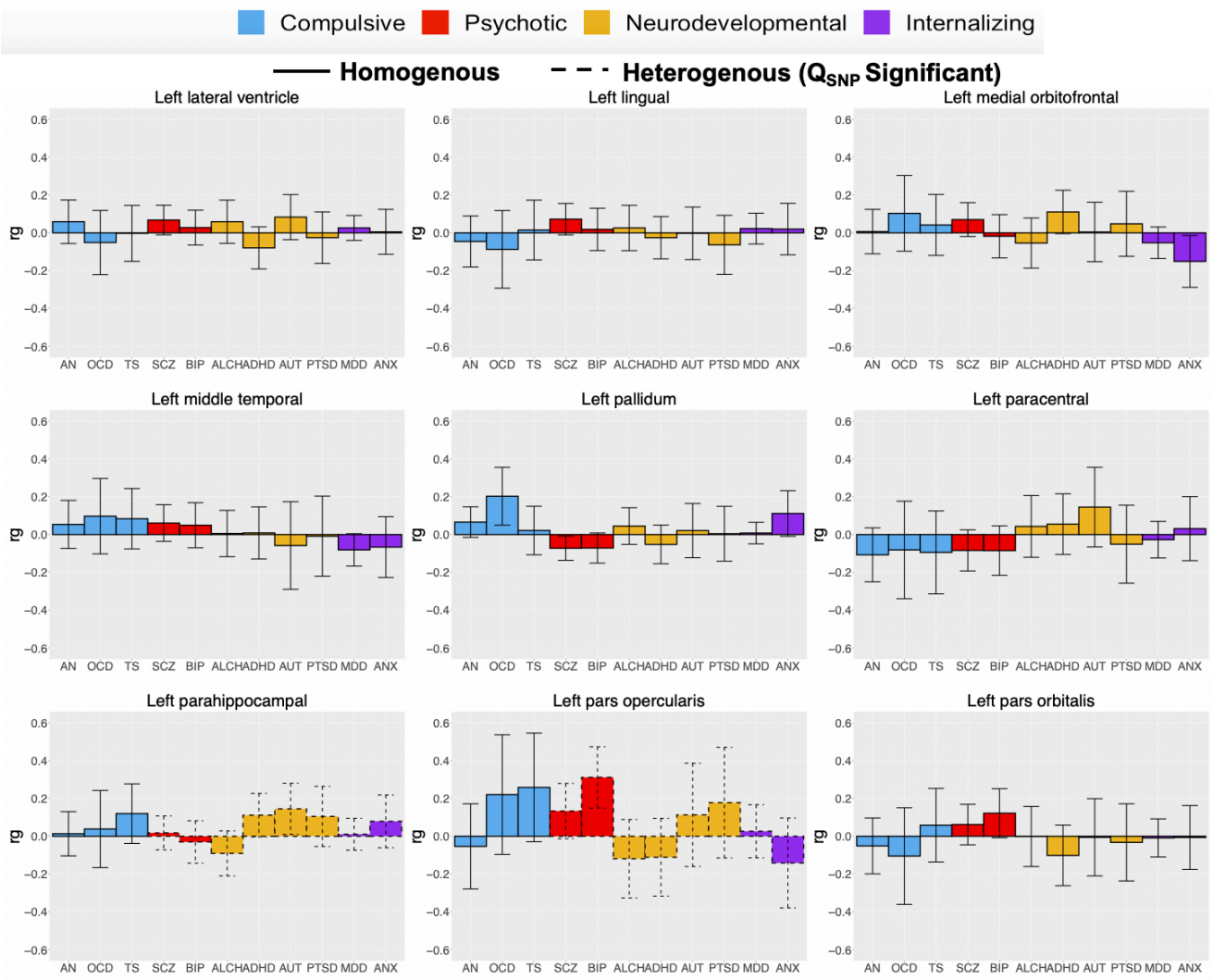

Supplementary Figure 4d. Genetic Correlations with Brain Morphology across Psychiatric Factors. Panels depict the genetic correlation point estimates in bar plots, with error bars depicting +/- 1.96 *SE*s, for associations with 9 of the 101 brain morphology metrics and the 11 psychiatric traits. The 11 psychiatric traits are grouped according to the correlated factor structure, with compulsive disorders depicted in light blue, psychotic disorders in red, neurodevelopmental disorders in golden yellow, and internalizing disorders in purple. For psychiatric traits that loaded on multiple latent factors (e.g., ALCH), the traits are colored to be grouped with the factor that they loaded on the strongest. Genetic correlations depicted with a dashed outline were significant at a Bonferroni corrected threshold for model comparisons indicating heterogeneity (i.e., significant Q_{Trait}) across the factor indicators in their genetic correlations with the brain morphology metric. The sample size for all brain morphology metrics was *N*= 19,629. The sample size for the psychiatric traits was: AN (*N*= 16,992 cases and 55,525 controls), OCD (*N*= 2,688 cases and 7,037 controls), TS (*N*= 4,819 cases and 9,488 controls), SCZ (*N*= 53,386 cases and 77,258 controls), BIP (*N*= 20,352 cases and 31,358 controls), ALCH (*N*= 176,024 observations), ADHD (*N*= 24,116 cases and 91,557 controls), AUT (*N*= 18,382 cases and 27,969 controls), PTSD (*N*= 12,255 cases and 26,338 controls), MDD (*N*= 249,227 cases and 553,712 controls), and ANX (*N*= 30,992 cases and 69,883 controls).

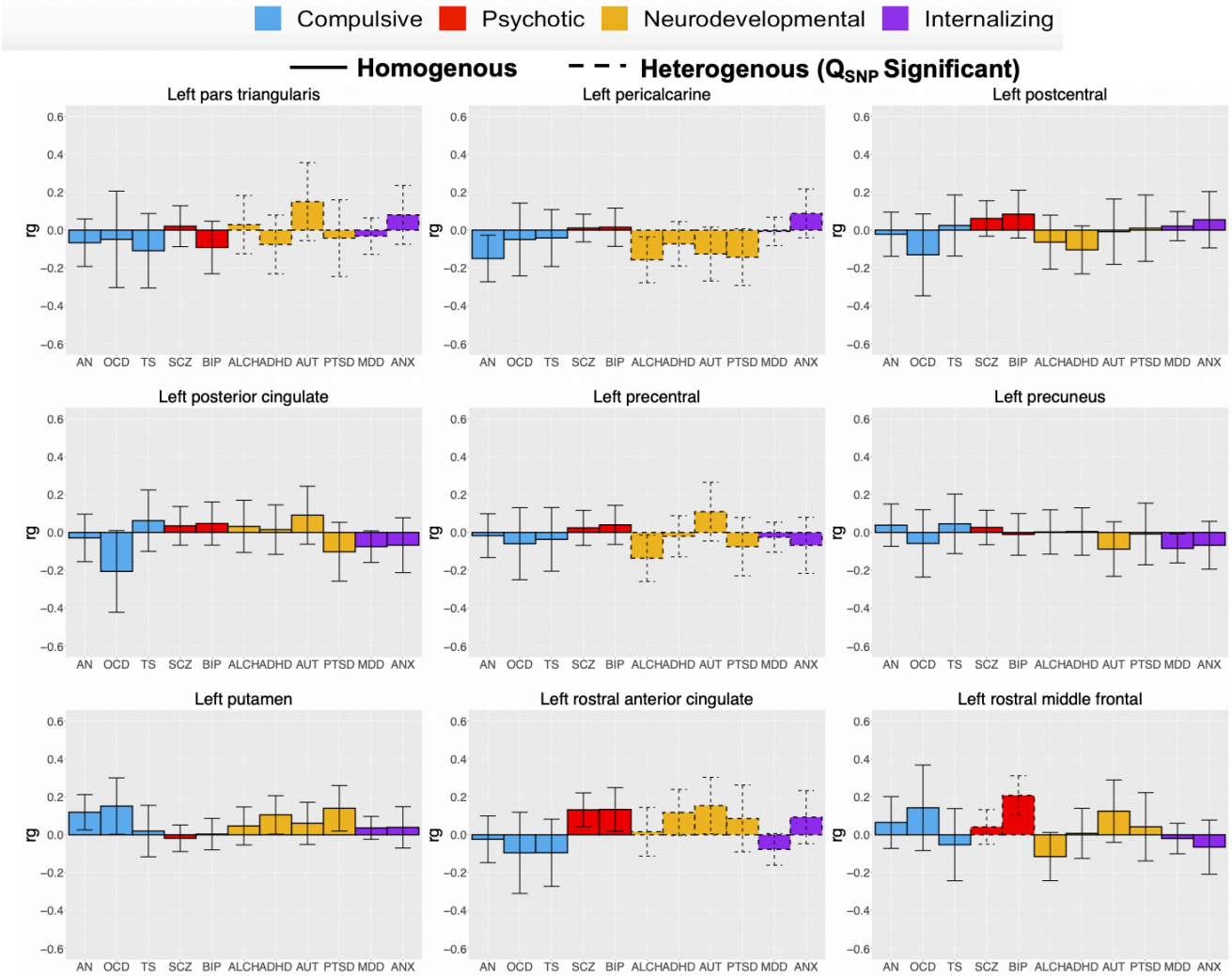

Supplementary Figure 4e. Genetic Correlations with Brain Morphology across Psychiatric Factors. Panels depict the genetic correlation point estimates in bar plots, with error bars depicting +/- 1.96 *SE*s, for associations with 9 of the 101 brain morphology metrics and the 11 psychiatric traits. The 11 psychiatric traits are grouped according to the correlated factor structure, with compulsive disorders depicted in light blue, psychotic disorders in red, neurodevelopmental disorders in golden yellow, and internalizing disorders in purple. For psychiatric traits that loaded on multiple latent factors (e.g., ALCH), the traits are colored to be grouped with the factor that they loaded on the strongest. Genetic correlations depicted with a dashed outline were significant at a Bonferroni corrected threshold for model comparisons indicating heterogeneity (i.e., significant Q_{Trait}) across the factor indicators in their genetic correlations with the brain morphology metric. The sample size for all brain morphology metrics was *N*= 19,629. The sample size for the psychiatric traits was: AN (*N*= 16,992 cases and 55,525 controls), OCD (*N*= 2,688 cases and 7,037 controls), TS (*N*= 4,819 cases and 9,488 controls), SCZ (*N*= 53,386 cases and 77,258 controls), BIP (*N*= 20,352 cases and 31,358 controls), ALCH (*N*= 176,024 observations), ADHD (*N*= 24,116 cases and 91,557 controls), AUT (*N*= 18,382 cases and 27,969 controls), PTSD (*N*= 12,255 cases and 26,338 controls), MDD (*N*= 249,227 cases and 553,712 controls), and ANX (*N*= 30,992 cases and 69,883 controls).

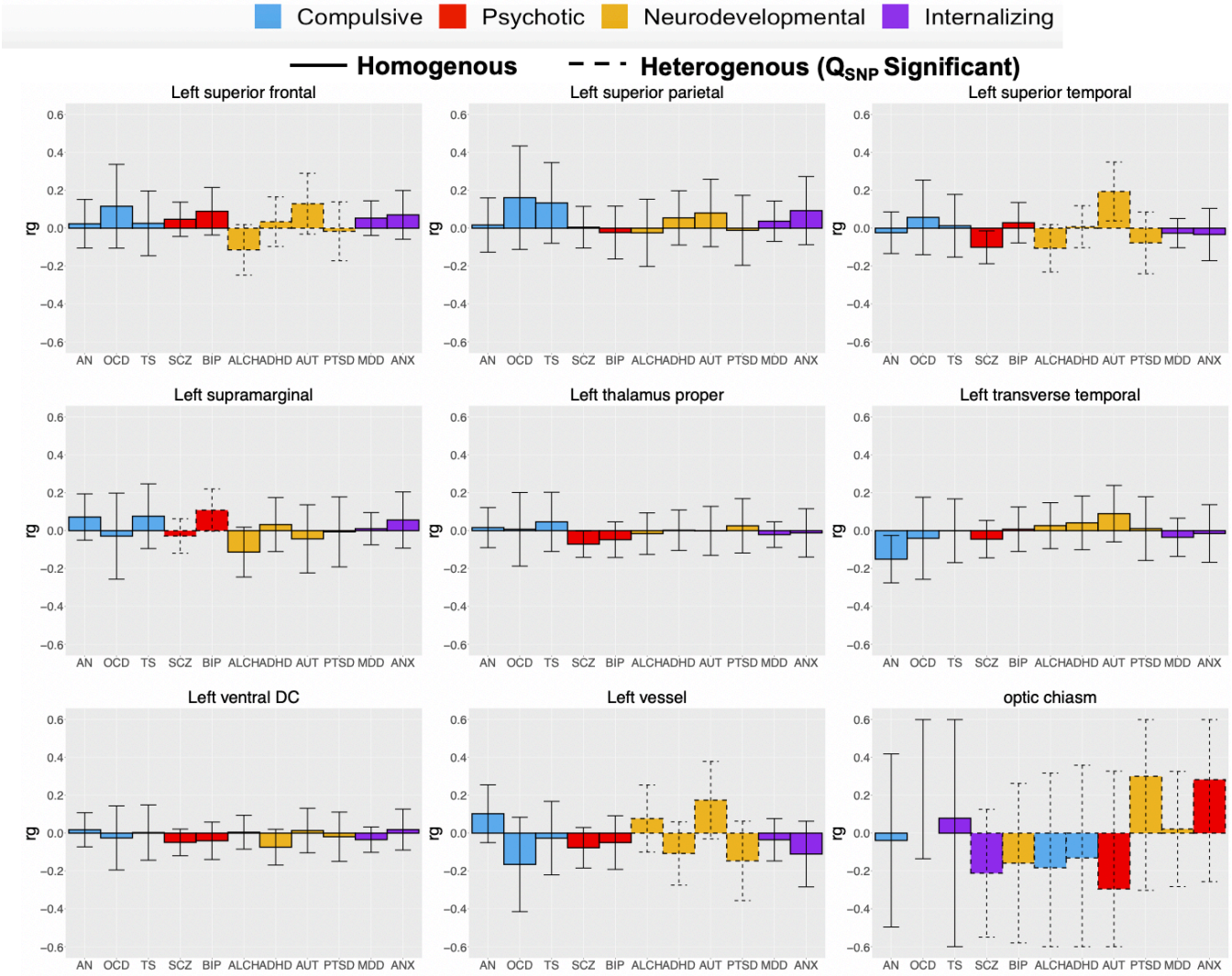

Supplementary Figure 4f. Genetic Correlations with Brain Morphology across Psychiatric Factors. Panels depict the genetic correlation point estimates in bar plots, with error bars depicting +/- 1.96 *SE*s, for associations with 9 of the 101 brain morphology metrics and the 11 psychiatric traits. The 11 psychiatric traits are grouped according to the correlated factor structure, with compulsive disorders depicted in light blue, psychotic disorders in red, neurodevelopmental disorders in golden yellow, and internalizing disorders in purple. For psychiatric traits that loaded on multiple latent factors (e.g., ALCH), the traits are colored to be grouped with the factor that they loaded on the strongest. Genetic correlations depicted with a dashed outline were significant at a Bonferroni corrected threshold for model comparisons indicating heterogeneity (i.e., significant Q_{Trait}) across the factor indicators in their genetic correlations with the brain morphology metric. The sample size for all brain morphology metrics was *N*= 19,629. The sample size for the psychiatric traits was: AN (*N*= 16,992 cases and 55,525 controls), OCD (*N*= 2,688 cases and 7,037 controls), TS (*N*= 4,819 cases and 9,488 controls), SCZ (*N*= 53,386 cases and 77,258 controls), BIP (*N*= 20,352 cases and 31,358 controls), ALCH (*N*= 176,024 observations), ADHD (*N*= 24,116 cases and 91,557 controls), AUT (*N*= 18,382 cases and 27,969 controls), PTSD (*N*= 12,255 cases and 26,338 controls), MDD (*N*= 249,227 cases and 553,712 controls), and ANX (*N*= 30,992 cases and 69,883 controls).

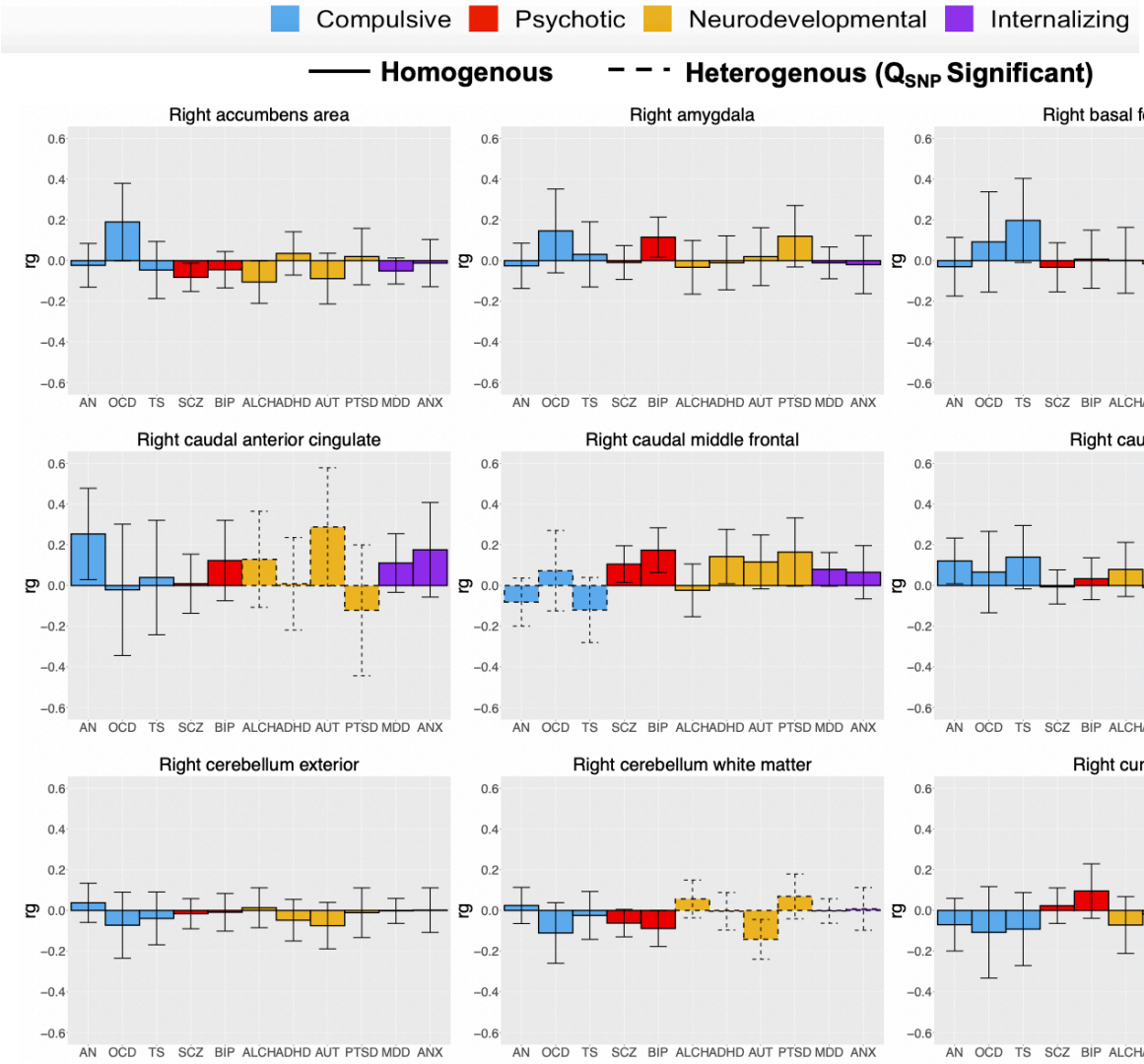

Supplementary Figure 4g. Genetic Correlations with Brain Morphology across Psychiatric Factors. Panels depict the genetic correlation point estimates in bar plots, with error bars depicting +/- 1.96 *SE*s, for associations with 9 of the 101 brain morphology metrics and the 11 psychiatric traits. The 11 psychiatric traits are grouped according to the correlated factor structure, with compulsive disorders depicted in light blue, psychotic disorders in red, neurodevelopmental disorders in golden yellow, and internalizing disorders in purple. For psychiatric traits that loaded on multiple latent factors (e.g., ALCH), the traits are colored to be grouped with the factor that they loaded on the strongest. Genetic correlations depicted with a dashed outline were significant at a Bonferroni corrected threshold for model comparisons indicating heterogeneity (i.e., significant Q_{Trait}) across the factor indicators in their genetic correlations with the brain morphology metric. The sample size for all brain morphology metrics was *N*= 19,629. The sample size for the psychiatric traits was: AN (*N*= 16,992 cases and 55,525 controls), OCD (*N*= 2,688 cases and 7,037 controls), TS (*N*= 4,819 cases and 9,488 controls), SCZ (*N*= 53,386 cases and 77,258 controls), BIP (*N*= 20,352 cases and 31,358 controls), ALCH (*N*= 176,024 observations), ADHD (*N*= 24,116 cases and 91,557 controls), AUT (*N*= 18,382 cases and 27,969 controls), PTSD (*N*= 12,255 cases and 26,338 controls), MDD (*N*= 249,227 cases and 553,712 controls), and ANX (*N*= 30,992 cases and 69,883 controls).

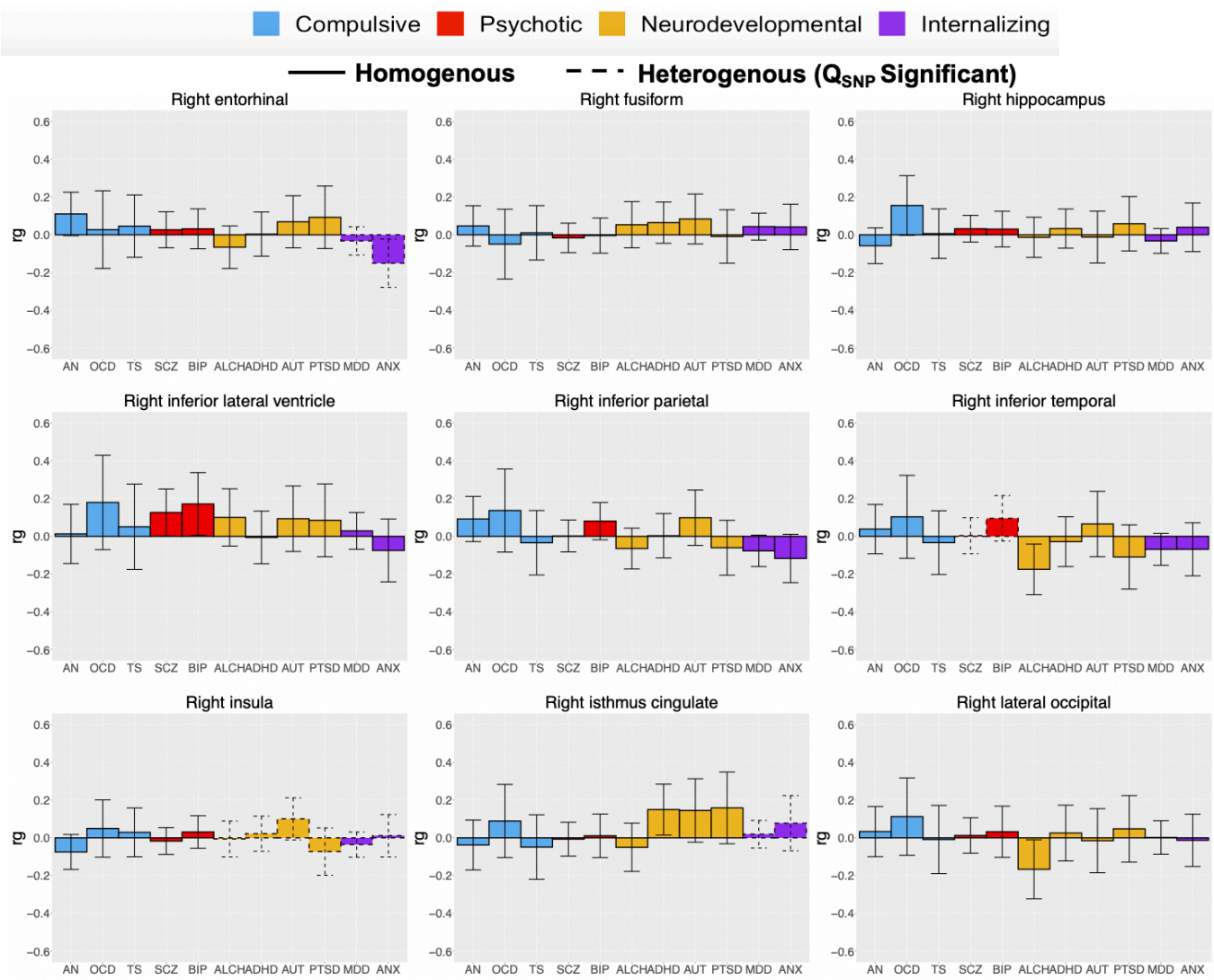

Supplementary Figure 4h. Genetic Correlations with Brain Morphology across Psychiatric Factors. Panels depict the genetic correlation point estimates in bar plots, with error bars depicting +/- 1.96 *SE*s, for associations with 9 of the 101 brain morphology metrics and the 11 psychiatric traits. The 11 psychiatric traits are grouped according to the correlated factor structure, with compulsive disorders depicted in light blue, psychotic disorders in red, neurodevelopmental disorders in golden yellow, and internalizing disorders in purple. For psychiatric traits that loaded on multiple latent factors (e.g., ALCH), the traits are colored to be grouped with the factor that they loaded on the strongest. Genetic correlations depicted with a dashed outline were significant at a Bonferroni corrected threshold for model comparisons indicating heterogeneity (i.e., significant Q_{Trait}) across the factor indicators in their genetic correlations with the brain morphology metric. The sample size for all brain morphology metrics was *N*= 19,629. The sample size for the psychiatric traits was: AN (*N*= 16,992 cases and 55,525 controls), OCD (*N*= 2,688 cases and 7,037 controls), TS (*N*= 4,819 cases and 9,488 controls), SCZ (*N*= 53,386 cases and 77,258 controls), BIP (*N*= 20,352 cases and 31,358 controls), ALCH (*N*= 176,024 observations), ADHD (*N*= 24,116 cases and 91,557 controls), AUT (*N*= 18,382 cases and 27,969 controls), PTSD (*N*= 12,255 cases and 26,338 controls), MDD (*N*= 249,227 cases and 553,712 controls), and ANX (*N*= 30,992 cases and 69,883 controls).

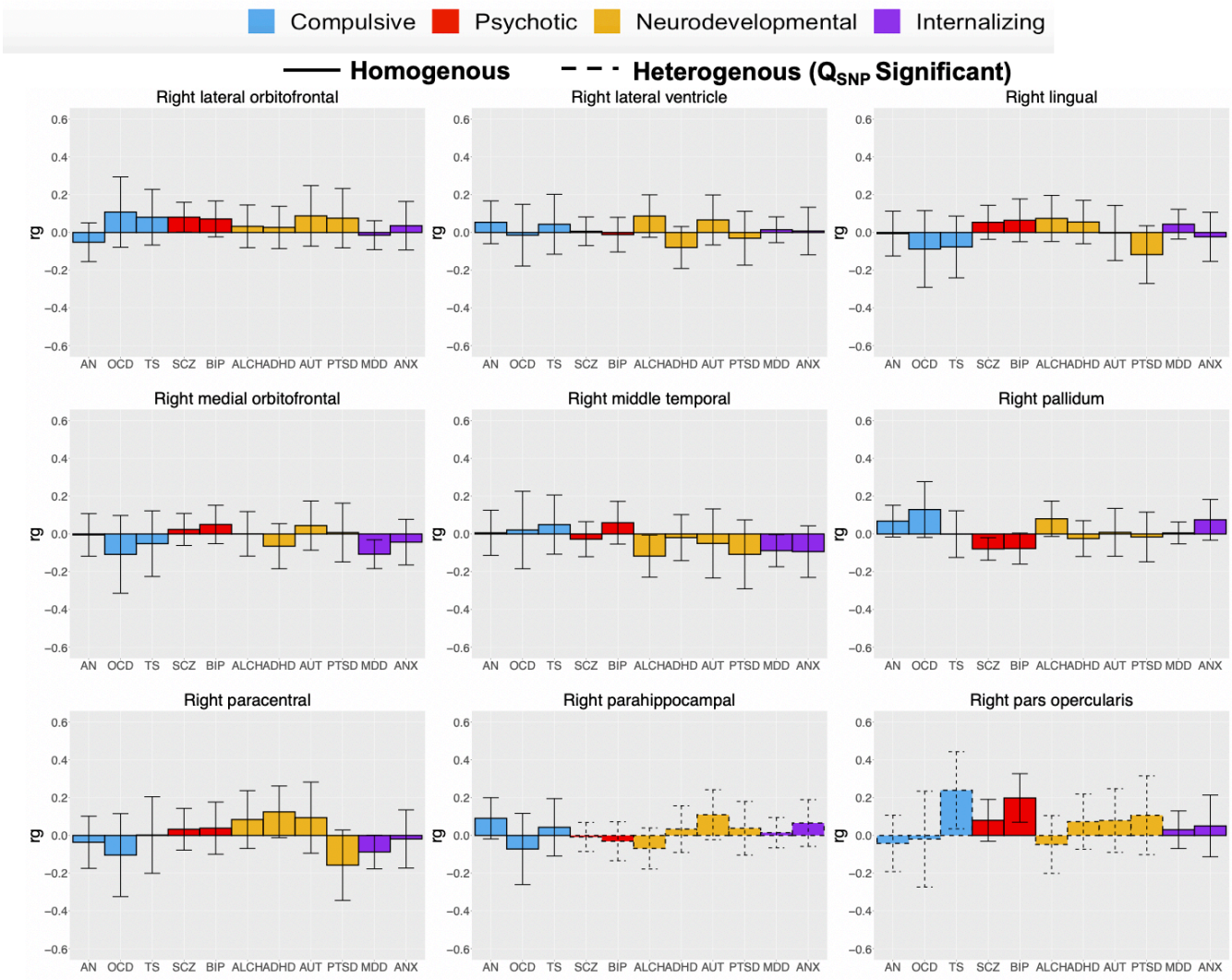

Supplementary Figure 4i. Genetic Correlations with Brain Morphology across Psychiatric Factors. Panels depict the genetic correlation point estimates in bar plots, with error bars depicting +/- 1.96 *SE*s, for associations with 9 of the 101 brain morphology metrics and the 11 psychiatric traits. The 11 psychiatric traits are grouped according to the correlated factor structure, with compulsive disorders depicted in light blue, psychotic disorders in red, neurodevelopmental disorders in golden yellow, and internalizing disorders in purple. For psychiatric traits that loaded on multiple latent factors (e.g., ALCH), the traits are colored to be grouped with the factor that they loaded on the strongest. Genetic correlations depicted with a dashed outline were significant at a Bonferroni corrected threshold for model comparisons indicating heterogeneity (i.e., significant Q_{Trait}) across the factor indicators in their genetic correlations with the brain morphology metric. The sample size for all brain morphology metrics was *N*= 19,629. The sample size for the psychiatric traits was: AN (*N*= 16,992 cases and 55,525 controls), OCD (*N*= 2,688 cases and 7,037 controls), TS (*N*= 4,819 cases and 9,488 controls), SCZ (*N*= 53,386 cases and 77,258 controls), BIP (*N*= 20,352 cases and 31,358 controls), ALCH (*N*= 176,024 observations), ADHD (*N*= 24,116 cases and 91,557 controls), AUT (*N*= 18,382 cases and 27,969 controls), PTSD (*N*= 12,255 cases and 26,338 controls), MDD (*N*= 249,227 cases and 553,712 controls), and ANX (*N*= 30,992 cases and 69,883 controls).

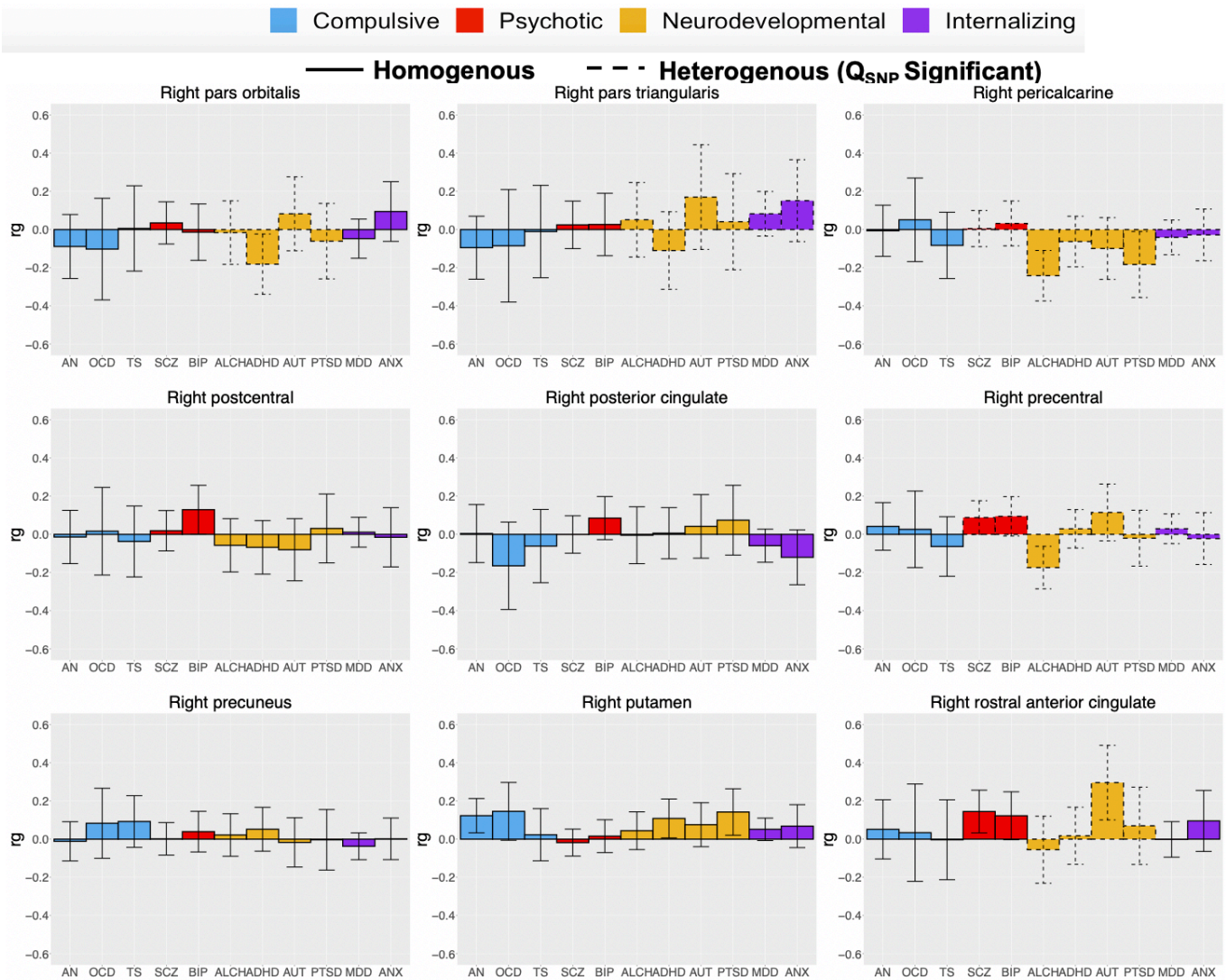

Supplementary Figure 4j. Genetic Correlations with Brain Morphology across Psychiatric Factors. Panels depict the genetic correlation point estimates in bar plots, with error bars depicting +/- 1.96 *SE*s, for associations with 9 of the 101 brain morphology metrics and the 11 psychiatric traits. The 11 psychiatric traits are grouped according to the correlated factor structure, with compulsive disorders depicted in light blue, psychotic disorders in red, neurodevelopmental disorders in golden yellow, and internalizing disorders in purple. For psychiatric traits that loaded on multiple latent factors (e.g., ALCH), the traits are colored to be grouped with the factor that they loaded on the strongest. Genetic correlations depicted with a dashed outline were significant at a Bonferroni corrected threshold for model comparisons indicating heterogeneity (i.e., significant Q_{Trait}) across the factor indicators in their genetic correlations with the brain morphology metric. The sample size for all brain morphology metrics was *N*= 19,629. The sample size for the psychiatric traits was: AN (*N*= 16,992 cases and 55,525 controls), OCD (*N*= 2,688 cases and 7,037 controls), TS (*N*= 4,819 cases and 9,488 controls), SCZ (*N*= 53,386 cases and 77,258 controls), BIP (*N*= 20,352 cases and 31,358 controls), ALCH (*N*= 176,024 observations), ADHD (*N*= 24,116 cases and 91,557 controls), AUT (*N*= 18,382 cases and 27,969 controls), PTSD (*N*= 12,255 cases and 26,338 controls), MDD (*N*= 249,227 cases and 553,712 controls), and ANX (*N*= 30,992 cases and 69,883 controls).

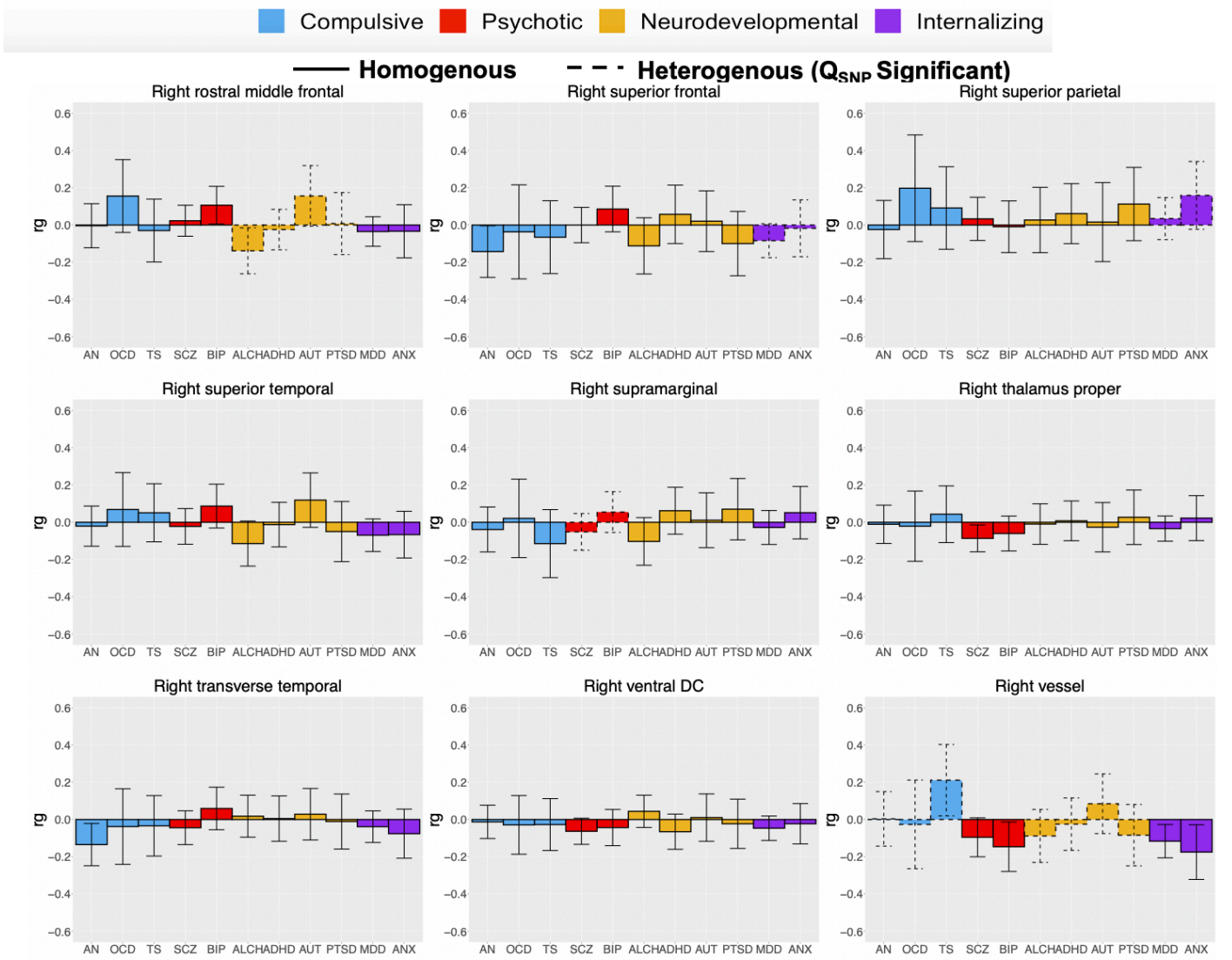

Supplementary Figure 4k. Genetic Correlations with Brain Morphology across Psychiatric Factors. Panels depict the genetic correlation point estimates in bar plots, with error bars depicting +/- 1.96 *SE*s, for associations with 9 of the 101 brain morphology metrics and the 11 psychiatric traits. The 11 psychiatric traits are grouped according to the correlated factor structure, with compulsive disorders depicted in light blue, psychotic disorders in red, neurodevelopmental disorders in golden yellow, and internalizing disorders in purple. For psychiatric traits that loaded on multiple latent factors (e.g., ALCH), the traits are colored to be grouped with the factor that they loaded on the strongest. Genetic correlations depicted with a dashed outline were significant at a Bonferroni corrected threshold for model comparisons indicating heterogeneity (i.e., significant Q_{Trait}) across the factor indicators in their genetic correlations with the brain morphology metric. The sample size for all brain morphology metrics was *N*= 19,629. The sample size for the psychiatric traits was: AN (*N*= 16,992 cases and 55,525 controls), OCD (*N*= 2,688 cases and 7,037 controls), TS (*N*= 4,819 cases and 9,488 controls), SCZ (*N*= 53,386 cases and 77,258 controls), BIP (*N*= 20,352 cases and 31,358 controls), ALCH (*N*= 176,024 observations), ADHD (*N*= 24,116 cases and 91,557 controls), AUT (*N*= 18,382 cases and 27,969 controls), PTSD (*N*= 12,255 cases and 26,338 controls), MDD (*N*= 249,227 cases and 553,712 controls), and ANX (*N*= 30,992 cases and 69,883 controls).

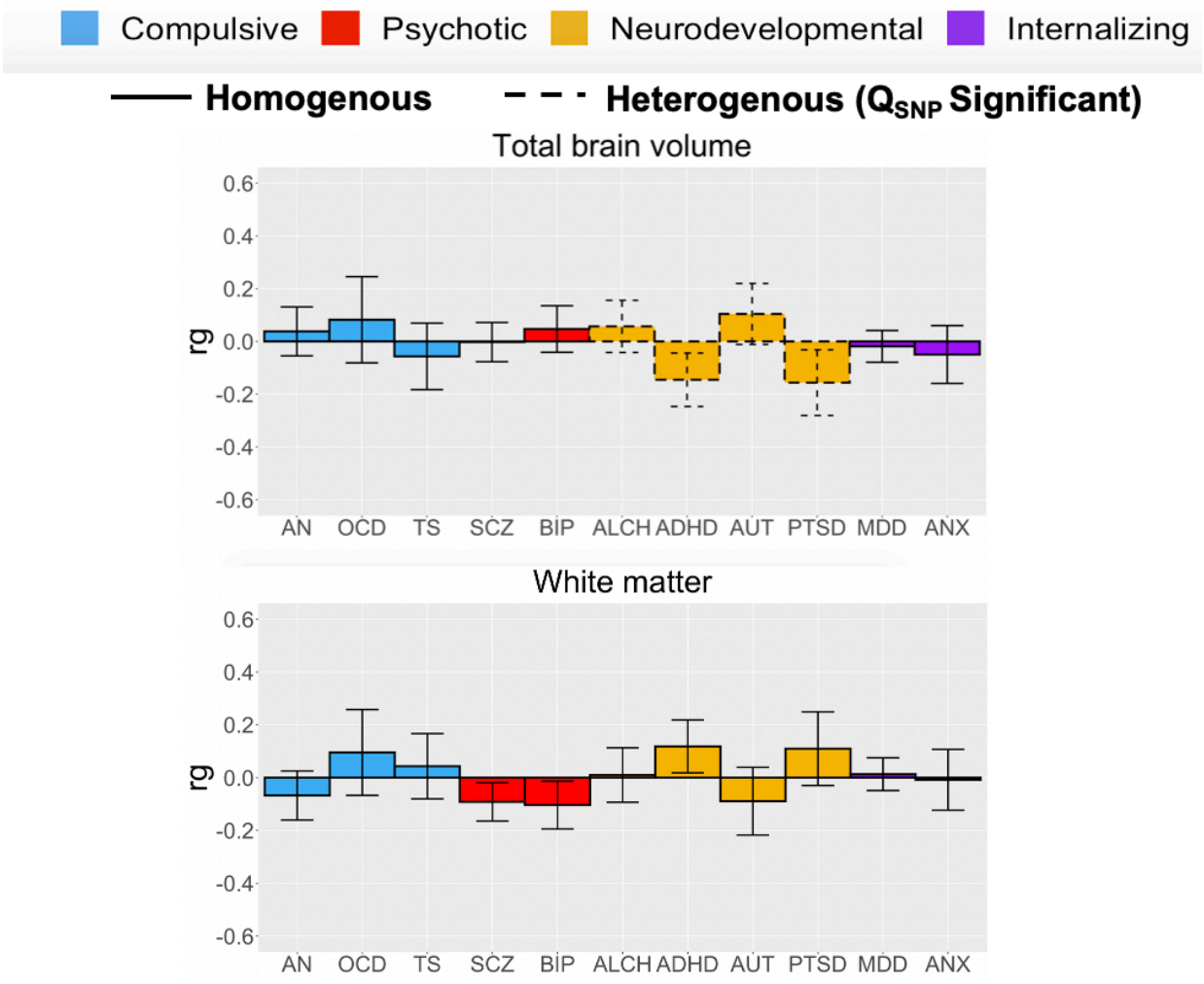

Supplementary Figure 4l. Genetic Correlations with Brain Morphology across Psychiatric Factors. Panels depict the genetic correlation point estimates in bar plots, with error bars depicting +/- 1.96 *SE*s, for associations with 2 of the 101 brain morphology metrics and the 11 psychiatric traits. The 11 psychiatric traits are grouped according to the correlated factor structure, with compulsive disorders depicted in light blue, psychotic disorders in red, neurodevelopmental disorders in golden yellow, and internalizing disorders in purple. For psychiatric traits that loaded on multiple latent factors (e.g., ALCH), the traits are colored to be grouped with the factor that they loaded on the strongest. Genetic correlations depicted with a dashed outline were significant at a Bonferroni corrected threshold for model comparisons indicating heterogeneity (i.e., significant Q_{Trait}) across the factor indicators in their genetic correlations with the brain morphology metric. The sample size for all brain morphology metrics was *N*= 19,629. The sample size for the psychiatric traits was: AN (*N*= 16,992 cases and 55,525 controls), OCD (*N*= 2,688 cases and 7,037 controls), TS (*N*= 4,819 cases and 9,488 controls), SCZ (*N*= 53,386 cases and 77,258 controls), BIP (*N*= 20,352 cases and 31,358 controls), ALCH (*N*= 176,024 observations), ADHD (*N*= 24,116 cases and 91,557 controls), AUT (*N*= 18,382 cases and 27,969 controls), PTSD (*N*= 12,255 cases and 26,338 controls), MDD (*N*= 249,227 cases and 553,712 controls), and ANX (*N*= 30,992 cases and 69,883 controls).

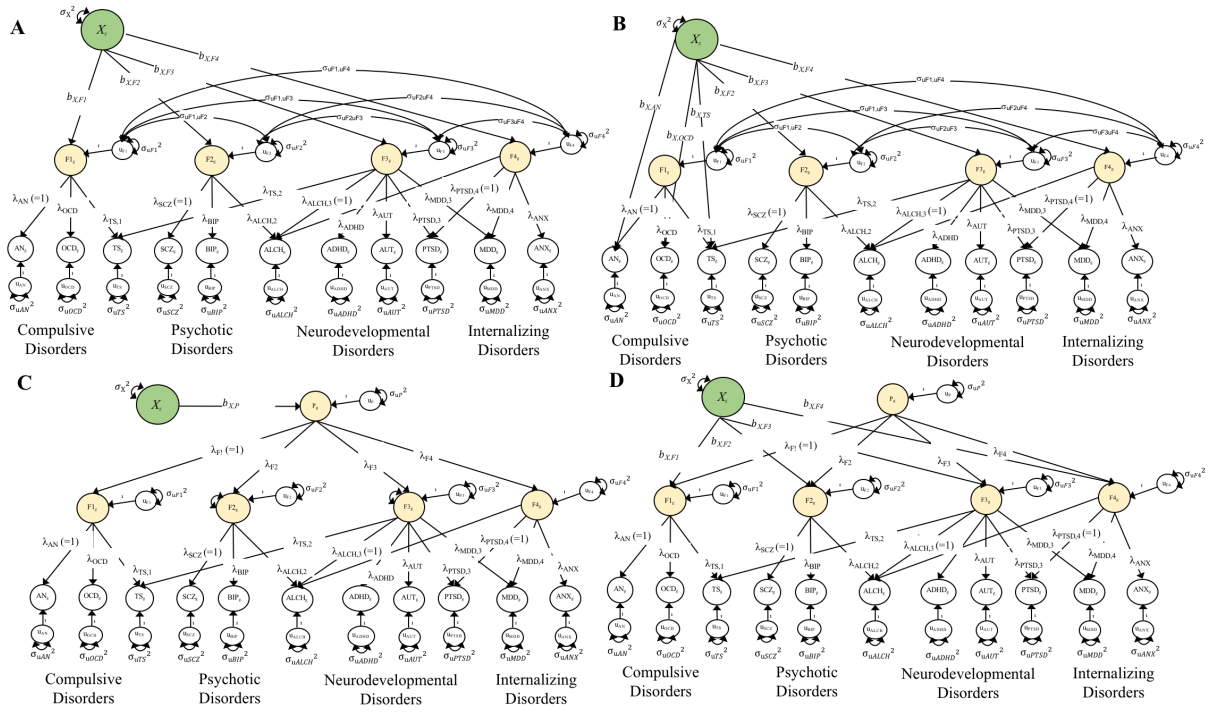

Supplementary Figure 5. Model Comparisons for Biobehavioral Traits used to produce Q_{Trait}. Panel A depicts the model run to obtain a model χ^2 for a model in which the biobevioral trait (X) predicted all four, correlated psychiatric factors. Panel B depicts the follow-up model for the compulsive disorders factor, where trait X predicts the indicators of the compulsive disorders factor, in addition to the remaing three factors. Model χ^2 difference tests between the model χ^2 for the model in panel A and model χ^2 in panel B index whether the pattern of correlations with trait X is well-accounted for by the factor. We term this heterogeneity index at the level of external correlates Q_{trait}. In order to produce model χ^2 difference tests for each factor, the model in Panel B was re-specified three additional times, such that trait X predicted the factor indicators for the remaining three factors. Panel C depicts the model run to obtain model χ^2 for the hierarchical factor model. Panel D depicts the follow-up model in which the trait directly predicts the four, first-order factors. As with the top two panels, comparing the model χ^2 across panels C and D indexes whether the pattern of correlations with trait X across the four, first-order factors is well-accounted for by the second-order, *p*-factor.

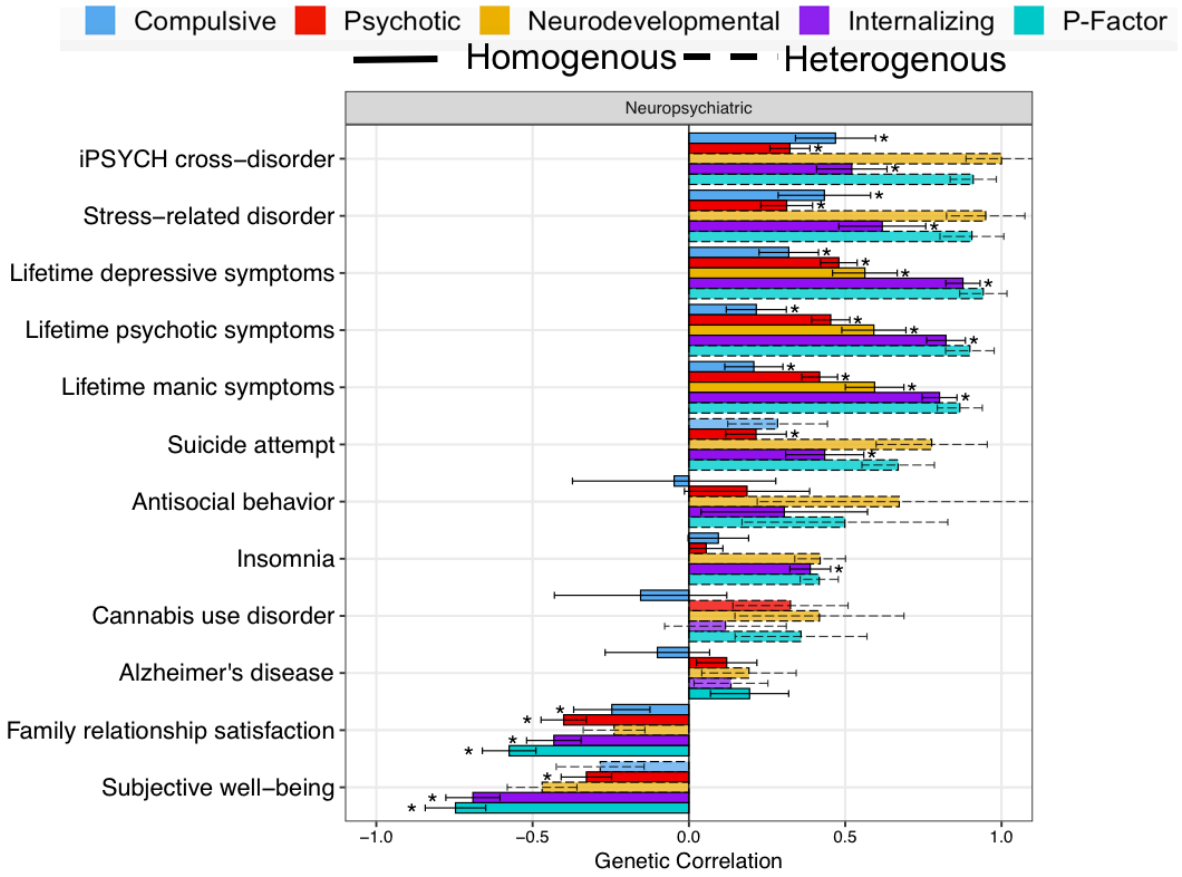

Supplementary Figure 6. Genetic Correlations with Neuropsychiatric Traits across Psychiatric Factors. Bar plots depict point estimates for genetic correlations with the 11 neuropscyhiatric complex traits with error bars depicted +/- 1.96 *SE*s. Correlations with the complex traits are depicted for each of the four psychiatric factors from the correlated factors model or the second-order, *p*-factor from the hierarchical model. Bars depicted with a dashed outline were significant at a Bonferroni corrected threshold for model comparisons indicating heterogeneity (i.e., significant Q_{Trait}) across the factor indicators in their genetic correlations with the outside trait. Bars depicted with an * above produced a genetic correlation that was significant at a Bonferroni corrected threshold and were not significantly heterogeneous. The total sample sizes were: iPSYCH cross-disorder (*N*= 65,534), stress-related disorder (*N*= 29,056), lifetime depressive symptoms (*N*= 126,494), lifetime psychotic symptoms (*N*= 126,494), lifetime manic symptoms (*N*= 126,494), suicide attempt (*N*= 50,265), antisocial behavior (*N*= 16,400), insomnia (*N*= 386,533), cannabis use disordeor (*N*= 357,806), Alzheimer's disease (*N*= 17,375), family relationship satisfcation (*N*= 361,194), and subjective well-being (*N*= 204,966). The effective sample size for the factors was: Compulsive Factor (*N*= 19,108), Psychotic Factor (*N*= 87,138), Neurodevelpomental Factor (*N*= 55,932), Internalizing Factor (*N*= 455,340), and hierarchical *p*-factor (*N*= 667,343).

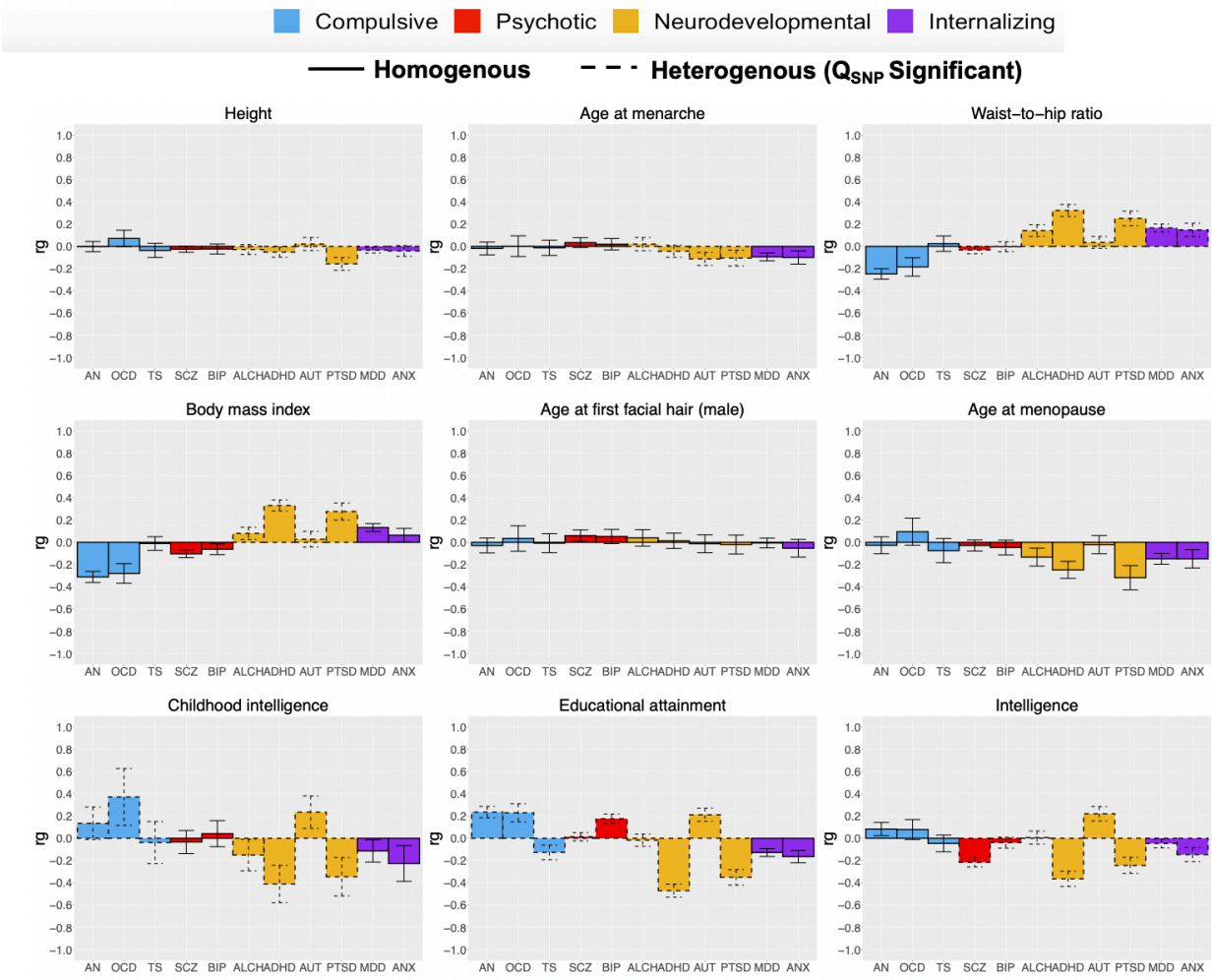

Supplementary Figure 7a. Genetic Correlations with Complex Traits across Psychiatric Factors. Panels depict the genetic correlation point estimates in bar plots, with error bars depicting +/- 1.96 *SE*s, for associations with 9 of the 49 biobehavioral complex traits and the 11 psychiatric traits. The 11 psychiatric traits are grouped according to the correlated factor structure, with compulsive disorders depicted in light blue, psychotic disorders in red, neurodevelopmental disorders in golden yellow, and internalizing disorders in purple. For traits that loaded on multiple factors (e.g., ALCH), they are colored to be grouped with the factor that they loaded on the strongest. Genetic correlations depicted with a dashed outline were significant at a Bonferroni corrected threshold for model comparisons indicating heterogeneity (i.e., significant Q_{Trait}) across the factor indicators in their genetic correlations with the outside trait. The total sample size for the complex traits was: Height (*N*= 709,703), age at menarche (*N*= 194,174), waist-to-hip ratio (*N*= 697,729), body mass index (*N*= 806,833), age at first facial hair (*N*= 167,020), age at menopause (*N*= 194,174), childhood intelligence (*N*= 12,441), educational attainment (*N*= 22,572), and inttelligence (*N*= 269,867). The sample size for the psychiatric traits was: AN (*N*= 16,992 cases and 55,525 controls), OCD (*N*= 2,688 cases and 7,037 controls), TS (*N*= 4,819 cases and 9,488 controls), SCZ (*N*= 53,386 cases and 77,258 controls), BIP (*N*= 20,352 cases and 31,358 controls), ALCH (*N*= 176,024 observations), ADHD (*N*= 24,116 cases and 91,557 controls), AUT (*N*= 18,382 cases and 27,969 controls), PTSD (*N*= 12,255 cases and 26,338 controls), MDD (*N*= 249,227 cases and 553,712 controls), and ANX (*N*= 30,992 cases and 69,883 controls).

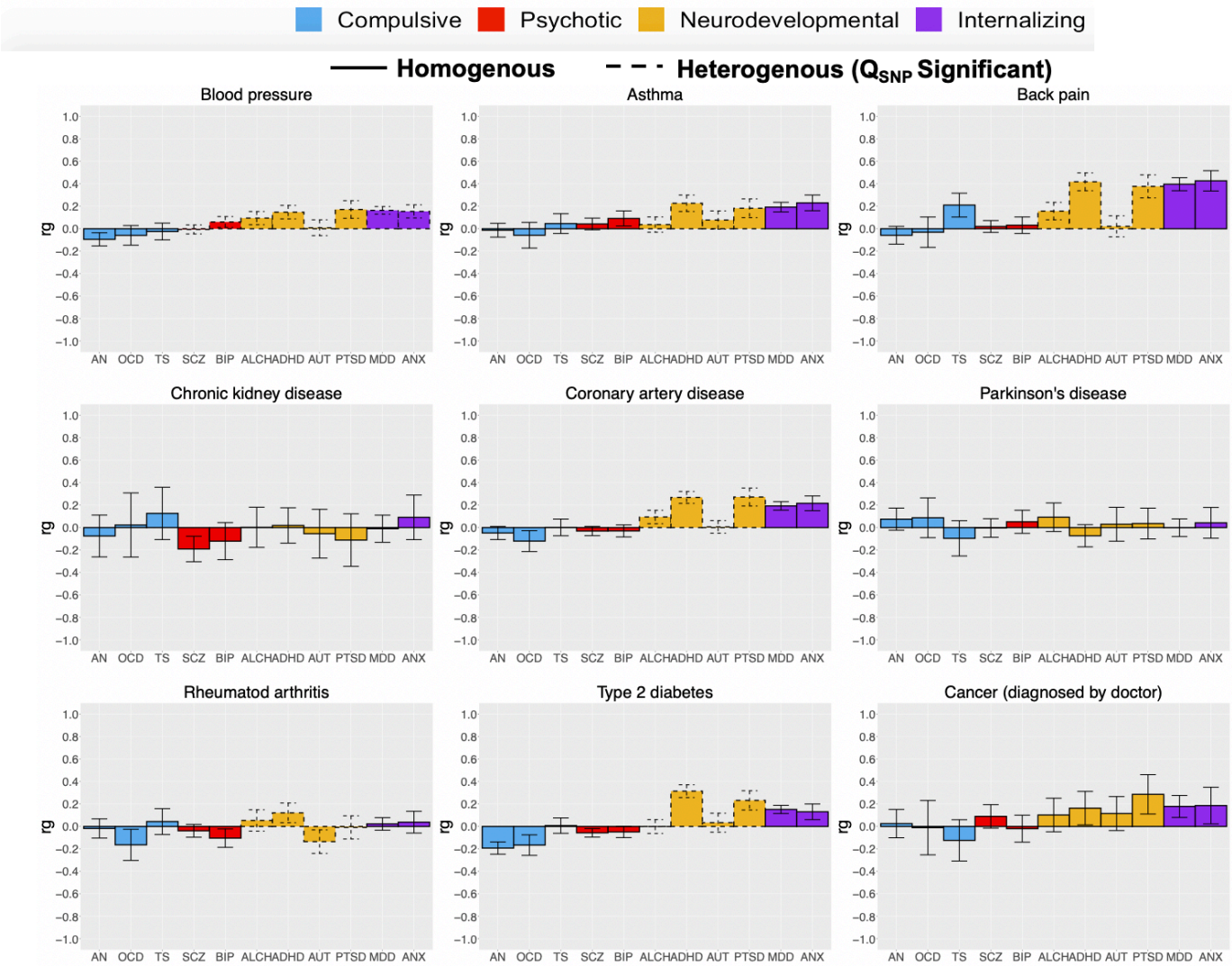

Supplementary Figure 7b. Genetic Correlations with Complex Traits across Psychiatric Factors. . Panels depict the genetic correlation point estimates in bar plots, with error bars depicting +/- 1.96 *SE*s, for associations with 9 of the 49 biobehavioral complex traits and the 11 psychiatric traits. The 11 psychiatric traits are grouped according to the correlated factor structure, with compulsive disorders depicted in light blue, psychotic disorders in red, neurodevelopmental disorders in golden yellow, and internalizing disorders in purple. For traits that loaded on multiple factors (e.g., ALCH), they are colored to be grouped with the factor that they loaded on the strongest. Genetic correlations depicted with a dashed outline were significant at a Bonferroni corrected threshold for model comparisons indicating heterogeneity (i.e., significant Q_{Trait}) across the factor indicators in their genetic correlations with the outside trait. The total sample size for the complex traits was: blood pressure (*N*= 361,194), asthma (*N*= 361,194), back pain (*N*= 361,194), chronic kidney disease (*N*= 118,147), coronary artery disease (*N*= 547,261), Parkinson's disease (*N*= 449,056), Rheumatoid arthritis (*N*= 58,284), Type 2 Diabetes (*N*= 898,130), and cancer (*N*= 361,194). The sample size for the psychiatric traits was: AN (*N*= 16,992 cases and 55,525 controls), OCD (*N*= 2,688 cases and 7,037 controls), TS (*N*= 4,819 cases and 9,488 controls), SCZ (*N*= 53,386 cases and 77,258 controls), BIP (*N*= 20,352 cases and 31,358 controls), ALCH (*N*= 176,024 observations), ADHD (*N*= 24,116 cases and 91,557 controls), AUT (*N*= 18,382 cases and 27,969 controls), PTSD (*N*= 12,255 cases and 26,338 controls), MDD (*N*= 249,227 cases and 553,712 controls), and ANX (*N*= 30,992 cases and 69,883 controls).

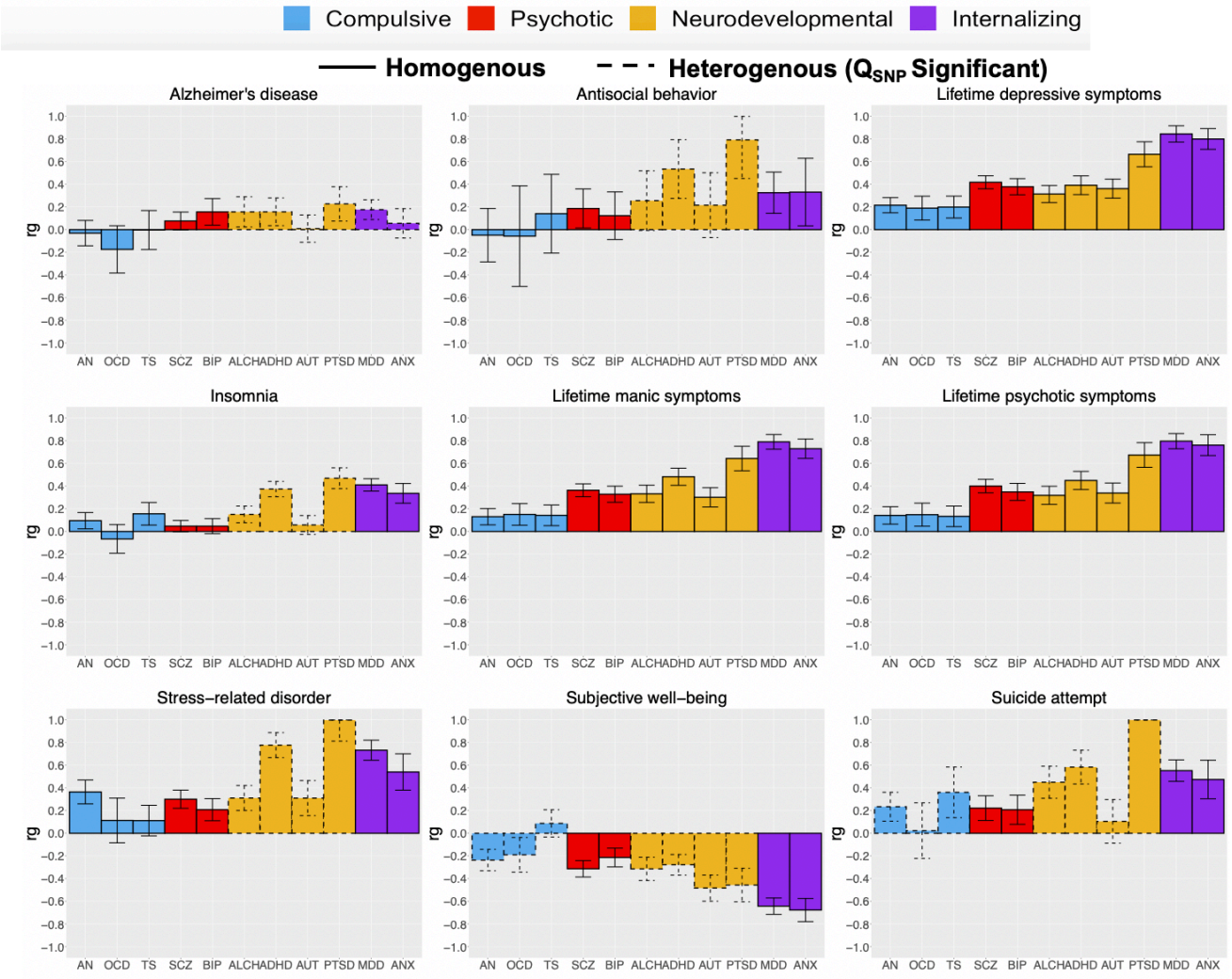

Supplementary Figure 7c. Genetic Correlations with Complex Traits across Psychiatric Factors. . Panels depict the genetic correlation point estimates in bar plots, with error bars depicting +/- 1.96 *SE*s, for associations with 9 of the 49 biobehavioral complex traits and the 11 psychiatric traits. The 11 psychiatric traits are grouped according to the correlated factor structure, with compulsive disorders depicted in light blue, psychotic disorders in red, neurodevelopmental disorders in golden yellow, and internalizing disorders in purple. For traits that loaded on multiple factors (e.g., ALCH), they are colored to be grouped with the factor that they loaded on the strongest. Genetic correlations depicted with a dashed outline were significant at a Bonferroni corrected threshold for model comparisons indicating heterogeneity (i.e., significant Q_{Trait}) across the factor indicators in their genetic correlations with the outside trait. The total sample sizes were: Alzheimer's disease (*N*= 17,375), antisocial behavior (*N*= 16,400), lifetime depressive symptoms (*N*= 126,494), insomnia (*N* = 386,533), lifetime psychotic symptoms (*N*= 126,494), lifetime manic symptoms (*N* = 126,494), stress-related disorder (*N* = 29,056), subjective well-being (*N* = 204,966), and suicide attempt (*N* = 50,265). The sample size for the psychiatric traits was: AN (*N*= 16,992 cases and 55,525 controls), OCD (*N*= 2,688 cases and 7,037 controls), TS (*N*= 4,819 cases and 9,488 controls), SCZ (*N*= 53,386 cases and 77,258 controls), BIP (*N*= 20,352 cases and 31,358 controls), ALCH (*N*= 176,024 observations), ADHD (*N*= 24,116 cases and 91,557 controls), AUT (*N*= 18,382 cases and 27,969 controls), PTSD (*N*= 12,255 cases and 26,338 controls), MDD (*N*= 249,227 cases and 553,712 controls), and ANX (*N*= 30,992 cases and 69,883 controls).

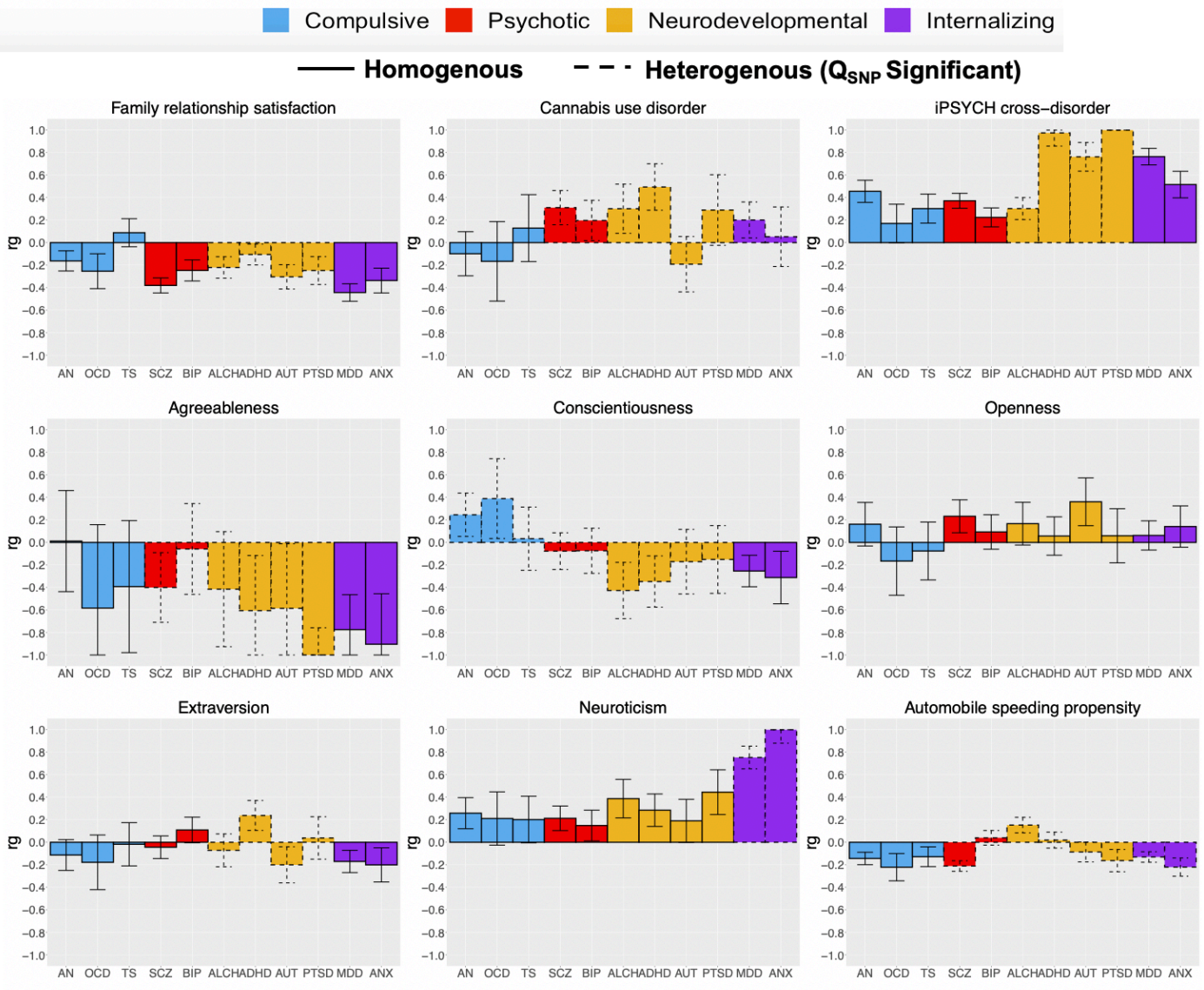

Supplementary Figure 7d. Genetic Correlations with Complex Traits across Psychiatric Factors. . Panels depict the genetic correlation point estimates in bar plots, with error bars depicting +/- 1.96 *SE*s, for associations with 9 of the 49 biobehavioral complex traits and the 11 psychiatric traits. The 11 psychiatric traits are grouped according to the correlated factor structure, with compulsive disorders depicted in light blue, psychotic disorders in red, neurodevelopmental disorders in golden yellow, and internalizing disorders in purple. For traits that loaded on multiple factors (e.g., ALCH), they are colored to be grouped with the factor that they loaded on the strongest. Genetic correlations depicted with a dashed outline were significant at a Bonferroni corrected threshold for model comparisons indicating heterogeneity (i.e., significant Q_{Trait}) across the factor indicators in their genetic correlations with the outside trait. The total sample sizes were: family relationship satisfcation (N = 361,194), cannabis use disorder (N= 357,806), iPSYCH cross-disorder (N = 65,534), agreeableness (N = 59,176), conscientiousness (N = 59,176), openness (N = 59,176), extraversion (N = 59,176), neuroticism (N = 63,661), automobile speeding propensity (N = 404,291). The sample size for the psychiatric traits was: AN (N= 16,992 cases and 55,525 controls), OCD (N= 2,688 cases and 7,037 controls), TS (N= 4,819 cases and 9,488 controls), SCZ (N= 53,386 cases and 77,258 controls), BIP (N= 20,352 cases and 31,358 controls), ALCH (N= 176,024 observations), ADHD (N= 24,116 cases and 91,557 controls), AUT (N= 18,382 cases and 27,969 controls), PTSD (N= 12,255 cases and 26,338 controls), MDD (N= 249,227 cases and 553,712 controls), and ANX (N= 30,992 cases and 69,883 controls).

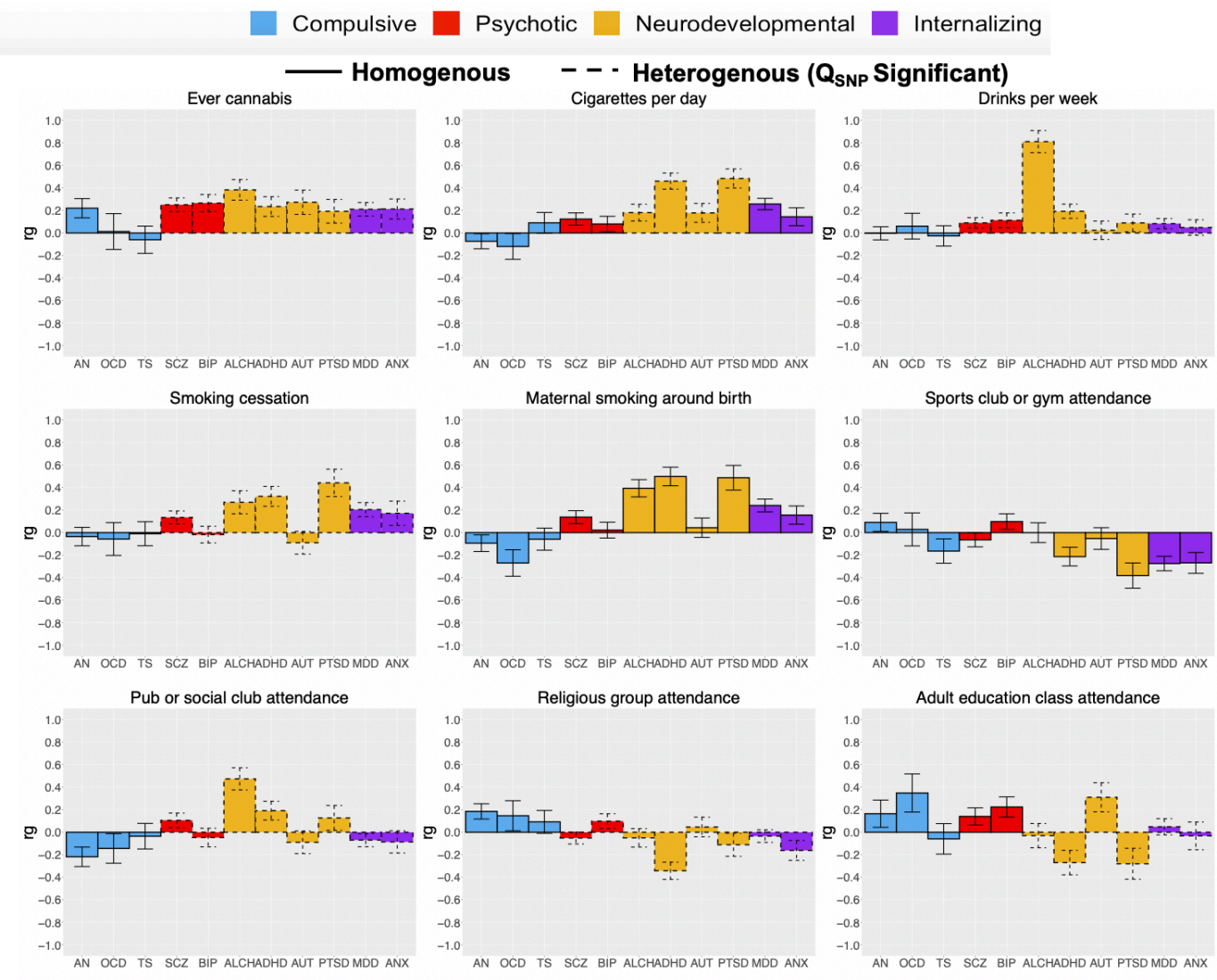

Supplementary Figure 7e. Genetic Correlations with Complex Traits across Psychiatric Factors. Panels depict the genetic correlation point estimates in bar plots, with error bars depicting +/- 1.96 *SE*s, for associations with 9 of the 49 biobehavioral complex traits and the 11 psychiatric traits. The 11 psychiatric traits are grouped according to the correlated factor structure, with compulsive disorders depicted in light blue, psychotic disorders in red, neurodevelopmental disorders in golden yellow, and internalizing disorders in purple. For traits that loaded on multiple factors (e.g., ALCH), they are colored to be grouped with the factor that they loaded on the strongest. Genetic correlations depicted with a dashed outline were significant at a Bonferroni corrected threshold for model comparisons indicating heterogeneity (i.e., significant Q_{Trait}) across the factor indicators in their genetic correlations with the outside trait. The total sample sizes were: ever cannabis (N = 162,082), cigarettes per day (N = 263,954), drinks per week (N = 537,349), smoking cessation (N = 312,821), maternal smoking around birth (N = 361,194), sports club or gym attendance (N = 361,194), pub or social club attendance (N = 361,194), religious group attendance (N = 361,194), adult education class attendance (N = 361,194). The sample size for the psychiatric traits was: AN (N= 16,992 cases and 55,525 controls), OCD (N= 2,688 cases and 7,037 controls), TS (N= 4,819 cases and 9,488 controls), SCZ (N= 53,386 cases and 77,258 controls), BIP (N= 20,352 cases and 31,358 controls), ALCH (N= 176,024 observations), ADHD (N= 24,116 cases and 91,557 controls), AUT (N= 18,382 cases and 27,969 controls), PTSD (N= 12,255 cases and 26,338 controls), MDD (N= 249,227 cases and 553,712 controls), and ANX (N= 30,992 cases and 69,883 controls).

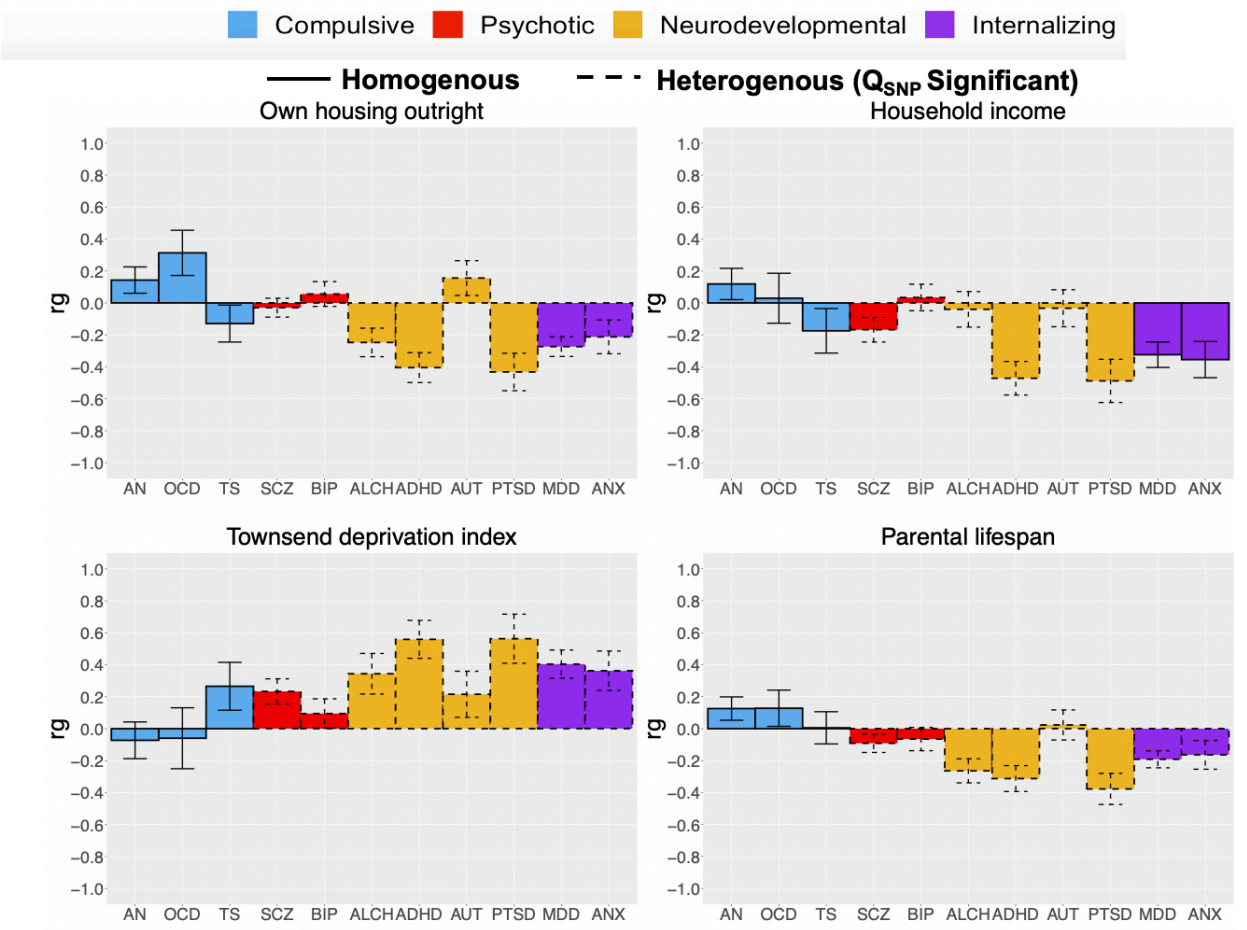

Supplementary Figure 7f. Genetic Correlations with Complex Traits across Psychiatric Factors. . Panels depict the genetic correlation point estimates in bar plots, with error bars depicting +/- 1.96 *SE*s, for associations with 4 of the 49 biobehavioral complex traits and the 11 psychiatric traits.The 11 psychiatric traits are grouped according to the correlated factor structure, with compulsive disorders depicted in light blue, psychotic disorders in red, neurodevelopmental disorders in golden yellow, and internalizing disorders in purple. For traits that loaded on multiple factors (e.g., ALCH), they are colored to be grouped with the factor that they loaded on the strongest. Genetic correlations depicted with a dashed outline were significant at a Bonferroni corrected threshold for model comparisons indicating heterogeneity (i.e., significant Q_{Trait}) across the factor indicators in their genetic correlations with the outside trait. The total sample sizes were: own housing outright (N = 361,194), household income (N = 112,151), townsend deprivation index (N = 112,151), parental lifespan (N = 640,189). The sample size for the psychiatric traits was: AN (N= 16,992 cases and 55,525 controls), OCD (N= 2,688 cases and 7,037 controls), TS (N= 4,819 cases and 9,488 controls), SCZ (N= 53,386 cases and 77,258 controls), BIP (N= 20,352 cases and 31,358 controls), ALCH (N= 176,024 observations), ADHD (N= 24,116 cases and 91,557 controls), AUT (N= 18,382 cases and 27,969 controls), PTSD (N= 12,255 cases and 26,338 controls), MDD (N= 249,227 cases and 553,712 controls), and ANX (N= 30,992 cases and 69,883 controls).

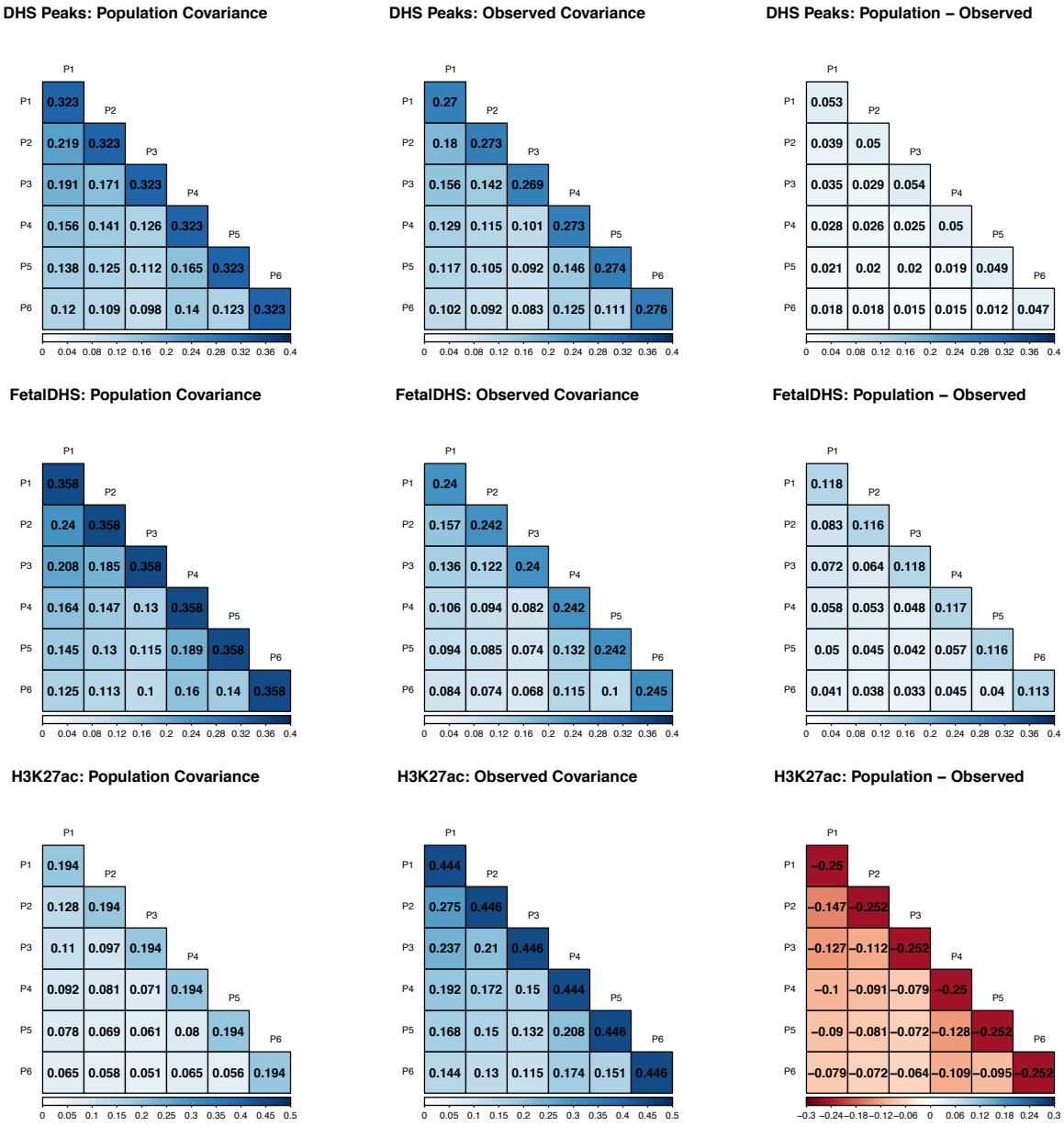

Supplementary Figure 8a. Population generating and observed zero-order (S0) covariance matrices. The first column depicts the genetic covariance matrix in the generating population. The second column depicts the average observed covariance across the 100 simulations runs. The last column reflects the difference between the population matrix and average observed covariance matrix. For the zero-order matrices, estimates are expected to be biased in the sense that an individual partition will be affected by population generating covariances in overlapping annotations. Results are shown for the DHS Peaks (top row), Fetal DHS (middle row) and H3K27ac (bottom row) annotations.

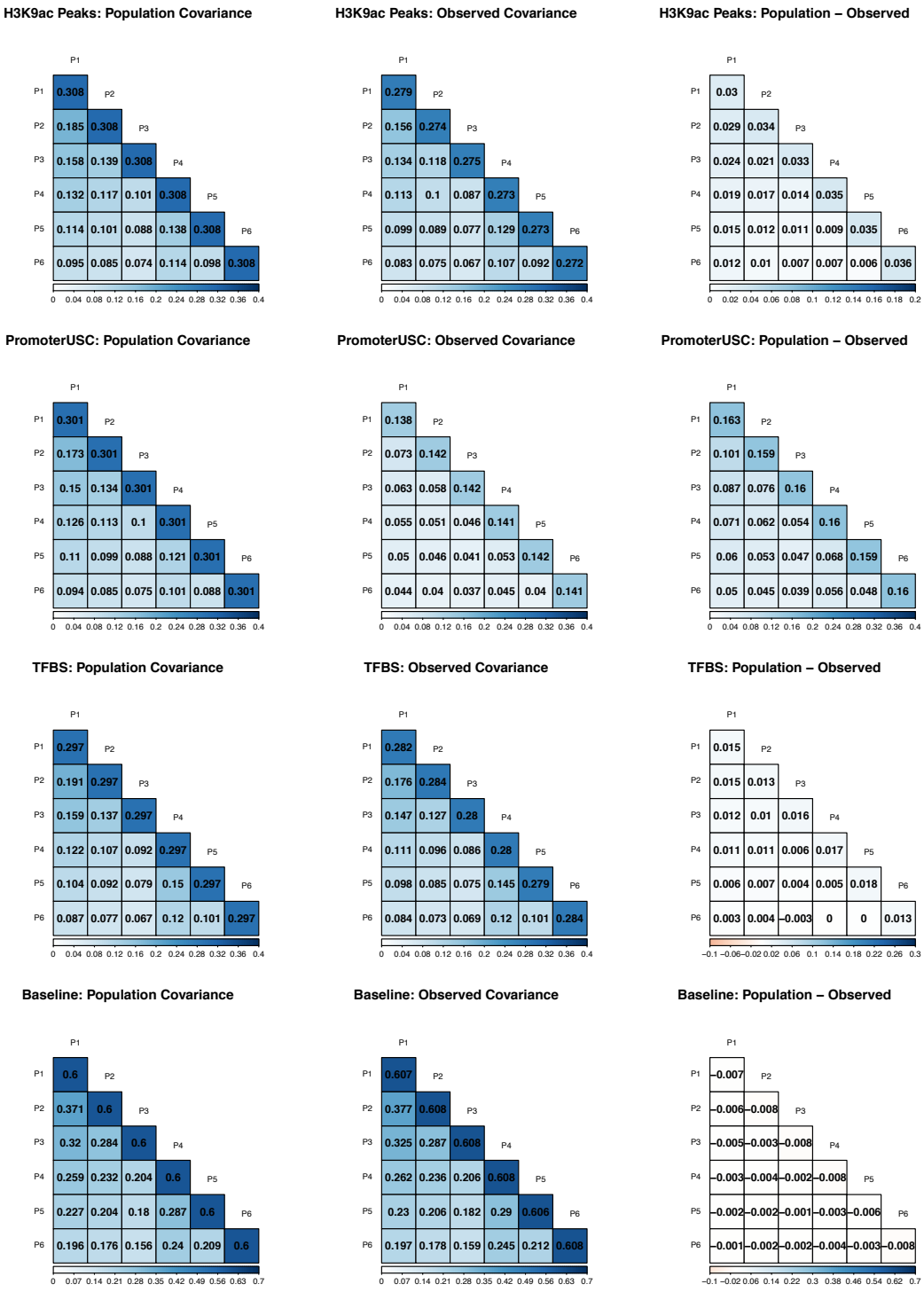

Supplementary Figure 8b. Population generating and observed zero-order (S0) covariance matrices. The first column depicts the genetic covariance matrix in the generating population. The second column depicts the average observed covariance across the 100 simulations runs. The last column reflects the difference between the population matrix and average observed covariance matrix. For the zero-order matrices, estimates are expected to be biased in the sense that an individual partition will be affected by population generating covariances in overlapping annotations. Results are shown for the H3K9ac Peaks (top row), PromoterUSC (second row), and TFBS (third row) annotations, and for the baseline genome-wide (bottom row) annotation containing all SNPs. Results for genome-wide estimates in the bottom row are unaffected by overlap with other annotations.

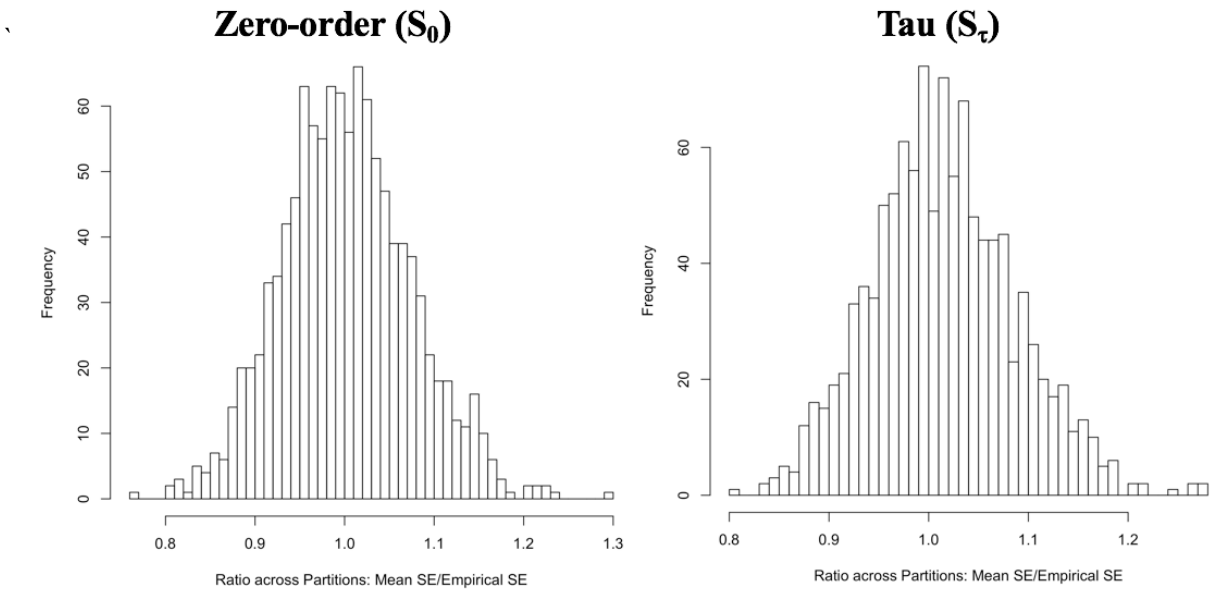

Supplementary Figure 9. Distributions of SE ratios. Panels depict mean *SE* ratios across the 100 simulations for the for mean *SE* over the empirical *SE* across the annotations for the S_τ (right panel) and zero-order (left panel) covariance matrices. Average ratios are shown for each cell of the covariance matrix for all annotations.

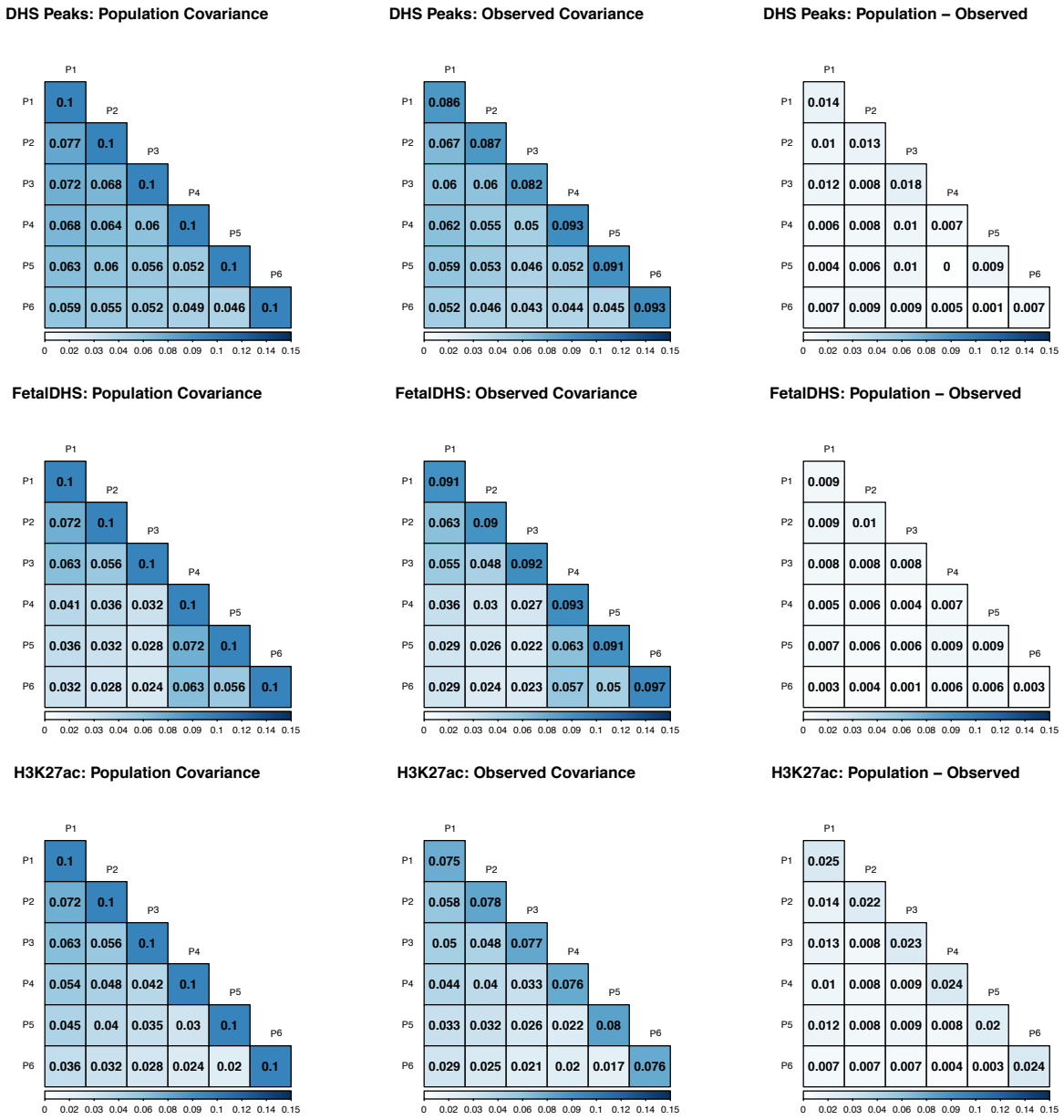

Supplementary Figure 10a. Stratified Sτ matrices covariance matrices. The first column depicts the genetic covariance matrix in the generating population. The second column depicts the average observed covariance across the 100 simulations runs. The last column reflects the difference between the population matrix and average observed covariance matrix. As observed, for the S_τ matrices, estimates are expected to be generally unbiased. Results are shown for the DHS Peaks (top row), Fetal DHS (middle row) and H3K27ac (bottom row) annotations.

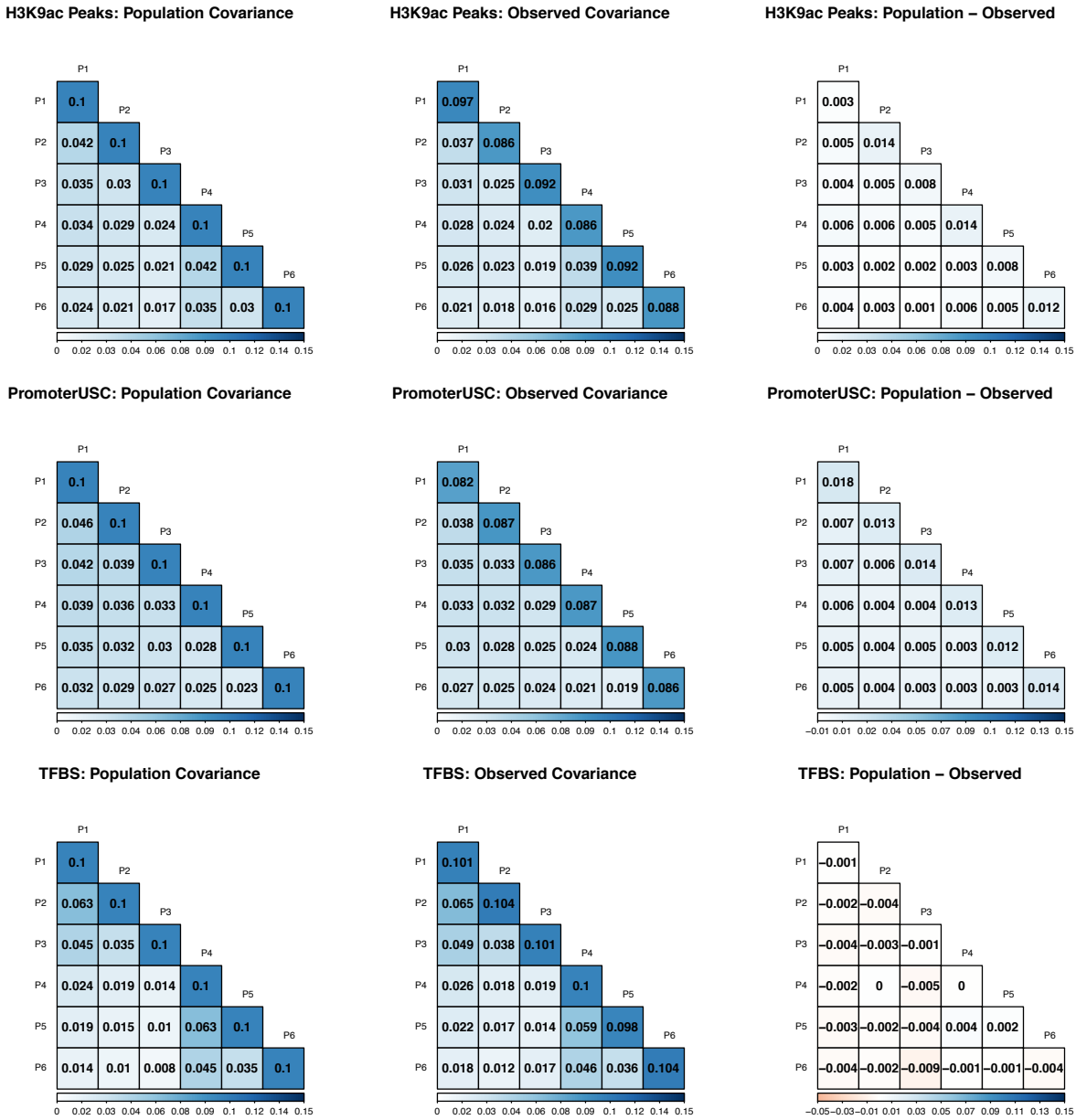

Supplementary Figure 10b. Stratified Sτ covariance matrices. The first column depicts the genetic covariance matrix in the generating population. The second column depicts the average observed covariance across the 100 simulations runs. The last column reflects the difference between the population matrix and average observed covariance matrix. As observed, for the S_τ matrices, estimates are expected to be generally unbiased. Results are shown for the H3K9ac Peaks (top row), PromoterUSC (second row), TFBS (third row), and genome-wide (bottom row) annotations. Results for genome-wide estimates are unaffected by overlap with other annotations as the genome-wide partition includes all SNPs.

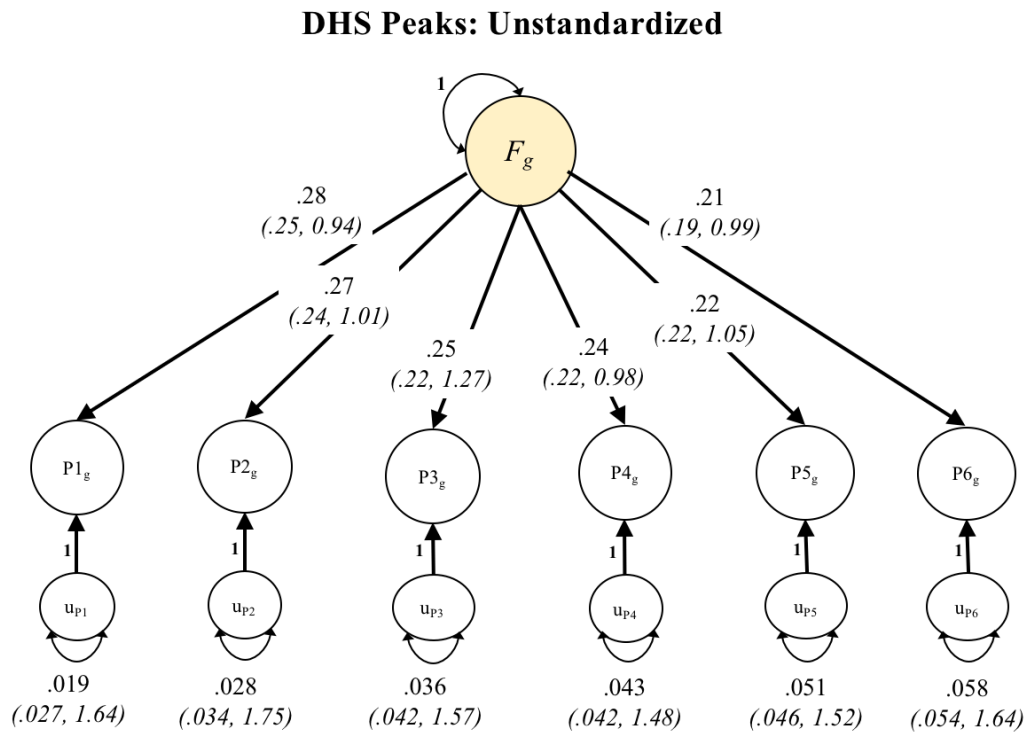

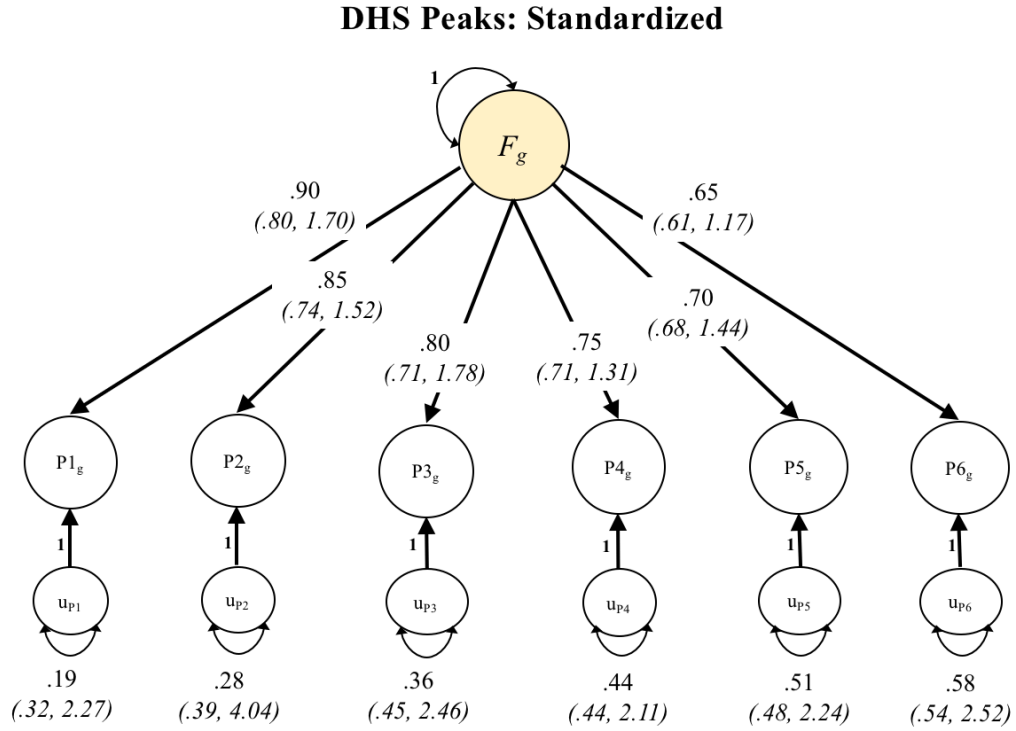

Supplementary Figure 11a. Genomic SEM simulation results for DHS partition. Parameters outside of the parentheses indicate those provided in the generating population. In parentheses, we provide the average point estimate followed by the ratio of the mean *SE estimate* across the 100 runs over the empirical *SE* (calculated as the standard deviation of the parameter estimates across the 100 runs). We note that *SE* estimates are expected to be upwardly biased in the standardized case, and for residual variances, due to upper or lower limits on the sampling distributions (e.g., residual variance > 0).

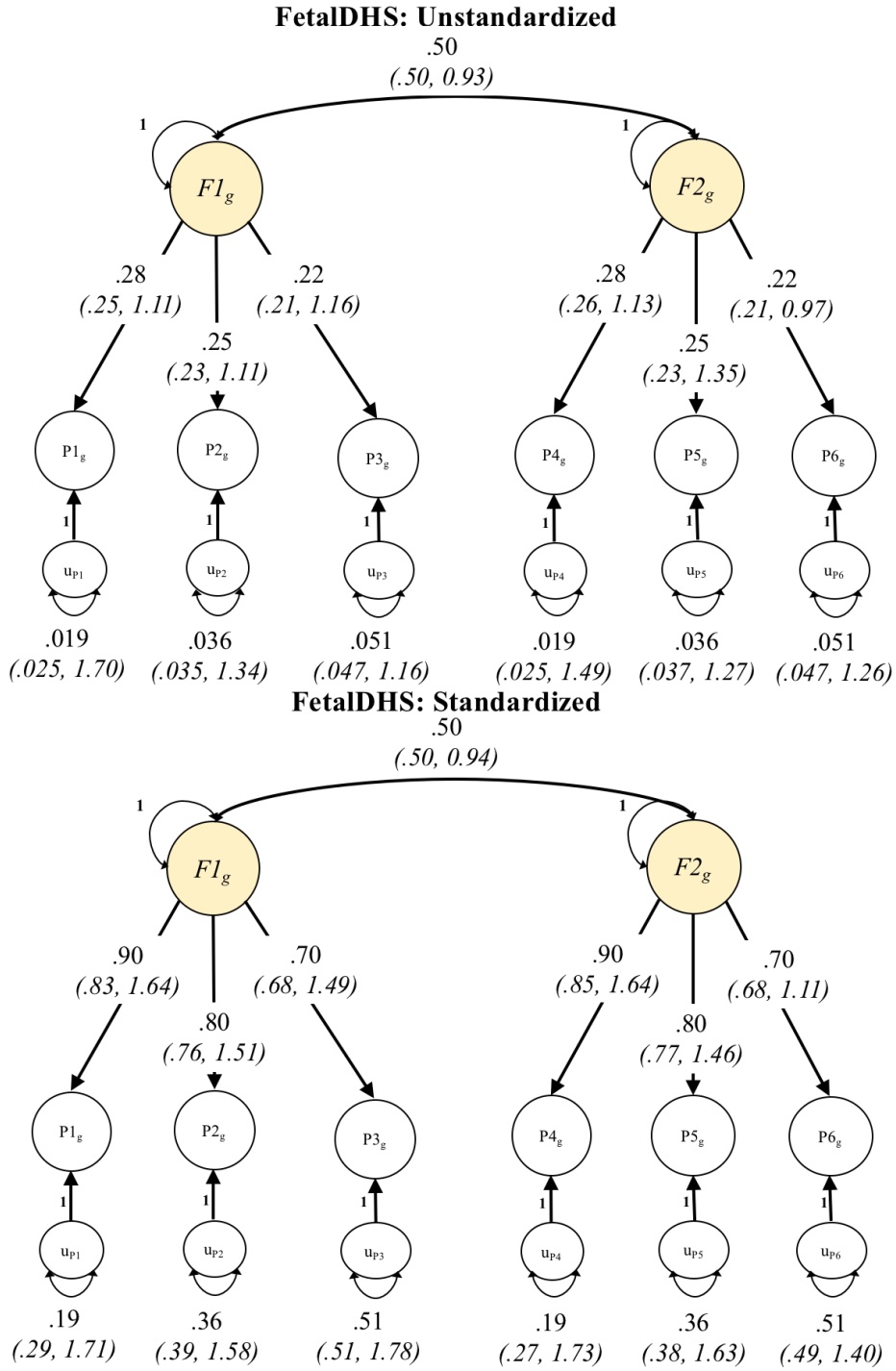

Supplementary Figure 11b. Genomic SEM simulation results for FetalDHS partition. Parameters outside of the parentheses indicate those provided in the generating population. In parentheses, we provide the average point estimate followed by the ratio of the mean *SE estimate* across the 100 runs over the empirical *SE* (calculated as the standard deviation of the parameter estimates across the 100 runs). We note that *SE* estimates are expected to be upwardly biased in the standardized case, and for residual variances, due to upper or lower limits on the sampling distributions (e.g., residual variance > 0).

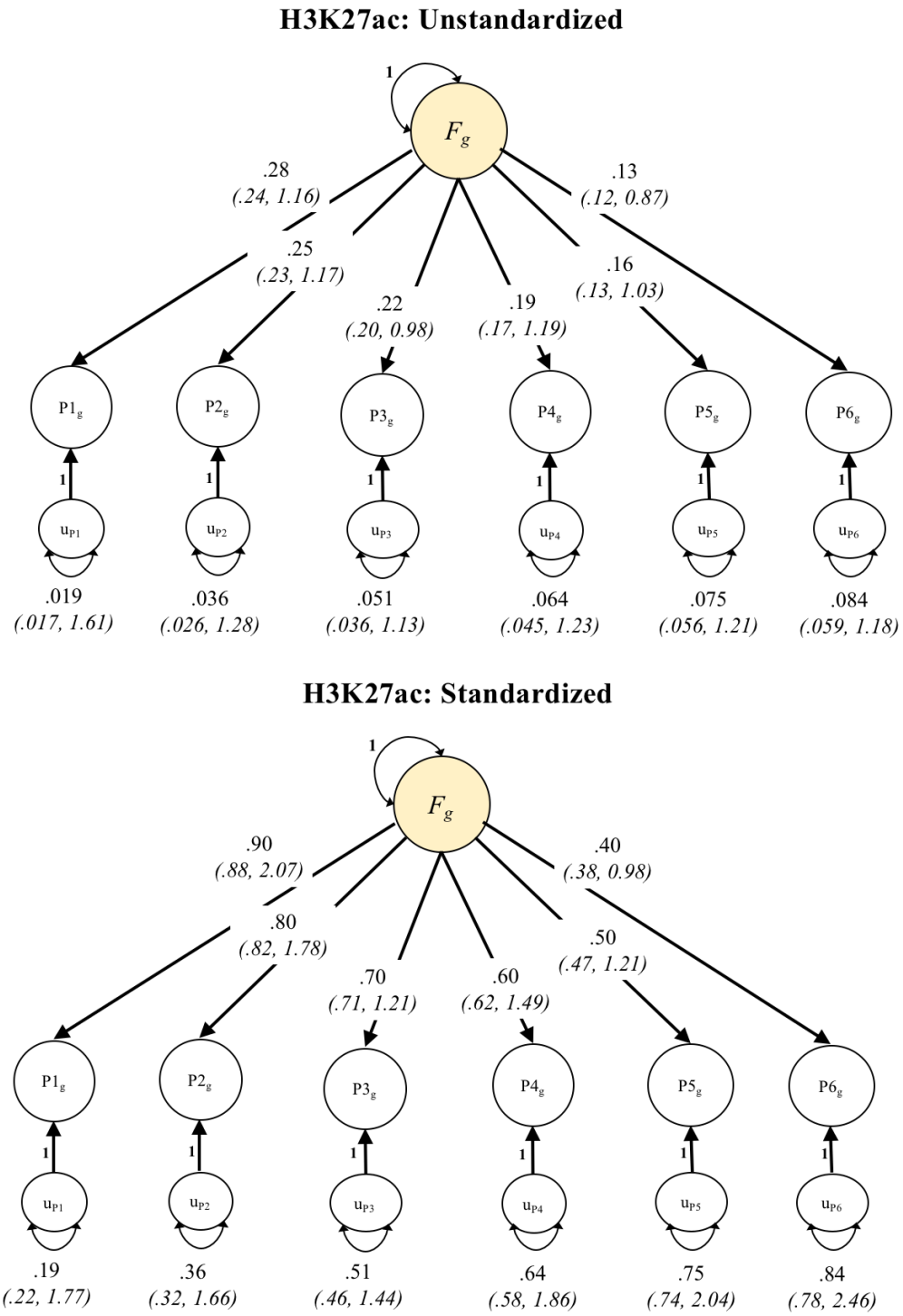

Supplementary Figure 11c. Genomic SEM simulation results for H3K27ac partition. Parameters outside of the parentheses indicate those provided in the generating population. In parentheses, we provide the average point estimate followed by the ratio of the mean *SE estimate* across the 100 runs over the empirical *SE* (calculated as the standard deviation of the parameter estimates across the 100 runs). We note that *SE* estimates are expected to be upwardly biased in the standardized case, and for residual variances, due to upper or lower limits on the sampling distributions (e.g., residual variance > 0).

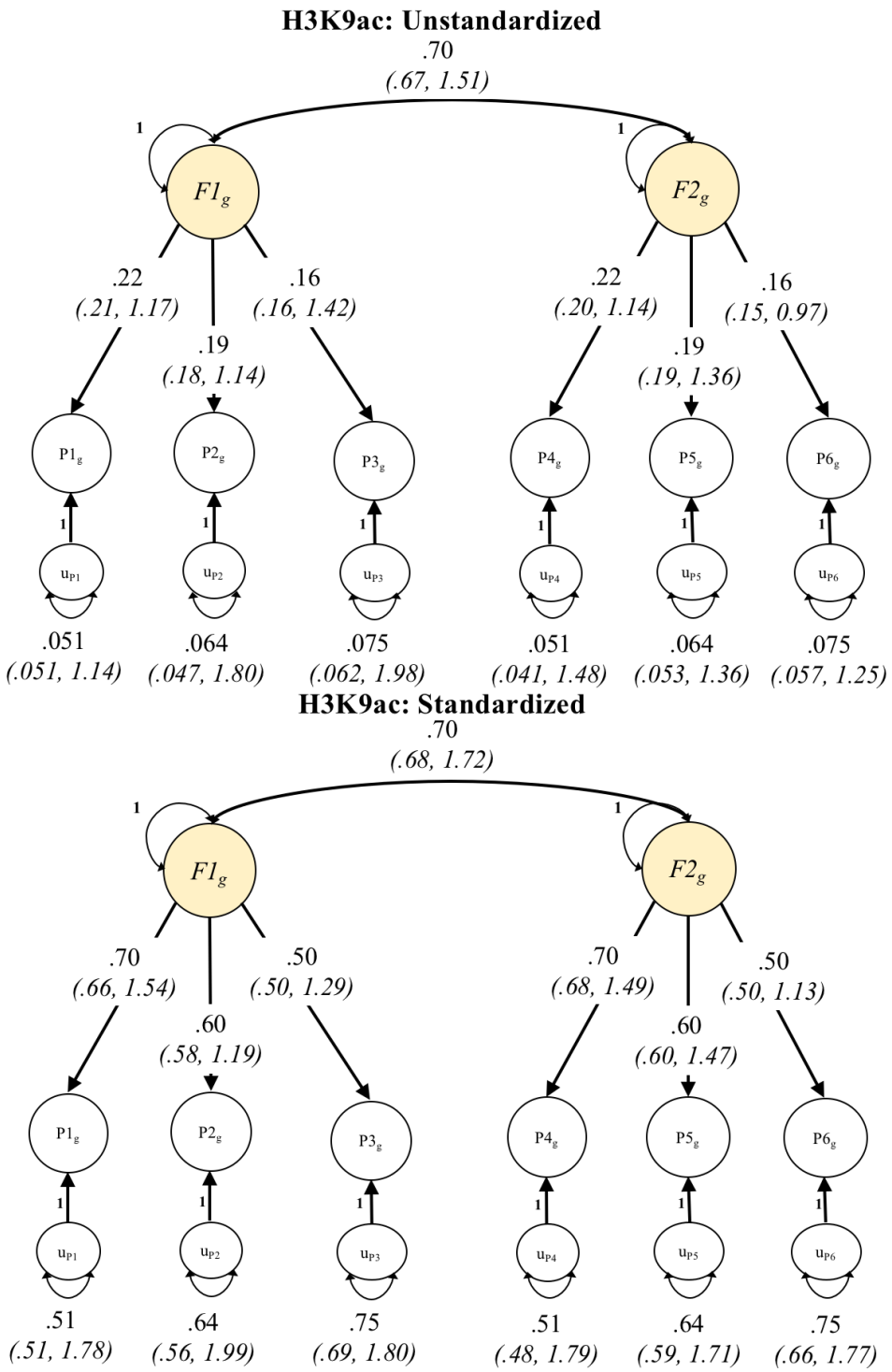

Supplementary Figure 11d. Genomic SEM simulation results for H3K9ac partition. Parameters outside of the parentheses indicate those provided in the generating population. In parentheses, we provide the average point estimate followed by the ratio of the mean *SE estimate* across the 100 runs over the empirical *SE* (calculated as the standard deviation of the parameter estimates across the 100 runs). We note that *SE* estimates are expected to be upwardly biased in the standardized case, and for residual variances, due to upper or lower limits on the sampling distributions (e.g., residual variance > 0).

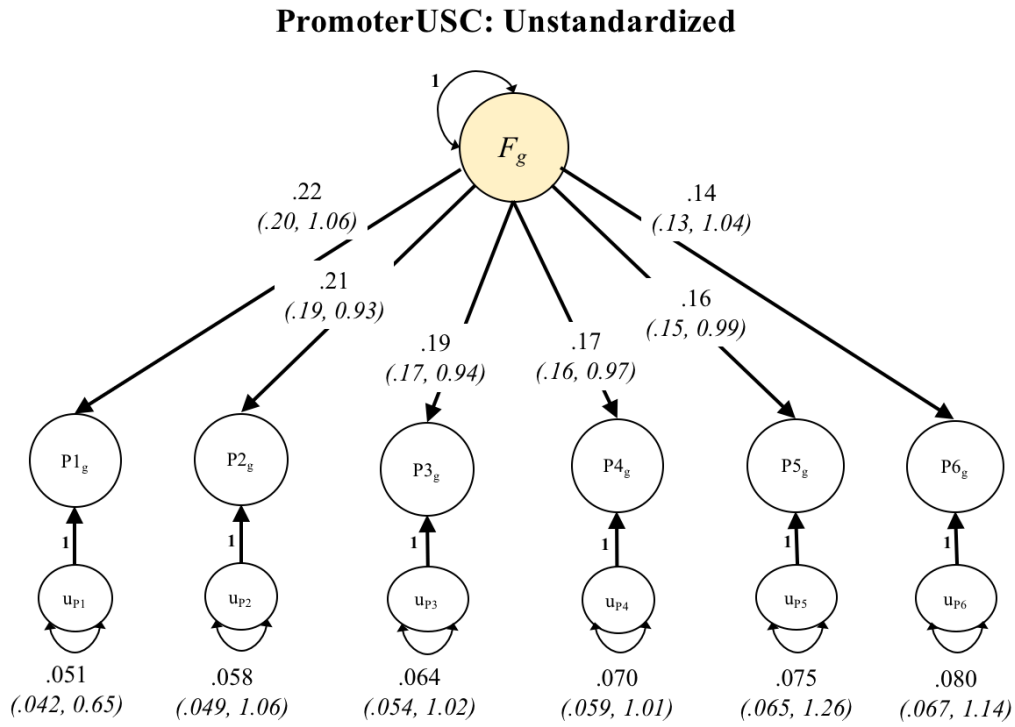

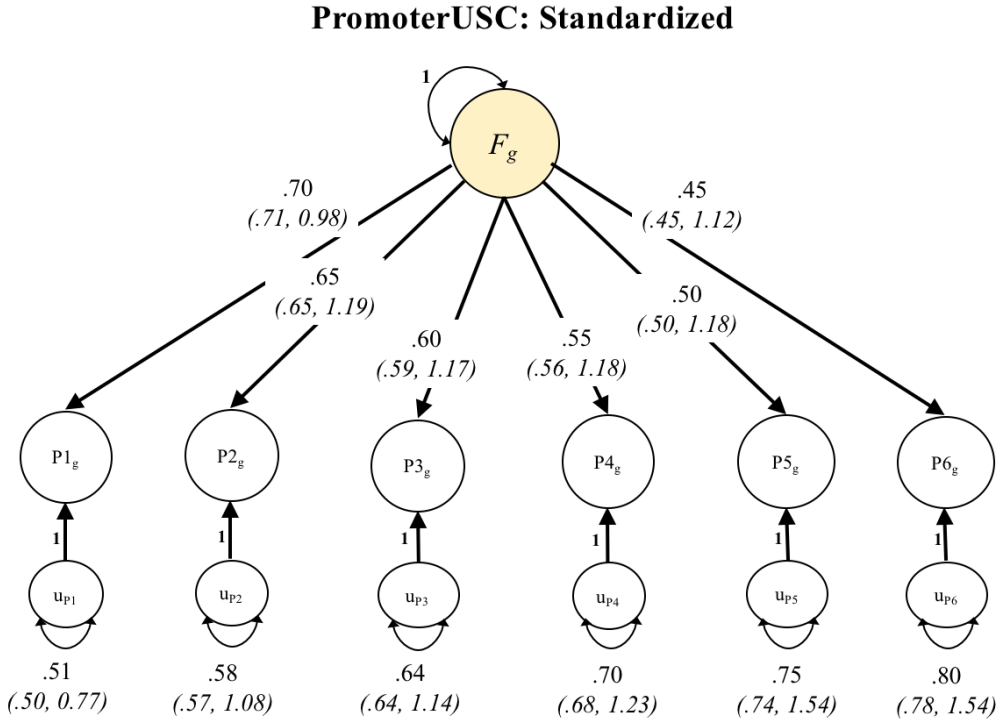

Supplementary Figure 11e. Genomic SEM simulation results for PromoterUSC partition. Parameters outside of the parentheses indicate those provided in the generating population. In parentheses, we provide the average point estimate followed by the ratio of the mean *SE estimate* across the 100 runs over the empirical *SE* (calculated as the standard deviation of the parameter estimates across the 100 runs). We note that *SE* estimates are expected to be upwardly biased in the standardized case, and for residual variances, due to upper or lower limits on the sampling distributions (e.g., residual variance > 0).

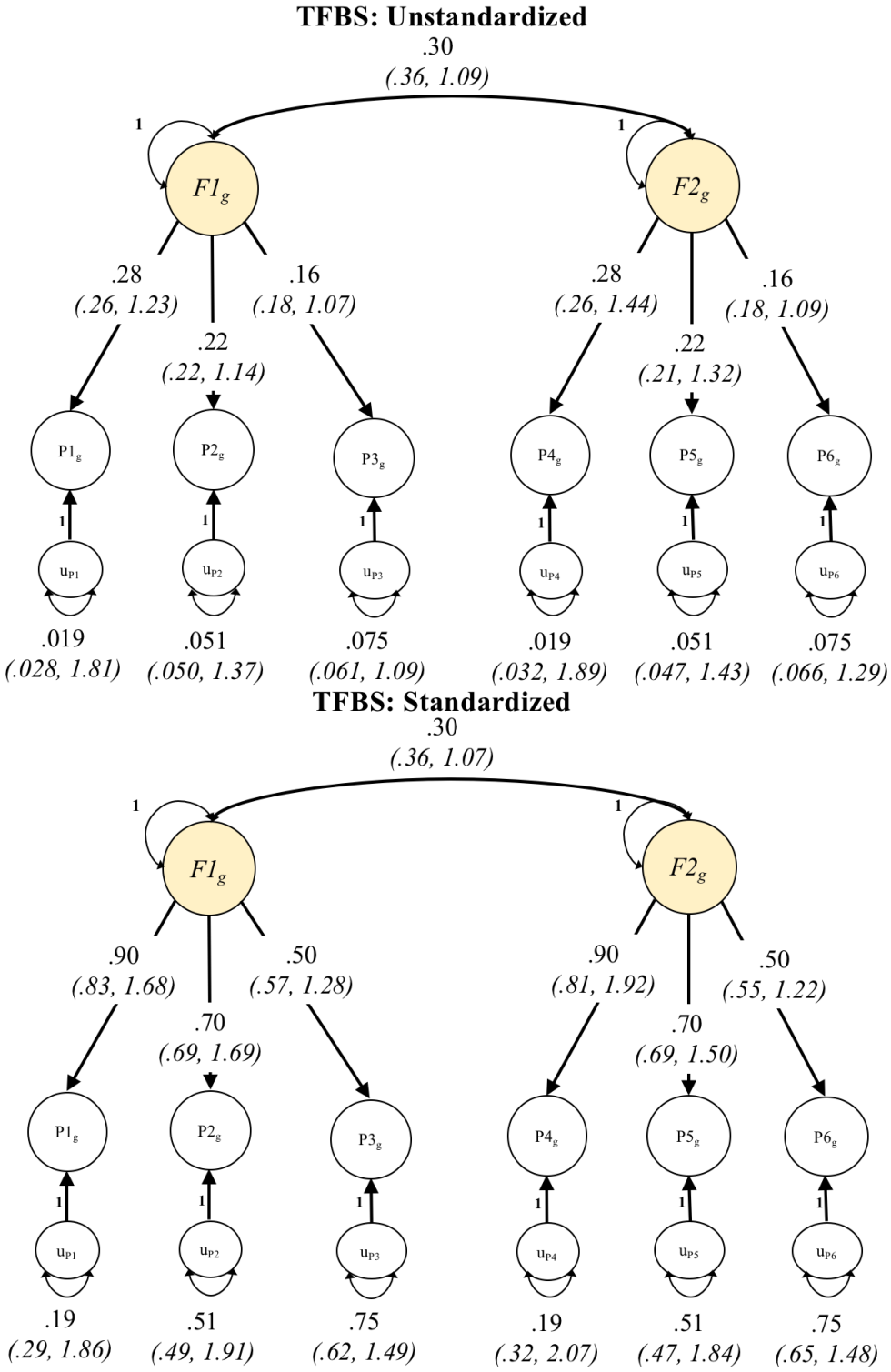

Supplementary Figure 11f. Genomic SEM simulation results for TFBS partition. Parameters outside of the parentheses indicate those provided in the generating population. In parentheses, we provide the average point estimate followed by the ratio of the mean *SE estimate* across the 100 runs over the empirical *SE* (calculated as the standard deviation of the parameter estimates across the 100 runs). We note that *SE* estimates are expected to be upwardly biased in the standardized case, and for residual variances, due to upper or lower limits on the sampling distributions (e.g., residual variance > 0).

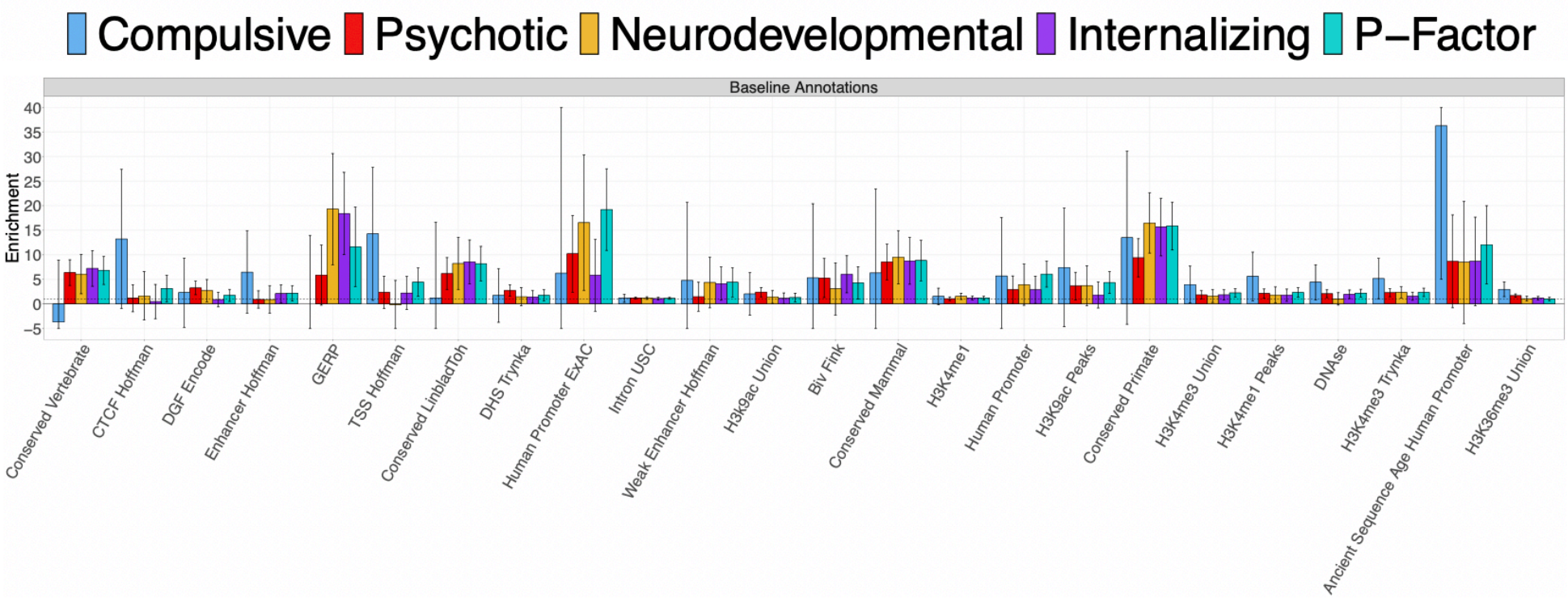

Supplementary Figure 12a. Genetic Enrichment of Psychiatric Factors for the Baseline Annotations. Figure depict enrichment point estimates, with error bars displaying +/- 1.96 SEs, for the compulsive (shown in blue), psychotic (shown in red), neurodevelopmental (shown in gold), and internalizing factors (shown in purple) from the correlated factors model and the second-order p-factor from the hierarchical factor model (shown in torqouise) for the baseline annotations. Enrichment is indexed by the ratio of the proportion of genome-wide relative risk sharing indexed by the annotation to that annotation's size as a proportion of the genome. The black dashed line reflects the null ration of 1.0, corresponding to no enrichment. Ratios greater than 1.0 indicate enrichment of pleiotropic signal whereas ratios less than 1.0 indicate depletion of pleiotropic signal. For panels A, C, and D, only the top ten annotations across the factors are depicted within each of the functional categories. Error bars depict 95% confidence intervals. For scaling purposes, error bars are capped at the y-axis limits for each panel for the compulsive disorders factor; no enrichment estimates were significant for this factor. The effective sample size for the factors was: Compulsive Factor (N = 19,108), Psychotic Factor (N = 87,138), Neurodevelpomental Factor (N = 55,932), Internalizing Factor (N = 455,340), and hierarchical p-factor (N = 667,343).

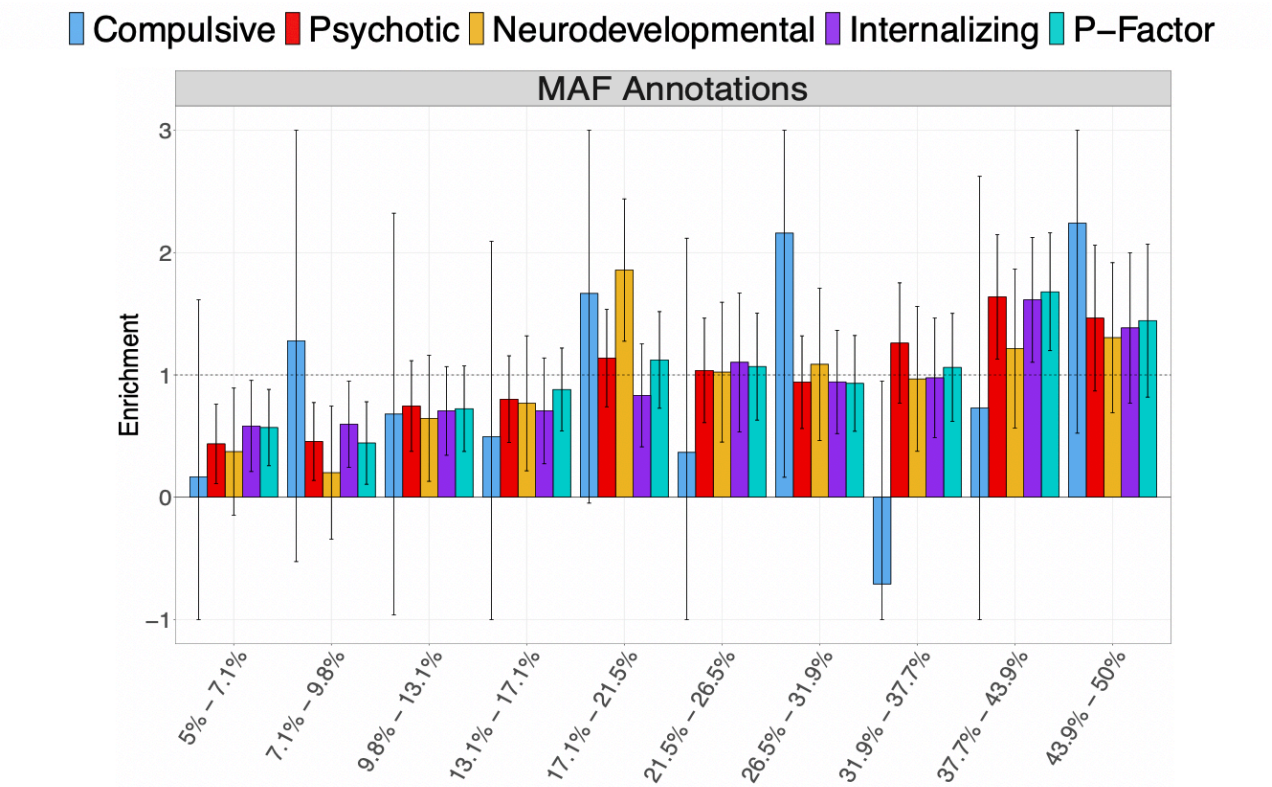

Supplementary Figure 12b. Genetic Enrichment of Psychiatric Factors for MAF Bins. Figure depict enrichment point estimates, with error bars displaying +/- 1.96 SEs, for the compulsive (shown in blue), psychotic (shown in red), neurodevelopmental (shown in gold), and internalizing factors (shown in purple) from the correlated factors model and the second-order p-factor from the hierarchical factor model (shown in torqouise) for the minor allele frequency annotations. Enrichment is indexed by the ratio of the proportion of genome-wide relative risk sharing indexed by the annotation to that annotation's size as a proportion of the genome. The black dashed line reflects the null ration of 1.0, corresponding to no enrichment. Ratios greater than 1.0 indicate enrichment of pleiotropic signal whereas ratios less than 1.0 indicate depletion of pleiotropic signal. For panels A, C, and D, only the top ten annotations across the factors are depicted within each of the functional categories. Error bars depict 95% confidence intervals. For scaling purposes, error bars are capped at the y-axis limits for each panel for the compulsive disorders factor; no enrichment estimates were significant for this factor. The effective sample size for the factors was: Compulsive Factor (N = 19,108), Psychotic Factor (N = 87,138), Neurodevelpomental Factor (N = 55,932), Internalizing Factor (N = 455,340), and hierarchical p-factor (N = 667,343).

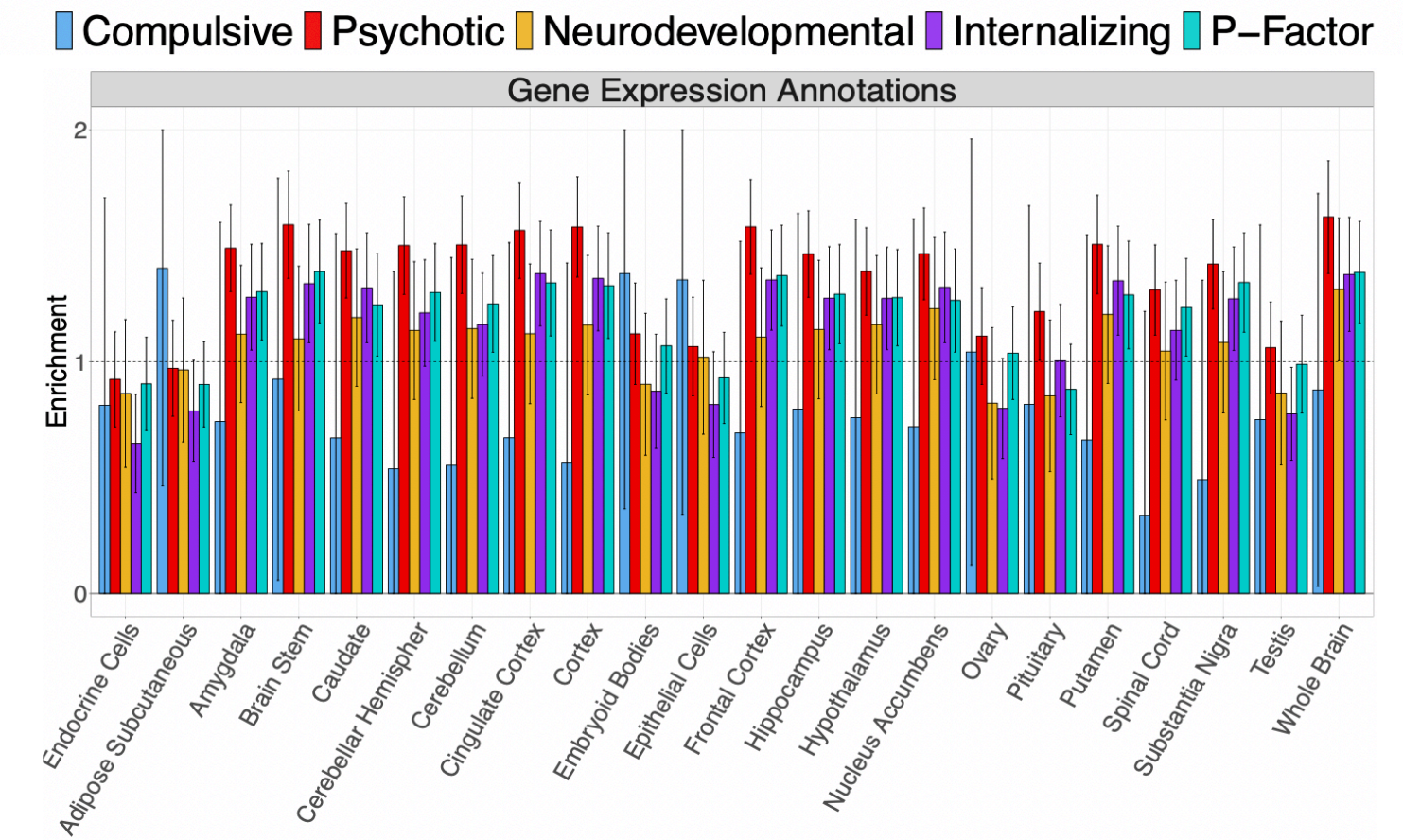

Supplementary Figure 12c. Genetic Enrichment of Psychiatric Factors for Gene Expression. Figure depict enrichment point estimates, with error bars displaying +/- 1.96 SEs, for the compulsive (shown in blue), psychotic (shown in red), neurodevelopmental (shown in gold), and internalizing factors (shown in purple) from the correlated factors model and the second-order p-factor from the hierarchical factor model (shown in torqouise) for the gene expression annotations. Enrichment is indexed by the ratio of the proportion of genome-wide relative risk sharing indexed by the annotation to that annotation's size as a proportion of the genome. The black dashed line reflects the null ration of 1.0, corresponding to no enrichment. Ratios greater than 1.0 indicate enrichment of pleiotropic signal whereas ratios less than 1.0 indicate depletion of pleiotropic signal. For panels A, C, and D, only the top ten annotations across the factors are depicted within each of the functional categories. Error bars depict 95% confidence intervals. For scaling purposes, error bars are capped at the y-axis limits for each panel for the compulsive disorders factor; no enrichment estimates were significant for this factor. The effective sample size for the factors was: Compulsive Factor (*N* = 19,108), Psychotic Factor (*N* = 87,138), Neurodevelpomental Factor (*N* = 55,932), Internalizing Factor (*N* = 455,340), and hierarchical p-factor (*N* = 667,343).

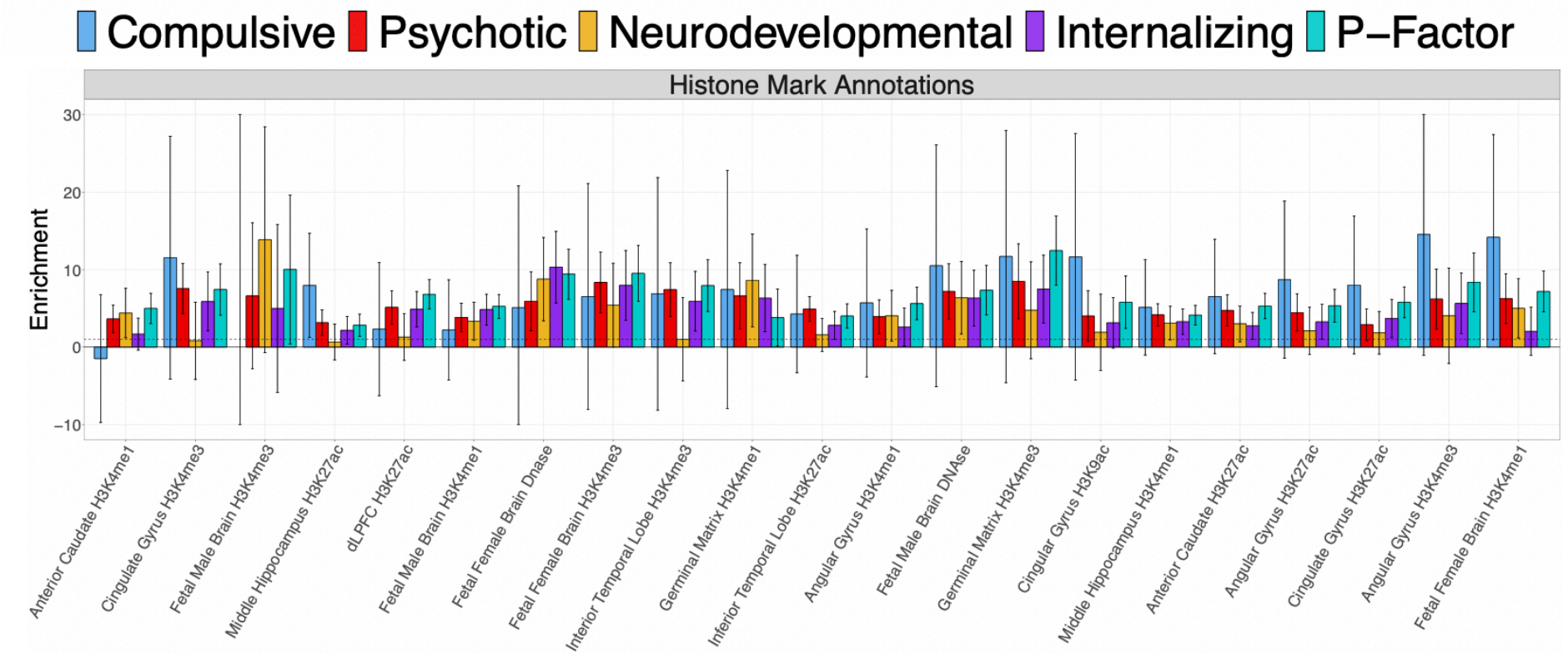

Supplementary Figure 12d. Genetic Enrichment of Psychiatric Factors for Histone Mark Annotations. Figure depict enrichment point estimates, with error bars displaying +/- 1.96 SEs, for the compulsive (shown in blue), psychotic (shown in red), neurodevelopmental (shown in gold), and internalizing factors (shown in purple) from the correlated factors model and the second-order p-factor from the hierarchical factor model (shown in torqouise) for the histone mark annotations. Enrichment is indexed by the ratio of the proportion of genome-wide relative risk sharing indexed by the annotation to that annotation's size as a proportion of the genome. The black dashed line reflects the null ration of 1.0, corresponding to no enrichment. Ratios greater than 1.0 indicate enrichment of pleiotropic signal whereas ratios less than 1.0 indicate depletion of pleiotropic signal. For panels A, C, and D, only the top ten annotations across the factors are depicted within each of the functional categories. Error bars depict 95% confidence intervals. For scaling purposes, error bars are capped at the y-axis limits for each panel for the compulsive disorders factor; no enrichment estimates were significant for this factor. The effective sample size for the factors was: Compulsive Factor (N = 19,108), Psychotic Factor (N = 87,138), Neurodevelpomental Factor (N = 55,932), Internalizing Factor (N = 455,340), and hierarchical p-factor (N = 667,343).

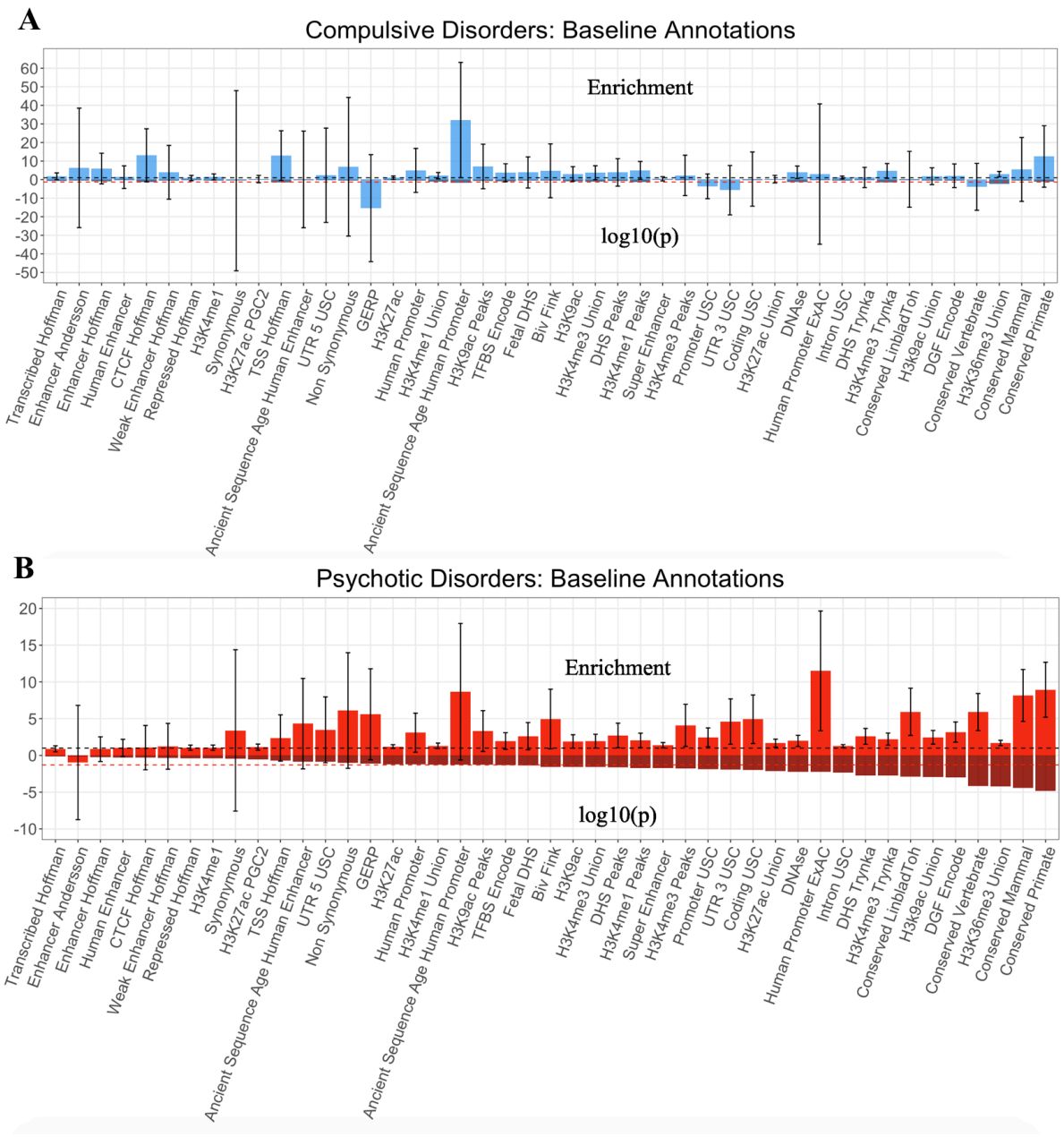

Supplementary Figure 13a. Enrichment of Baseline Annotations from Correlated Factors Model. The top half of each panel depicts the enrichment point estimates, with error bars depicting +/- 1.96 *SEs.* The black dashed line on the top half reflects the null (enrichment = 1). The bottom half of each panel depicts the log10(p) values. The red dashed line on the bottom half reflects log10(p = .05). For comparative purposes across factors, all graphs for the correlated factors model are based on increasing significance for the psychotic disorders factor. The scaling of the y-axis across panels differs due to widely discrepant ranges in CIs across factors. Estimates are shown for compulsive disorders (panel A) and psychotic disorders (panel B). The effective sample size for the factors was: Compulsive Factor (*N*= 19,108) and Psychotic Factor (*N*= 87,138).

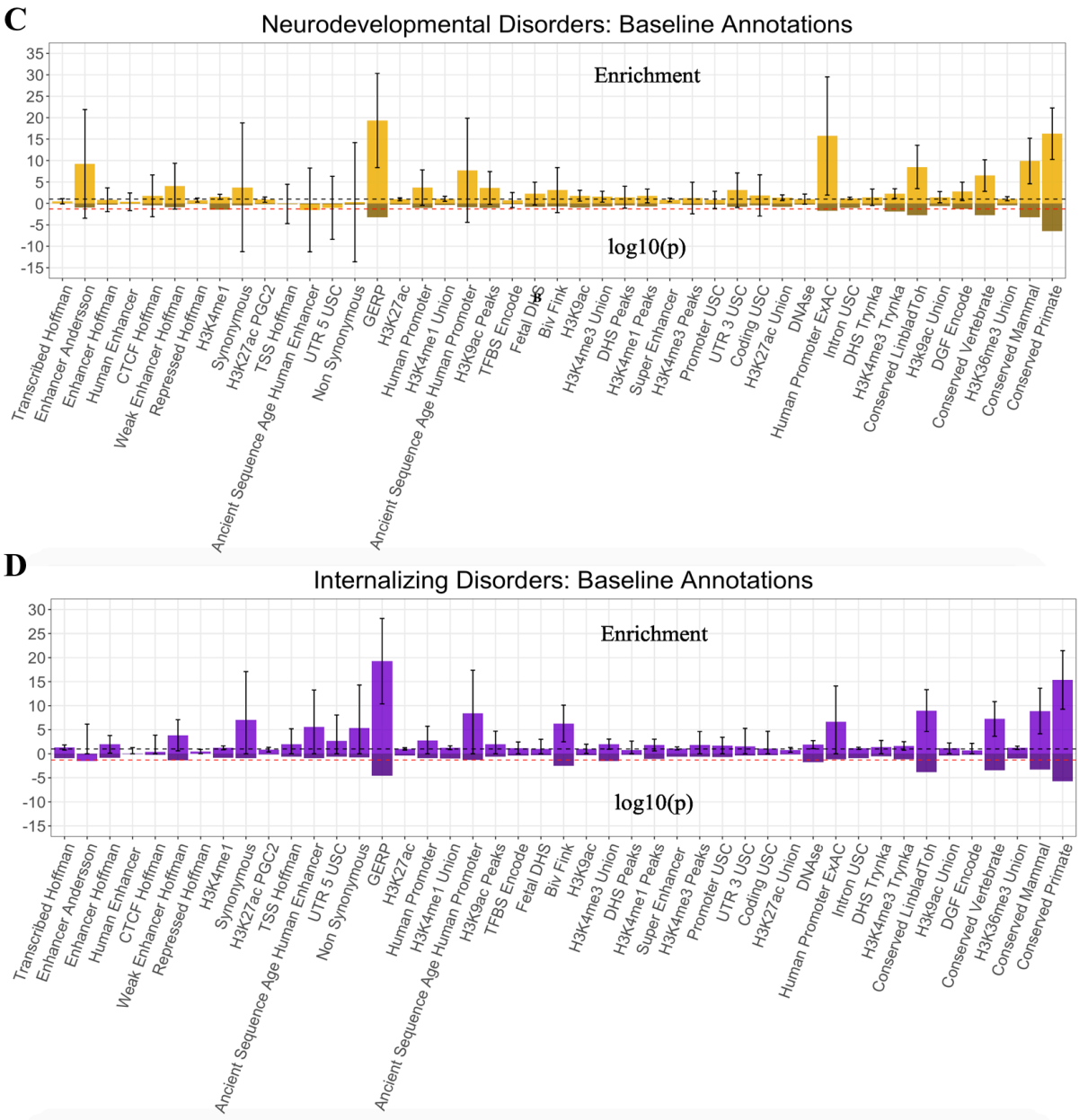

Supplementary Figure 13b. Enrichment of Baseline Annotations from Correlated Factors Model. The top half of each panel depicts the enrichment point estimates, with error bars depicting +/- 1.96 *SEs.* The black dashed line on the top half reflects the null (enrichment = 1). The bottom half of each panel depicts the log10(p) values. The red dashed line on the bottom half reflects log10(p = .05). For comparative purposes across factors, all graphs for the correlated factors model are based on increasing significance for the Psychotic Disorders factor. The scaling of the y-axis across panels differs due to widely discrepant ranges in CIs across factors. Estimates are shown for neurodevelopmental disorders (panel C), and internalizing disorders (panel D). The effective sample size for the factors was Neurodevelpomental Factor (N = 55,932) and Internalizing Factor (N = 455,340).

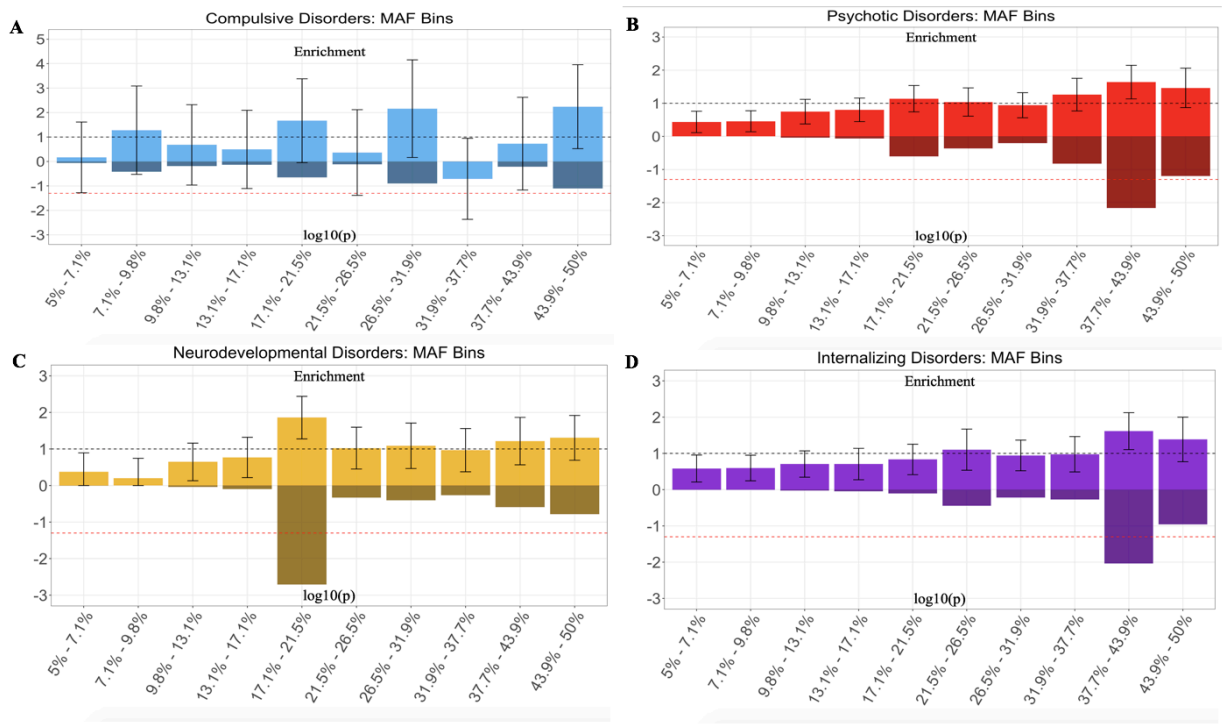

Supplementary Figure 14. Enrichment of MAF Annotations from Correlated Factors Model. The top half of each panel depicts the enrichment point estimates, with error bars depicting +/- 1.96 *SEs.* The black dashed line on the top half reflects the null (enrichment = 1). The bottom half of each panel depicts the log10(p) values. The red dashed line on the bottom half reflects log10(p = .05). For comparative purposes across factors, all graphs for the correlated factors model are based on increasing significance for the psychotic disorders factor. The scaling of the y-axis across panels differs due to widely discrepant ranges in CIs across factors. Estimates are shown for compulsive disorders (panel A), psychotic disorders (panel B), neurodevelopmental disorders (panel C), and internalizing disorders (panel D). The effective sample size for the factors was: Compulsive Factor (*N*= 19,108), Psychotic Factor (*N* = 87,138), Neurodevelpomental Factor (*N* = 55,932), Internalizing Factor (*N* = 455,340), and hierarchical p-factor (*N* = 667,343).

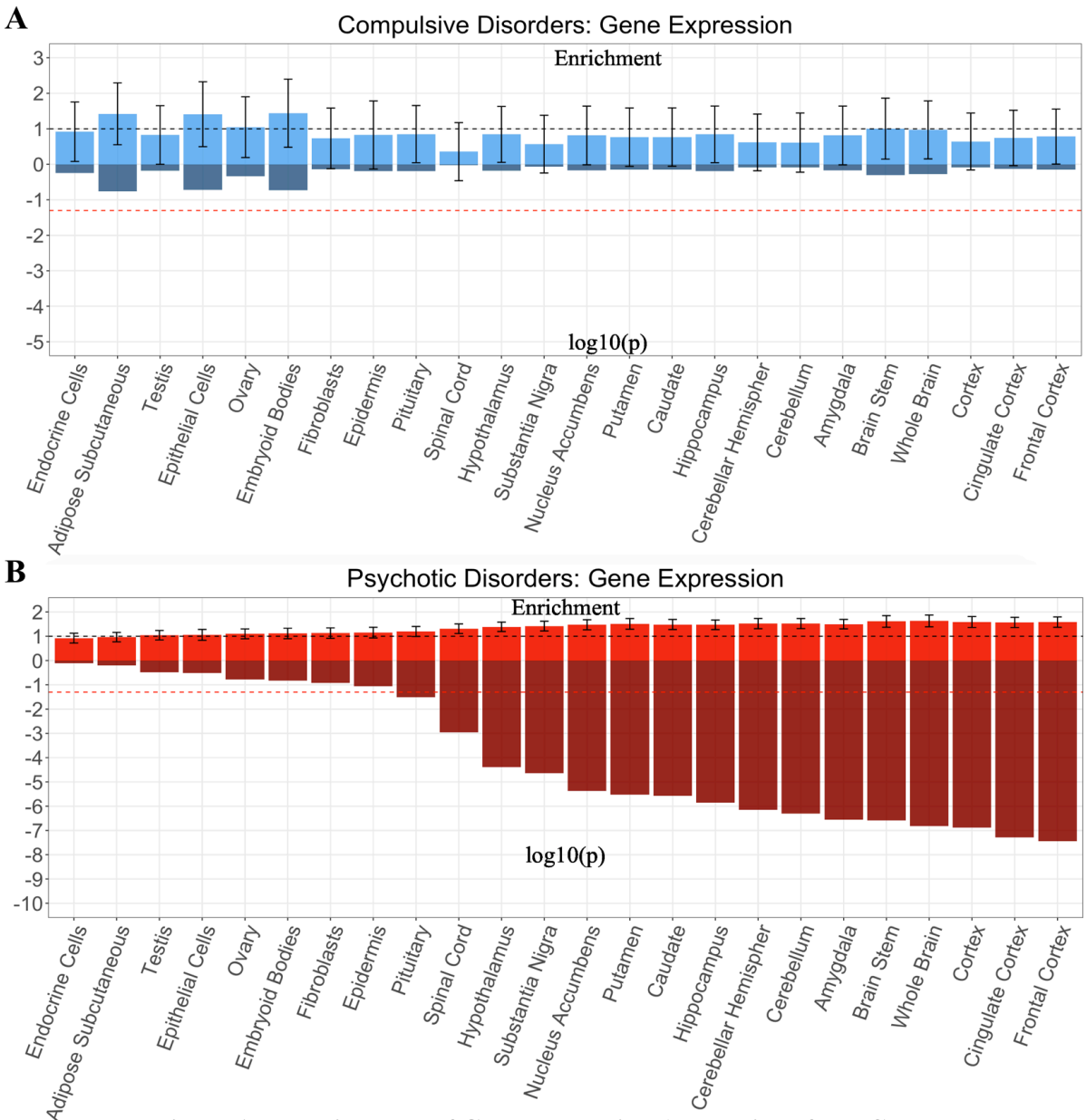

Supplementary Figure 15a. Enrichment of Gene Expression Annotations from Correlated Factors Model. The top half of each panel depicts the enrichment point estimates, with error bars depicting +/- 1.96 *SEs*. The black dashed line on the top half reflects the null (enrichment = 1). The bottom half of each panel depicts the log10(p) values. The red dashed line on the bottom half reflects log10(p = .05). For comparative purposes across factors, all graphs for the correlated factors model are based on increasing significance for the psychotic disorders factor. The scaling of the y-axis across panels differs due to widely discrepant ranges in CIs across factors. Estimates are shown for compulsive disorders (panel A) and psychotic disorders (panel B). The effective sample size for the factors was: Compulsive Factor (*N*= 19,108) and Psychotic Factor (*N*= 87,138).

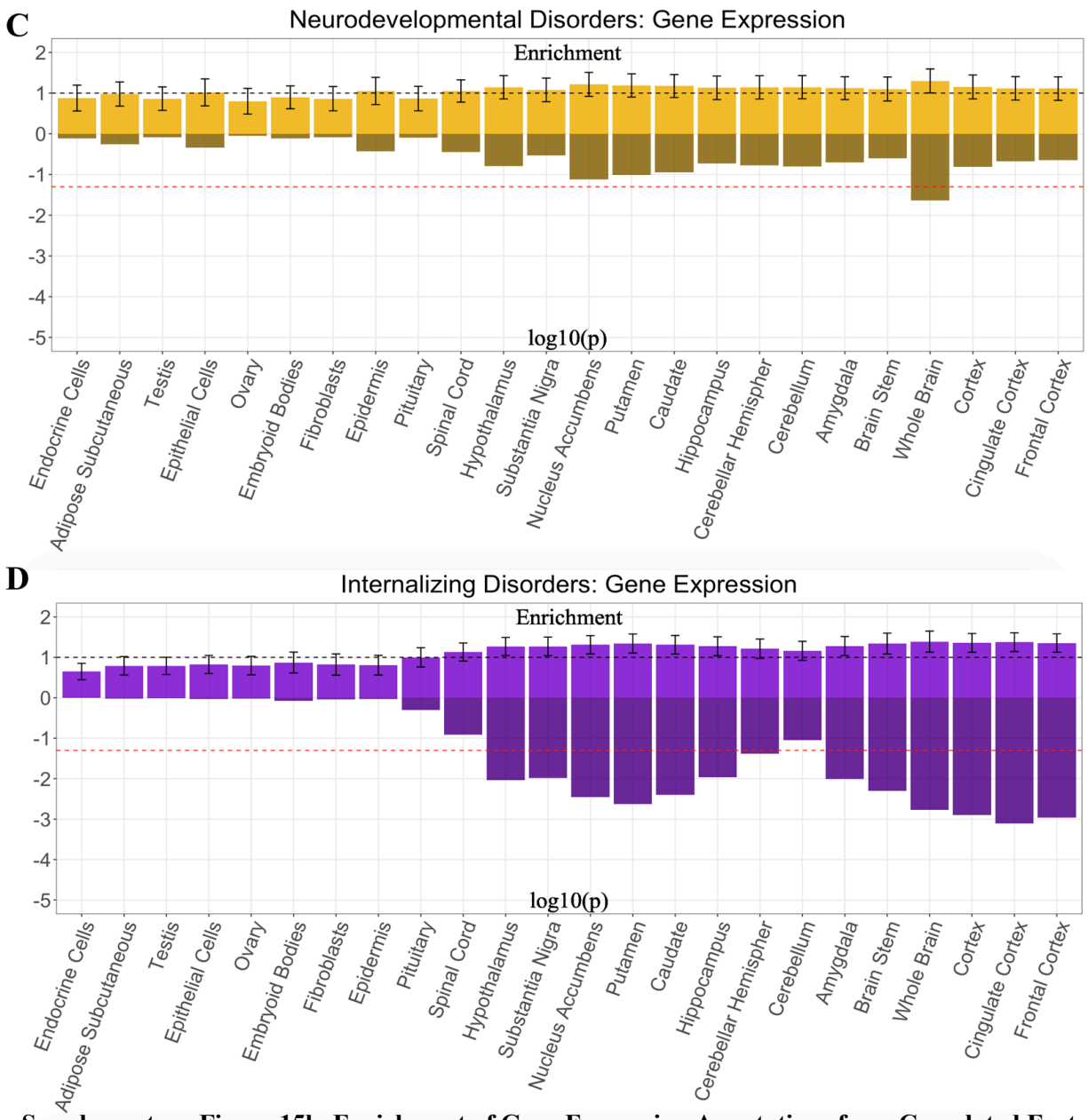

Supplementary Figure 15b. Enrichment of Gene Expression Annotations from Correlated Factors Model. The top half of each panel depicts the enrichment point estimates, with error bars depicting +/- 1.96 *SEs.* The black dashed line on the top half reflects the null (enrichment = 1). The bottom half of each panel depicts the log10(p) values. The red dashed line on the bottom half reflects log10(p = .05). For comparative purposes across factors, all graphs for the correlated factors model are based on increasing significance for the Psychotic Disorders factor. The scaling of the y-axis across panels differs due to widely discrepant ranges in CIs across factors. Estimates are shown for neurodevelopmental disorders (panel C), and internalizing disorders (panel D). The effective sample size for the factors was Neurodevelpomental Factor (N = 55,932) and Internalizing Factor (N = 455,340).

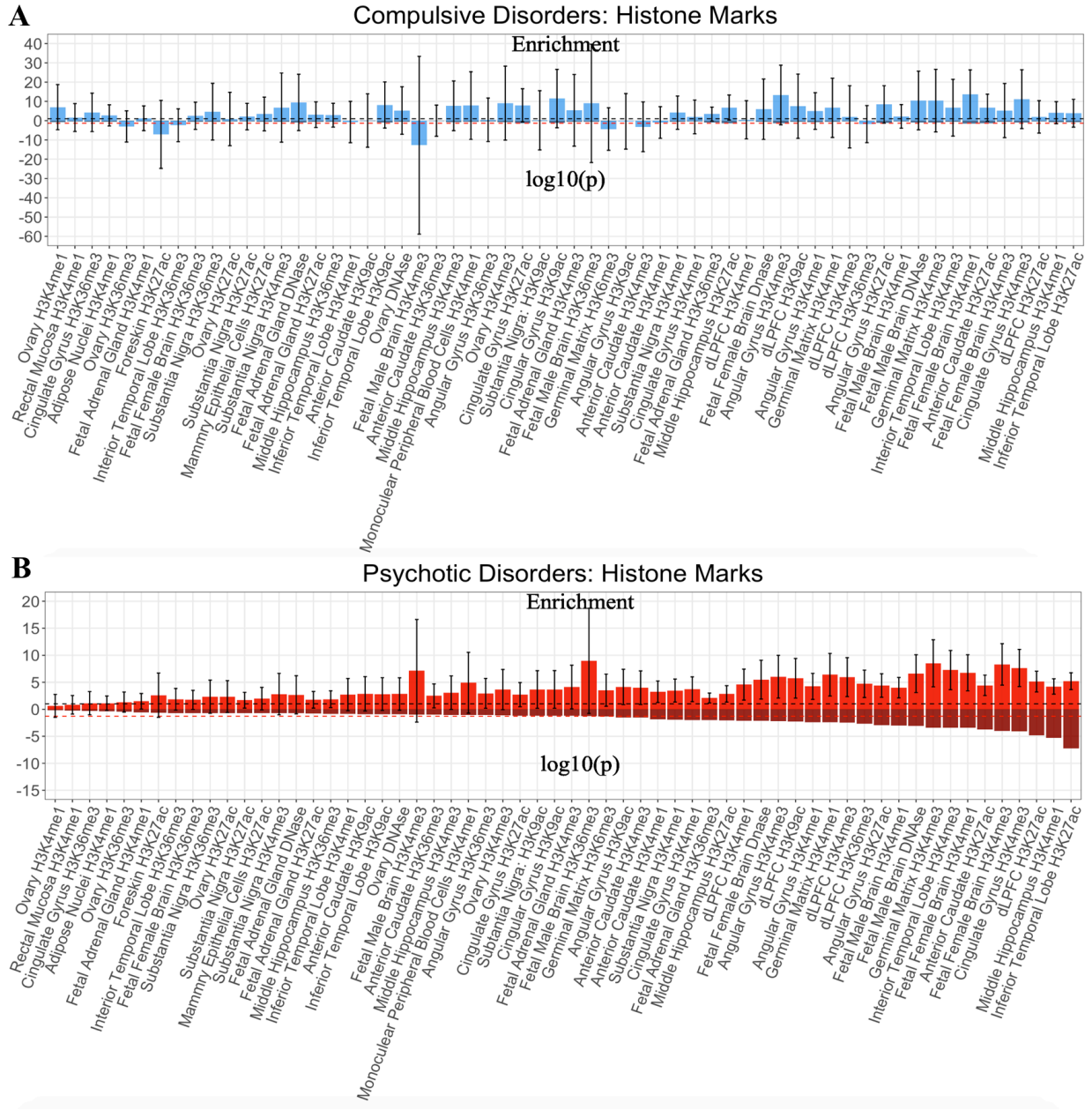

Supplementary Figure 16a. Enrichment of Histone Marks Annotations from Correlated Factors Model. The top half of each panel depicts the enrichment point estimates, with error bars depicting +/- 1.96 *SEs.* The black dashed line on the top half reflects the null (enrichment = 1). The bottom half of each panel depicts the log10(p) values. The red dashed line on the bottom half reflects log10(p = .05). For comparative purposes across factors, all graphs for the correlated factors model are based on increasing significance for the psychotic disorders factor. The scaling of the y-axis across panels differs due to widely discrepant ranges in CIs across factors. Estimates are shown for compulsive disorders (panel A) and psychotic disorders (panel B). The effective sample size for the factors was: Compulsive Factor (*N*= 19,108) and Psychotic Factor (*N*= 87,138).

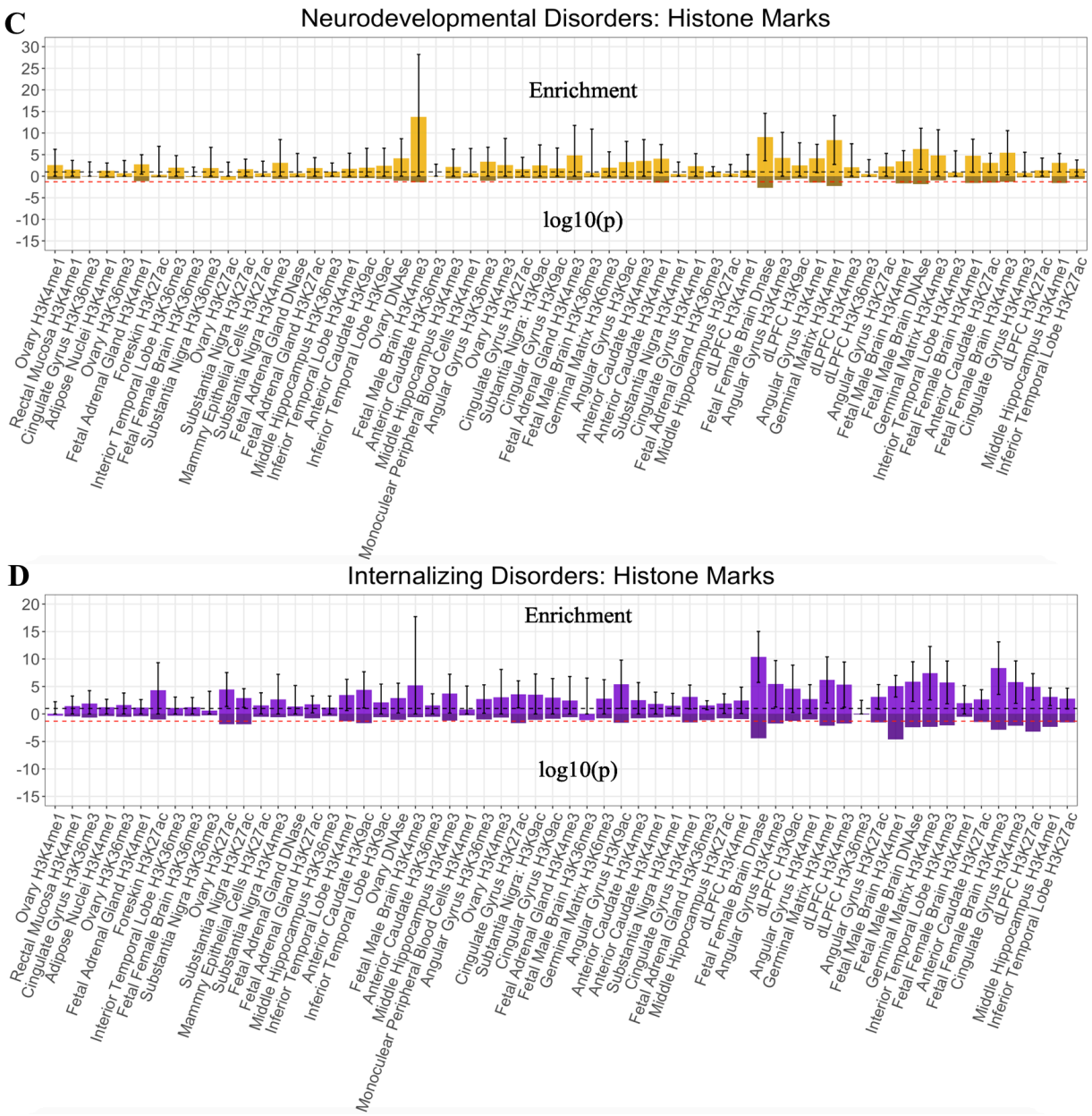

Supplementary Figure 16b. Enrichment of Histone Marks Annotations from Correlated Factors Model. The top half of each panel depicts the enrichment point estimates, with error bars depicting +/- 1.96 *SEs.* The black dashed line on the top half reflects the null (enrichment = 1). The bottom half of each panel depicts the log10(p) values. The red dashed line on the bottom half reflects log10(p = .05). For comparative purposes across factors, all graphs for the correlated factors model are based on increasing significance for the Psychotic Disorders factor. The scaling of the y-axis across panels differs due to widely discrepant ranges in CIs across factors. Estimates are shown for neurodevelopmental disorders (panel C), and internalizing disorders (panel D). The effective sample size for the factors was Neurodevelpomental Factor (N = 55,932) and Internalizing Factor (N = 455,340).

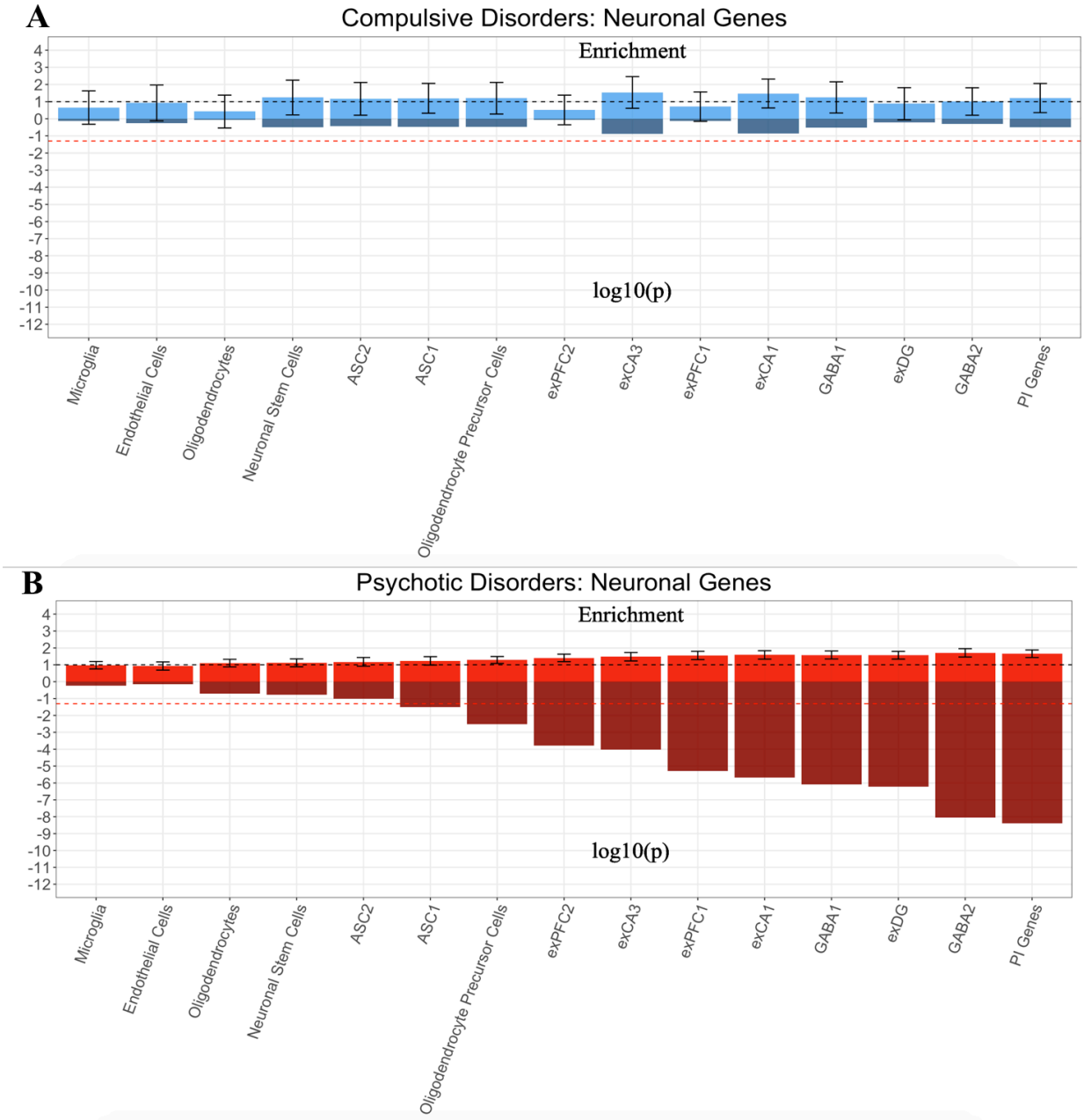

Supplementary Figure 17a. Enrichment of Brain Cell Annotations from Correlated Factors Model. The top half of each panel depicts the enrichment point estimates, with error bars depicting +/- 1.96 *SEs*. The black dashed line on the top half reflects the null (enrichment = 1). The bottom half of each panel depicts the log10(p) values. The red dashed line on the bottom half reflects log10(p = .05). For comparative purposes across factors, all graphs for the correlated factors model are based on increasing significance for the psychotic disorders factor. The scaling of the y-axis across panels differs due to widely discrepant ranges in CIs across factors. Estimates are shown for compulsive disorders (panel A) and psychotic disorders (panel B). The effective sample size for the factors was: Compulsive Factor (*N*= 19,108) and Psychotic Factor (*N*= 87,138).

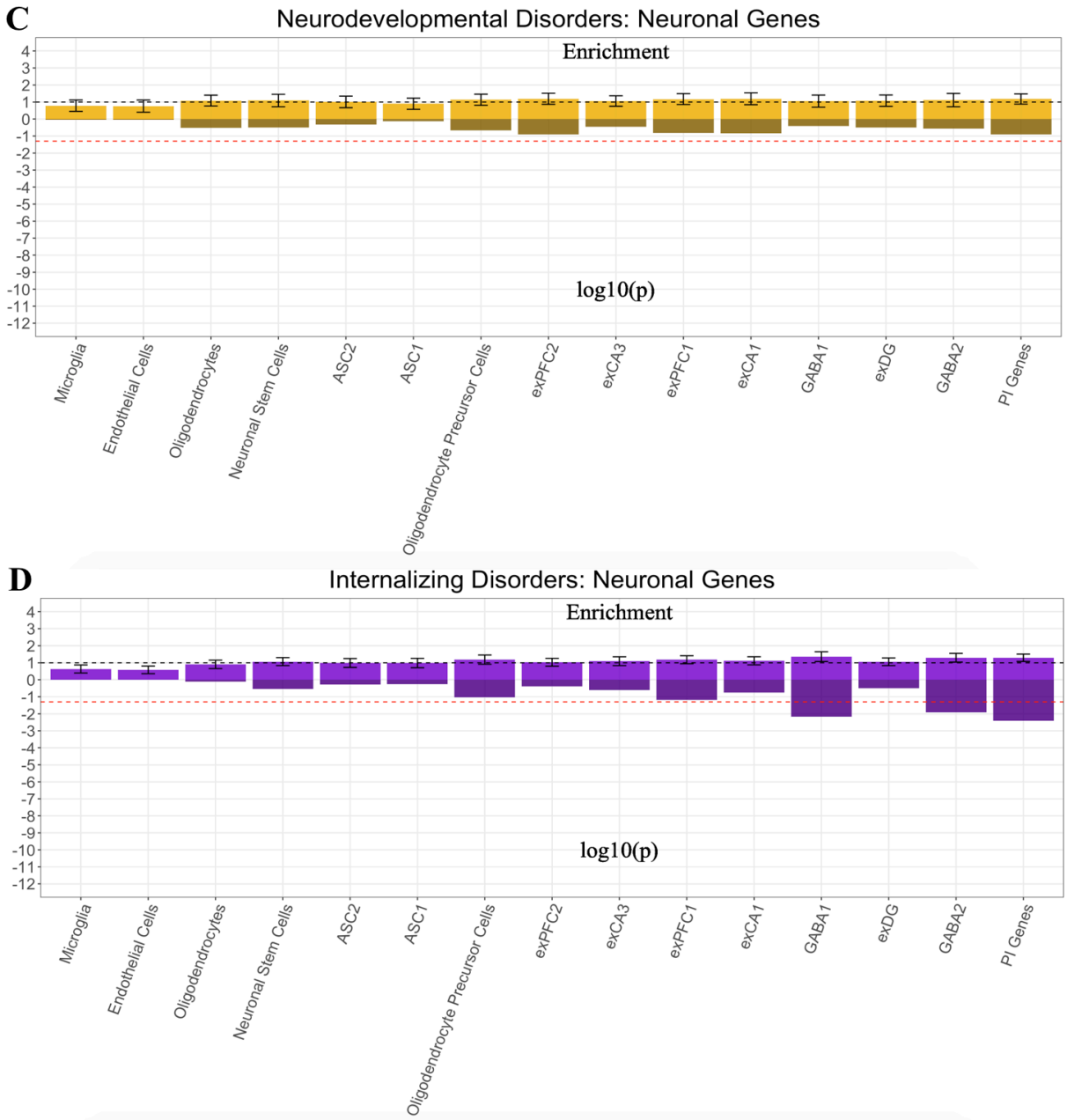

Supplementary Figure 17b. Enrichment of Brain Cell Annotations from Correlated Factors Model. The top half of each panel depicts the enrichment point estimates, with error bars depicting +/- 1.96 *SEs.* The black dashed line on the top half reflects the null (enrichment = 1). The bottom half of each panel depicts the log10(p) values. The red dashed line on the bottom half reflects log10(p = .05). For comparative purposes across factors, all graphs for the correlated factors model are based on increasing significance for the Psychotic Disorders factor. The scaling of the y-axis across panels differs due to widely discrepant ranges in CIs across factors. Estimates are shown for neurodevelopmental disorders (panel C), and internalizing disorders (panel D). The effective sample size for the factors was Neurodevelpomental Factor (N = 55,932) and Internalizing Factor (N = 455,340).

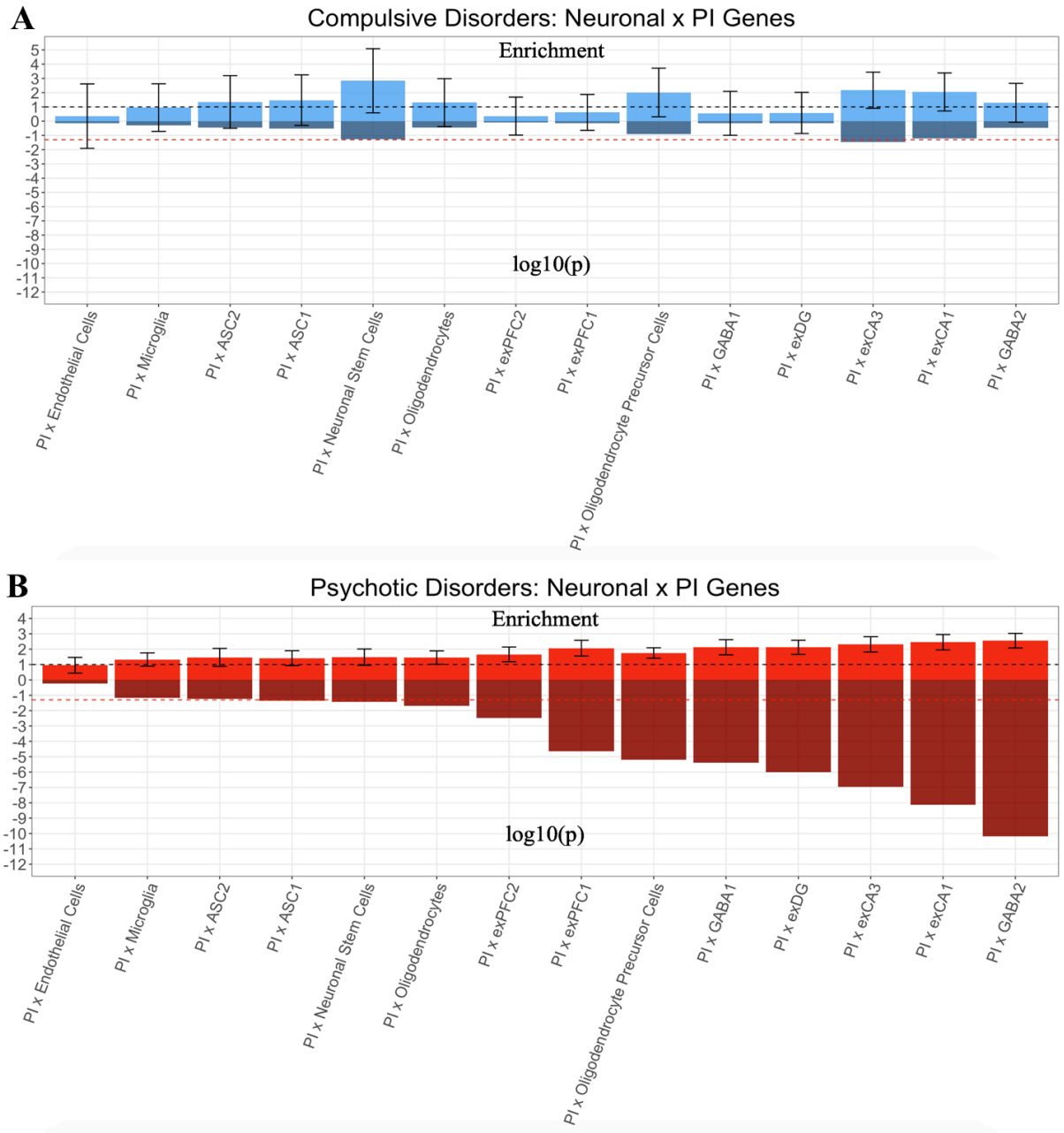

Supplementary Figure 18a. Enrichment of Brain Cell × PI Gene Annotations from Correlated Factors Model. The top half of each panel depicts the enrichment point estimates, with error bars depicting +/- 1.96 *SEs*. The black dashed line on the top half reflects the null (enrichment = 1). The bottom half of each panel depicts the log10(p) values. The red dashed line on the bottom half reflects log10(p = .05). For comparative purposes across factors, all graphs for the correlated factors model are based on increasing significance for the psychotic disorders factor. The scaling of the y-axis across panels differs due to widely discrepant ranges in CIs across factors. Estimates are shown for compulsive disorders (panel A) and psychotic disorders (panel B). The effective sample size for the factors was: Compulsive Factor (*N*= 19,108) and Psychotic Factor (*N*= 87,138).

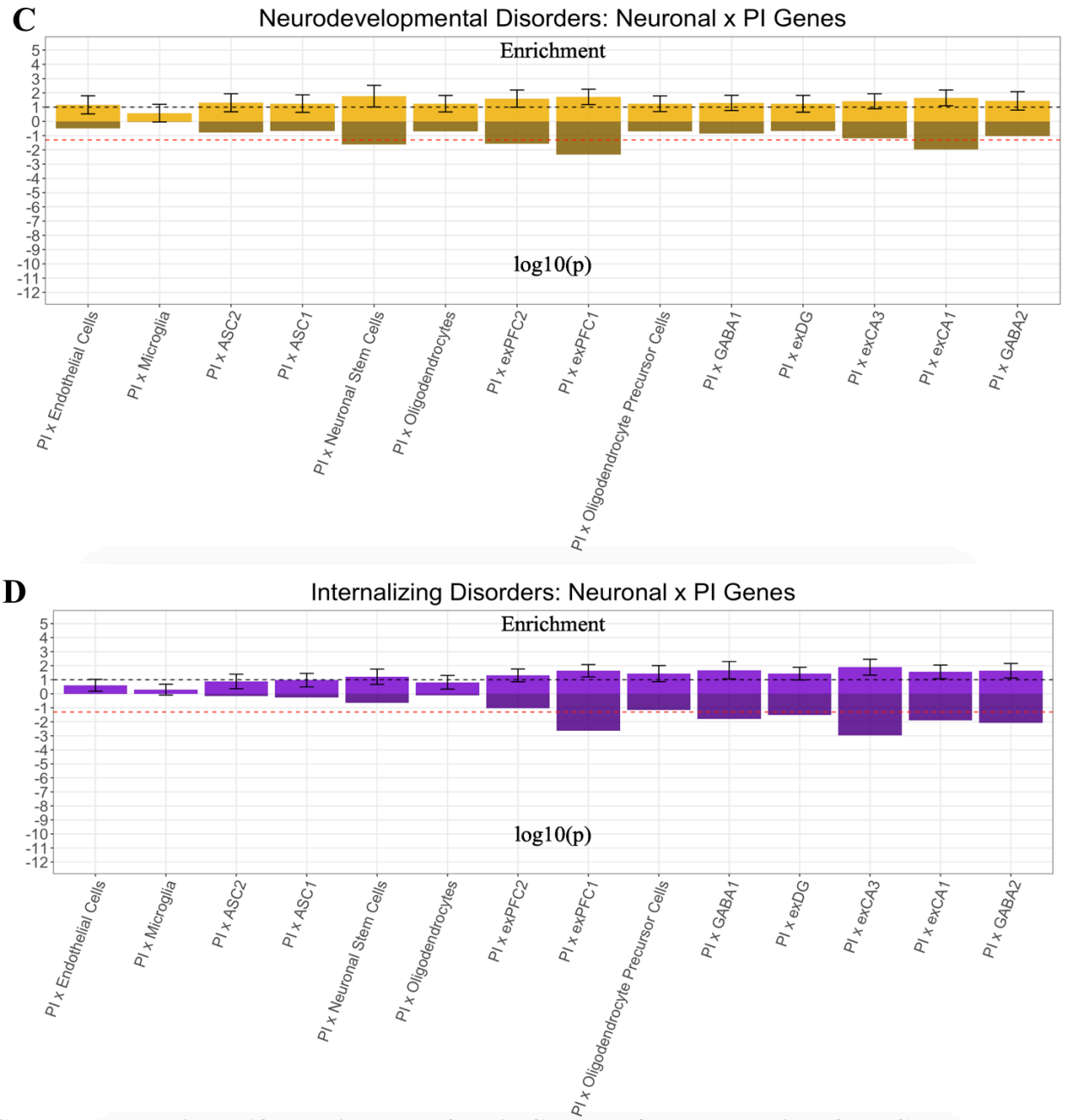

Supplementary Figure 18b. Enrichment of Brain Cell × PI Gene Annotations from Correlated Factors Model. The top half of each panel depicts the enrichment point estimates, with error bars depicting +/- 1.96 *SEs.* The black dashed line on the top half reflects the null (enrichment = 1). The bottom half of each panel depicts the log10(p) values. The red dashed line on the bottom half reflects log10(p = .05). For comparative purposes across factors, all graphs for the correlated factors model are based on increasing significance for the Psychotic Disorders factor. The scaling of the y-axis across panels differs due to widely discrepant ranges in CIs across factors. Estimates are shown for neurodevelopmental disorders (panel C), and internalizing disorders (panel D). The effective sample size for the factors was Neurodevelpomental Factor (*N* = 55,932) and Internalizing Factor (*N* = 455,340).

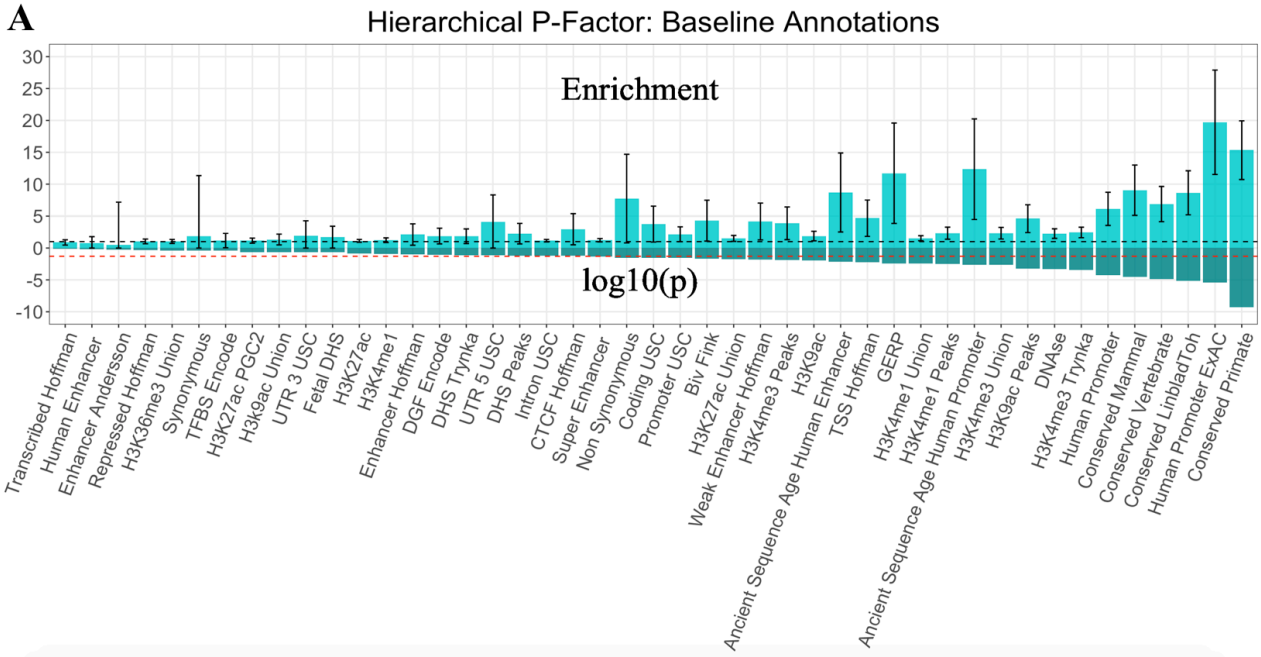

Supplementary Figure 19a. Enrichment of Baseline Annotations from Hierarchical Model. The top half of each panel depicts the enrichment point estimates, with error bars indicating +/- 1.96 *SE*s. The black dashed line on the top half reflects the null (enrichment = 1). The bottom half of each panel depicts the log10(p) values. The red dashed line on the bottom half reflects log10(p = .05). The scaling of the y-axis across panels differs due to widely discrepant ranges in CIs across factors. For comparative purposes across factors, all graphs for the hierarchical factor model are based on increasing significance for the hierarchical *p*-factor. Estimates are shown for the hierarchical *p*-factor (panel A). The effective sample size for the *p*-factor was N = 667,343.

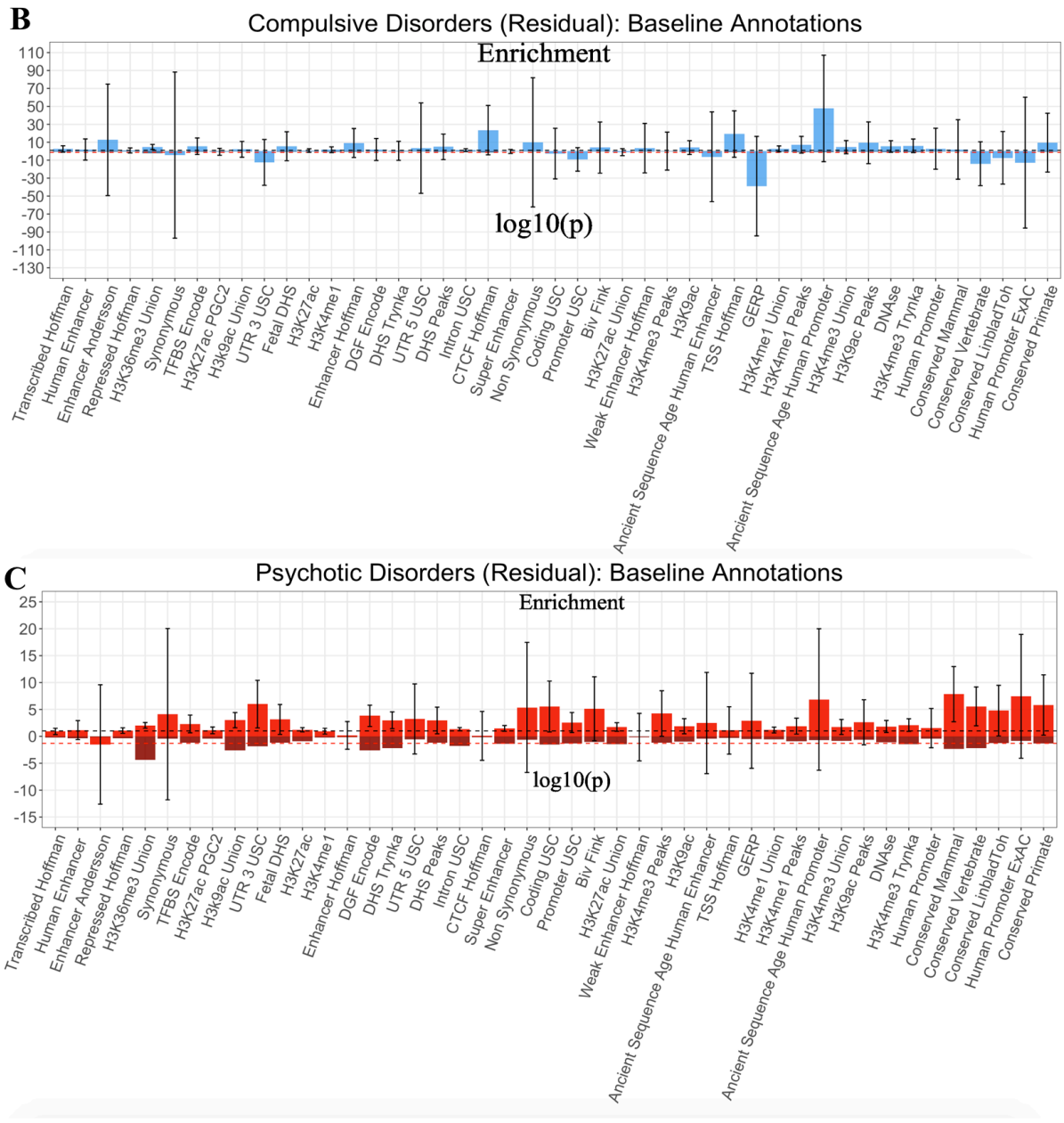

Supplementary Figure 19b. Enrichment of Baseline Annotations from Hierarchical Model. The top half of each panel depicts the enrichment point estimates, with error bars indicating +/- 1.96 *SEs.* The black dashed line on the top half reflects the null (enrichment = 1). The bottom half of each panel depicts the log10(p) values. The red dashed line on the bottom half reflects log10(p = .05). scaling of the y-axis across panels differs due to widely discrepant ranges in CIs across factors. For comparative purposes across factors, all graphs for the hierarchical factor model are based on increasing significance for the hierarchical *p*-factor. Estimates are shown for the residuals of the compulsive disorders (panel B) and psychotic disorders (panel C) factors after accounting for variance explained by the *p*-factor. The total effective sample size for the factors was: Compulsive Factor (*N*= 19,108) and Psychotic Factor (*N* = 87,138); however, it is important to note that these are enrichment estimates for the residual variance in the factors such that the effective *N* for just these residual components will be much smaller.

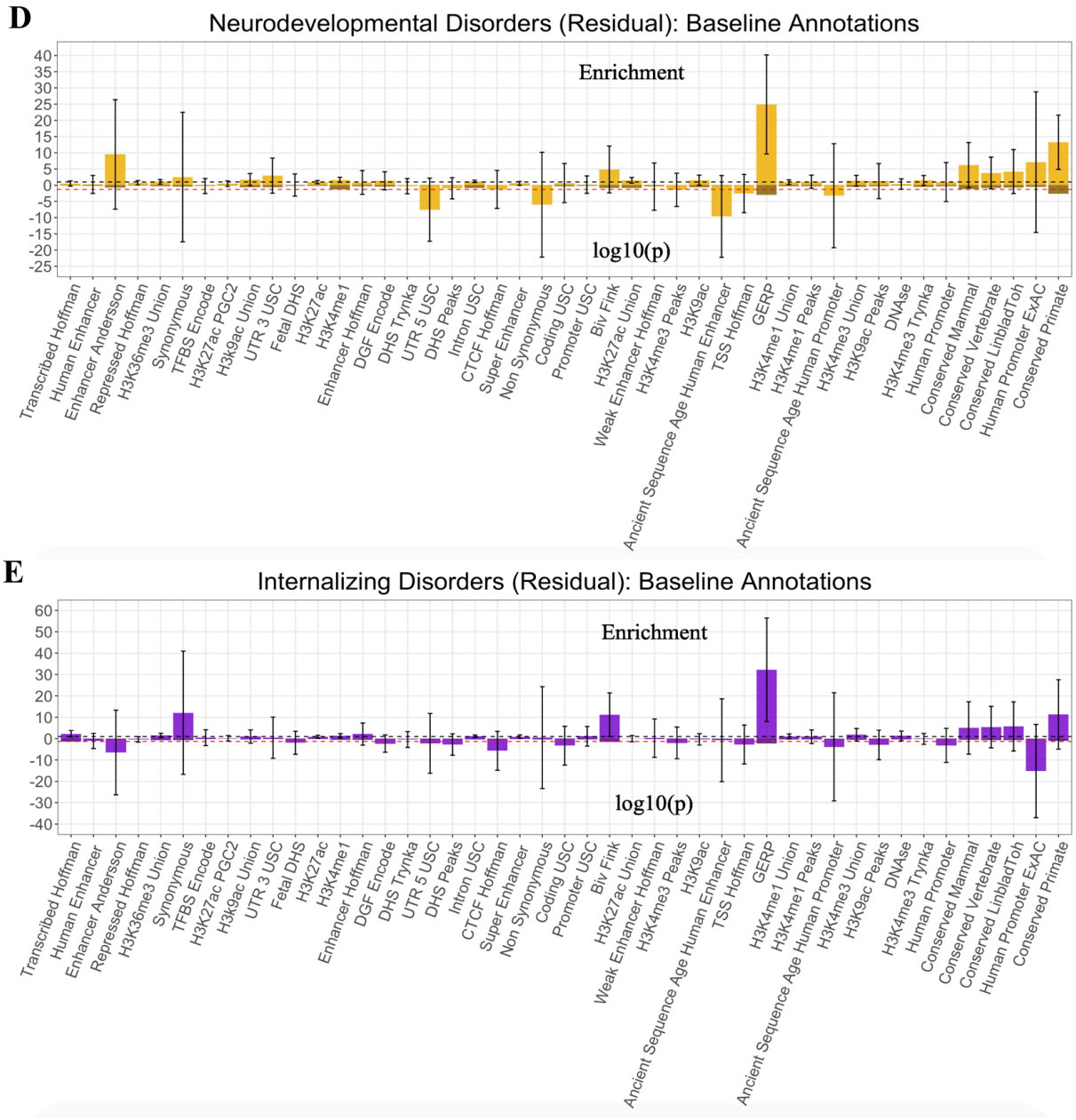

Supplementary Figure 19c. Enrichment of Baseline Annotations from Hierarchical Model. The top half of each panel depicts the enrichment point estimates, with error bars indicating +/- 1.96 *SE*s. The black dashed line on the top half reflects the null (enrichment = 1). The bottom half of each panel depicts the log10(p) values. The red dashed line on the bottom half reflects log10(p = .05). The scaling of the y-axis across panels differs due to widely discrepant ranges in CIs across factors. For comparative purposes across factors, all graphs for the hierarchical factor model are based on increasing significance for the hierarchical *p*-factor. Estimates are shown for the residuals of the neurodevelopmental disorders (panel D) and internalizing (panel C) factors after accounting for variance explained by the *p*-factor. The effective sample size for the factors was Neurodevelpomental Factor (N= 55,932) and Internalizing Factor (N= 455,340) ; however, it is important to note that these are enrichment estimates for the residual variance in the factors such that the effective N for just these residual components will be much smaller.

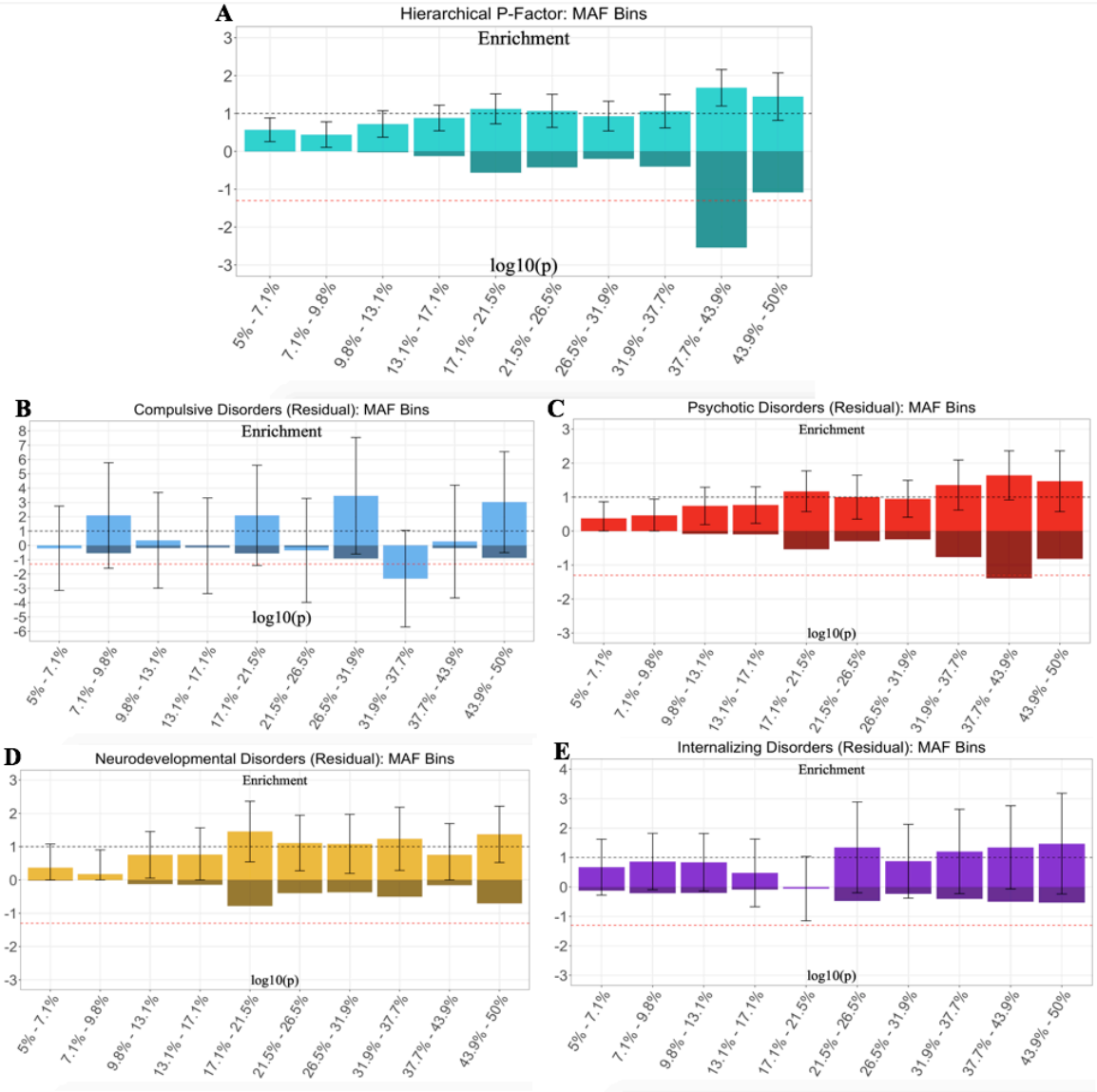

Supplementary Figure 20. Enrichment of MAF Annotations from Hierarchical Model. The top half of each panel depicts the enrichment point estimates, with error bars indicating 95% confidence intervals. The black dashed line on the top half reflects the null (enrichment = 1). The bottom half of each panel depicts the log10(p) values. The red dashed line on the bottom half reflects log10(p = .05). The scaling of the y-axis across panels differs due to widely discrepant ranges in CIs across factors. For comparative purposes across factors, all graphs for the hierarchical factor model are based on increasing significance for the hierarchical *p*-factor. Estimates are shown for the hierarchical *p*-factor (panel A), and the residuals of the 4 factors after accounting for variance explained by the *p*-factor: compulsive disorders (panel B), psychotic disorders (panel C), neurodevelopmental disorders (panel D), and internalizing disorders (panel E). The effective sample size for the *p*-factor was N = 667,343. The total effective sample size for the factors was: Compulsive Factor (N = 19,108), Psychotic Factor (N = 87,138), Neurodevelpomental Factor (N = 55,932) and Internalizing Factor (N = 455,340); however, it is important to note that these are enrichment estimates for the residual variance in the factors such that the effective N for just these residual components will be much smaller.

Supplementary Figure 21a. Enrichment of Gene Expression Annotations from Hierarchical Model. The top half of each panel depicts the enrichment point estimates, with error bars indicating +/- 1.96 *SE*s. The black dashed line on the top half reflects the null (enrichment = 1). The bottom half of each panel depicts the log10(p) values. The red dashed line on the bottom half reflects log10(p = .05). The scaling of the y-axis across panels differs due to widely discrepant ranges in CIs across factors. For comparative purposes across factors, all graphs for the hierarchical factor model are based on increasing significance for the hierarchical *p*-factor. Estimates are shown for the hierarchical *p*-factor (panel A). The effective sample size for the *p*-factor was N = 667,343.

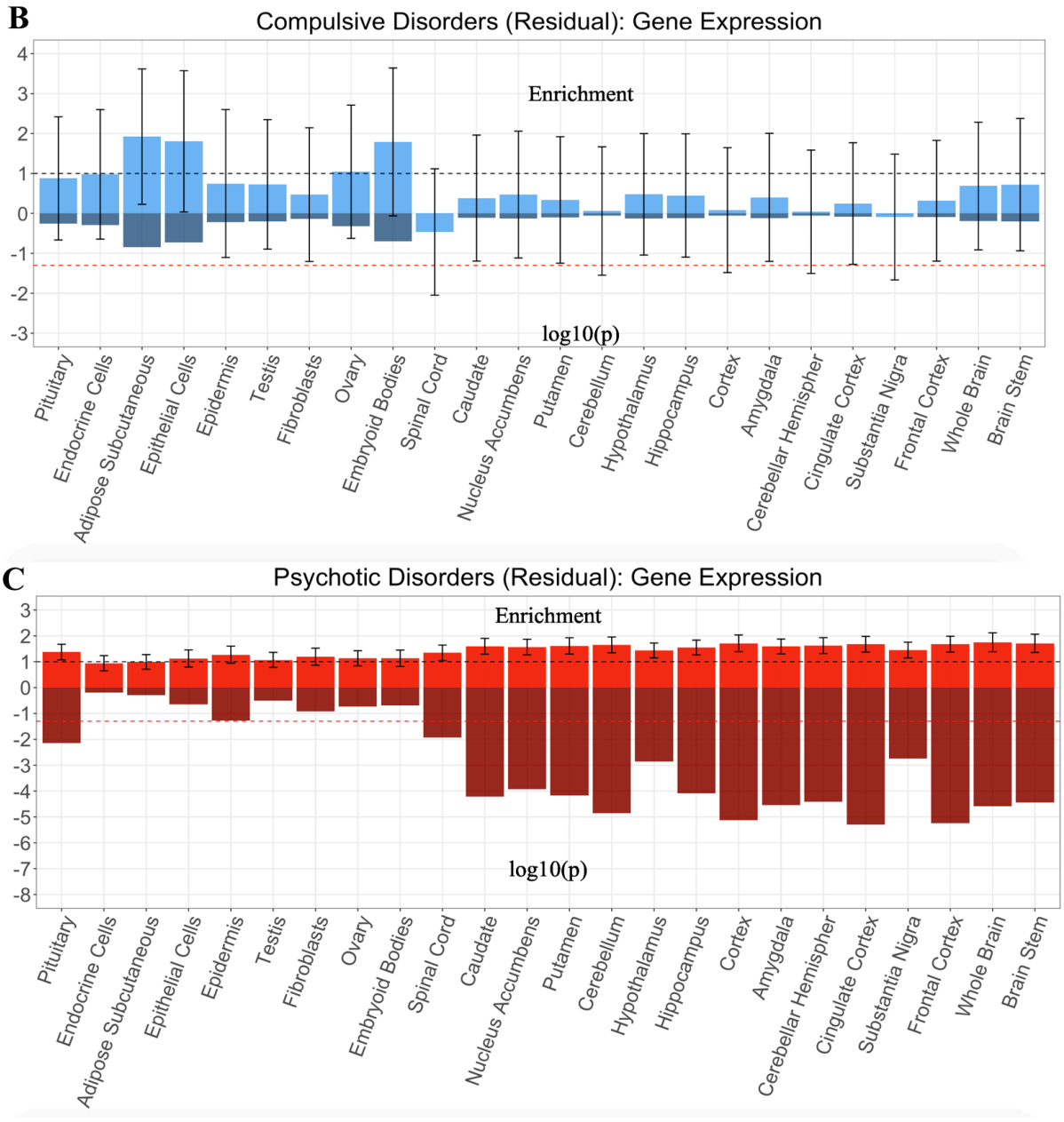

Supplementary Figure 21b. Enrichment of Gene Expression Annotations from Hierarchical Model. The top half of each panel depicts the enrichment point estimates, with error bars indicating +/- 1.96 *SEs.* The black dashed line on the top half reflects the null (enrichment = 1). The bottom half of each panel depicts the log10(p) values. The red dashed line on the bottom half reflects log10(p = .05). scaling of the y-axis across panels differs due to widely discrepant ranges in CIs across factors. For comparative purposes across factors, all graphs for the hierarchical factor model are based on increasing significance for the hierarchical *p*-factor. Estimates are shown for the residuals of the compulsive disorders (panel B) and psychotic disorders (panel C) factors after accounting for variance explained by the *p*-factor. The total effective sample size for the factors was: Compulsive Factor (*N*= 19,108) and Psychotic Factor (*N* = 87,138); however, it is important to note that these are enrichment estimates for the residual variance in the factors such that the effective *N* for just these residual components will be much smaller.

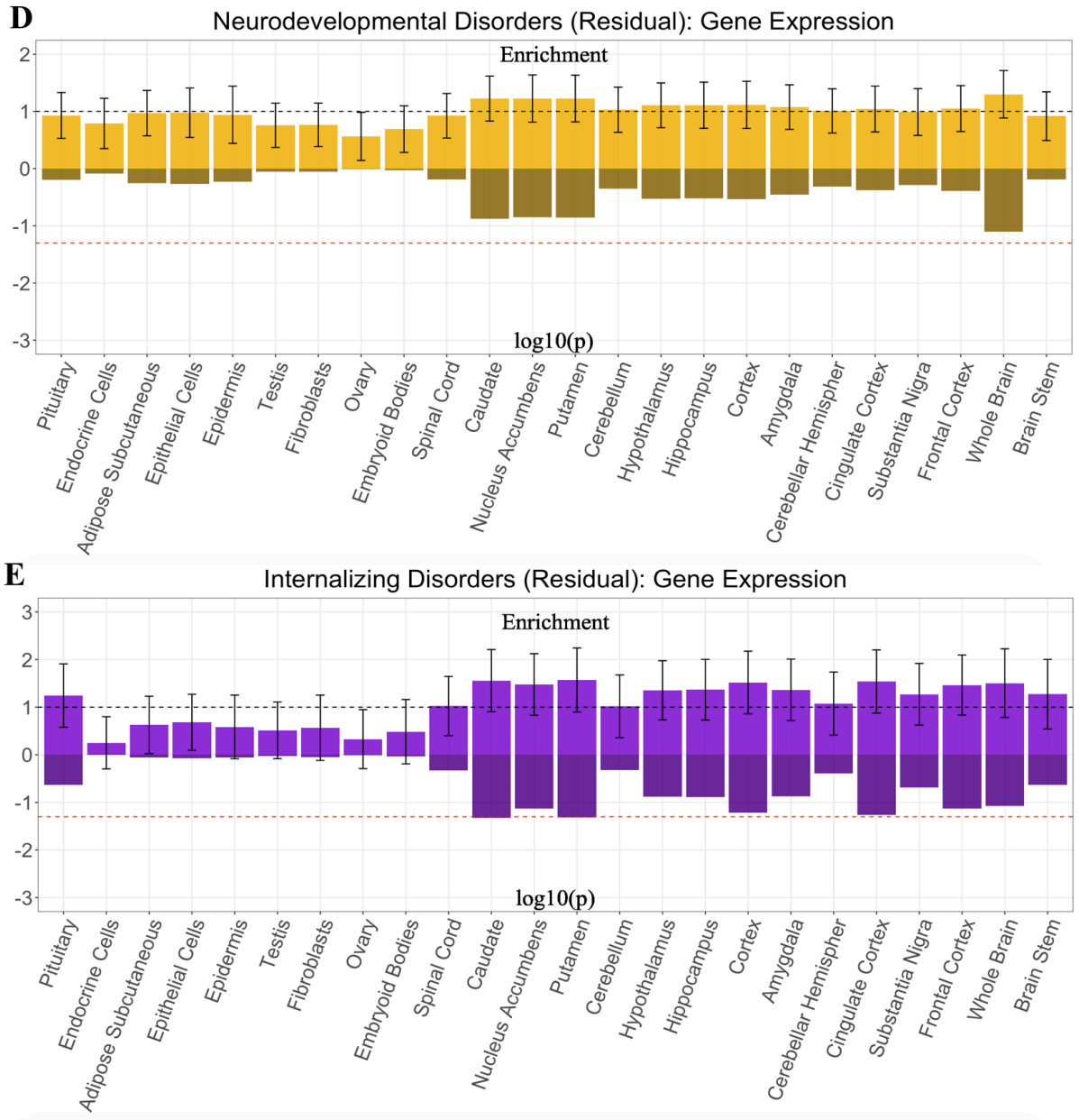

Supplementary Figure 21c. Enrichment of Gene Expression Annotations from Hierarchical Model. The top half of each panel depicts the enrichment point estimates, with error bars indicating +/- 1.96 *SE*s. The black dashed line on the top half reflects the null (enrichment = 1). The bottom half of each panel depicts the log10(p) values. The red dashed line on the bottom half reflects log10(p = .05). The scaling of the y-axis across panels differs due to widely discrepant ranges in CIs across factors. For comparative purposes across factors, all graphs for the hierarchical factor model are based on increasing significance for the hierarchical *p*-factor. Estimates are shown for the residuals of the neurodevelopmental disorders (panel D) and internalizing (panel C) factors after accounting for variance explained by the *p*-factor. The effective sample size for the factors was Neurodevelpomental Factor (*N*= 55,932) and Internalizing Factor (*N*= 455,340) ; however, it is important to note that these are enrichment estimates for the residual variance in the factors such that the effective *N* for just these residual components will be much smaller.

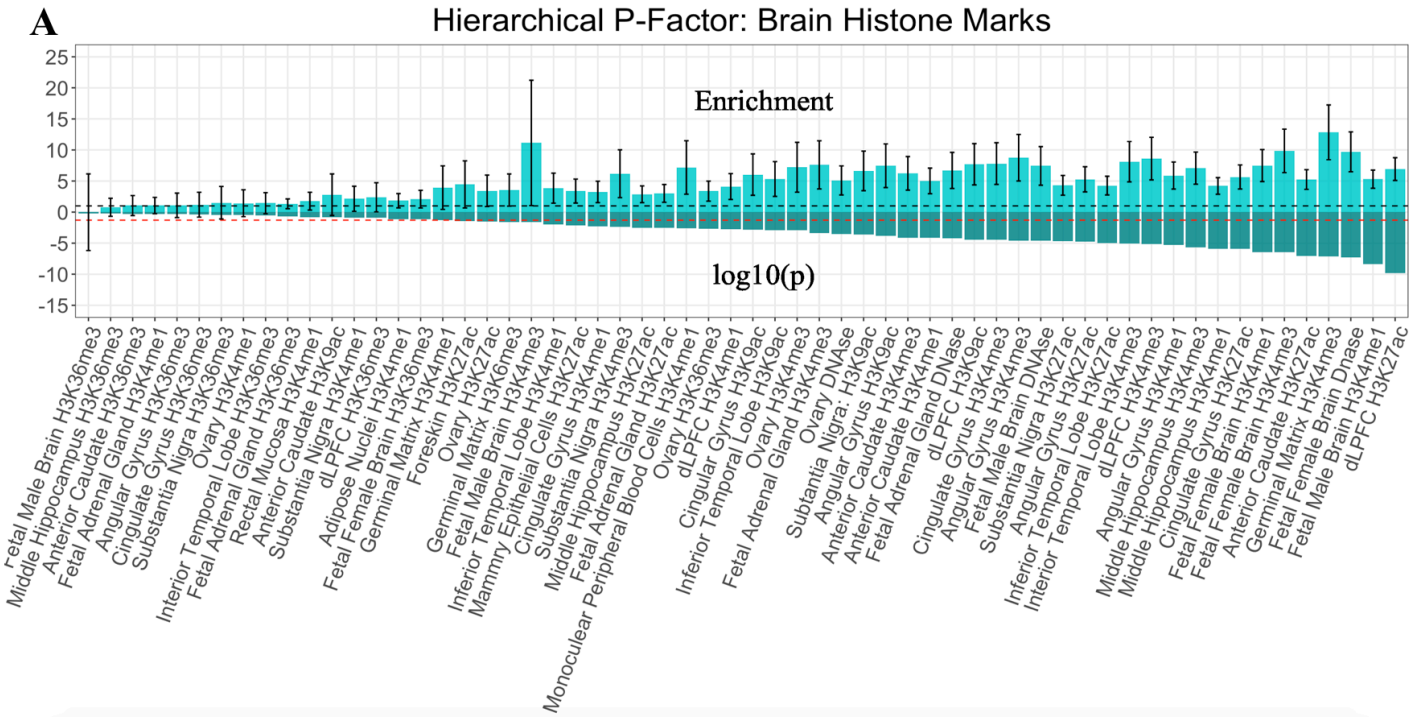

Supplementary Figure 22a. Enrichment of Histone Marks Annotations from Hierarchical Model. The top half of each panel depicts the enrichment point estimates, with error bars indicating +/- 1.96 *SE*s. The black dashed line on the top half reflects the null (enrichment = 1). The bottom half of each panel depicts the log10(p) values. The red dashed line on the bottom half reflects log10(p = .05). The scaling of the y-axis across panels differs due to widely discrepant ranges in CIs across factors. For comparative purposes across factors, all graphs for the hierarchical factor model are based on increasing significance for the hierarchical *p*-factor. Estimates are shown for the hierarchical *p*-factor (panel A). The effective sample size for the *p*-factor was N = 667,343.

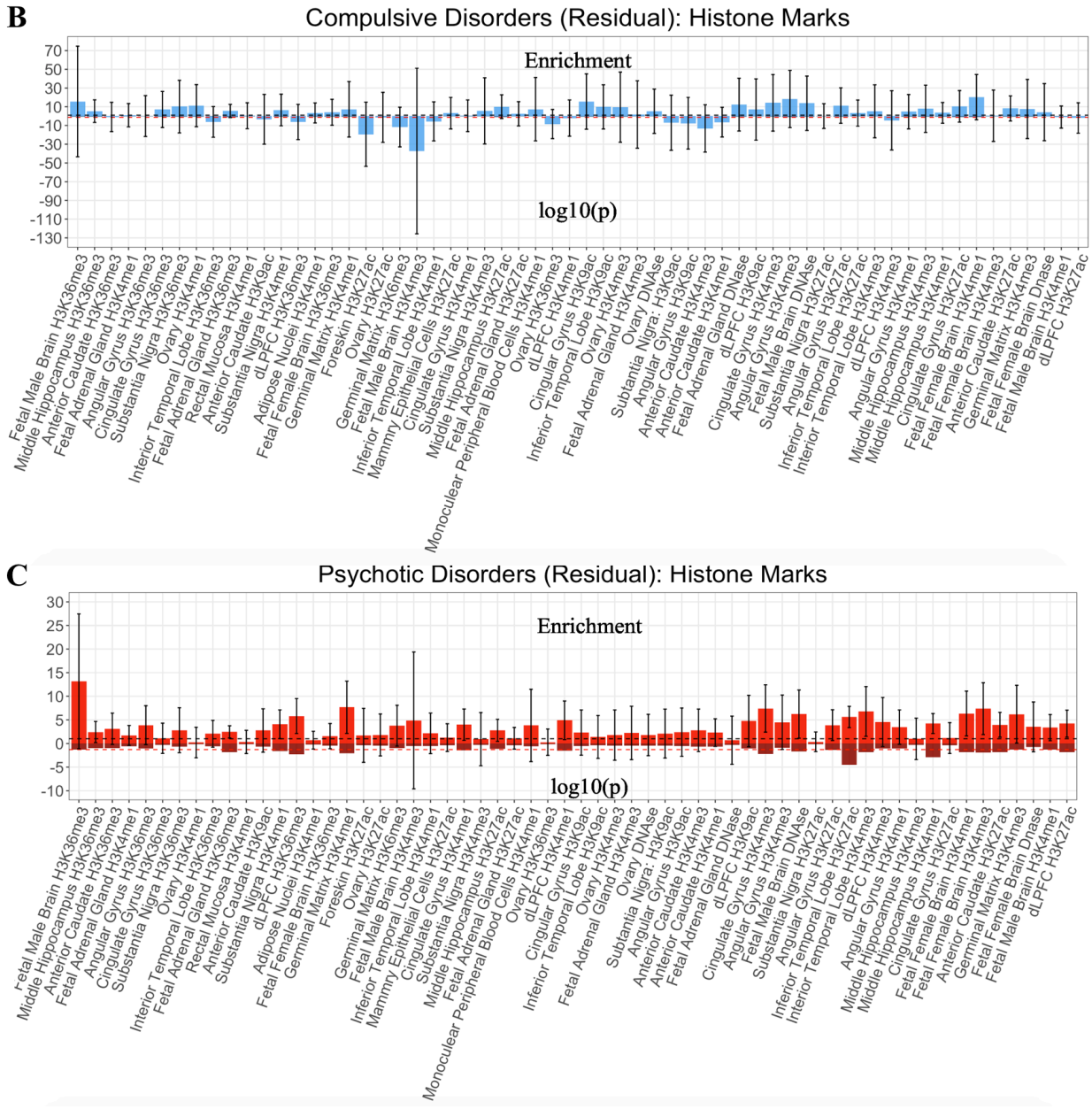

Supplementary Figure 22b. Enrichment of Histone Marks Annotations from Hierarchical Model. The top half of each panel depicts the enrichment point estimates, with error bars indicating +/- 1.96 *SEs.* The black dashed line on the top half reflects the null (enrichment = 1). The bottom half of each panel depicts the log10(p) values. The red dashed line on the bottom half reflects log10(p = .05). scaling of the y-axis across panels differs due to widely discrepant ranges in CIs across factors. For comparative purposes across factors, all graphs for the hierarchical factor model are based on increasing significance for the hierarchical *p*-factor. Estimates are shown for the residuals of the compulsive disorders (panel B) and psychotic disorders (panel C) factors after accounting for variance explained by the *p*-factor. The total effective sample size for the factors was: Compulsive Factor (*N*= 19,108) and Psychotic Factor (*N* = 87,138); however, it is important to note that these are enrichment estimates for the residual variance in the factors such that the effective *N* for just these residual components will be much smaller.

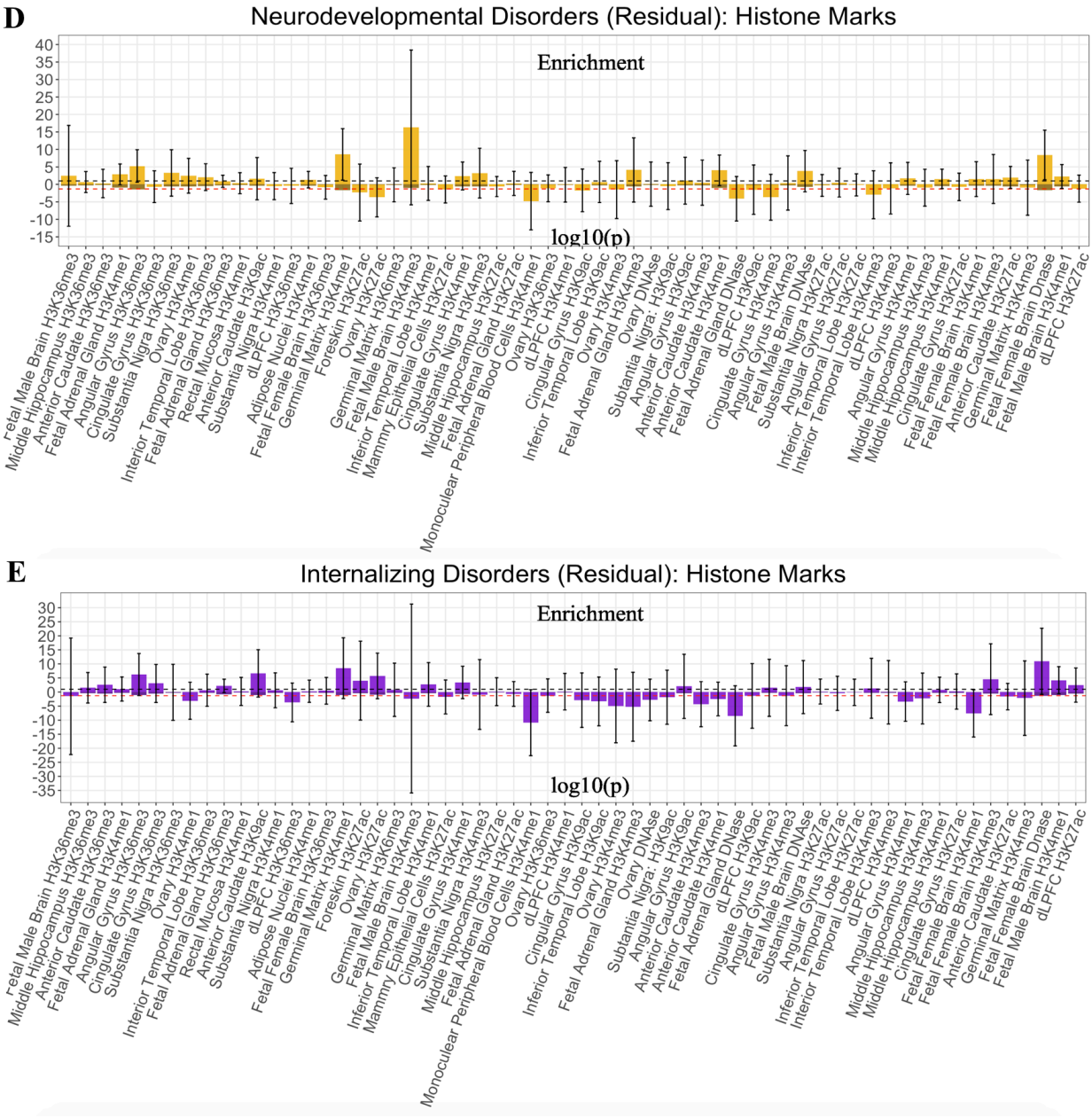

Supplementary Figure 22c. Enrichment of Histone Marks Annotations from Hierarchical Model. The top half of each panel depicts the enrichment point estimates, with error bars indicating +/- 1.96 *SE*s. The black dashed line on the top half reflects the null (enrichment = 1). The bottom half of each panel depicts the log10(p) values. The red dashed line on the bottom half reflects log10(p = .05). The scaling of the y-axis across panels differs due to widely discrepant ranges in CIs across factors. For comparative purposes across factors, all graphs for the hierarchical factor model are based on increasing significance for the hierarchical *p*-factor. Estimates are shown for the residuals of the neurodevelopmental disorders (panel D) and internalizing (panel C) factors after accounting for variance explained by the *p*-factor. The effective sample size for the factors was Neurodevelpomental Factor (*N*= 55,932) and Internalizing Factor (*N*= 455,340) ; however, it is important to note that these are enrichment estimates for the residual variance in the factors such that the effective *N* for just these residual components will be much smaller.

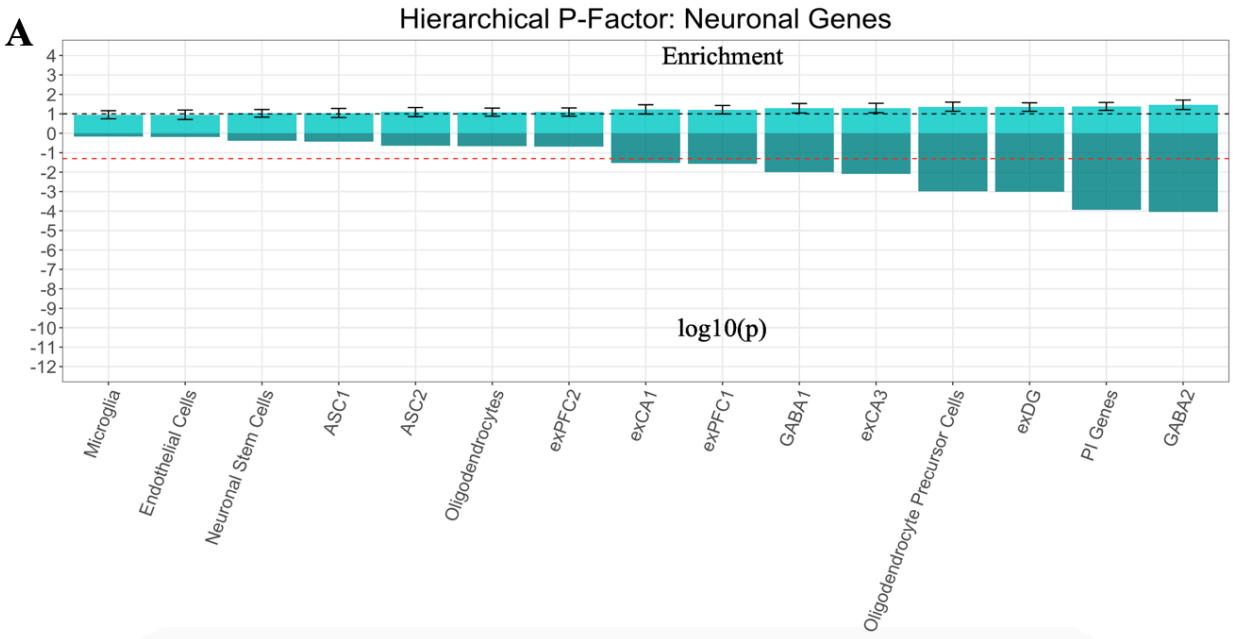

Supplementary Figure 23a. Enrichment of Brain Cell Annotations from Hierarchical Model. The top half of each panel depicts the enrichment point estimates, with error bars indicating +/- 1.96 *SE*s. The black dashed line on the top half reflects the null (enrichment = 1). The bottom half of each panel depicts the log10(p) values. The red dashed line on the bottom half reflects log10(p = .05). The scaling of the y-axis across panels differs due to widely discrepant ranges in CIs across factors. For comparative purposes across factors, all graphs for the hierarchical factor model are based on increasing significance for the hierarchical *p*-factor. Estimates are shown for the hierarchical *p*-factor (panel A). The effective sample size for the *p*-factor was N = 667,343.

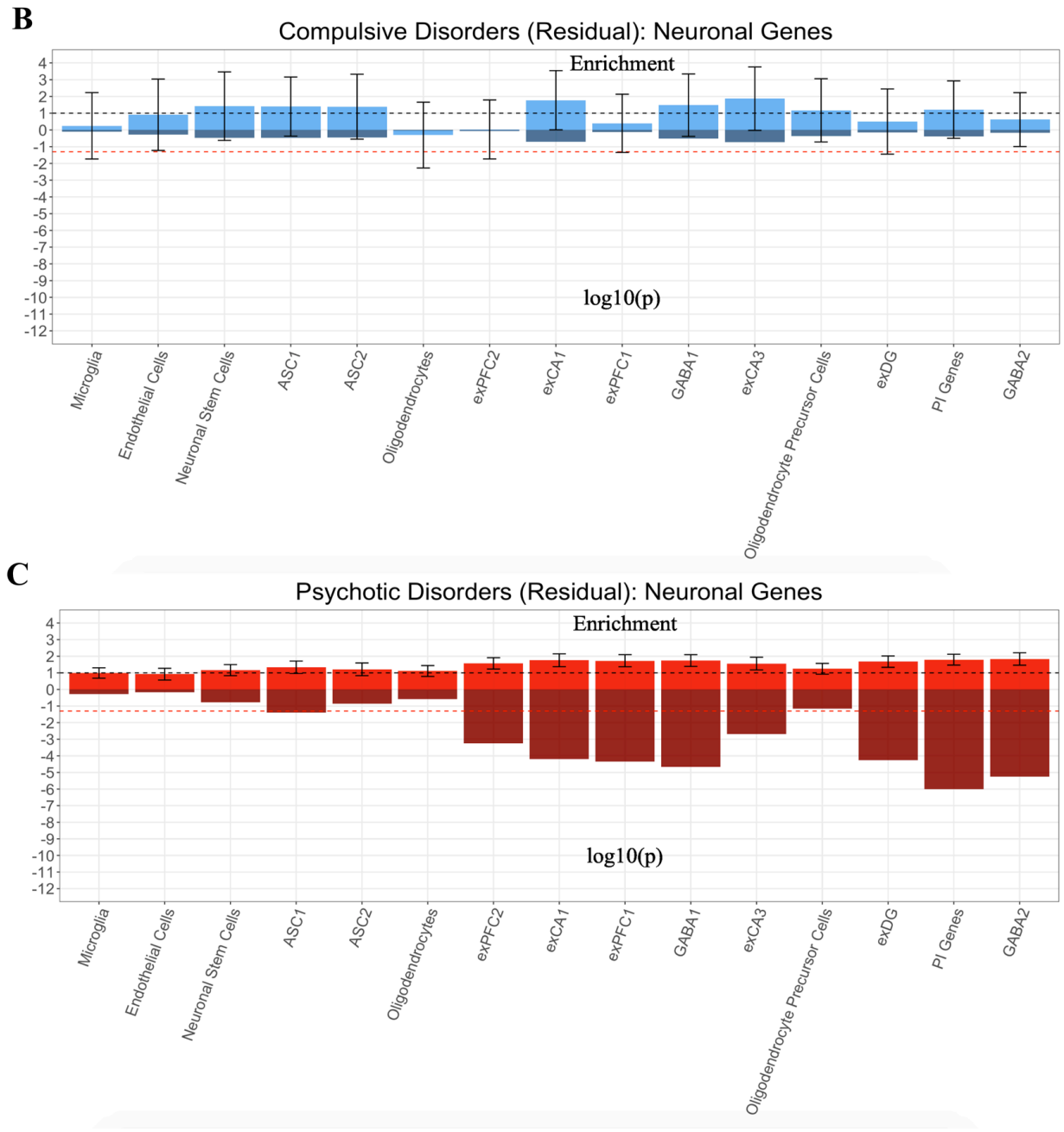

Supplementary Figure 23b. Enrichment of Brain Cell Annotations from Hierarchical Model. The top half of each panel depicts the enrichment point estimates, with error bars indicating +/- 1.96 *SEs.* The black dashed line on the top half reflects the null (enrichment = 1). The bottom half of each panel depicts the log10(p) values. The red dashed line on the bottom half reflects log10(p = .05). scaling of the y-axis across panels differs due to widely discrepant ranges in CIs across factors. For comparative purposes across factors, all graphs for the hierarchical factor model are based on increasing significance for the hierarchical *p*-factor. Estimates are shown for the residuals of the compulsive disorders (panel B) and psychotic disorders (panel C) factors after accounting for variance explained by the *p*-factor. The total effective sample size for the factors was: Compulsive Factor (*N*= 19,108) and Psychotic Factor (*N* = 87,138); however, it is important to note that these are enrichment estimates for the residual variance in the factors such that the effective *N* for just these residual components will be much smaller.

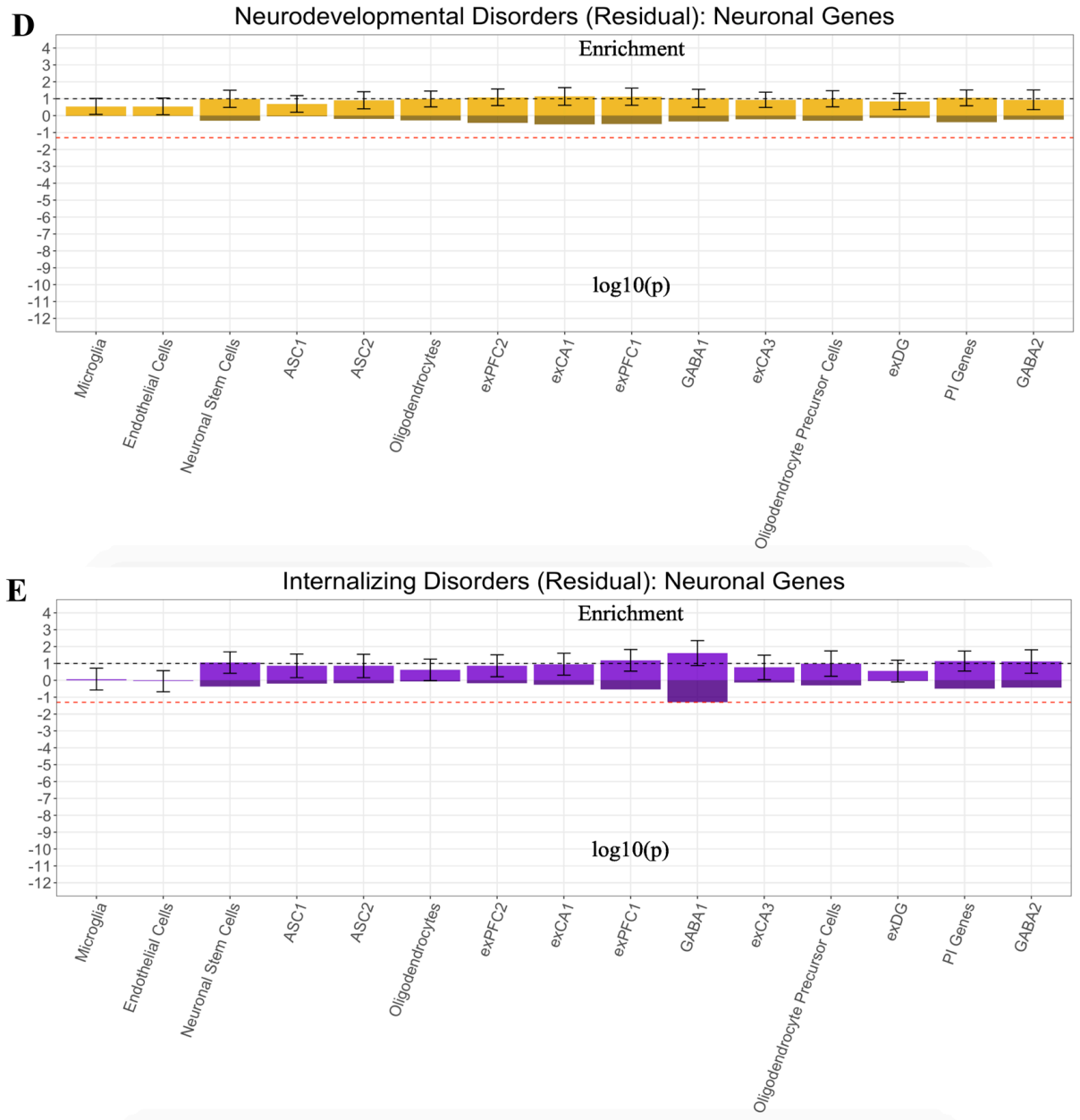

Supplementary Figure 23c. Enrichment of Brain Cell Annotations from Hierarchical Model. The top half of each panel depicts the enrichment point estimates, with error bars indicating +/- 1.96 *SE*s. The black dashed line on the top half reflects the null (enrichment = 1). The bottom half of each panel depicts the log10(p) values. The red dashed line on the bottom half reflects log10(p = .05). The scaling of the y-axis across panels differs due to widely discrepant ranges in CIs across factors. For comparative purposes across factors, all graphs for the hierarchical factor model are based on increasing significance for the hierarchical *p*-factor. Estimates are shown for the residuals of the neurodevelopmental disorders (panel D) and internalizing (panel C) factors after accounting for variance explained by the *p*-factor. The effective sample size for the factors was Neurodevelpomental Factor (*N*= 55,932) and Internalizing Factor (*N*= 455,340) ; however, it is important to note that these are enrichment estimates for the residual variance in the factors such that the effective *N* for just these residual components will be much smaller.

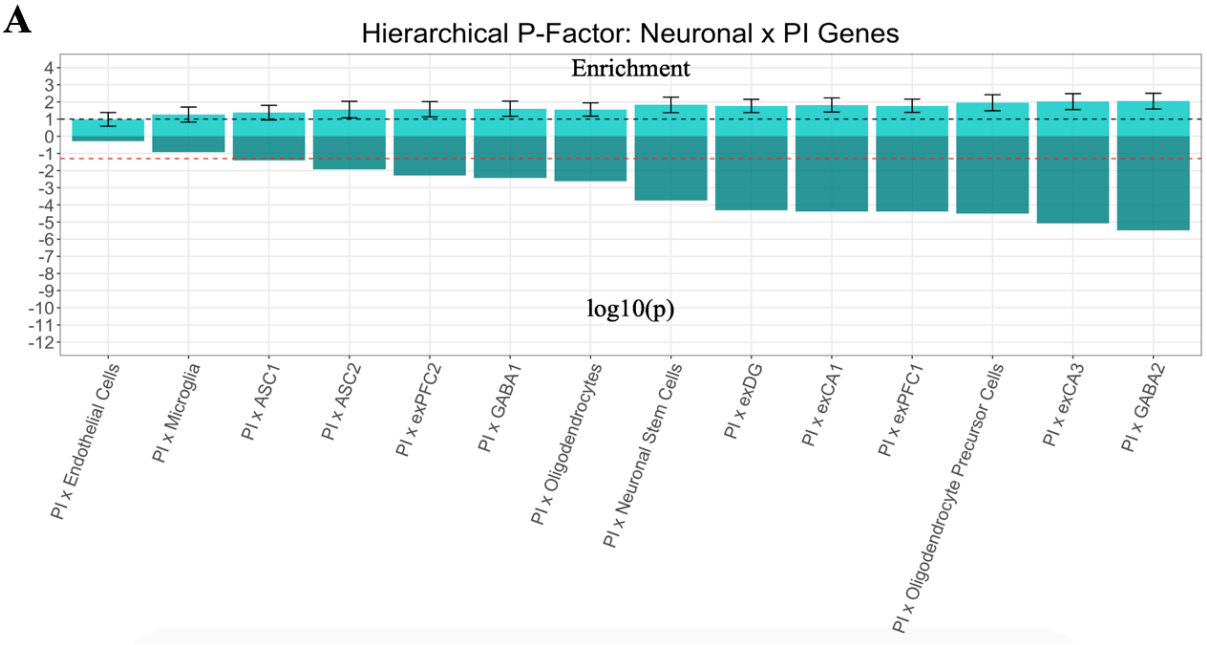

Supplementary Figure 24a. Enrichment of Brain Cell × PI Gene Annotations from Hierarchical Model. The top half of each panel depicts the enrichment point estimates, with error bars indicating +/- 1.96 *SE*s. The black dashed line on the top half reflects the null (enrichment = 1). The bottom half of each panel depicts the log10(p) values. The red dashed line on the bottom half reflects log10(p = .05). The scaling of the y-axis across panels differs due to widely discrepant ranges in CIs across factors. For comparative purposes across factors, all graphs for the hierarchical factor model are based on increasing significance for the hierarchical *p*-factor. Estimates are shown for the hierarchical *p*-factor (panel A). The effective sample size for the *p*-factor was N = 667,343.

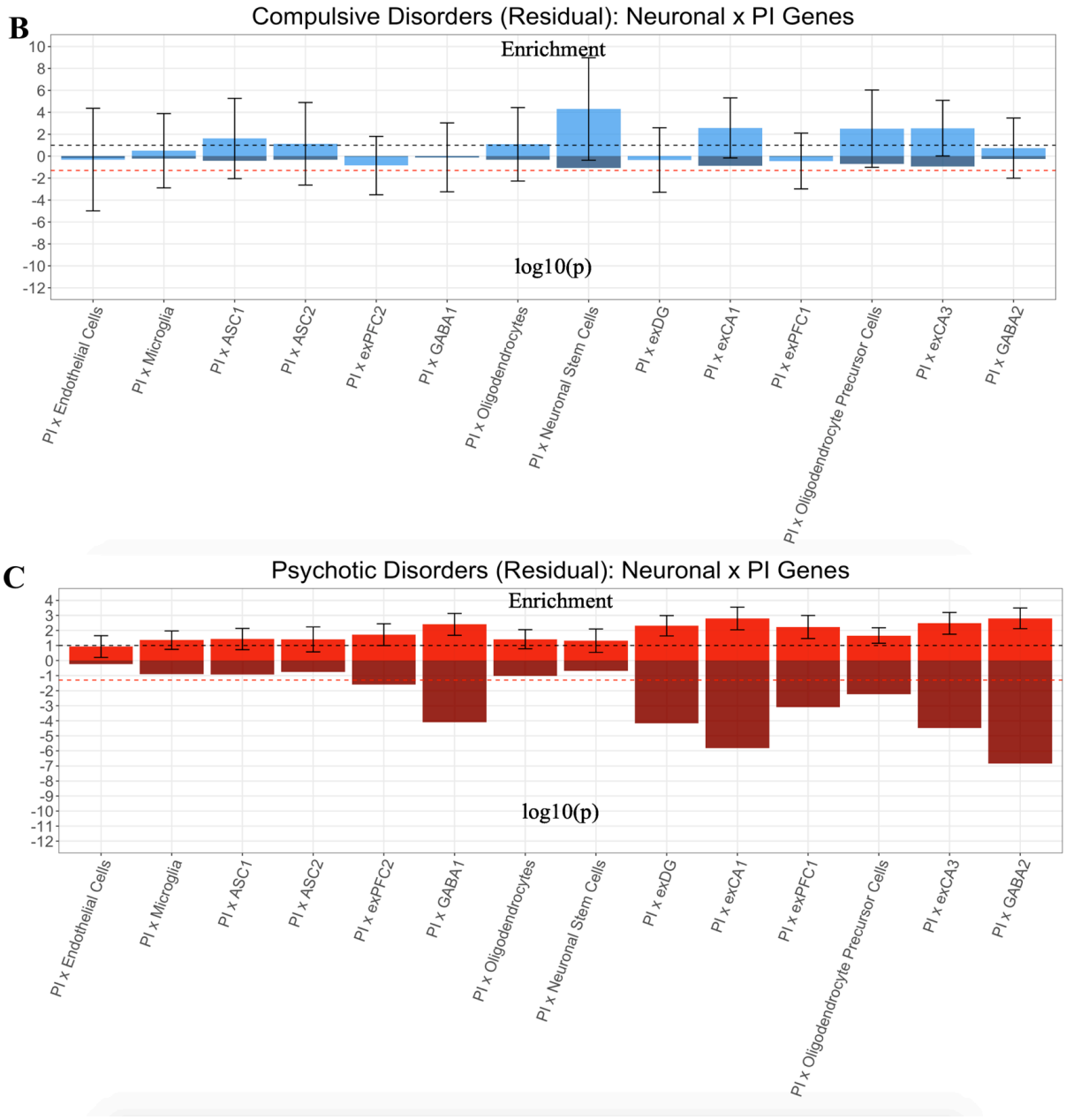

Supplementary Figure 24b. Enrichment of Brain Cell × PI Gene Annotations from Hierarchical Model. The top half of each panel depicts the enrichment point estimates, with error bars indicating +/- 1.96 *SEs.* The black dashed line on the top half reflects the null (enrichment = 1). The bottom half of each panel depicts the log10(p) values. The red dashed line on the bottom half reflects log10(p = .05). scaling of the y-axis across panels differs due to widely discrepant ranges in CIs across factors. For comparative purposes across factors, all graphs for the hierarchical factor model are based on increasing significance for the hierarchical *p*-factor. Estimates are shown for the residuals of the compulsive disorders (panel B) and psychotic disorders (panel C) factors after accounting for variance explained by the *p*-factor. The total effective sample size for the factors was: Compulsive Factor (*N*= 19,108) and Psychotic Factor (*N* = 87,138); however, it is important to note that these are enrichment estimates for the residual variance in the factors such that the effective *N* for just these residual components will be much smaller.

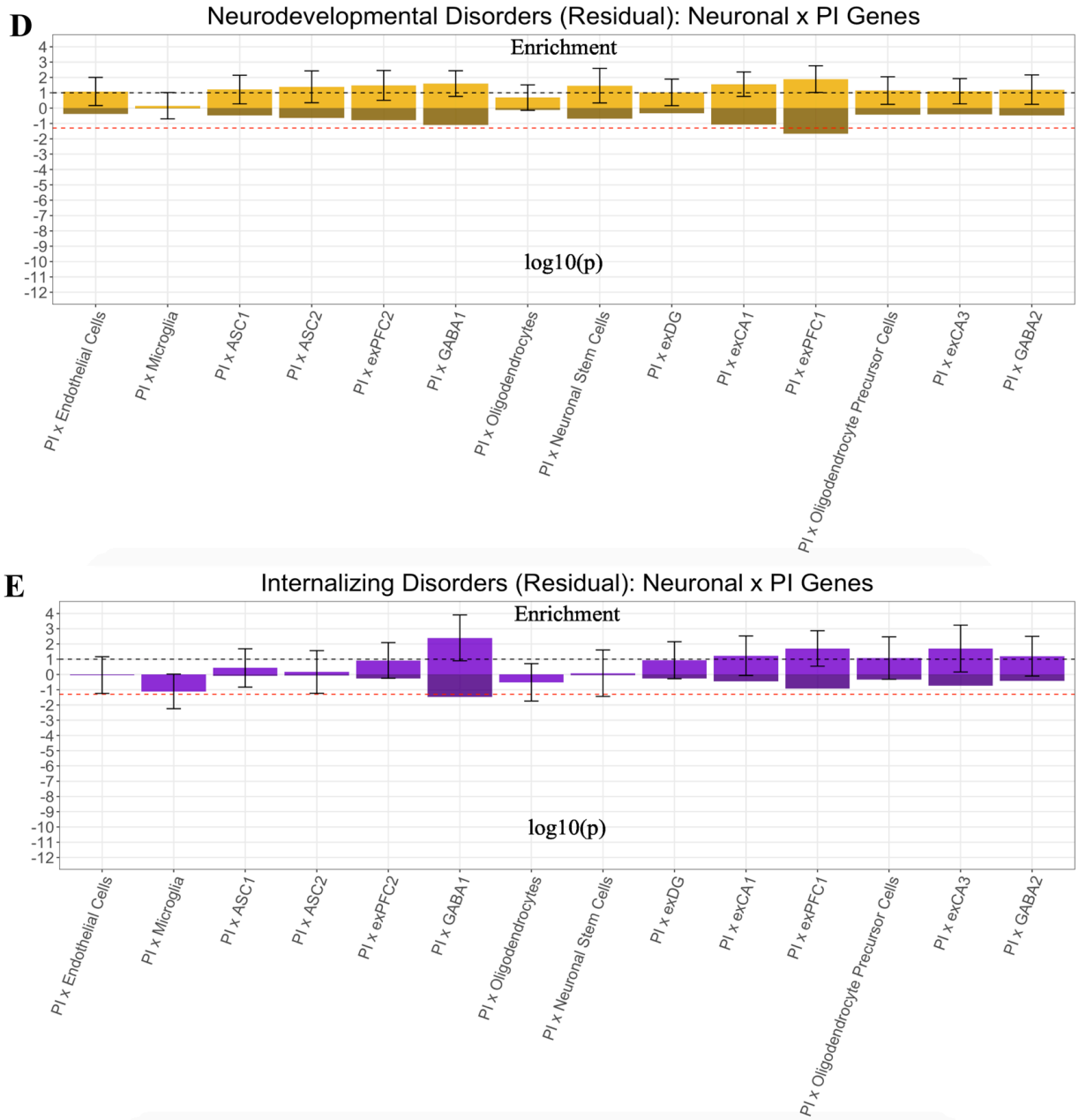

Supplementary Figure 24c. Enrichment of Brain Cell × PI Gene Annotations from Hierarchical Model. The top half of each panel depicts the enrichment point estimates, with error bars indicating +/- 1.96 *SE*s. The black dashed line on the top half reflects the null (enrichment = 1). The bottom half of each panel depicts the log10(p) values. The red dashed line on the bottom half reflects log10(p = .05). The scaling of the y-axis across panels differs due to widely discrepant ranges in CIs across factors. For comparative purposes across factors, all graphs for the hierarchical factor model are based on increasing significance for the hierarchical *p*-factor. Estimates are shown for the residuals of the neurodevelopmental disorders (panel D) and internalizing (panel C) factors after accounting for variance explained by the *p*-factor. The effective sample size for the factors was Neurodevelpomental Factor (*N*= 55,932) and Internalizing Factor (*N*= 455,340); however, it is important to note that these are enrichment estimates for the residual variance in the factors such that the effective *N* for just these residual components will be much smaller.

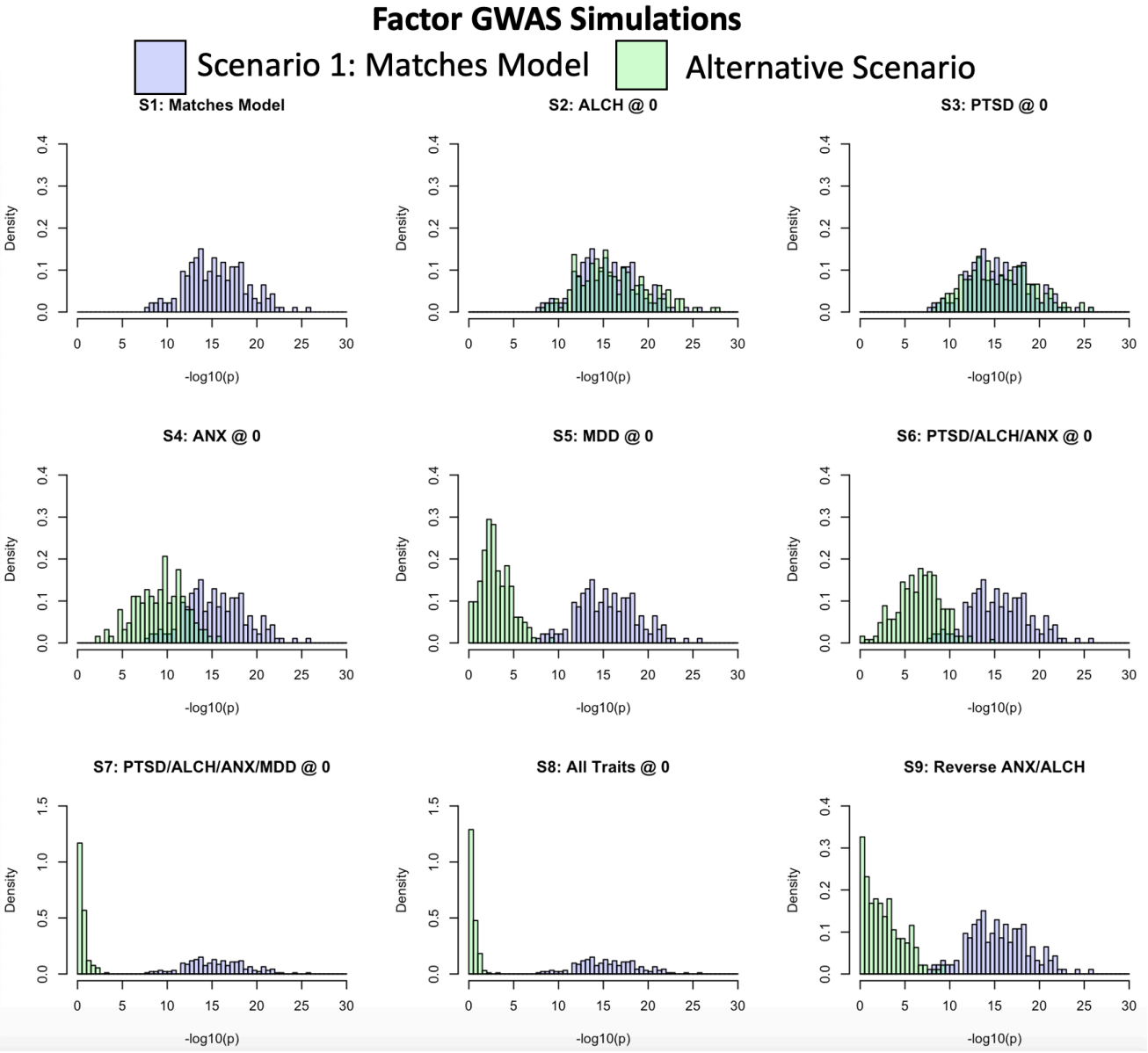

Supplementary Figure 25. Histograms of Genomic SEM Factor GWAS Simulation Results. Panels depict the -log10(p) values for SNP effects on the Internalizing disorders factor across the 9 different population generating scenarios. All panels depict in blue as a reference point the simulation scenario that exactly matched the factor model (i.e., Scenario 1 depicted in upper left panel) and in green the specific scenario indicated in the histogram title.

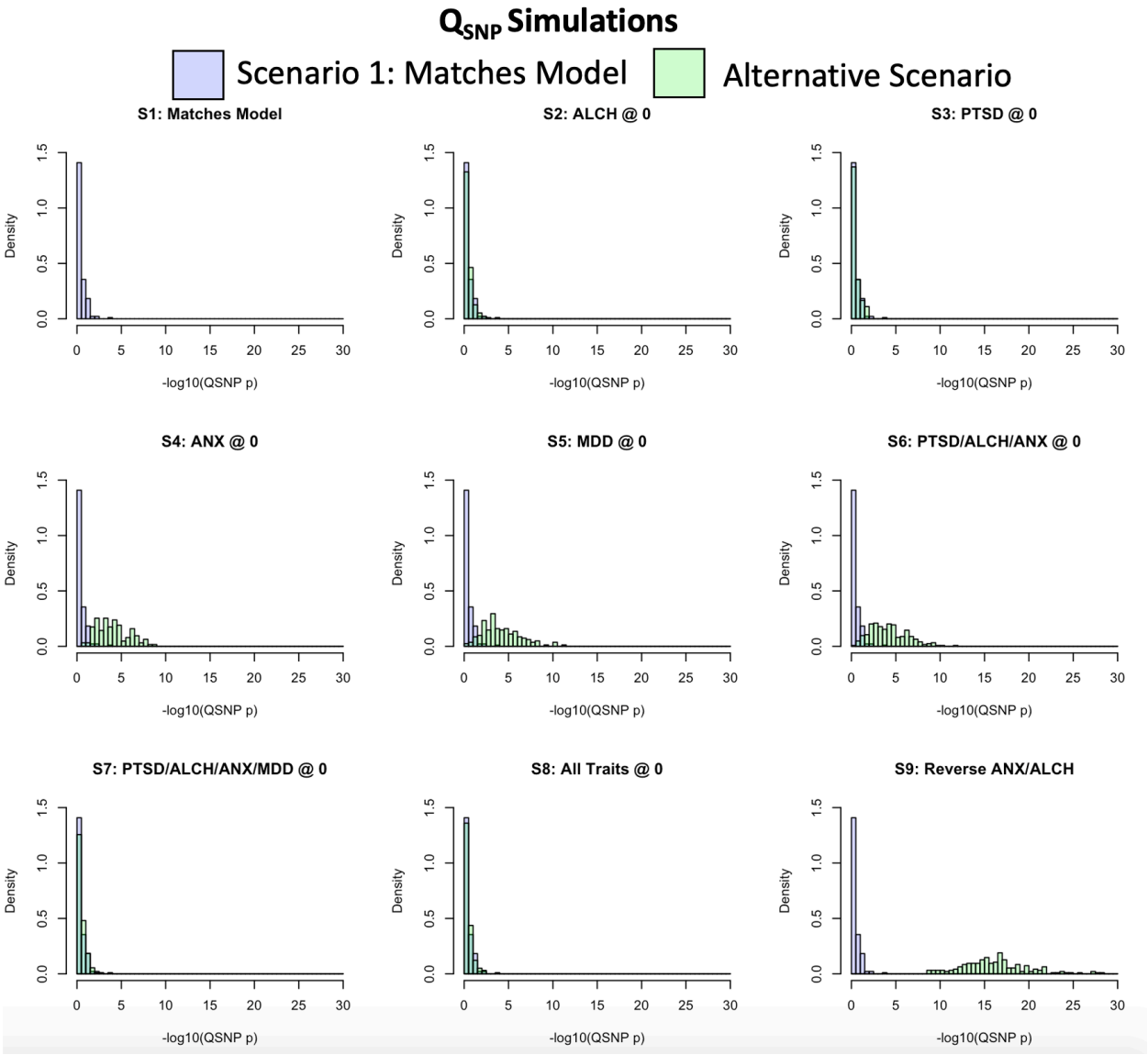

Supplementary Figure 26. Histograms of Factor GWAS Q_{SNP} Simulation Results. Panels depict the -log10(p) values for Q_{SNP} for the Internalizing disorders factor across the 9 different population generating scenarios. All panels depict in blue as a reference point the simulation scenario that exactly matched the factor model (i.e., Scenario 1 depicted in upper left panel) and in green the specific population generating scenario indicated in the histogram title.

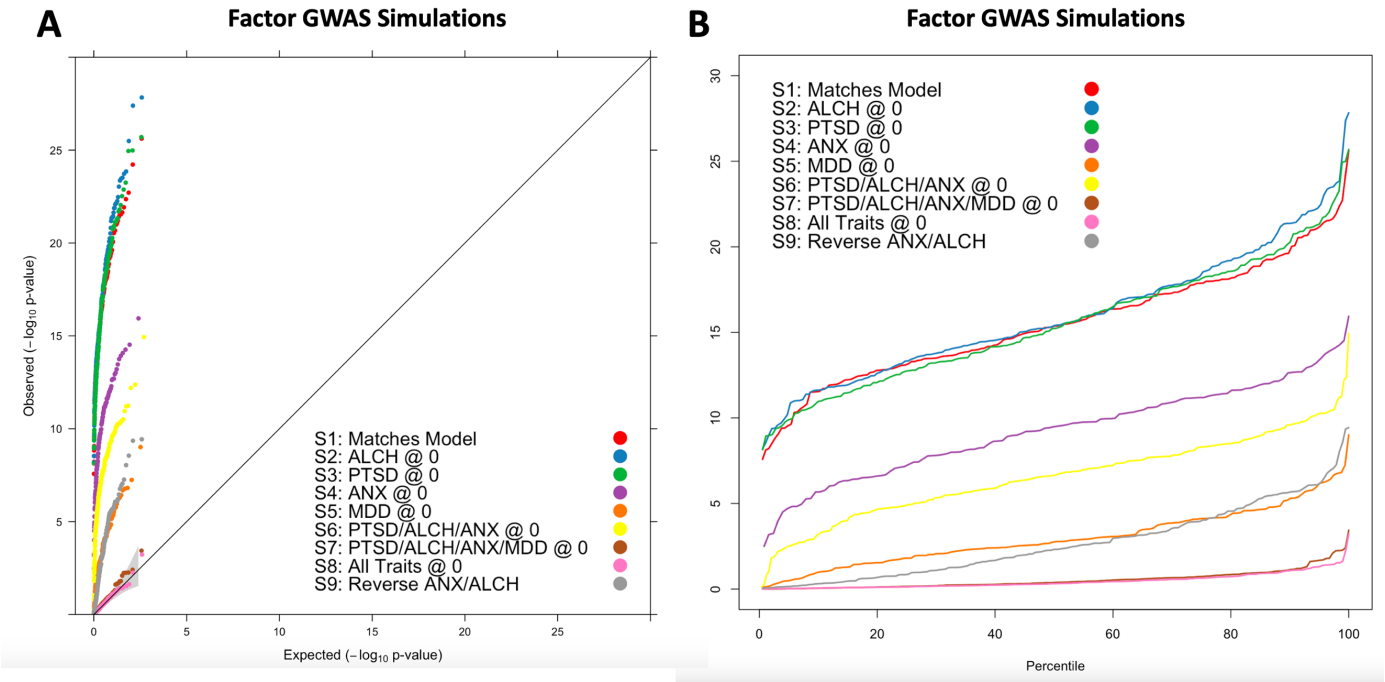

Supplementary Figure 27. Genomic SEM Factor GWAS Simulation Results. *Panel A* depicts the -log10(p) values as a QQ-plot for SNP effects on the Internalizing disorders factor for the 9 different population generating scenarios with. *Panel B* depicts the same simulation results also with -log10(p) values on the y-axis while the x-axis depicts rank orderered simulation results from the 0% percentile to 100% percentile across the 250 simulation runs. In both panels the different simulation scenarios are depicted as: Scenario 1 that matches the factor model depicted in red; Scenario 2 with the covariance between the SNP and ALCH set at 0 in the generating population in blue; Scenario 3 with the covariance between the SNP and PTSD set at 0 in the generating population in green; Scenario 4 with the covariance between the SNP and ANX set at 0 in the in the generating population in purple; Scenario 5 with the covariance between the SNP and MDD set at 0 in the generating population in orange; Scenario 6 with the covariance between the SNP and PTSD, ALCH and ANX set at 0 in the generating population in yellow; Scenario 7 with the covariance between the SNP and PTSD, ALCH, ANX, and MDD set at 0 in the generating population in brown; Scenario 8 with the covariance between the SNP and all psychiatric traits set at 0 in pink; and Scenario 9 with the sign reversed for the covariance between the SNP and ANX and ALCH (i.e., multiplied by -1) in grey.

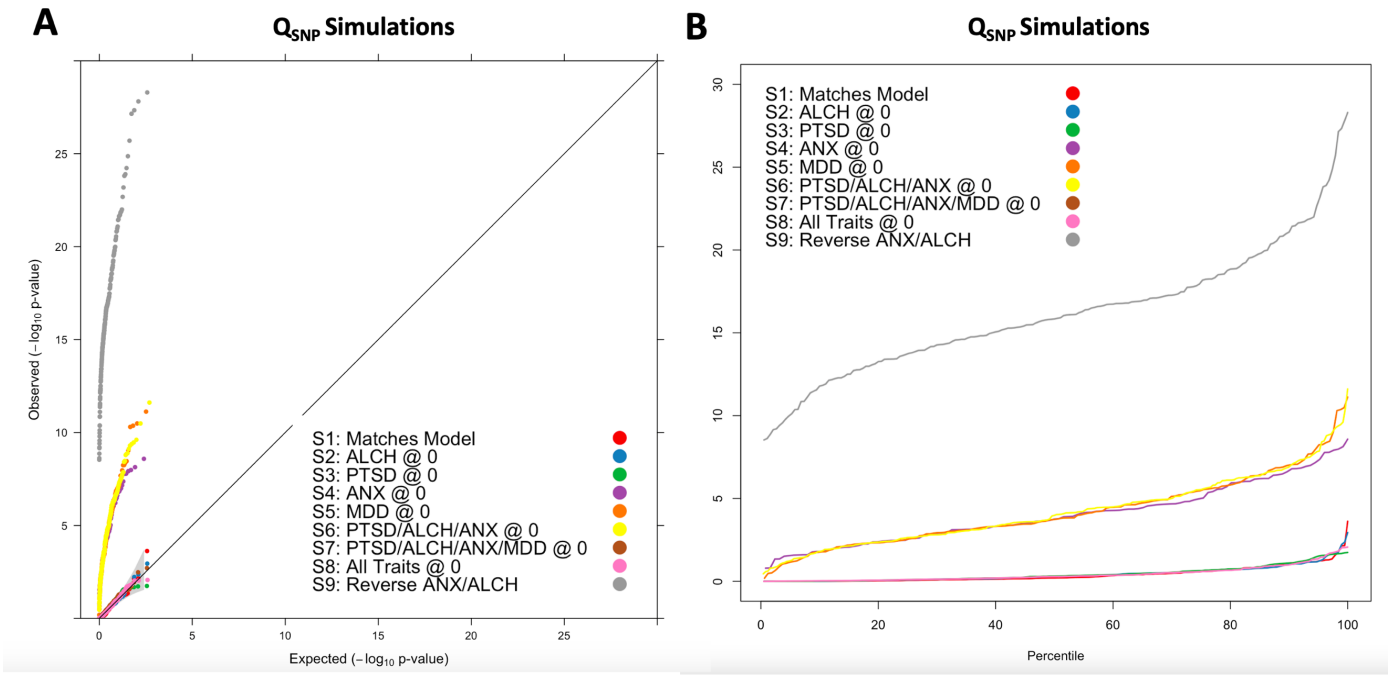

Supplementary Figure 28. Genomic SEM Factor GWAS Q_{SNP} Simulation Results. *Panel A* depicts the QQ-plot -log10(p) values for Q_{SNP} for the internalizing disorders factor for the 9 different population generating scenarios. *Panel B* depicts the same simulation results also with -log10(p) values on the y-axis while the x-axis depicts rank orderered simulation results from the 0% percentile to 100% percentile across the 250 simulation runs. Note that Q_{SNP} was calculated as the factor specific Q_{SNP} for the internalizing disorders factor. The 9 population generating scenarios were: Scenario 1 that matches the factor model depicted in red; Scenario 2 with the covariance between the SNP and ALCH set at 0 in the generating population in blue; Scenario 3 with the covariance between the SNP and PTSD set at 0 in the generating population in green; Scenario 4 with the covariance between the SNP and ANX set at 0 in the in the generating population in purple; Scenario 5 with the covariance between the SNP and MDD set at 0 in the generating population in orange; Scenario 6 with the covariance between the SNP and PTSD, ALCH and ANX set at 0 in the generating population in yellow; Scenario 7 with the covariance between the SNP and PTSD, ALCH, ANX, and MDD set at 0 in the generating population in brown; Scenario 8 with the covariance between the SNP and all psychiatric traits set at 0 in pink; and Scenario 9 with the sign reversed for the covariance between the SNP and ANX and ALCH (i.e., multiplied by -1) in grey.

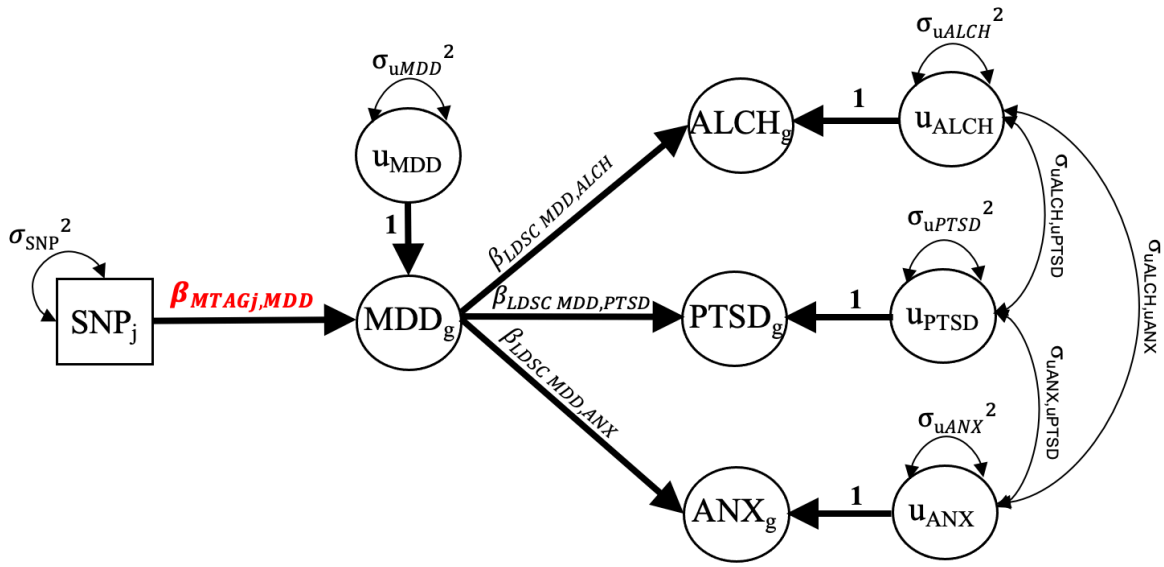

Supplementary Figure 29. MTAG Model Specified in Genomic SEM. Figure depicts the path diagram for the MTAG model for MDD as specified in a Genomic SEM model. The regression path between a given SNPj and MDD is highlighted in red as this reflects the regression path that statistically mirrors the output from MTAG and as such is the MTAG outcome reported in the simulation results. In addition, we refer the reader to the Online Supplement of the original Genomic SEM publication[22] for a formal explication on the equivalence of this model specification to the MTAG model

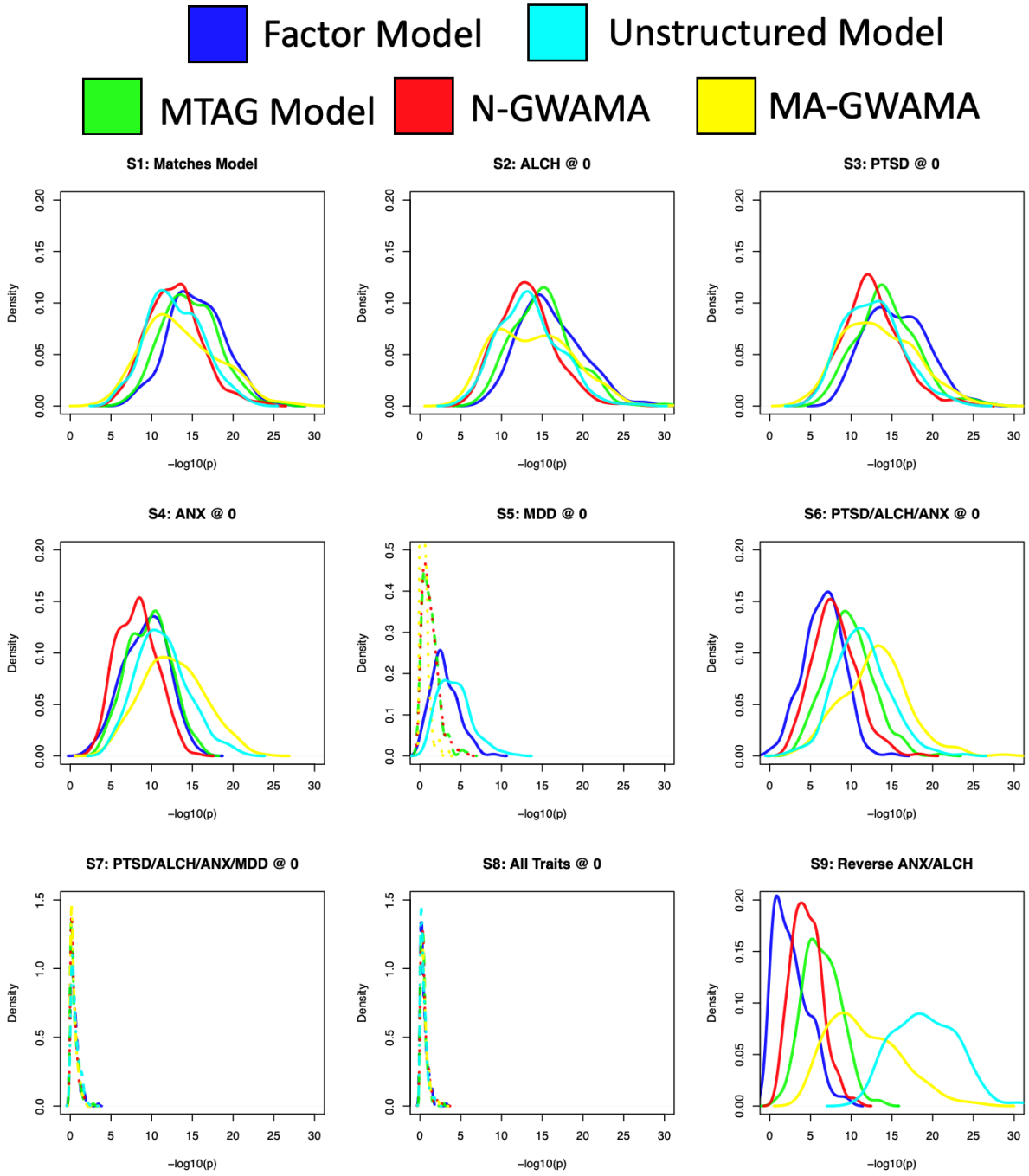

Supplementary Figure 30. Density Plots of Multivariate GWAS Simulation Results across Multivariate Methods. Panels depict the -log10(p) values across the 9 different population generating scenarios for the Factor Model (in dark blue), Unstructured Mode (in light blue), MTAG Model (in green), N-GWAMA (in red), and MA-GWAMA (in yellow). Note that the scaling of the y-axis varies for certain population generating scenarios due to a density of observations around -log10(p) of 0 while the scaling of the x-axis is kept consistent. Lines are depicted as dashed for certain panels when similar results were obtained across methods and, consequently, the lines laid on top of one another.

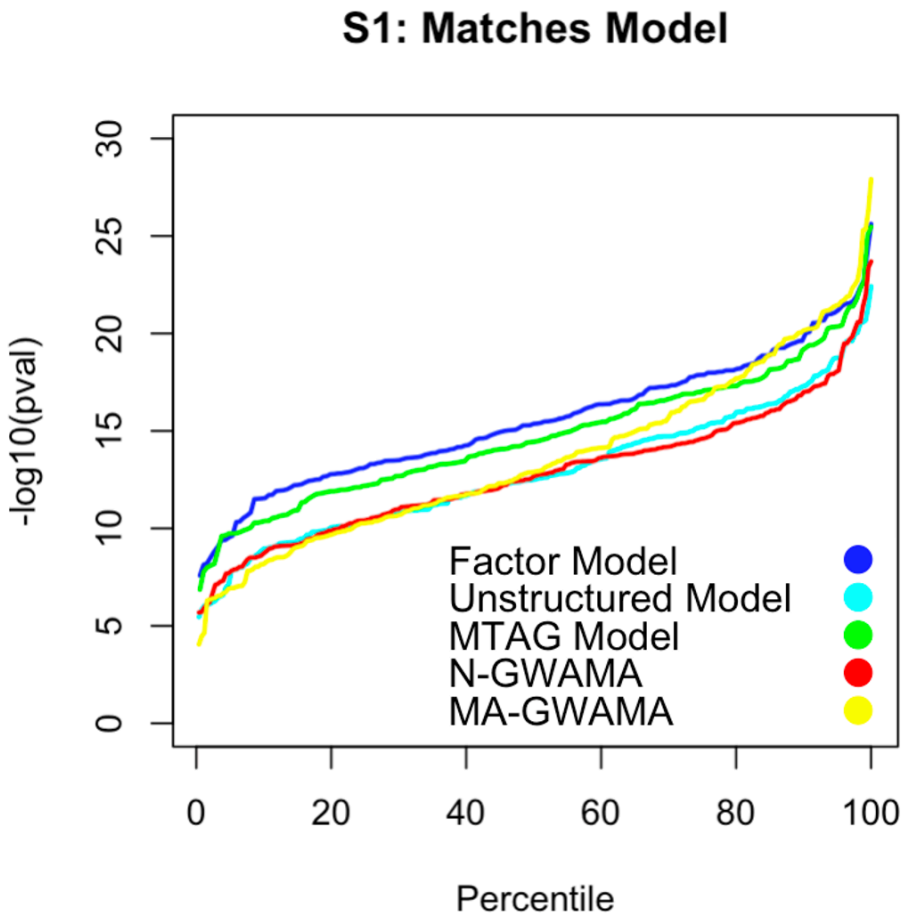

Supplementary Figure 31a. QQ-plot of Simulation Results for Scenario 1 Across Multivariate Methods. Figure depicts the simulation results for the population generating Scenario 1 that mirrored the factor structure. Results are depicted for the Factor Model (in dark blue), Unstructured Model (in light blue), MTAG Model (in green), N-GWAMA (in red), and MA-GWAMA (in yellow). The x-axis depicts rank orderered simulation results within each method in percentile from 0% percentile to 100% percentile across the 250 simulation runs. The y-axis depicts the -log10(*p*-value) for each simulation run.

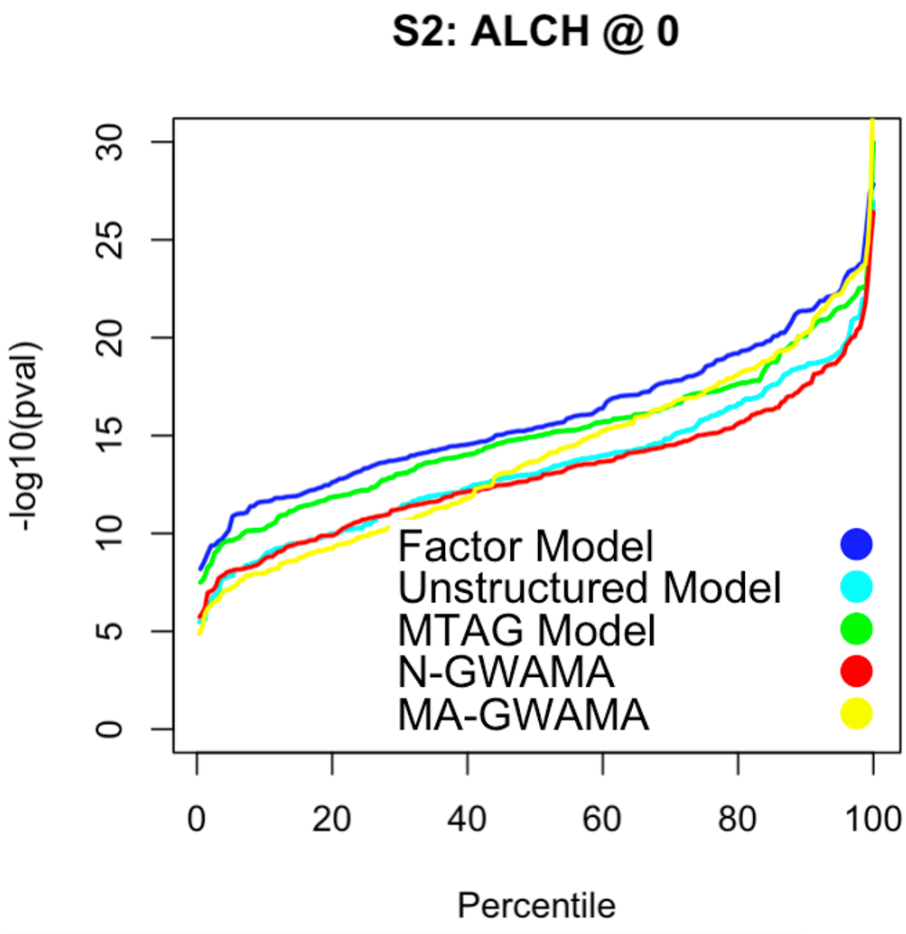

Supplementary Figure 31b. QQ-plot of Simulation Results for Scenario 2 across Multivariate Methods. Figure depicts the simulation results for the population generating Scenario 2 that set the association between the SNP and ALCH to 0 in the population. Results are depicted for the Factor Model (in dark blue), Unstructured Model (in light blue), MTAG Model (in green), N-GWAMA (in red), and MA-GWAMA (in yellow). The x-axis depicts rank orderered simulation results within each method in percentile from 0% percentile to 100% percentile across the 250 simulation runs. The y-axis depicts the -log10(*p*-value) for each simulation run.

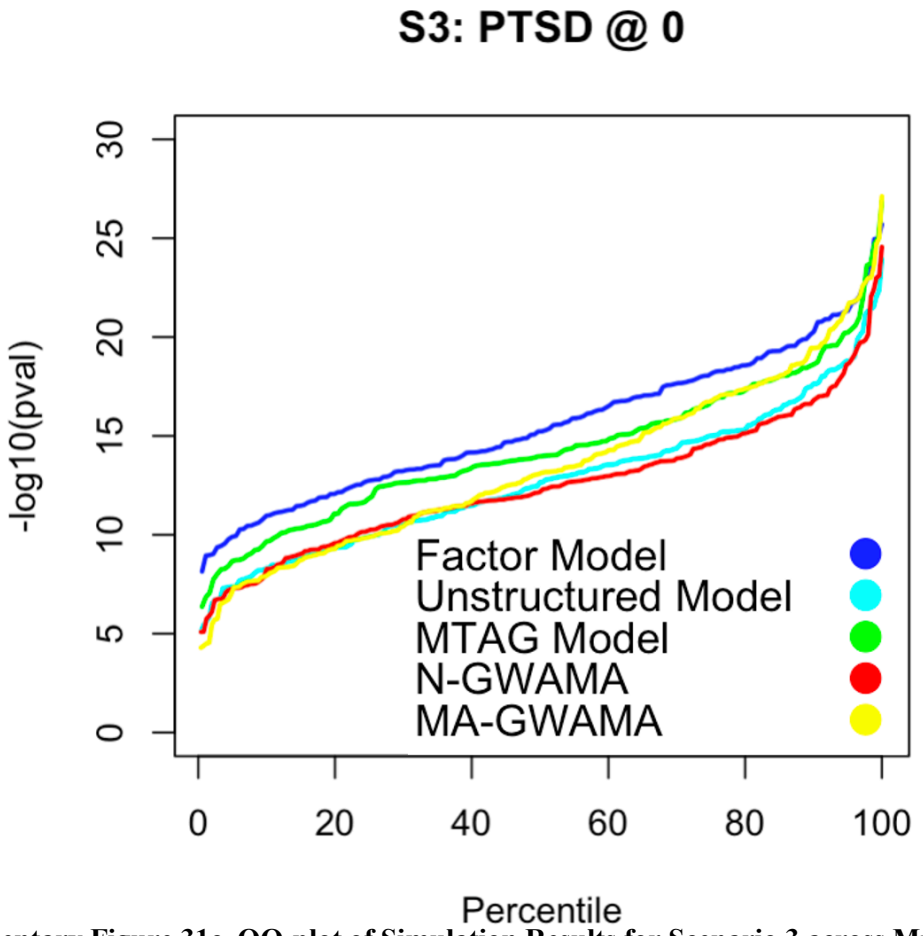

Supplementary Figure 31c. QQ-plot of Simulation Results for Scenario 3 across Multivariate Methods. Figure depicts the simulation results for the population generating Scenario 3 that set the association between the SNP and PTSD to 0 in the population. Results are depicted for the Factor Model (in dark blue), Unstructured Model (in light blue), MTAG Model (in green), N-GWAMA (in red), and MA-GWAMA (in yellow). The x-axis depicts rank orderered simulation results within each method in percentile from 0% percentile to 100% percentile across the 250 simulation runs. The y-axis depicts the -log10(*p*-value) for each simulation run.

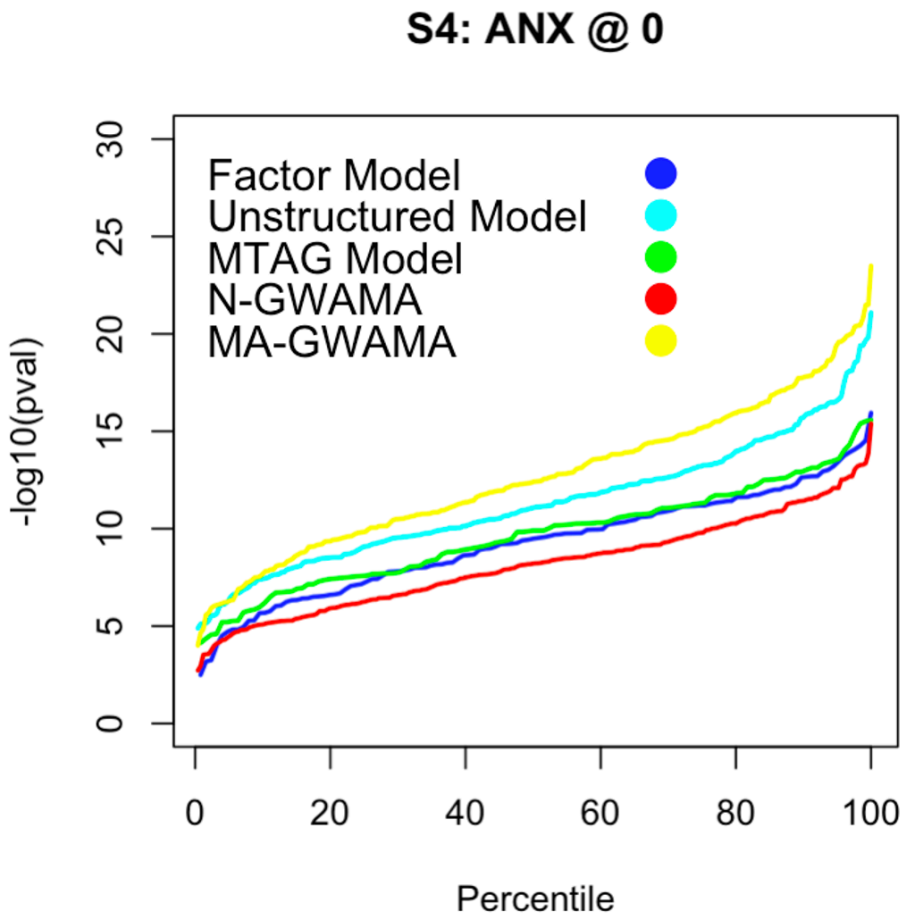

Supplementary Figure 31d. QQ-plot of Simulation Results for Scenario 4 across Multivariate Methods. Figure depicts the simulation results for the population generating Scenario 4 that set the association between the SNP and ANX to 0 in the population. Results are depicted for the Factor Model (in dark blue), Unstructured Model (in light blue), MTAG Model (in green), N-GWAMA (in red), and MA-GWAMA (in yellow). The x-axis depicts rank orderered simulation results within each method in percentile from 0% percentile to 100% percentile across the 250 simulation runs. The y-axis depicts the -log10(*p*-value) for each simulation run.

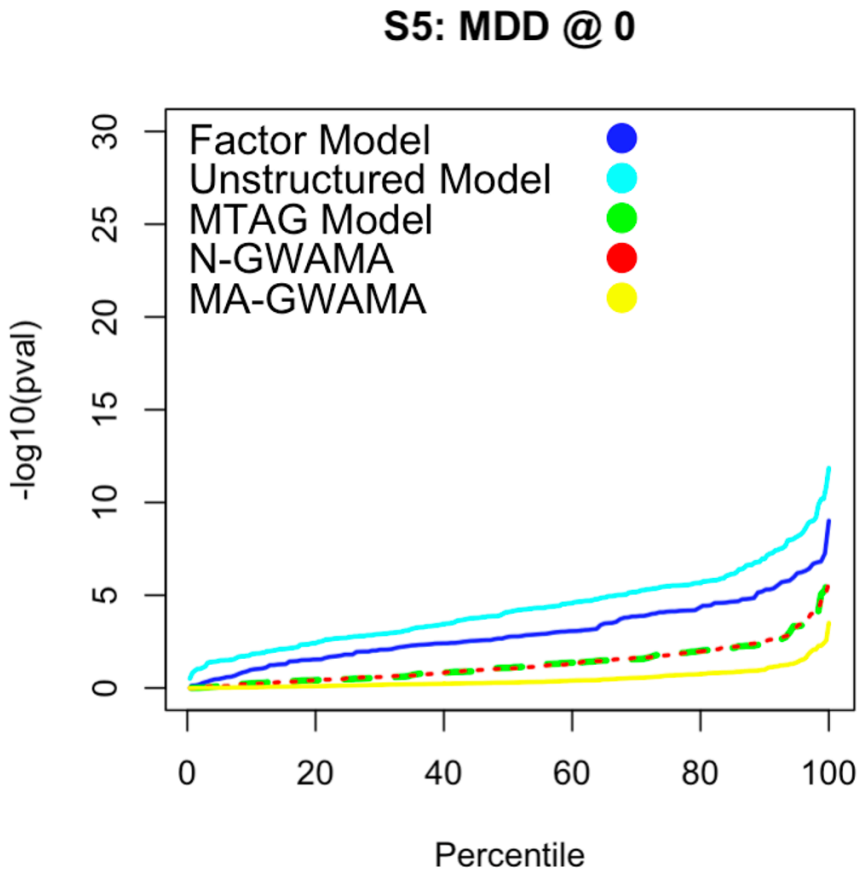

Supplementary Figure 31e. QQ-plot of Simulation Results for Scenario 5 across Multivariate Methods. Figure depicts the simulation results for the population generating Scenario 5 that set the association between the SNP and MDD to 0 in the population. Results are depicted for the Factor Model (in dark blue), Unstructured Model (in light blue), MTAG Model (in green), N-GWAMA (in red), and MA-GWAMA (in yellow). The x-axis depicts rank orderered simulation results within each method in percentile from 0% percentile to 100% percentile across the 250 simulation runs. The y-axis depicts the -log10(*p*-value) for each simulation run. Lines are depicted as dashed for MTAG and N-GWAMA as similar results were obtained across these methods and, consequently, the lines laid on top of one another.

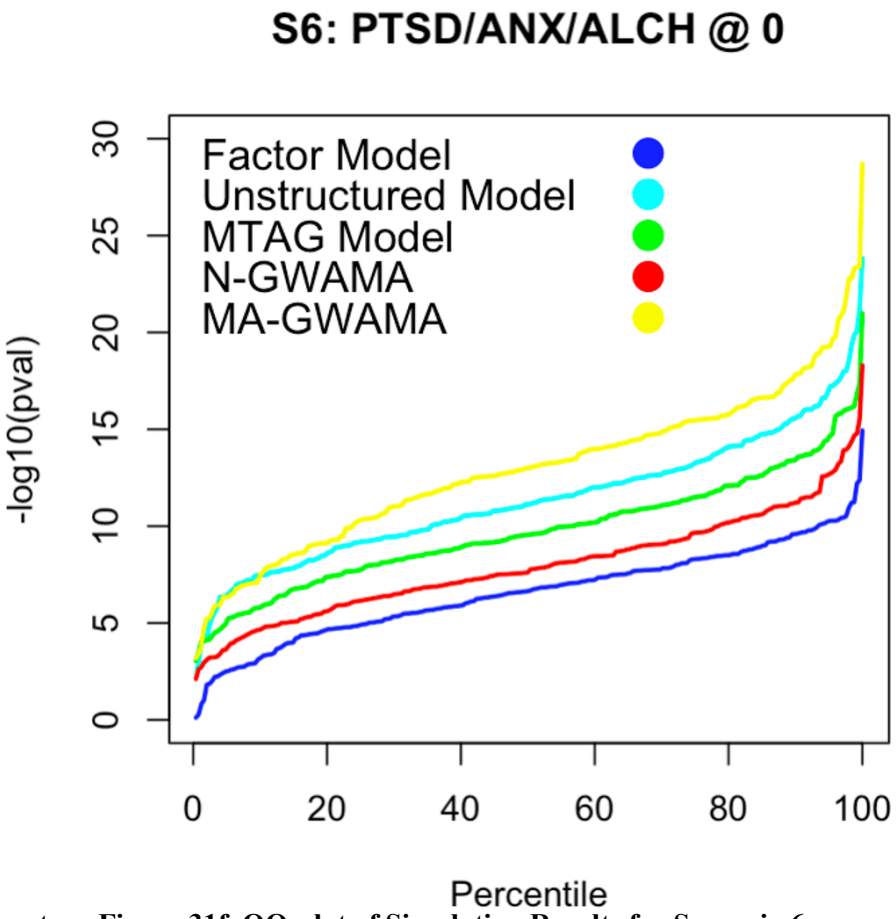

Supplementary Figure 31f. QQ-plot of Simulation Results for Scenario 6 across Multivariate Methods. Figure depicts the simulation results for the population generating Scenario 6 that set the association between the SNP and PTSD, ANX, and ALCH to 0 in the population. Results are depicted for the Factor Model (in dark blue), Unstructured Model (in light blue), MTAG Model (in green), N-GWAMA (in red), and MA-GWAMA (in yellow). The x-axis depicts rank orderered simulation results within each method in percentile from 0% percentile to 100% percentile across the 250 simulation runs. The y-axis depicts the -log10(*p*-value) for each simulation run.

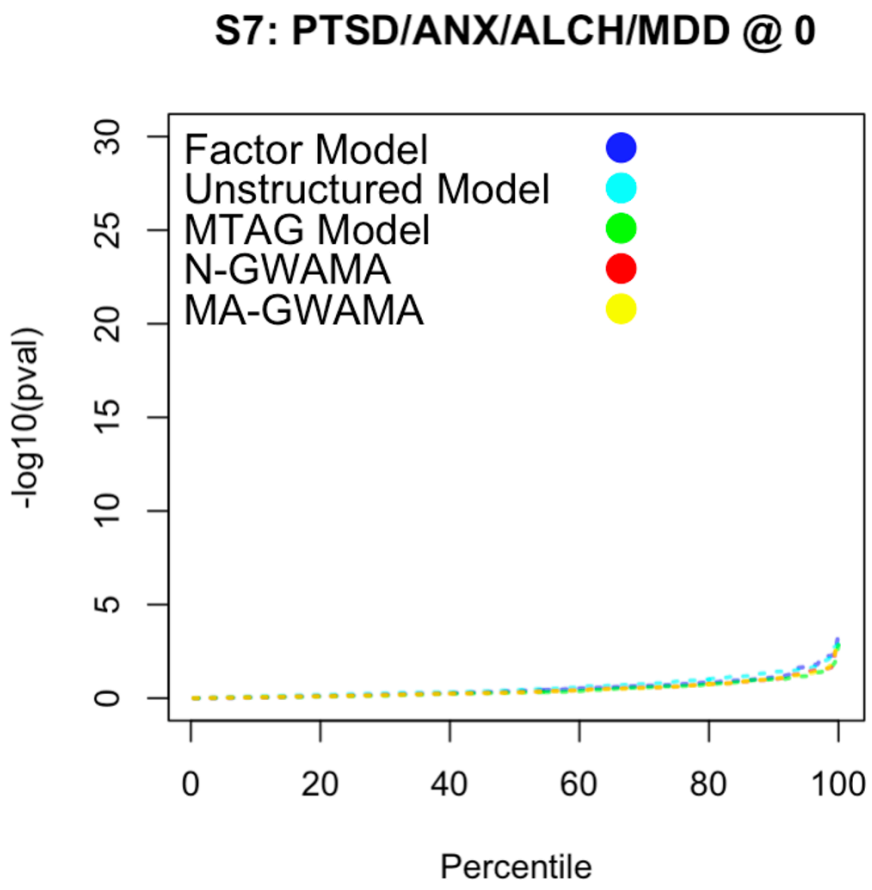

Supplementary Figure 31h. QQ-plot of Simulation Results for Scenario 7 across Multivariate Methods. Figure depicts the simulation results for the population generating Scenario 7 that set the association between the SNP and MDD, PTSD, ANX, and ALCH to 0 in the population. Results are depicted for the Factor Model (in dark blue), Unstructured Model (in light blue), MTAG Model (in green), N-GWAMA (in red), and MA-GWAMA (in yellow). The x-axis depicts rank orderered simulation results within each method in percentile from 0% percentile to 100% percentile across the 250 simulation runs. The y-axis depicts the -log10(*p*-value) for each simulation run. Lines are depicted as dashed as similar results were obtained across these methods and, consequently, the lines laid on top of one another.

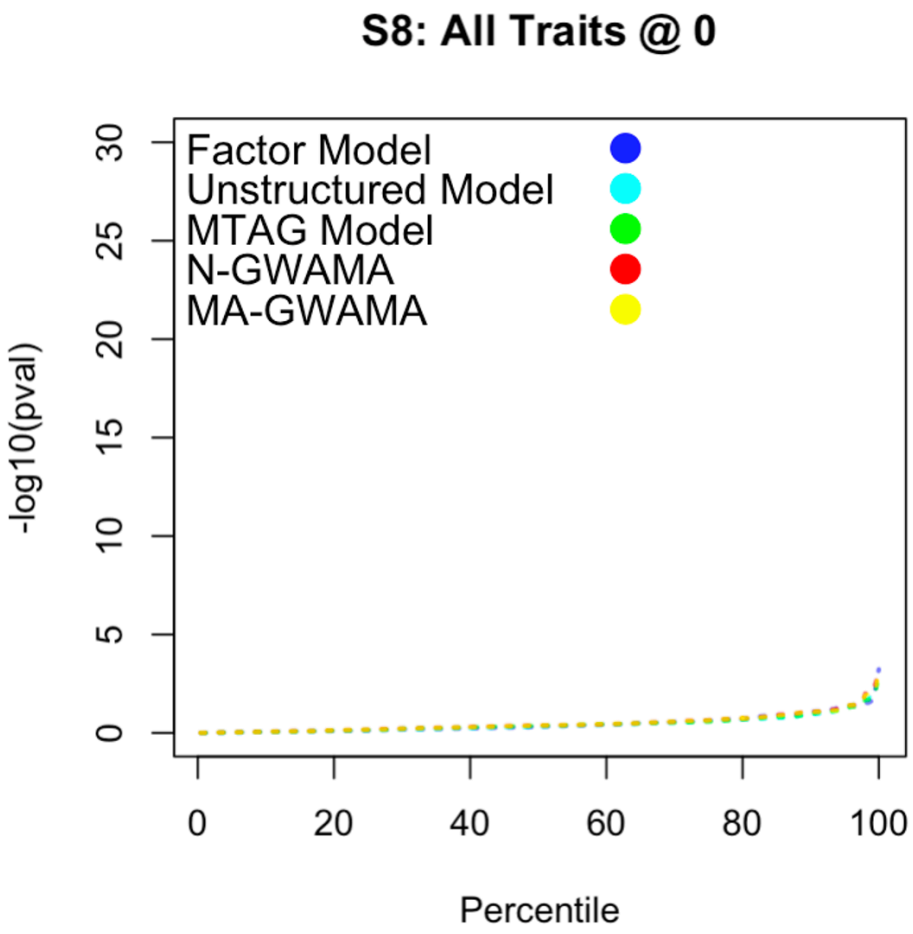

Supplementary Figure 31i. QQ-plot of Simulation Results for Scenario 8 across Multivariate Methods. Figure depicts the simulation results for the population generating Scenario 8 that set the association between the SNP and all psychiatric traits at 0 in the population. Results are depicted for the Factor Model (in dark blue), Unstructured Model (in light blue), MTAG Model (in green), N-GWAMA (in red), and MA-GWAMA (in yellow). The x-axis depicts rank orderered simulation results within each method in percentile from 0% percentile to 100% percentile across the 250 simulation runs. The y-axis depicts the -log10(*p*-value) for each simulation run. Lines are depicted as dashed as similar results were obtained across methods and, consequently, the lines laid on top of one another.

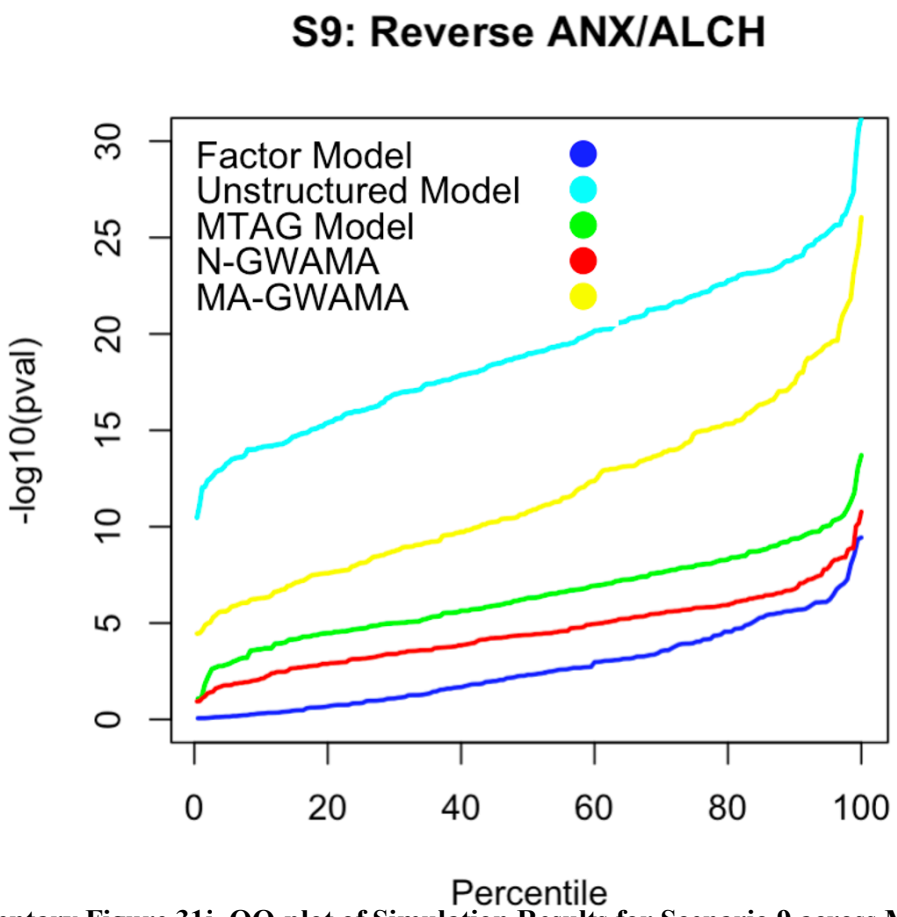

Supplementary Figure 31j. QQ-plot of Simulation Results for Scenario 9 across Multivariate Methods. Figure depicts the simulation results for the population generating Scenario 9 that reversed the direction of the association between the SNP and ANX and ALCH. Results are depicted for the Factor Model (in dark blue), Unstructured Model (in light blue), MTAG Model (in green), N-GWAMA (in red), and MA-GWAMA (in yellow). The x-axis depicts rank orderered simulation results within each method in percentile from 0% percentile to 100% percentile across the 250 simulation runs. The y-axis depicts the -log10(*p*-value) for each simulation run.

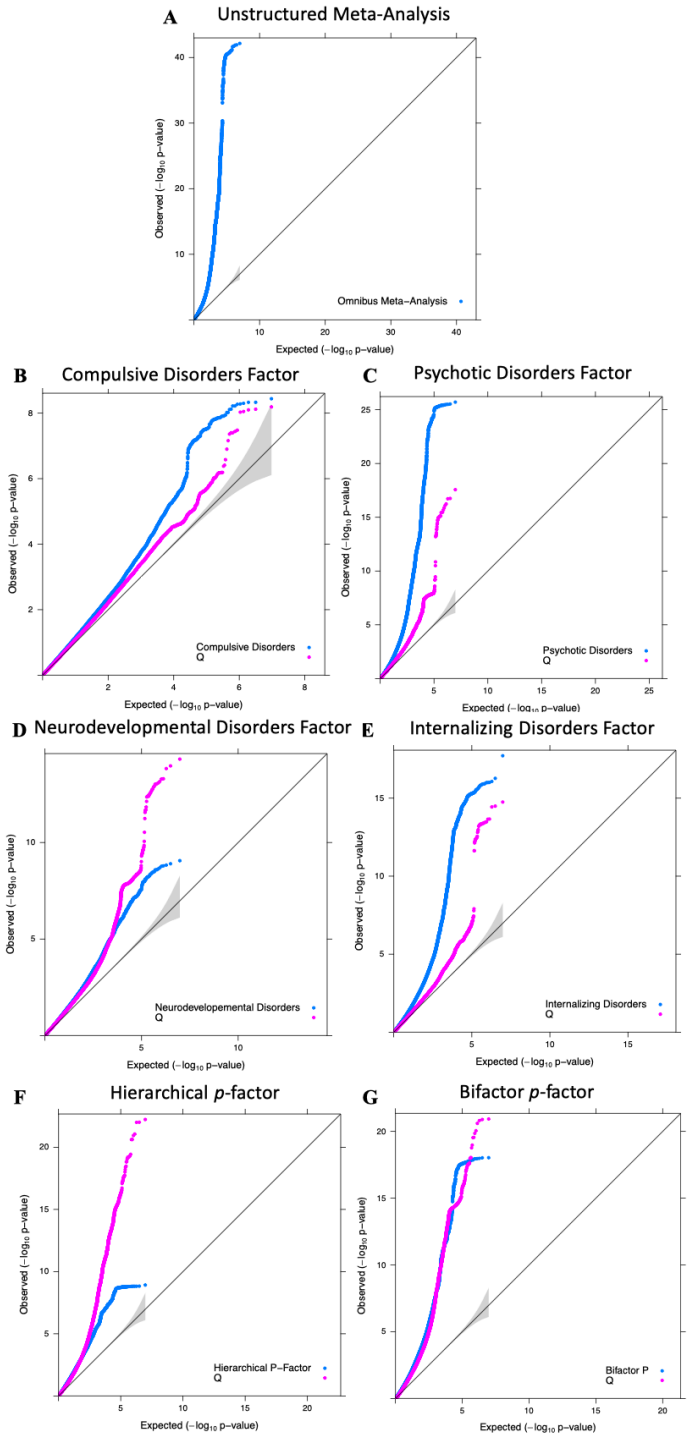

Supplementary Figure 32a. QQ-plots for Multivariate GWAS using LDSC. Expected −log10(*p*)-values are those expected under the null hypothesis. The shaded area indicates the 95% confidence interval with the line on the diagonal indicating the null. In the top panel, results are shown for the unstructured meta-analysis (panel A) reflecting an 11 *df* omnibus meta-analysis across all 11 psychiatric indicators. The middle four panels depict the compulsive disorders (panel B), psychotic disorders (panel C), neurodevelopmental disorders (panel D), and internalizing disorders (panel E) factors from the correlated factors model. Panel F depicts results for the hierarchical, second-order factor. Panel G depicts results for the bifactor *p*-factor. Blue lines depict results for the psychiatric factors. Pink lines depict the factor specific Q_{SNP} estimates.

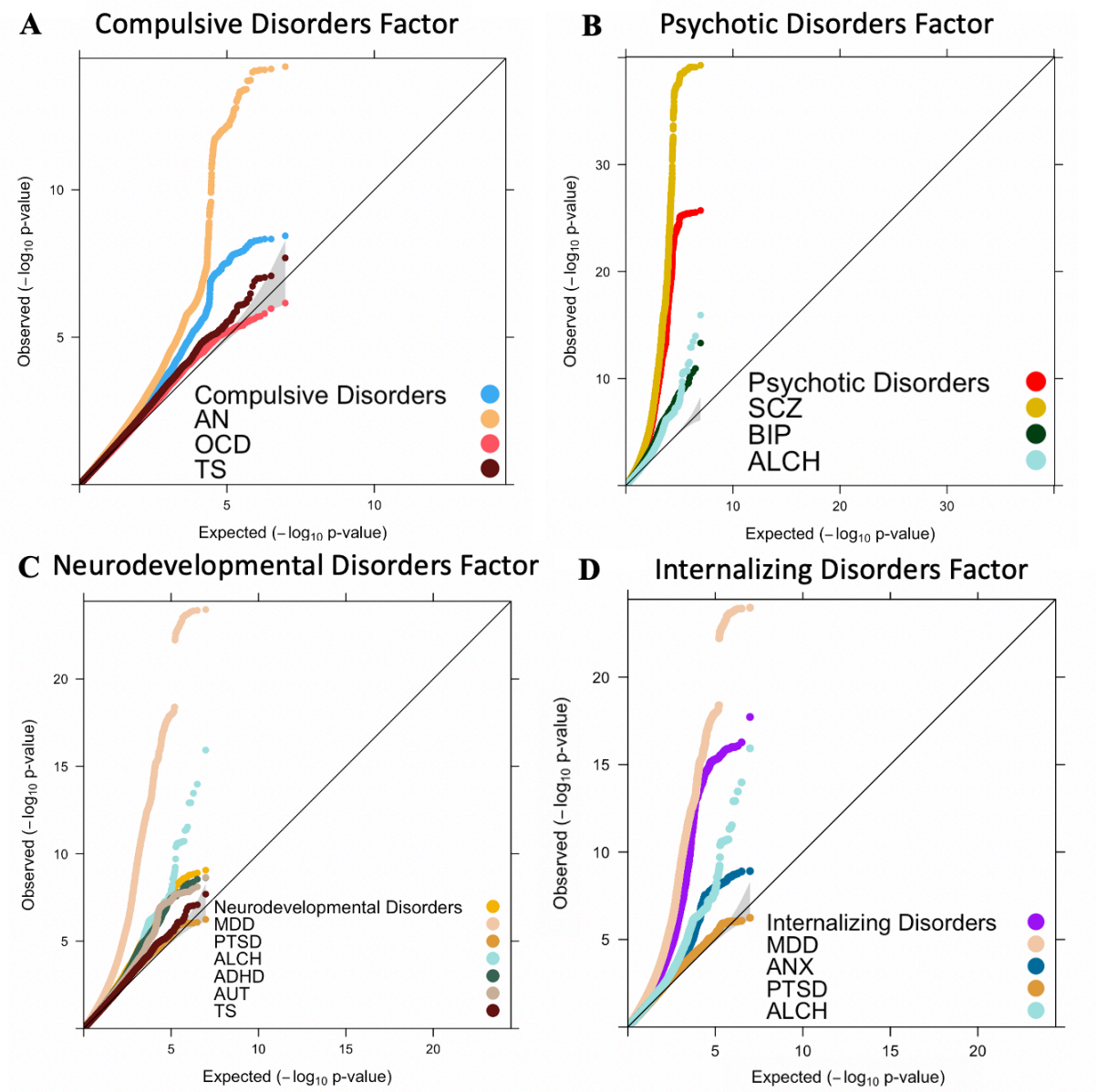

Supplementary Figure 32b. QQ-plots for Multivariate GWAS using LDSC Against Univariate GWAS. Expected −log10(*p*)-values are those expected under the null hypothesis. The shaded area indicates the 95% confidence interval with the line on the diagonal indicating the null. Results are shown for all indicators that loaded on a given factor along with the factor results for the compulsive (panel A), psychotic (panel B), neurodevelopmental (panel C), and internalizing disorders (panel D) factors. Note that the y-axes are scaled to be unique to each panel.

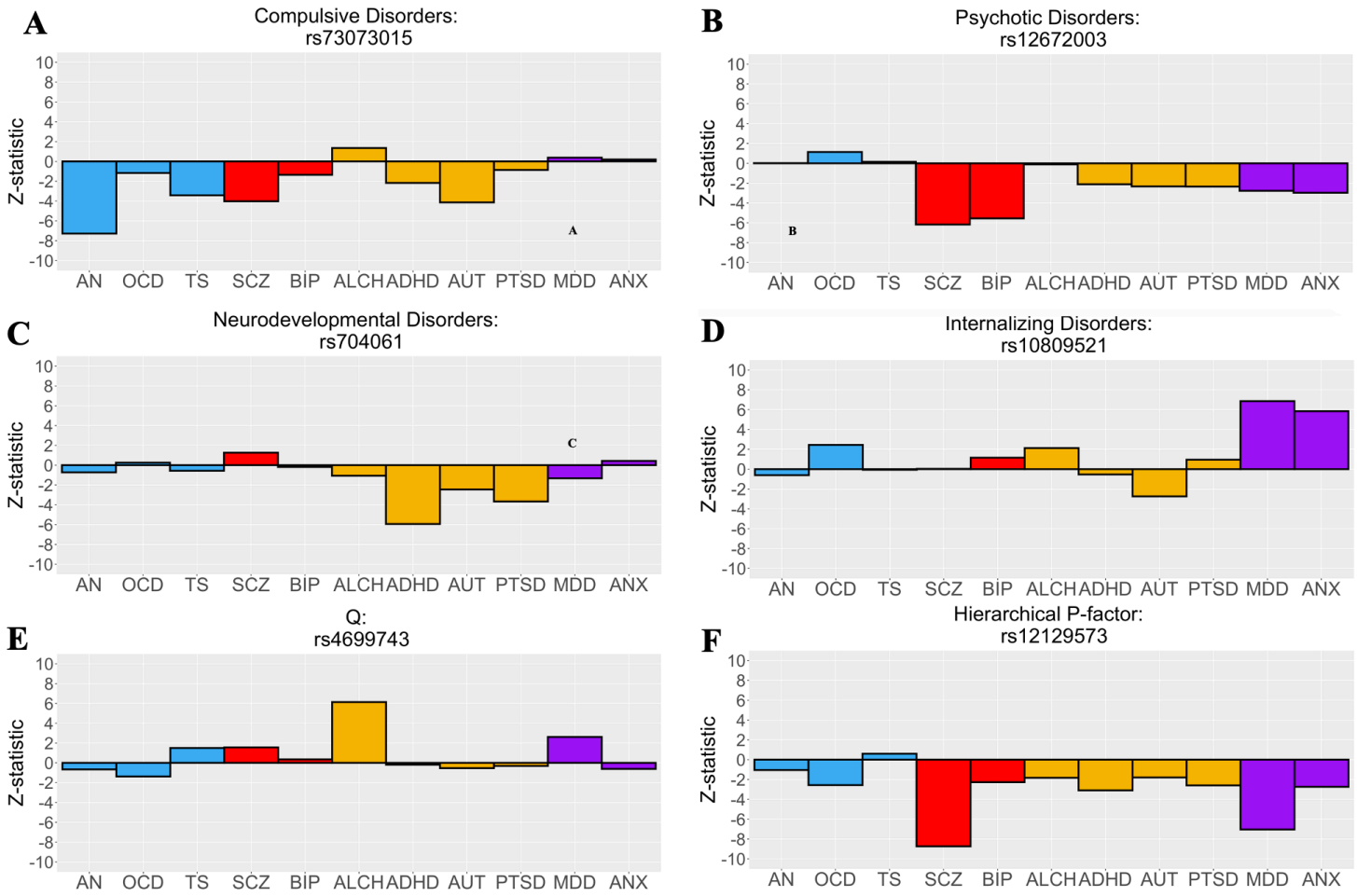

Supplementary Figure 33. Bar plots of SNP level effects. Figure displays Z-statistics from univariate summary statistics for individual variants estimated as genome-wide significant for the Compulsive disorders (panel A), Psychotic disorders (panel B), Neurodevelopmental disorders (panel C), and Internalizing disorders factor (panel D) from the correlated factors model. Panel E depicts a variant that was significant across all factor specific Q_{SNP} estimates. This particular variant lies within the well described ADH1B gene. Panel F displays a variant that was significant for the second-order, *p*-factor from the hierarchical factor model.

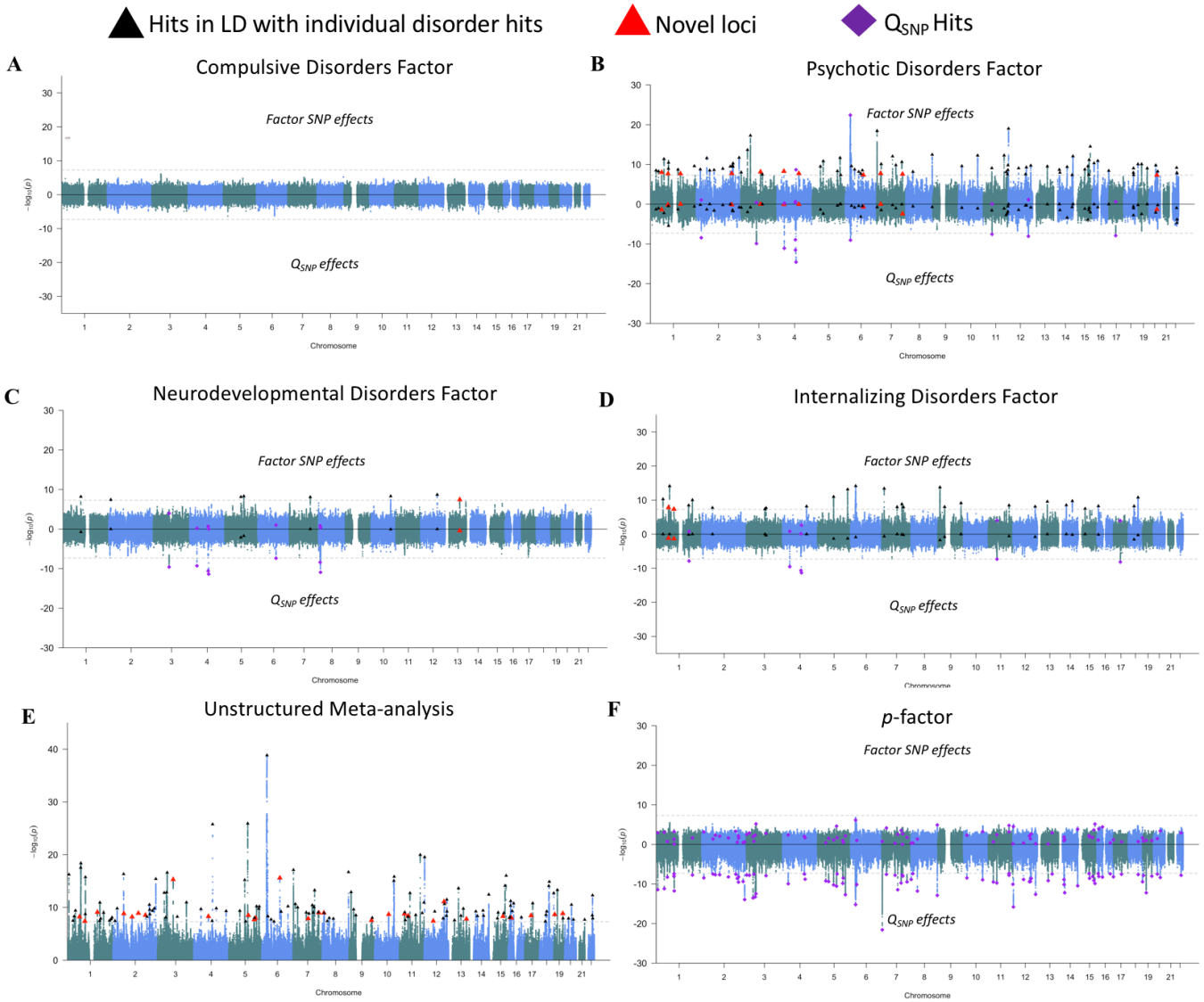

Supplementary Figure 34. Miami plots for Psychiatric Factors using S-LDSC Matrix. Genomic SEM was used to conduct a multivariate GWAS from the correlated factors model for compulsive disorders (Factor 1; panel A), psychotic disorders (Factor 2; panel B), neurodevelopmental disorders (Factor 3; panel C), and internalizing disorders (Factor 4; panel D) using the genome-wide S-LDSC matrix. Panel E depicts results from the omnibus test across all 11 psychiatric traits. Panel F depicts the results of the SNP effect on the second-order general liability factor from the hierarchical model. The top half of the hierarchical and correlated factors plots depicts the -log10(p) values for SNP effects on the factor; the bottom half depicts the log(10)p values for the factor specific Q_{SNP} effects. The gray dashed line marks the threshold for genome-wide significance ($p < 5 \times 10^{-8}$). Black triangles denote independent factor hits that were in LD with hits for one of the univariate indicators and were not in LD factor-specific Q_{SNP} hits. Large red triangles denote novel loci that were not in LD with any of the univariate GWAS or factor-specific Q_{SNP} hits. Purple diamonds denote Q_{SNP} hits.

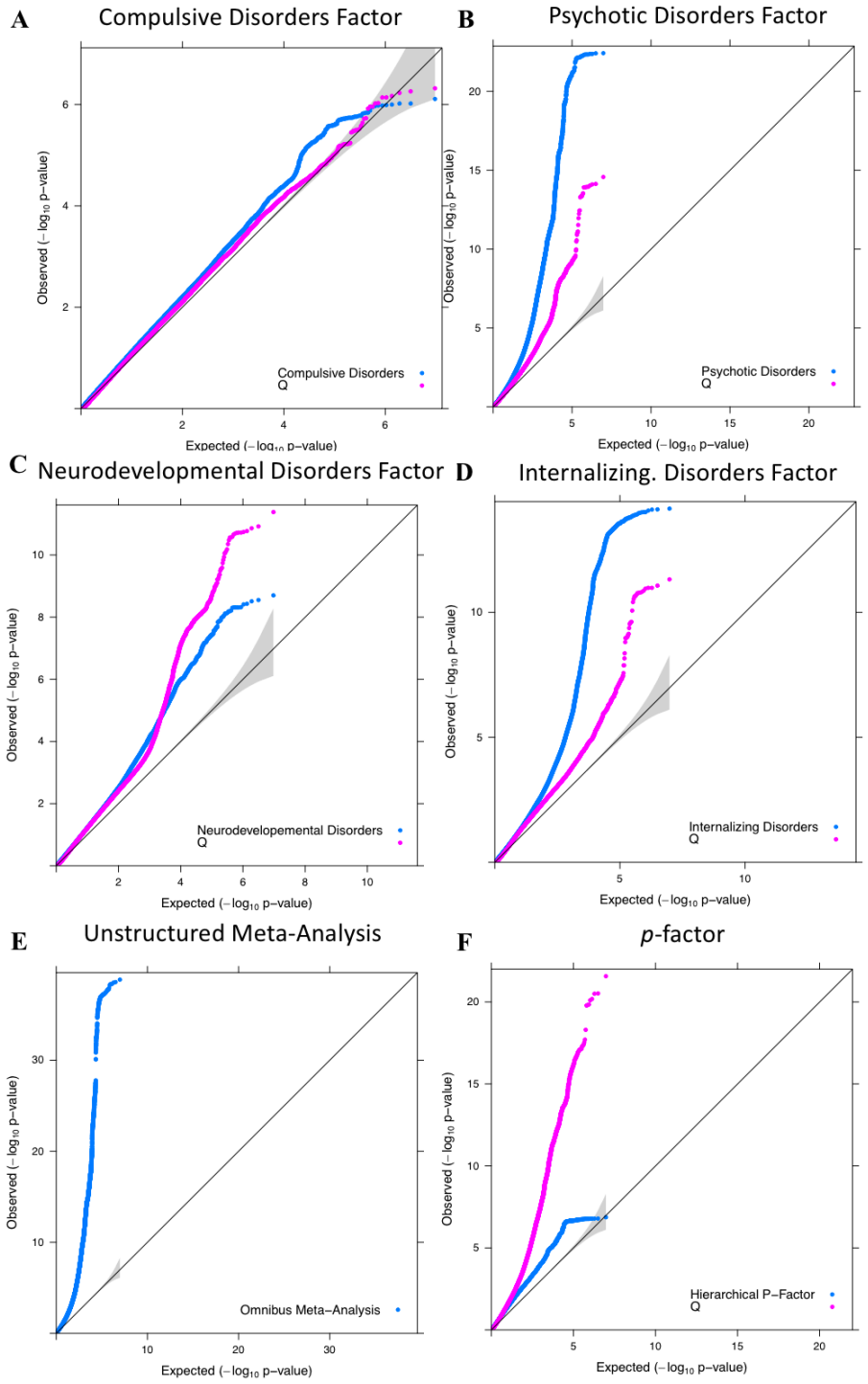

Supplementary Figure 35. QQ-plots for Multivariate GWAS using S-LDSC. Expected −log10(*p*)-values are those expected under the null hypothesis. The shaded area indicates the 95% confidence interval with the line on the diagonal indicating the null. In the top four panels, results are shown for the compulsive disorders (panel A), psychotic disorders (panel B), neurodevelopmental disorders (panel C), and internalizing disorders (panel D) factors from the correlated factors model. Panel E depicts the results from the 11 *df* omnibus meta-analysis across all 11 psychiatric indicators. Panel F depicts results for the hierarchical, second-order factor. Blue lines depict results for the psychiatric factors. Pink lines depict the factor specific Q_{SNP} estimates.

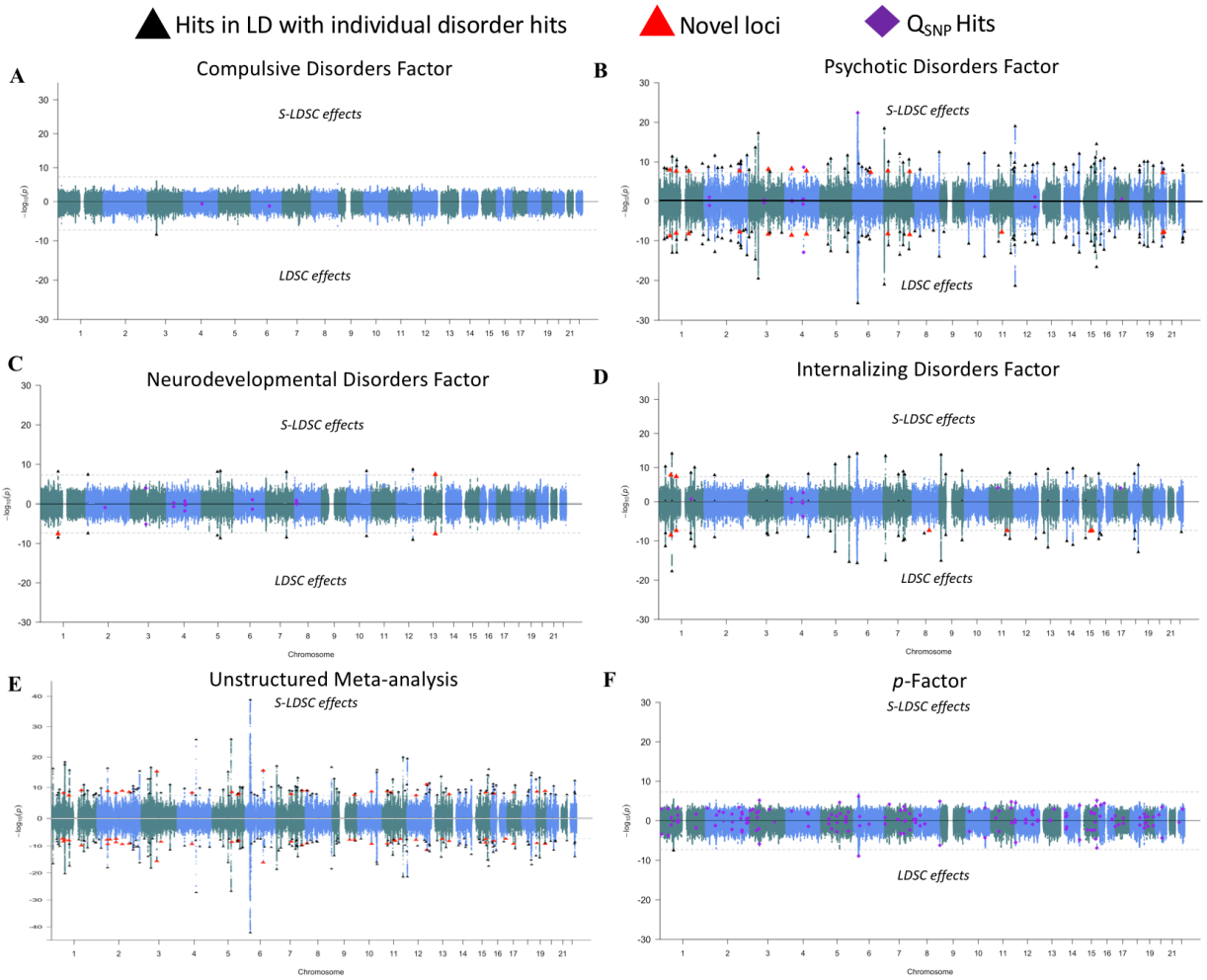

Supplementary Figure 36. Miami plots of Multivariate GWAS using S-LDSC (top) and LDSC (bottom). Genomic SEM was used to conduct a multivariate GWAS using both the S-LDSC and LDSC genome-wide, genetic covariance matrices. For all panels, results from S-LDSC and LDSC are shown on the top half and bottom half of the Miami plots, respectively. Results are shown from the correlated factors model for compulsive disorders (Factor 1; panel A), psychotic disorders (Factor 2; panel B), neurodevelopmental disorders (Factor 3; panel C), and internalizing disorders (Factor 4; panel D) using the genome-wide S-LDSC matrix. Panel E depicts results from the omnibus test across all 11 psychiatric traits. Panel F depicts the results of the SNP effect on the second-order general liability factor from the hierarchical model. The gray dashed line marks the threshold for genome-wide significance ($p < 5 \times 10^{-8}$). Black triangles denote independent factor hits that were in LD with hits for one of the univariate indicators and were not in LD factor-specific Q_{SNP} hits. Large red triangles denote novel loci that were not in LD with any of the univariate GWAS or factor-specific Q_{SNP} hits. Purple diamonds denote Q_{SNP} hits.

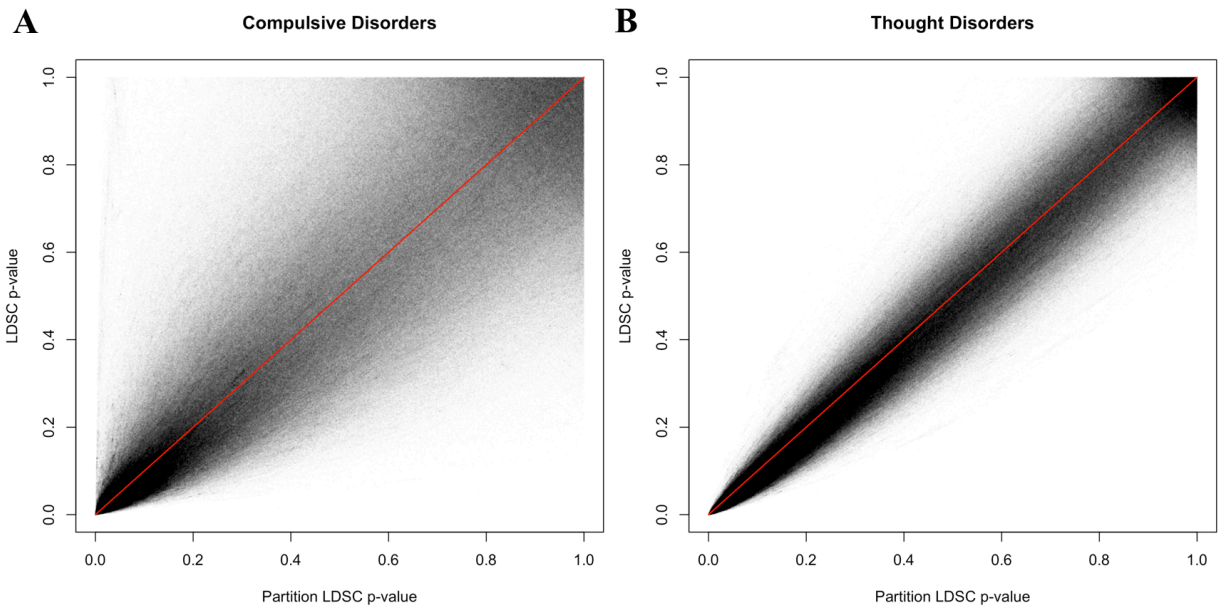

Supplementary Figure 37a. Comparison of GWAS p-values for LDSC and S-LDSC. Scatter plot comparing *p*-values between LDSC (y-axis) and S-LDSC (x-axis) estimation for the compulsive disorders factor (panel A) and the thought disorders factor (panel B). Red line reflects the regression line for LDSC predicting itself (i.e., a slope of 1), with dots above the line estimated as less significant for LDSC.

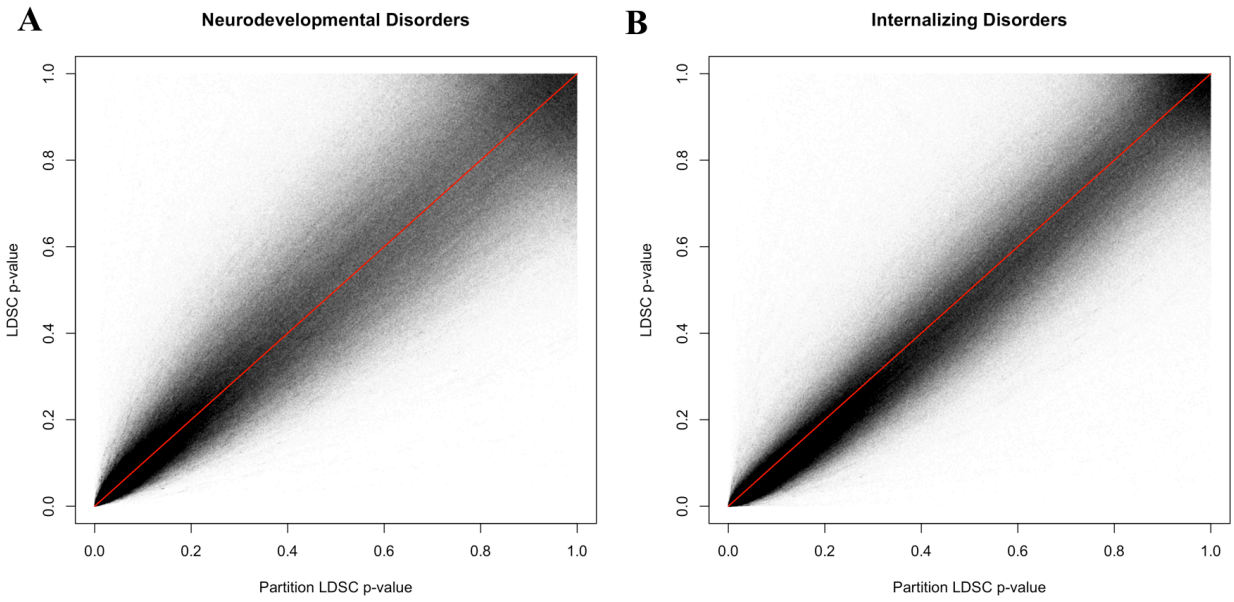

Supplementary Figure 37b. Comparison of GWAS p-values for LDSC and S-LDSC. Scatter plot comparing *p*-values between LDSC (y-axis) and S-LDSC (x-axis) estimation for the neurodevelopmental disorders factor (panel A) and the internalizing disorders factor (panel B). Red line reflects the regression line for LDSC predicting itself (i.e., a slope of 1), with dots above the line estimated as less significant for LDSC.

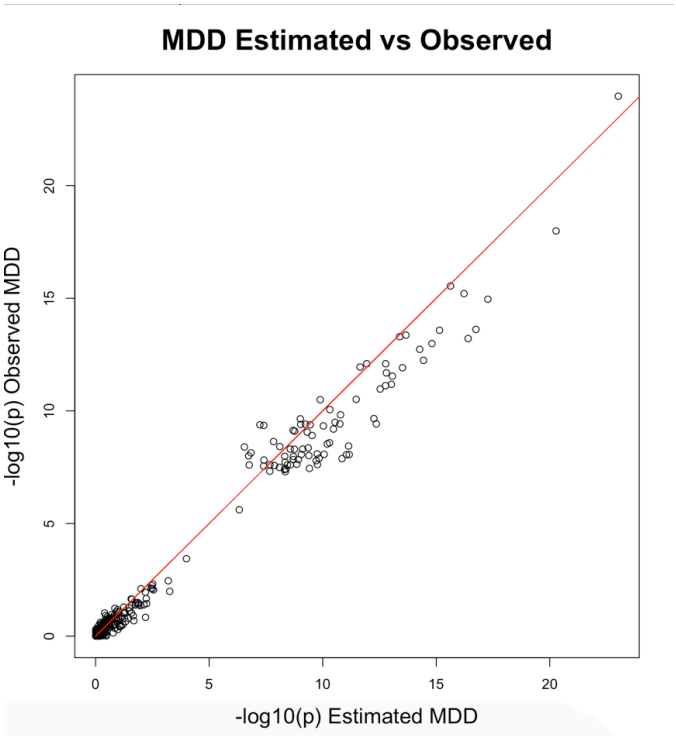

Supplementary Figure 38. Comparison of GWAS -log10(p-values) estimated and observed for MDD. Scatter plot compares -log10(*p*-values) between what was observed for MDD versus computing an indirect, estimated effect of the SNP effect on MDD in the context of the correlated factors model. This indirect effect was estimated in Genomic SEM and computed as the sum of the product of the effect of the SNP on the neurodevelopmental factors by the factor loading for MDD on this factor and the product of the effect of the SNP on the internalizing factor by the factor loading of MDD on the internalizing factor. Scatterplot displays these effects for the 109 independent loci for MDD and 200 randomly selected loci. Red line reflects the regression line for observed MDD predicting itself (i.e., a slope of 1), with dots above the line more significant for observed -log10(*p*-values). The correlation in this plot between the observed and estimated MDD -log10(*p*-values) was > .99.

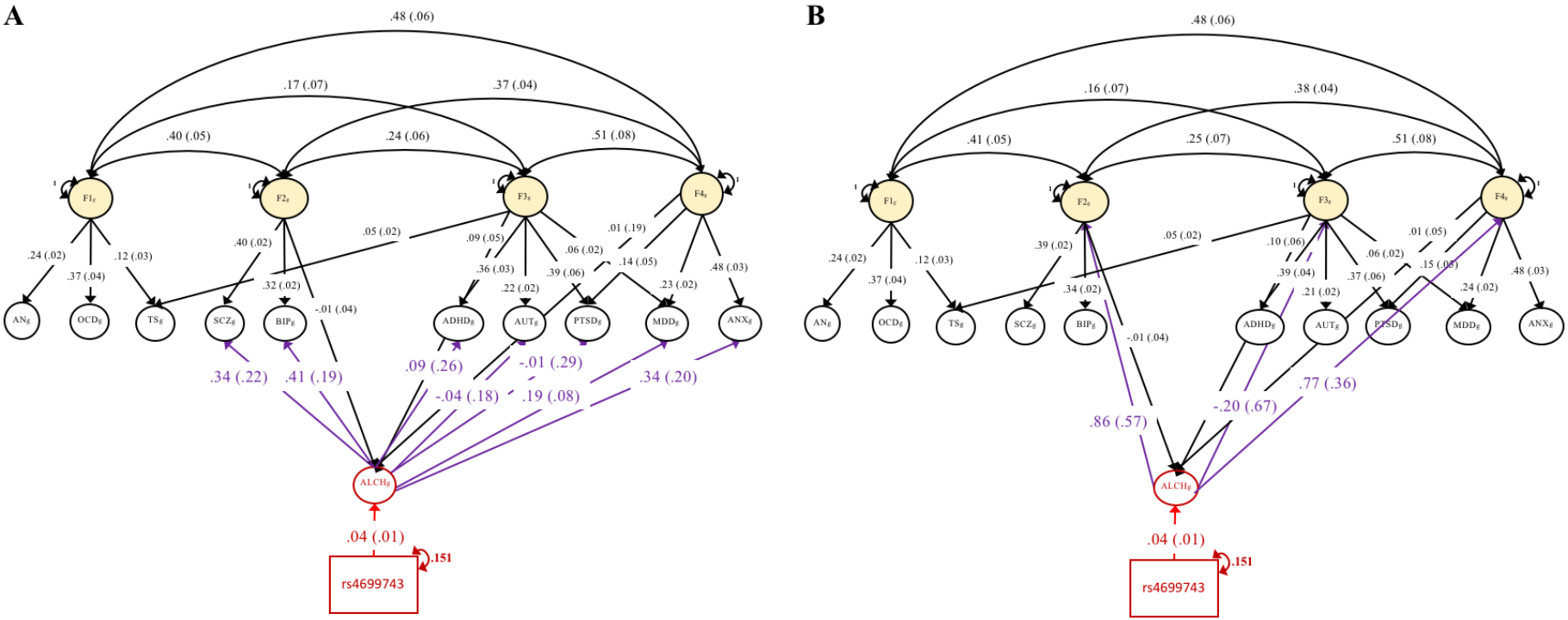

Supplementary Figure 39. Multi-Trait Mendelian Randomization Model for ADH1B as Instrument of Problematic Alcohol Use. Figures display unstandardized parameter estimates (and standard errors in parentheses) from a model in which a SNP in the ADH1B gene was specified to predict ALCH, and ALCH to predict the indicators of the Psychotic, Neurodevelopmental, and Internalizing disorders factors (panel A) or the factors themselves (panel B). Paths from the SNP to ALCH are depicted in red, while direct paths from ALCH to disorders or factors are depicted in purple. For simplicity, residual variances for the disorders are not depicted. We note that the ADH1B showed a smaller effect on ALCH due to the lead ADH1B variant (rs1229984; p =1.135E-60 for univariate effect on ALCH) from our ALCH meta-analysis being listwise deleted across all 11 psychiatric traits. We also note that models in which the SNP was specified to additionally predict the compulsive disorders factor all fit slightly worse, while producing equivalent point estimates to those displayed here. Finally, we note that the factor variances of 1 depicted in panel B reflect the residual variances of the factor.

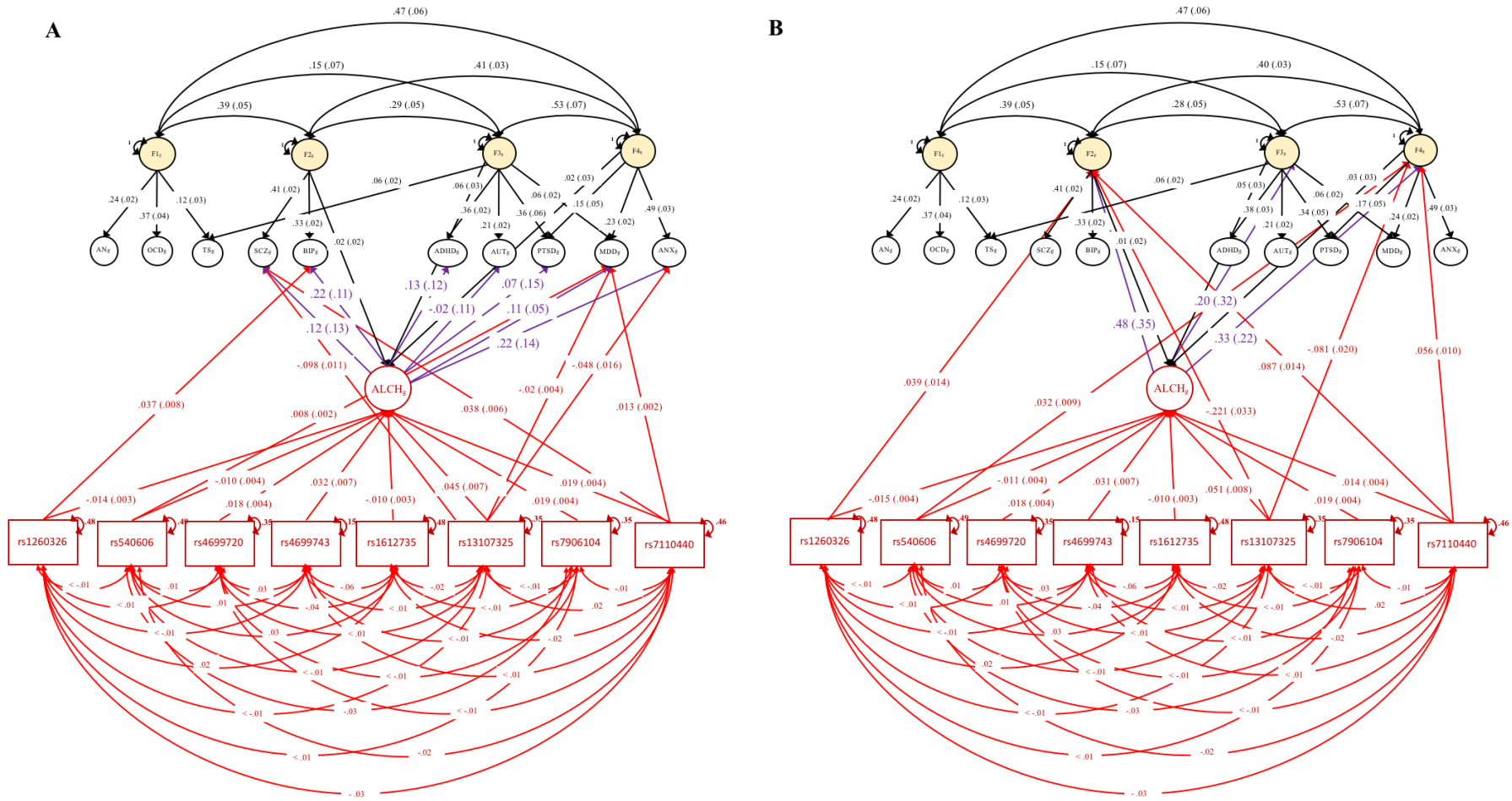

Supplementary Figure 40. Multi-Trait, Multi-SNP Mendelian Randomization Models for Problematic Alcohol Use. Figures display unstandardized parameter estimates (and standard errors in parentheses) from models that examined the causal effect of ALCH on the disorders (panel A) and the more general psychiatric factors (panel B). The 8 SNPs used as instruments for ALCH were identified from an independent discovery GWAS of problematic alcohol use. Paths from SNPs to disorders are depicted in red, while direct paths from ALCH to disorders or factors are depicted in purple. Results revealed a causal effect of ALCH on MDD and BIP (panel A), but not on the more general Internalizing or Psychotic disorders factors (panel B), or the remaining factors or disorders. For simplicity, residual variances for the disorders are not depicted. We note that the factor variances of 1 depicted in panel B reflect the residual variances of the factor

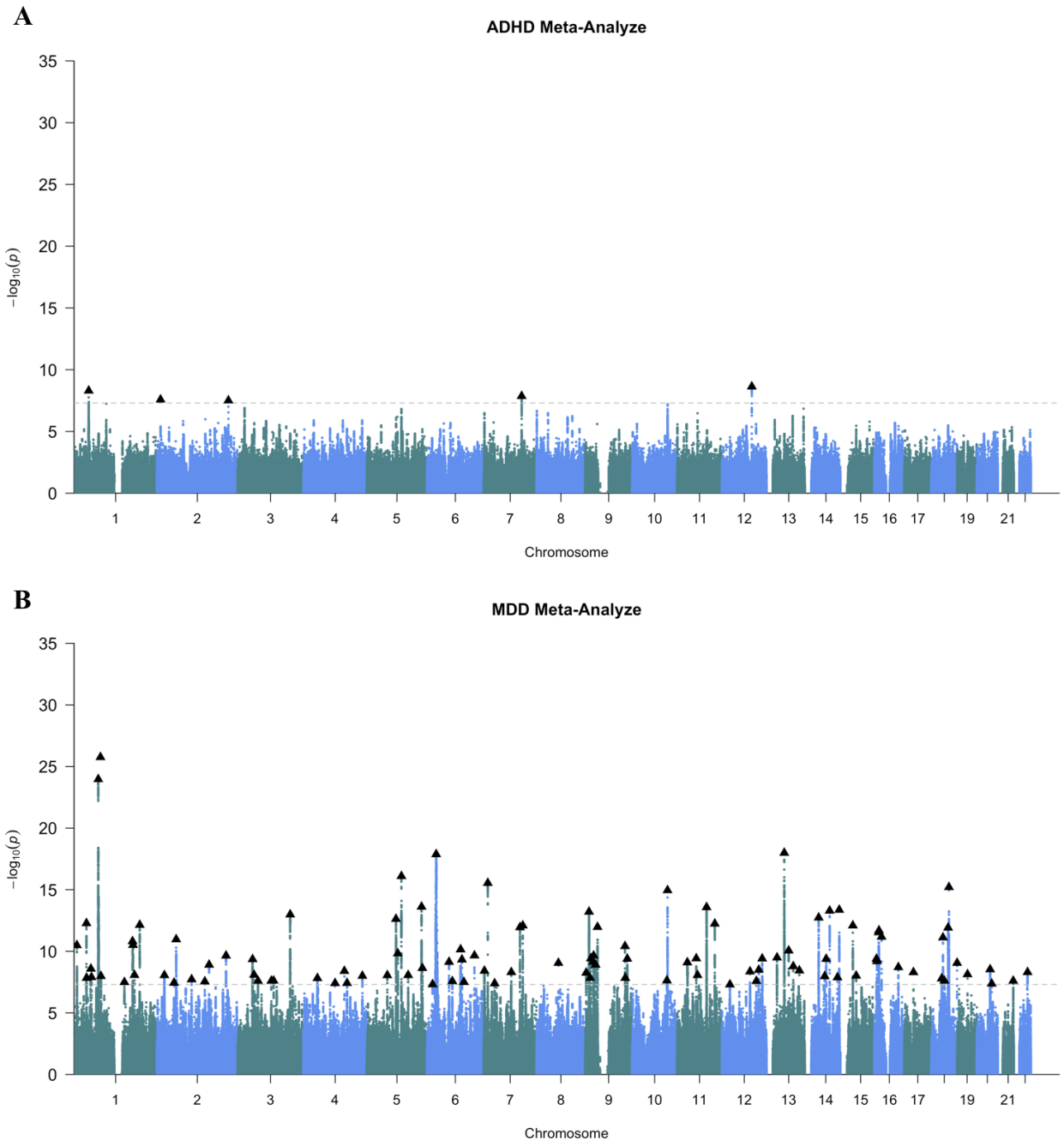

Supplementary Figure 41a. Manhattan plots from meta-analyses of ADHD and MDD. Genomic SEM was used to conduct a meta-analysis of attention-deficit/hyperactivity disorder (ADHD; panel A) and major depressive disorder (MDD; panel B). The gray dashed line marks the threshold for genome-wide significance ($p < 5 \times 10^{-8}$). Black triangles denote independent loci.

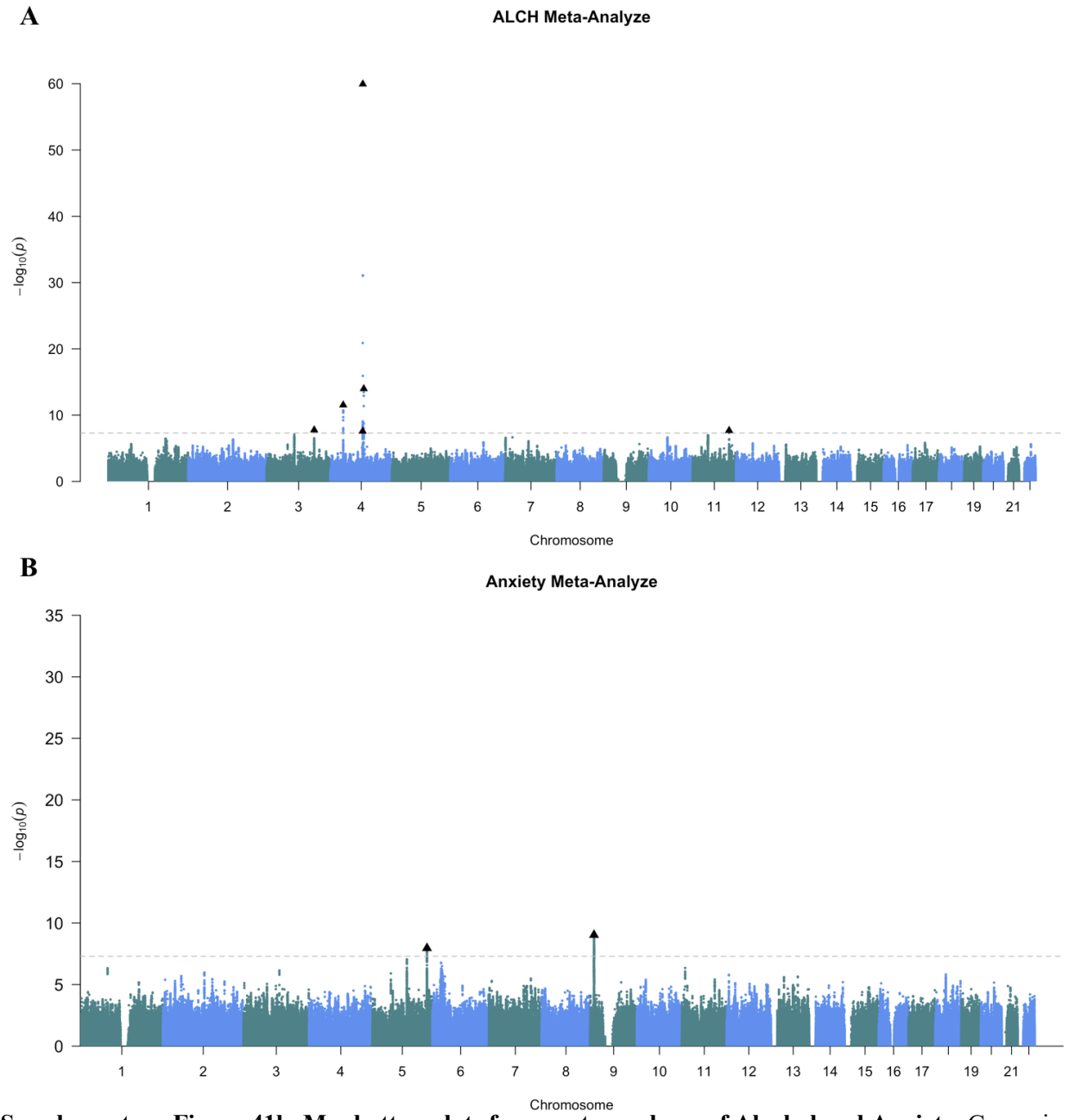

Supplementary Figure 41b. Manhattan plots from meta-analyses of Alcohol and Anxiety. Genomic SEM was used to conduct a meta-analysis of problematic alcohol use (panel A) and anxiety disorders (panel B). The gray dashed line marks the threshold for genome-wide significance ($p < 5 \times 10^{-8}$). Black triangles denote independent loci.

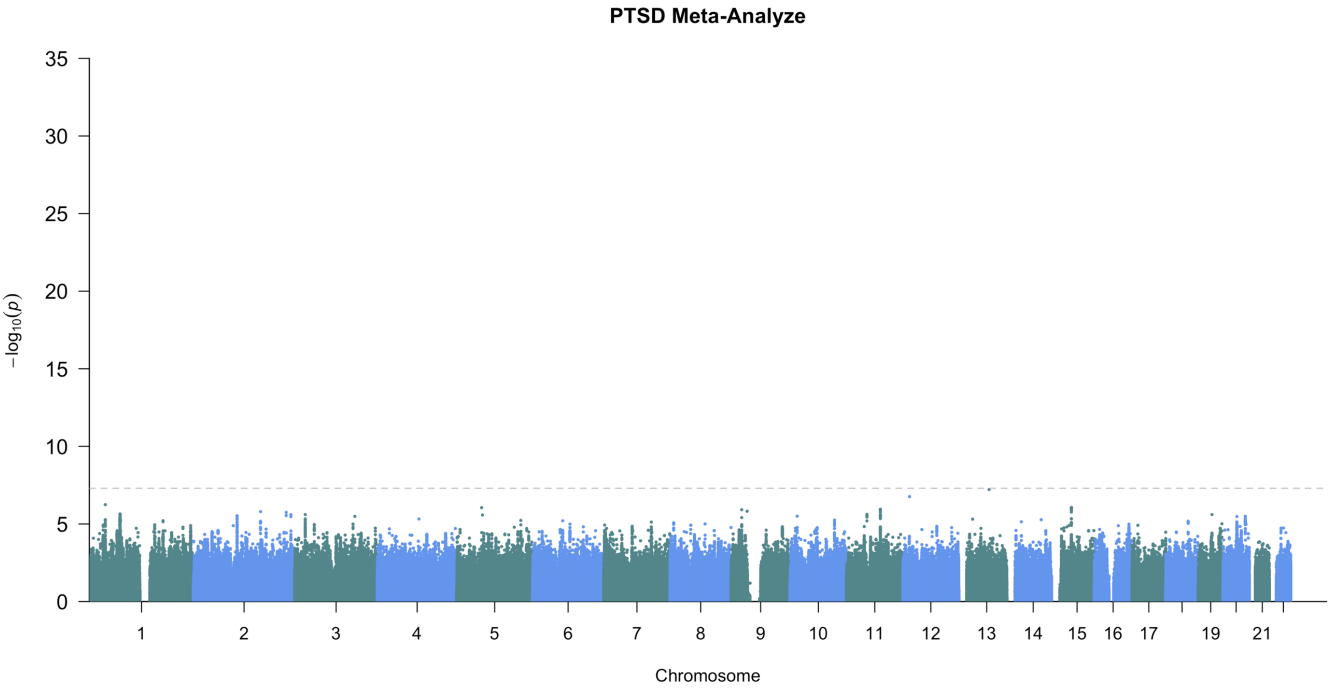

Supplementary Figure 41c. Manhattan plots from meta-analysis of PTSD. Genomic SEM was used to conduct a meta-analysis of post-traumatic stress disorder (PTSD). The gray dashed line marks the threshold for genome-wide significance ($p < 5 \times 10^{-8}$).

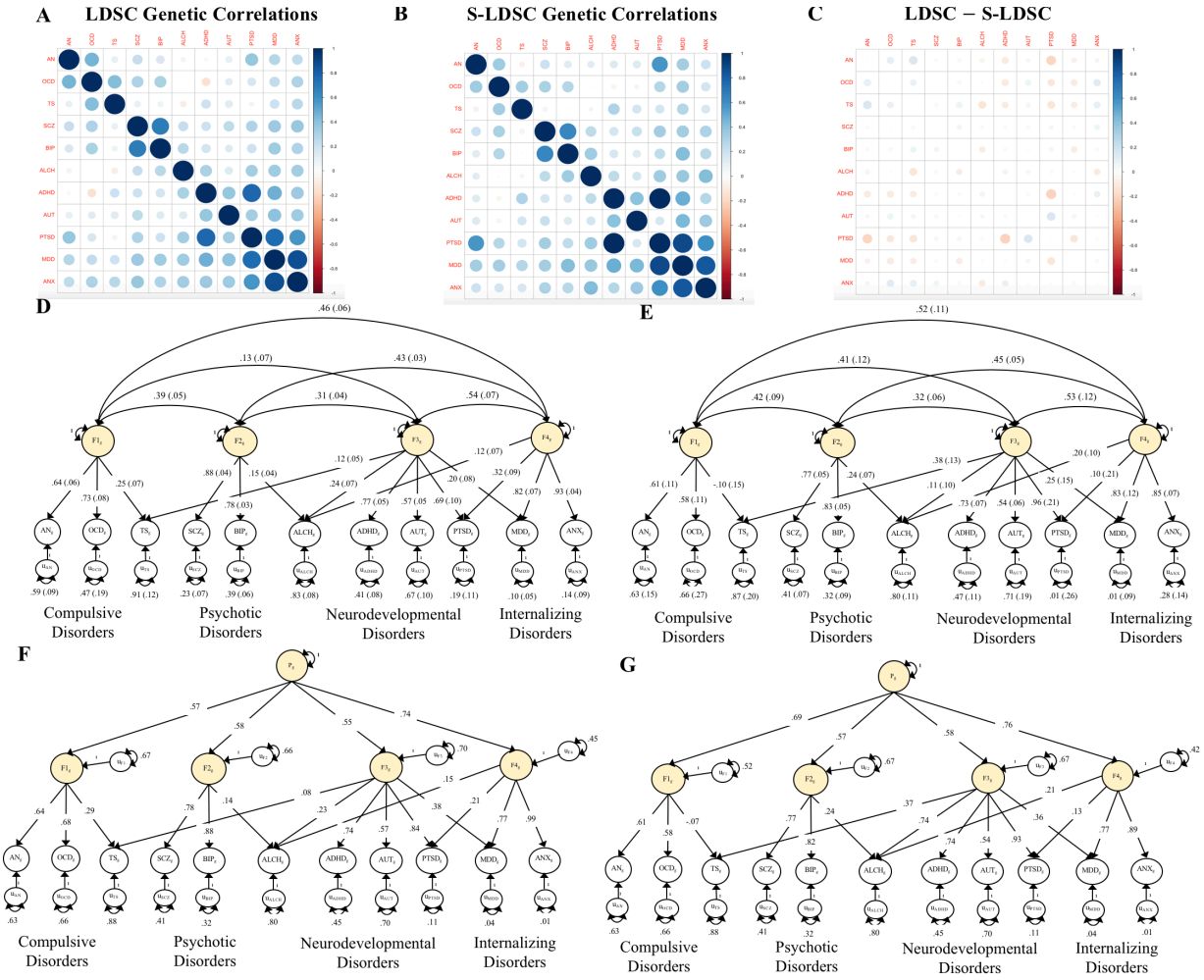

Supplementary Figure 42. Heatmap of Genetic Correlations and Factor Models. Panel A: LD-score regression was used to estimate the genetic correlations among the eleven psychiatric traits. The heatmap was hierarchically clustered using the *corrplot* R package. **Panel B:** S-LDSC was used to estimate the genetic correlations across the same eleven psychiatric traits. The heatmap was ordered based on that in Panel A for comparative purposes. **Panel C:** Figure presents difference LDSC and S-LDSC estimates. **Panel D:** Standardized results for correlated factors model fit to LDSC matrix. **Panel E:** Standardized results for correlated factors model fit to S-LDSC matrix. **Panel F:** Standardized results for hierarchical factor model fit to LDSC matrix. **Panel G:** Standardized results for hierarchical factor model fit to S-LDSC matrix. ADHD = attention-deficit/hyperactivity disorder; OCD = obsessive-compulsive disorder; TS = Tourette syndrome; PTSD = post-traumatic stress disorder; AN = anorexia nervosa; AUT = autism spectrum disorder; ALCH = problematic alcohol use; ANX = anxiety; MDD = major depressive disorder; BIP = bipolar disorder; SCZ = schizophrenia.

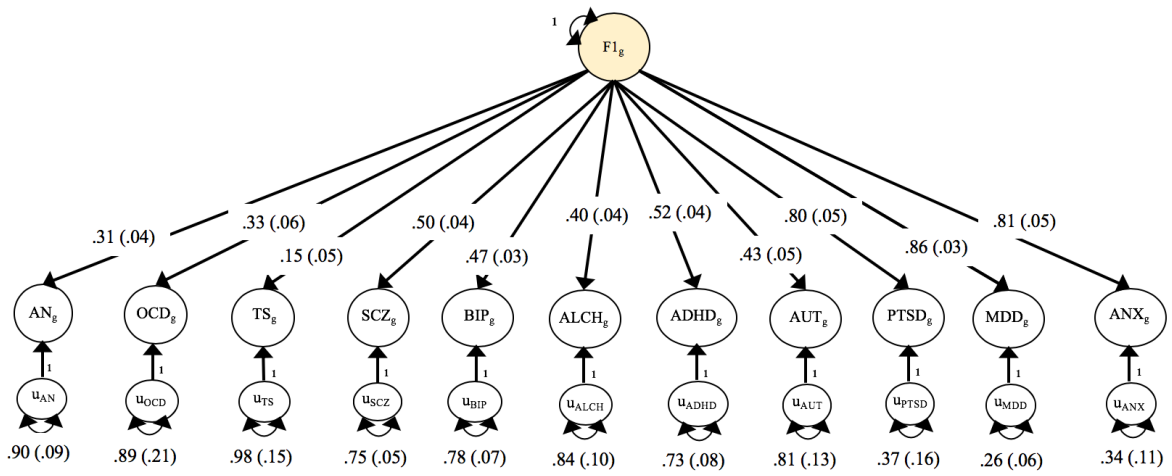

Supplementary Figure 43a. Even-autosome Genetic CFA for Common Factor Model. Figure presents the standardized results for a CFA fit to an even-autosome genetic covariance matrix for a common factor model. ADHD = attention-deficit/hyperactivity disorder; OCD = obsessive-compulsive disorder; TS = Tourette syndrome; PTSD = post-traumatic stress disorder; AN = anorexia nervosa; AUT = autism spectrum disorder; ALCH = problematic alcohol use; ANX = anxiety; MDD = major depressive disorder; BIP = bipolar disorder; SCZ = schizophrenia.

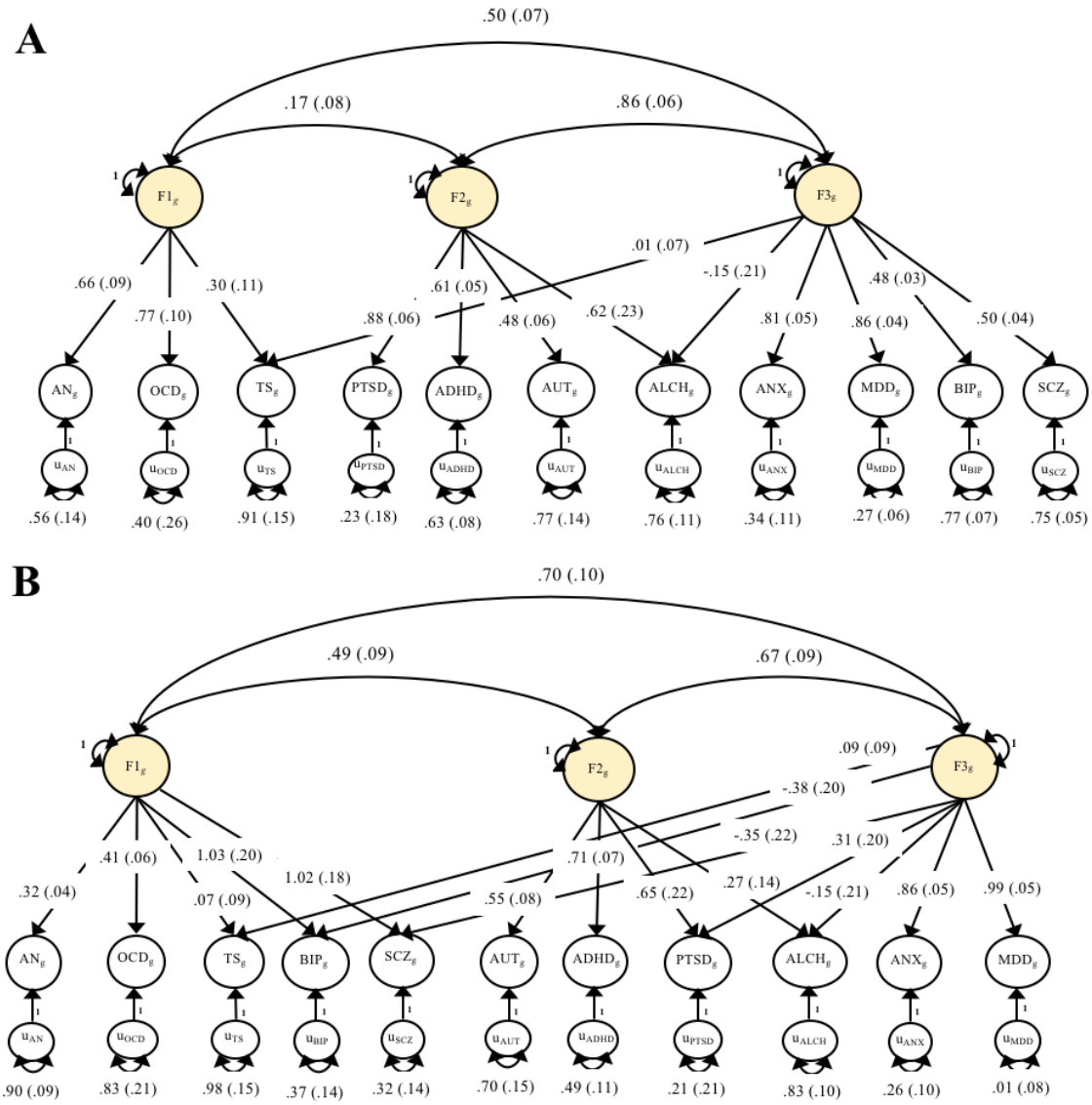

Supplementary Figure 43b. Three-Factor Genetic CFAs in Even Autosomes. Figure presents the standardized results for CFA fit to an even-autosome genetic covariance matrix based on a four-factor oblique (panel A) and orthogonal (panel B) EFAs fit to an odd autosome genetic covariance matrix. There is one less factor than was estimated in the EFA as TS was initially estimated to load on a factor as its only indicator. CFAs based on orthogonal EFAs included factor correlations as pruning factor loadings from the EFA solution will re-introduce these correlations. ADHD = attention-deficit/hyperactivity disorder; OCD = obsessive-compulsive disorder; TS = Tourette syndrome; PTSD = post-traumatic stress disorder; AN = anorexia nervosa; AUT = autism spectrum disorder; ALCH = problematic alcohol use; ANX = anxiety; MDD = major depressive disorder; BIP = bipolar disorder; SCZ = schizophrenia.

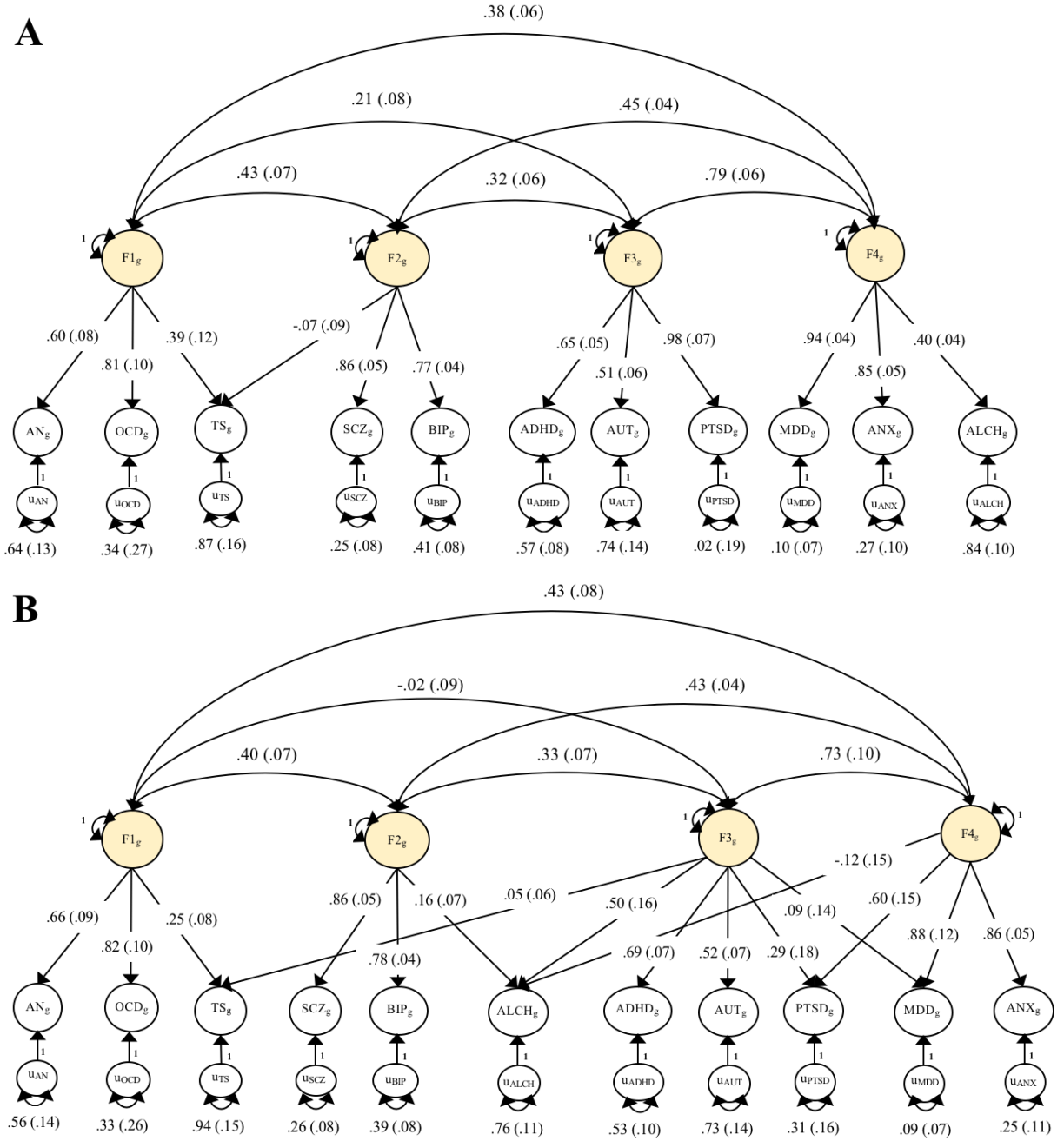

Supplementary Figure 43c. Four-Factor Genetic CFAs in Even Autosomes. Figure presents the standardized results for CFA fit to an even-autosome genetic covariance matrix based on a five-factor oblique (panel A) and orthogonal (panel B) EFAs fit to an odd autosome genetic covariance matrix. There is one less factor than was estimated in the EFA as TS was initially estimated to load on a factor as its only indicator. CFAs based on orthogonal EFAs included factor correlations as pruning factor loadings from the EFA solution will re-introduce these correlations. ADHD = attention-deficit/hyperactivity disorder; OCD = obsessive-compulsive disorder; TS = Tourette syndrome; PTSD = post-traumatic stress disorder; AN = anorexia nervosa; AUT = autism spectrum disorder; ALCH = problematic alcohol use; ANX = anxiety; MDD = major depressive disorder; BIP = bipolar disorder; SCZ = schizophrenia.

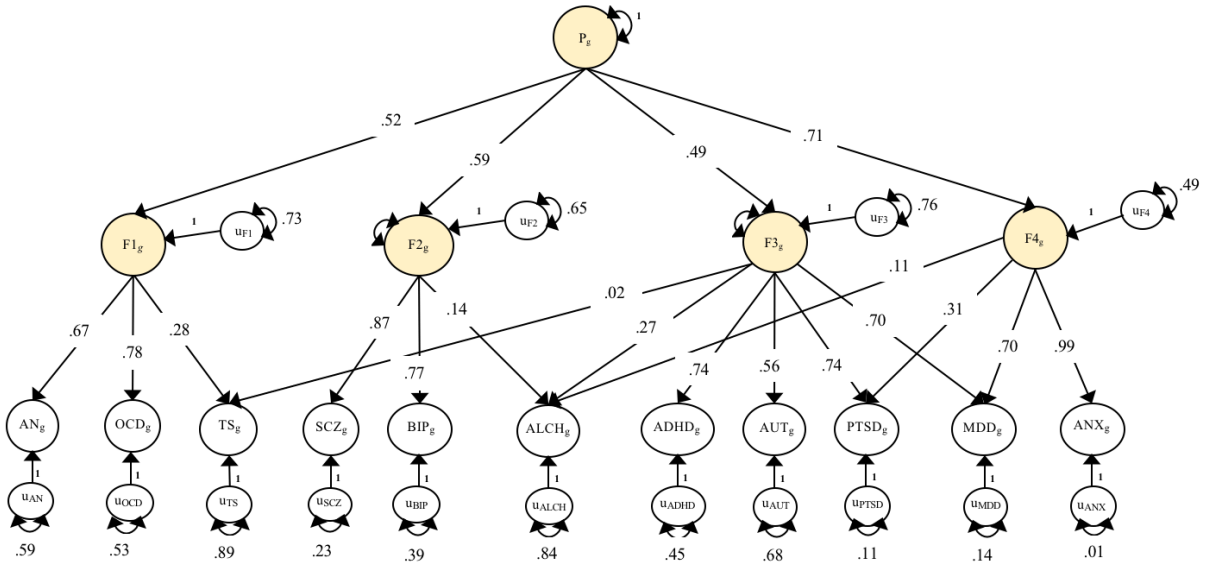

Supplementary Figure 43d. Genetic Hierarchical CFA in Even Autosomes. Figure presents the standardized results for a hierarchical CFA fit to an even-autosome genetic covariance matrix. ADHD = attention-deficit/hyperactivity disorder; OCD = obsessive-compulsive disorder; TS = Tourette syndrome; PTSD = post-traumatic stress disorder; AN = anorexia nervosa; AUT = autism spectrum disorder; ALCH = problematic alcohol use; ANX = anxiety; MDD = major depressive disorder; BIP = bipolar disorder; SCZ = schizophrenia.

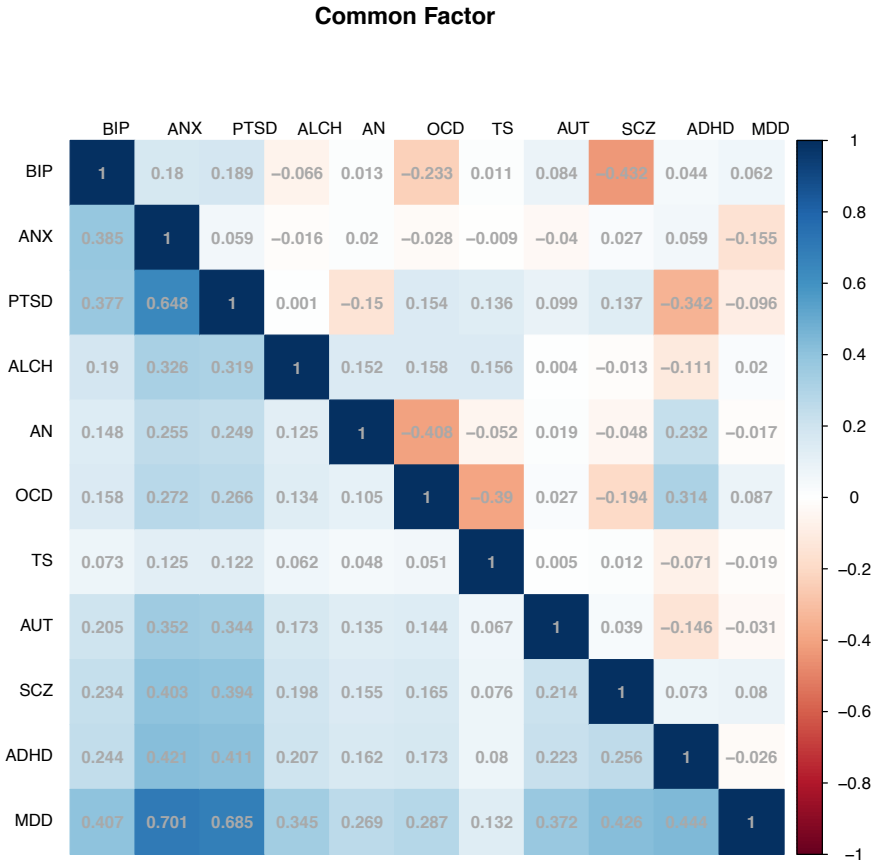

Supplementary Figure 44a. Heatmap of Model Implied Genetic Correlation Matrix for Common Factor Solution in Even Autosomes. The lower diagonal of the heatmap presents the model implied correlation matrix for the common factor CFA fit to the even autosome genetic correlation matrix. The upper diagonal depicts the observed even autosome genetic correlation matrix subtracted from the model implied correlation matrix, with positive values indicating upwardly biased estimates. ADHD = attention-deficit/hyperactivity disorder; OCD = obsessive-compulsive disorder; TS = Tourette syndrome; PTSD = post-traumatic stress disorder; AN = anorexia nervosa; AUT = autism spectrum disorder; ALCH = problematic alcohol use; ANX = anxiety; MDD = major depressive disorder; BIP = bipolar disorder; SCZ = schizophrenia.

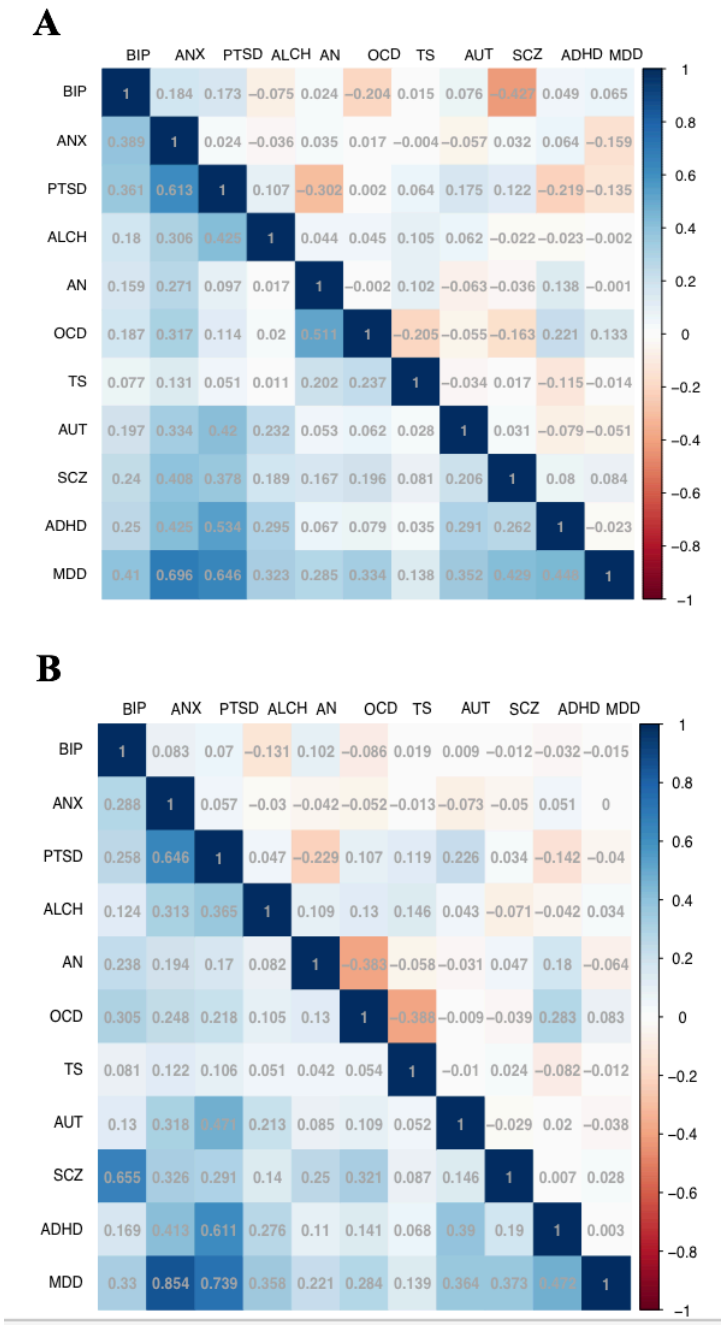

Supplementary Figure 44b. Heatmap of Model Implied Genetic Correlation Matrix for Three-Factor CFA Solutions fit in Even Autosomes. The lower diagonal of the heatmap presents the model implied correlation matrix for the three correlated factor CFAs fit in the even autosome genetic correlation matrix that was specified based on the oblique (panel A) or orthogonal (panel B) EFAs. CFAs based on orthogonal EFAs included factor correlations as pruning factor loadings from the EFA solution will re-introduce these correlations. The upper diagonal depicts the observed even autosome genetic correlation matrix subtracted from the model implied correlation matrix, with positive values indicating upwardly biased estimates. ADHD = attention-deficit/hyperactivity disorder; OCD = obsessive-compulsive disorder; TS = Tourette syndrome; PTSD = post-traumatic stress disorder; AN = anorexia nervosa; AUT = autism spectrum disorder; ALCH = problematic alcohol use; ANX = anxiety; MDD = major depressive disorder; BIP = bipolar disorder; SCZ = schizophrenia.

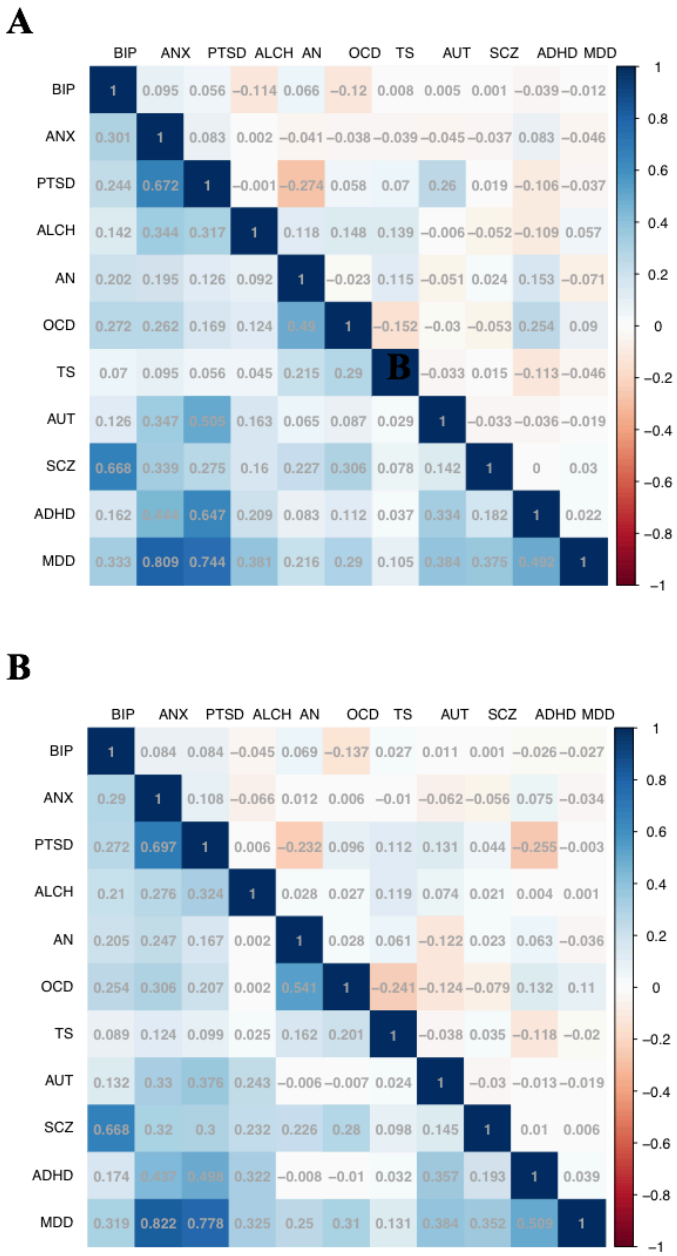

Supplementary Figure 44c. Heatmap of Model Implied Genetic Correlation Matrix for Four-Factor CFA Solutions fit in Even Autosomes. The lower diagonal of the heatmap presents the model implied correlation matrix for the four correlated factor CFAs fit in an even autosome correlation matrix that were specified based on the oblique (panel A) or orthogonal (panel B) EFAs. CFAs based on orthogonal EFAs included factor correlations as pruning factor loadings from the EFA solution will re-introduce these correlations. The upper diagonal depicts the observed even autosome genetic correlation matrix subtracted from the model implied correlation matrix, with positive values indicating upwardly biased estimates. ADHD = attention-deficit/hyperactivity disorder; OCD = obsessive-compulsive disorder; TS = Tourette syndrome; PTSD = post-traumatic stress disorder; AN = anorexia nervosa; AUT = autism spectrum disorder; ALCH = problematic alcohol use; ANX = anxiety; MDD = major depressive disorder; BIP = bipolar disorder; SCZ = schizophrenia.

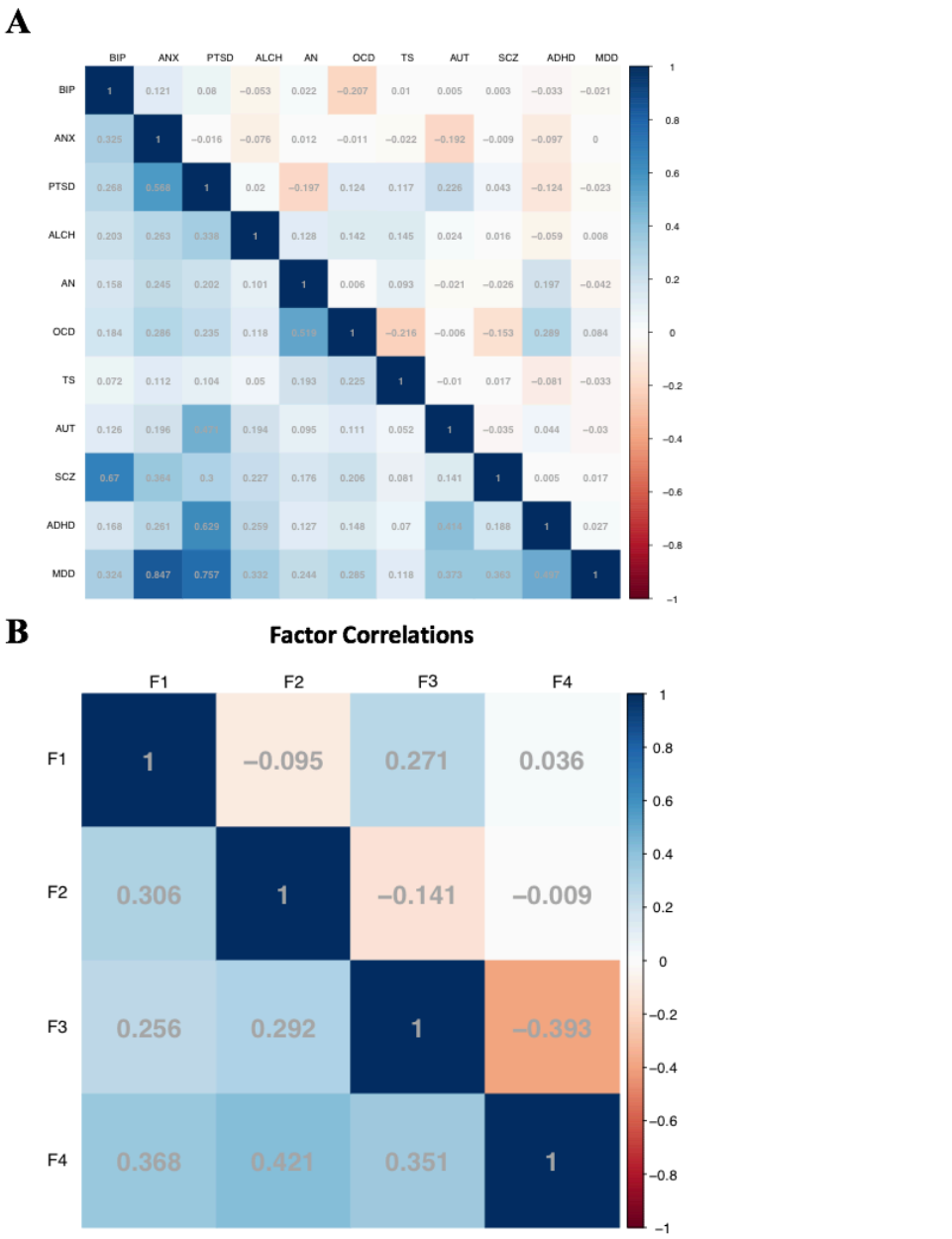

Supplementary Figure 44d. Heatmap of Model Implied Genetic Correlation Matrix for Hierarchical Solution in Even Autosomes. In panel A, the lower diagonal of the heatmap presents the model implied correlation matrix for the hierarchical CFA fit to the even autosome genetic correlation matrix. The upper diagonal depicts the observed even autosome genetic correlation matrix subtracted from the model implied correlation matrix, with positive values indicating upwardly biased estimates. The lower diagonal of Panel B depicts the model implied factor correlations from the hierarchical CFA. The upper diagonal depicts the correlations estimated in the corresponding non-hierarchical CFA subtracted from the model implied factor correlations in the hierarchical CFA. ADHD = attention-deficit/hyperactivity disorder; OCD = obsessive-compulsive disorder; TS = Tourette syndrome; PTSD = post-traumatic stress disorder; AN = anorexia nervosa; AUT = autism spectrum disorder; ALCH = problematic alcohol use; ANX = anxiety; MDD = major depressive disorder; BIP = bipolar disorder; SCZ = schizophrenia.

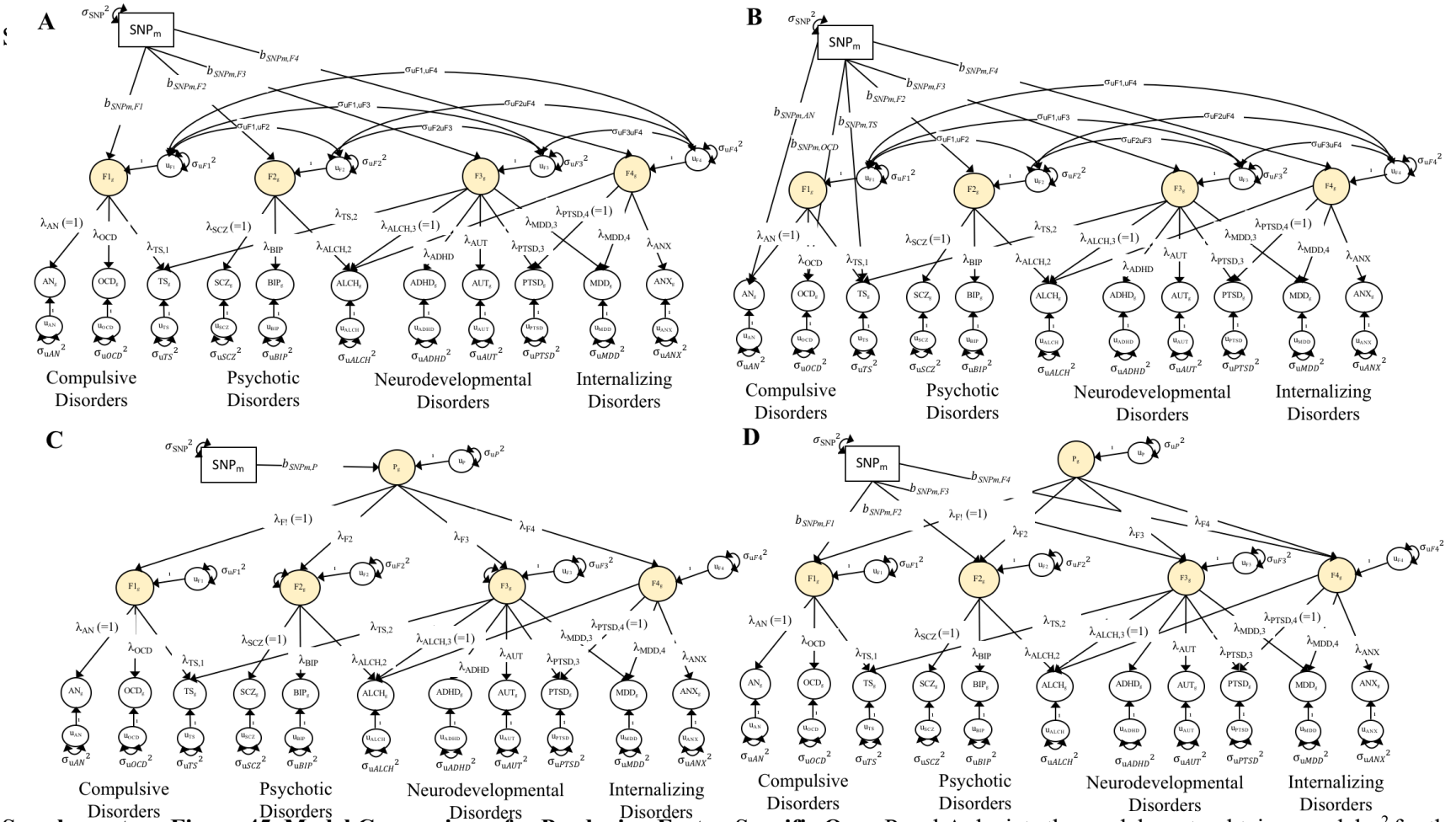

Supplementary Figure 45. Model Comparisons for Producing Factor-Specific Q_{SNP}. Panel A depicts the model run to obtain a model χ^2 for the multivariate GWAS of the correlated factors model. Panel B depicts the follow-up model for the compulsive disorders factor, where a given SNP predicts the indicators of the compulsive disorders factor, in addition to the remaing three factors. Model χ^2 difference tests between the model χ^2 for the model in panels A and B index whether the pattern of associations with a given SNP is well-accounted for by the factor. In order to produce factor-specific Q_{SNP} estimates for the remaining three factors, the model in Panel B was re-specified three additional times, such that the SNP simultanesouly predicted three of the factors and the factor indicators for the remaining factor. Panel C depicts the model run to obtain model χ^2 for the hierarchical factor model. Panel D depicts the follow-up model in which the SNP directly predicts the four, first-order factors. As with the top two panels, comparing the model χ^2 across panels C and D produces indexes whether the pattern of associations with a given SNP is well-accounted for by the factor structure of the second-order, *p*-factor. The loading of the first indicator for each factor is fixed to 1 in all panels for identification purposes.

Supplemental References

1. Willer, C. J., Li, Y. & Abecasis, G. R. METAL: fast and efficient meta-analysis of genomewide association scans. *Bioinformatics* **26,** 2190–2191 (2010).
2. Howard, D. M. *et al.* Genome-wide meta-analysis of depression identifies 102 independent variants and highlights the importance of the prefrontal brain regions. *Nature Neuroscience* **22,** 343 (2019).
3. Demontis, D. *et al.* Discovery of the first genome-wide significant risk loci for attention deficit/hyperactivity disorder. *Nature Genetics* **51,** 63 (2019).
4. Howard, D. M. *et al.* Genome-wide meta-analysis of depression identifies 102 independent variants and highlights the importance of the prefrontal brain regions. *Nature Neuroscience* **22,** 343–352 (2019).
5. Wray, N. R. *et al.* Genome-wide association analyses identify 44 risk variants and refine the genetic architecture of major depression. *Nature Genetics* **50,** 668 (2018).
6. Sanchez-Roige, S. *et al.* Genome-Wide Association Study Meta-Analysis of the Alcohol Use Disorders Identification Test (AUDIT) in Two Population-Based Cohorts. *American Journal of Psychiatry* **176,** 107–118 (2018).
7. Nievergelt, C. M. *et al.* International meta-analysis of PTSD genome-wide association studies identifies sex-and ancestry-specific genetic risk loci. *Nat Comms* **10,** 1–16 (2019).
8. Markon, K. E. Bifactor and hierarchical models: Specification, inference, and interpretation. *Annual review of clinical psychology* **15,** 51–69 (2019).
9. Zugman, A. *et al.* Reduced dorso-lateral prefrontal cortex in treatment resistant schizophrenia. *Schizophrenia research* **148,** 81–86 (2013).
10. Abé, C. *et al.* Manic episodes are related to changes in frontal cortex: a longitudinal neuroimaging study of bipolar disorder 1. *Brain, Behavior, and Immunity* **138,** 3440–3448 (2015).
11. Seidman, L. J., Valera, E. M. & Makris, N. Structural brain imaging of attention-deficit/hyperactivity disorder. *Biological Psychiatry* **57,** 1263–1272 (2005).
12. Kikinis, Z. *et al.* Gray matter volume reduction in rostral middle frontal gyrus in patients with chronic schizophrenia. *Schizophrenia research* **123,** 153–159 (2010).
13. Knöchel, C. *et al.* Cortical thinning in bipolar disorder and schizophrenia. *Schizophrenia research* **172,** 78–85 (2016).
14. Zarei, M. *et al.* Changes in gray matter volume and white matter microstructure in adolescents with obsessive-compulsive disorder. *Biological Psychiatry* **70,** 1083–1090 (2011).
15. Roessner, V. *et al.* Increased putamen and callosal motor subregion in treatment-naïve boys with Tourette syndrome indicates changes in the bihemispheric motor network. *Journal of Child Psychology and Psychiatry* **52,** 306–314 (2011).
16. Bloch, M. H., Leckman, J. F., Zhu, H. & Peterson, B. S. Caudate volumes in childhood predict symptom severity in adults with Tourette syndrome. *Neurology* **65,** 1253–1258 (2005).
17. Sato, W. *et al.* Increased putamen volume in adults with autism spectrum disorder. *Frontiers in Human Neuroscience* **8,** 957 (2014).
18. Scheel, C. *et al.* Imaging derived cortical thickness reduction in high-functioning autism: key regions and temporal slope. *Neuroimage* **58,** 391–400 (2011).
19. Kühn, S., Schubert, F. & Gallinat, J. Structural correlates of trait anxiety: reduced thickness in medial orbitofrontal cortex accompanied by volume increase in nucleus accumbens. *Journal of affective disorders* **134,** 315–319 (2011).
20. Canu, E. *et al.* Brain structural abnormalities in patients with major depression with or without generalized anxiety disorder comorbidity. *Journal of neurology* **262,** 1255–1265 (2015).
21. Watanabe, K. *et al.* A global overview of pleiotropy and genetic architecture in complex traits. *Nature Genetics* **51,** 1339–1348 (2019).

22. Zhao, B. *et al.* GWAS of 19,629 individuals identifies novel genetic variants for regional brain volumes and refines their genetic co-architecture with cognitive and mental health traits. *bioRxiv* 586339 (2019).
23. Jiang, L. *et al.* A resource-efficient tool for mixed model association analysis of large-scale data. (2019).
24. Vöhringer, P. A. M. S. M. P. H. *et al.* Cognitive Impairment in Bipolar Disorder and Schizophrenia: A Systematic Review. *Front. Psychiatry* **4,** (2013).
25. Kahn, R. S. & Keefe, R. S. E. Schizophrenia Is a Cognitive Illness: Time for a Change in Focus. *JAMA Psychiatry* **70,** 1107–1112 (2013).
26. Griffith, J. W. *et al.* Neuroticism as a common dimension in the internalizing disorders. *Psychological Medicine* **40,** 1125–1136 (2010).
27. John M Hettema, M. D. P. D., Michael C Neale, P. D., John M Myers, M. S., Carol A Prescott, P. D. & Kenneth S Kendler, M. D. A Population-Based Twin Study of the Relationship Between Neuroticism and Internalizing Disorders. *American Journal of Psychiatry* **163,** 857–864 (2006).
28. Thorp, J. G. *et al.* Symptom-level genetic modelling identifies novel risk loci and unravels the shared genetic architecture of anxiety and depression. *medRxiv* **37,** 2020.04.08.20057653 (2020).
29. McArdle, J. J. & Goldsmith, H. H. Alternative common factor models for multivariate biometric analyses. *Behav Genet* **20,** 569–608 (1990).
30. Grotzinger, A. D. *et al.* Genomic structural equation modelling provides insights into the multivariate genetic architecture of complex traits. *Nat Hum Behav* **3,** 513 (2019).
31. la Fuente, de, J., Davies, G., Grotzinger, A. D., Tucker-Drob, E. M. & Deary, I. J. A general dimension of genetic sharing across diverse cognitive traits inferred from molecular data. *Nat Hum Behav* 1–10 (2020).
32. Lee, P. H. *et al.* Genomic relationships, novel loci, and pleiotropic mechanisms across eight psychiatric disorders. *Cell* **179,** 1469–1482. e11 (2019).
33. Watanabe, K., Taskesen, E., Van Bochoven, A. & Posthuma, D. Functional mapping and annotation of genetic associations with FUMA. *Nat Comms* **8,** 1826 (2017).
34. Turley, P. *et al.* Multi-trait analysis of genome-wide association summary statistics using MTAG. *Nature Genetics* 1 (2018).
35. Baselmans, B. M. L. *et al.* Multivariate genome-wide analyses of the well-being spectrum. *Nature Genetics* **51,** 445–451 (2019).
36. Clarke, T.-K. *et al.* Genome-wide association study of alcohol consumption and genetic overlap with other health-related traits in UK Biobank (N= 112 117). *Molecular Psychiatry* **22,** 1376–1384 (2017).
37. Macgregor, S. *et al.* Associations of ADH and ALDH2 gene variation with self report alcohol reactions, consumption and dependence: an integrated analysis. *Hum Mol Genet* **18,** 580–593 (2009).
38. Bierut, L. J. *et al.* ADH1B is associated with alcohol dependence and alcohol consumption in populations of European and African ancestry. *Molecular Psychiatry* **17,** 445–450 (2012).
39. Gelernter, J. *et al.* Genome-wide association study of alcohol dependence: significant findings in African-and European-Americans including novel risk loci. *Molecular Psychiatry* **19,** 41–49 (2014).
40. Polimanti, R. & Gelernter, J. ADH1B: From alcoholism, natural selection, and cancer to the human phenome. *American Journal of Medical Genetics Part B: Neuropsychiatric Genetics* **177,** 113–125 (2018).
41. Kranzler, H. R. *et al.* Genome-wide association study of alcohol consumption and use disorder in 274,424 individuals from multiple populations. *Nat Comms* **10,** 1–11 (2019).
42. Muthén, B. O. Latent variable modeling in heterogeneous populations. *Psychometrika* **54,** 557–585 (1989).
43. Zhu, Z. *et al.* Causal associations between risk factors and common diseases inferred from GWAS summary data. *Nat Comms* **9,** 1–12 (2018).

44. Finucane, H. K. *et al.* Partitioning heritability by functional annotation using genome-wide association summary statistics. *Nature Genetics* **47,** 1228 (2015).
45. Cai, N. *et al.* Minimal phenotyping yields genome-wide association signals of low specificity for major depression. *Nature Genetics* 1–11 (2020).
46. Newson, J. J., Hunter, D. & Thiagarajan, T. C. The Heterogeneity of Mental Health Assessment. *Front. Psychiatry* **11,** 76 (2020).
47. Thorp, J. G. *et al.* Genetic heterogeneity in self-reported depressive symptoms identified through genetic analyses of the PHQ-9. *Psychological Medicine* 1–12 (2019).
48. Klein, A. & Tourville, J. 101 labeled brain images and a consistent human cortical labeling protocol. *Frontiers in neuroscience* **6,** 171 (2012).

Major Depressive Disorder Working Group of the Psychiatric Genomics Consortium

Naomi R Wray* 1, 2
Stephan Ripke* 3, 4, 5
Manuel Mattheisen* 6, 7, 8
Maciej Trzaskowski 1
Enda M Byrne 1
Abdel Abdellaoui 9
Mark J Adams 10
Esben Agerbo 11, 12, 13
Tracy M Air 14
Till F M Andlauer 15, 16
Silviu-Alin Bacanu 17
Marie Bækvad-Hansen 13, 18
Aartjan T F Beekman 19
Tim B Bigdeli 17, 20
Elisabeth B Binder 15, 21
Julien Bryois 22
Henriette N Buttenschøn 13, 23, 24
Jonas Bybjerg-Grauholm 13, 18
Na Cai 25, 26
Enrique Castelao 27
Jane Hvarregaard Christensen 8, 13, 24
Toni-Kim Clarke 10
Jonathan R I Coleman 28
Lucía Colodro-Conde 29
Baptiste Couvy-Duchesne 2, 30
Nick Craddock 31
Gregory E Crawford 32, 33
Gail Davies 34
Ian J Deary 34
Franziska Degenhardt 35
Eske M Derks 29
Nese Direk 36, 37
Conor V Dolan 9
Erin C Dunn 38, 39, 40
Thalia C Eley 28
Valentina Escott-Price 41
Farnush Farhadi Hassan Kiadeh 42
Hilary K Finucane 43, 44
Jerome C Foo 45
Andreas J Forstner 35, 46, 47, 48
Josef Frank 45
Héléna A Gaspar 28
Michael Gill 49
Fernando S Goes 50
Scott D Gordon 29
Jakob Grove 8, 13, 24, 51
Lynsey S Hall 10, 52
Christine Søholm Hansen 13, 18
Thomas F Hansen 53, 54, 55
Stefan Herms 35, 47
Ian B Hickie 56
Per Hoffmann 35, 47
Georg Homuth 57
Carsten Horn 58
Jouke-Jan Hottenga 9
David M Hougaard 13,18
David M Howard 10, 28
Marcus Ising 59
Rick Jansen 19
Ian Jones 60
Lisa A Jones 61
Eric Jorgenson 62
James A Knowles 63
Isaac S Kohane 64, 65, 66
Julia Kraft 4
Warren W. Kretzschmar 67
Zoltán Kutalik 68, 69
Yihan Li 67
Penelope A Lind 29
Donald J MacIntyre 70, 71
Dean F MacKinnon 50
Robert M Maier 2
Wolfgang Maier 72
Jonathan Marchini 73
Hamdi Mbarek 9
Patrick McGrath 74
Peter McGuffin 28
Sarah E Medland 29
Divya Mehta 2, 75
Christel M Middeldorp 9, 76, 77
Evelin Mihailov 78
Yuri Milaneschi 19
Lili Milani 78
Francis M Mondimore 50
Grant W Montgomery 1
Sara Mostafavi 79, 80
Niamh Mullins 28
Matthias Nauck 81, 82
Bernard Ng 80
Michel G Nivard 9
Dale R Nyholt 83
Paul F O'Reilly 28
Hogni Oskarsson 84
Michael J Owen 60
Jodie N Painter 29
Carsten Bøcker Pedersen 11, 12, 13
Marianne Giørtz Pedersen 11, 12, 13
Roseann E Peterson 17, 85
Erik Pettersson 22
Wouter J Peyrot 19
Giorgio Pistis 27
Danielle Posthuma 86, 87
Jorge A Quiroz 88
Per Qvist 8, 13, 24
John P Rice 89
Brien P. Riley 17
Margarita Rivera 28, 90
Saira Saeed Mirza 36
Robert Schoevers 91
Eva C Schulte 92, 93
Ling Shen 62
Jianxin Shi 94
Stanley I Shyn 95
Engilbert Sigurdsson 96
Grant C B Sinnamon 97
Johannes H Smit 19
Daniel J Smith 98
Hreinn Stefansson 99
Stacy Steinberg 99
Fabian Streit 45
Jana Strohmaier 45
Katherine E Tansey 100
Henning Teismann 101
Alexander Teumer 102
Wesley Thompson 13, 54, 103, 104
Pippa A Thomson 105
Thorgeir E Thorgeirsson 99
Matthew Traylor 106
Jens Treutlein 45
Vassily Trubetskoy 4
Andrés G Uitterlinden 107
Daniel Umbricht 108
Sandra Van der Auwera 109

1, Institute for Molecular Bioscience, The University of Queensland, Brisbane, QLD, AU
2, Queensland Brain Institute, The University of Queensland, Brisbane, QLD, AU
3, Analytic and Translational Genetics Unit, Massachusetts General Hospital, Boston, MA, US
4, Department of Psychiatry and Psychotherapy, Universitätsmedizin Berlin Campus Charité Mitte, Berlin, DE
5, Medical and Population Genetics, Broad Institute, Cambridge, MA, US
6, Department of Psychiatry, Psychosomatics and Psychotherapy, University of Wurzburg, Wurzburg, DE
7, Centre for Psychiatry Research, Department of Clinical Neuroscience, Karolinska Institutet, Stockholm, SE
8, Department of Biomedicine, Aarhus University, Aarhus, DK
9, Dept of Biological Psychology & EMGO+ Institute for Health and Care Research, Vrije Universiteit Amsterdam, Amsterdam, NL
10, Division of Psychiatry, University of Edinburgh, Edinburgh, GB
11, Centre for Integrated Register-based Research, Aarhus University, Aarhus, DK
12, National Centre for Register-Based Research, Aarhus University, Aarhus, DK
13, iPSYCH, The Lundbeck Foundation Initiative for Integrative Psychiatric Research,, DK
14, Discipline of Psychiatry, University of Adelaide, Adelaide, SA, AU
15, Department of Translational Research in Psychiatry, Max Planck Institute of Psychiatry, Munich, DE
16, Department of Neurology, Klinikum rechts der Isar, Technical University of Munich, Munich, DE
17, Department of Psychiatry, Virginia Commonwealth University, Richmond, VA, US
18, Center for Neonatal Screening, Department for Congenital Disorders, Statens Serum Institut, Copenhagen, DK
19, Department of Psychiatry, Vrije Universiteit Medical Center and GGZ inGeest, Amsterdam, NL
20, Virginia Institute for Psychiatric and Behavior Genetics, Richmond, VA, US
21, Department of Psychiatry and Behavioral Sciences, Emory University School of Medicine, Atlanta, GA, US
22, Department of Medical Epidemiology and Biostatistics, Karolinska Institutet, Stockholm, SE
23, Department of Clinical Medicine, Translational Neuropsychiatry Unit, Aarhus University, Aarhus, DK
24, iSEQ, Centre for Integrative Sequencing, Aarhus University, Aarhus, DK
25, Human Genetics, Wellcome Trust Sanger Institute, Cambridge, GB
26, Statistical genomics and systems genetics, European Bioinformatics Institute (EMBL-EBI), Cambridge, GB
27, Department of Psychiatry, Lausanne University Hospital and University of Lausanne, Lausanne, CH
28, Social, Genetic and Developmental Psychiatry Centre, King's College London, London, GB
29, Genetics and Computational Biology, QIMR Berghofer Medical Research Institute, Brisbane, QLD, AU
30, Centre for Advanced Imaging, The University of Queensland, Brisbane, QLD, AU
31, Psychological Medicine, Cardiff University, Cardiff, GB
32, Center for Genomic and Computational Biology, Duke University, Durham, NC, US
33, Department of Pediatrics, Division of Medical Genetics, Duke University, Durham, NC, US
34, Centre for Cognitive Ageing and Cognitive Epidemiology, University of Edinburgh, Edinburgh, GB
35, Institute of Human Genetics, University of Bonn, School of Medicine & University Hospital Bonn, Bonn, DE
36, Epidemiology, Erasmus MC, Rotterdam, Zuid-Holland, NL
37, Psychiatry, Dokuz Eylul University School Of Medicine, Izmir, TR
38, Department of Psychiatry, Massachusetts General Hospital, Boston, MA, US
39, Psychiatric and Neurodevelopmental Genetics Unit (PNGU), Massachusetts General Hospital, Boston, MA, US
40, Stanley Center for Psychiatric Research, Broad Institute, Cambridge, MA, US

41, Neuroscience and Mental Health, Cardiff University, Cardiff, GB
42, Bioinformatics, University of British Columbia, Vancouver, BC, CA
43, Department of Epidemiology, Harvard T.H. Chan School of Public Health, Boston, MA, US
44, Department of Mathematics, Massachusetts Institute of Technology, Cambridge, MA, US
45, Department of Genetic Epidemiology in Psychiatry, Central Institute of Mental Health, Medical Faculty Mannheim, Heidelberg University, Mannheim, Baden-Württemberg, DE
46, Department of Psychiatry (UPK), University of Basel, Basel, CH
47, Department of Biomedicine, University of Basel, Basel, CH
48, Centre for Human Genetics, University of Marburg, Marburg, DE
49, Department of Psychiatry, Trinity College Dublin, Dublin, IE
50, Psychiatry & Behavioral Sciences, Johns Hopkins University, Baltimore, MD, US
51, Bioinformatics Research Centre, Aarhus University, Aarhus, DK
52, Institute of Genetic Medicine, Newcastle University, Newcastle upon Tyne, GB
53, Danish Headache Centre, Department of Neurology, Rigshospitalet, Glostrup, DK
54, Institute of Biological Psychiatry, Mental Health Center Sct. Hans, Mental Health Services Capital Region of Denmark, Copenhagen, DK
55, iPSYCH, The Lundbeck Foundation Initiative for Psychiatric Research, Copenhagen, DK
56, Brain and Mind Centre, University of Sydney, Sydney, NSW, AU
57, Interfaculty Institute for Genetics and Functional Genomics, Department of Functional Genomics, University Medicine and Ernst Moritz Arndt University Greifswald, Greifswald, Mecklenburg-Vorpommern, DE
58, Roche Pharmaceutical Research and Early Development, Pharmaceutical Sciences, Roche Innovation Center Basel, F. Hoffmann-La Roche Ltd, Basel, CH
59, Max Planck Institute of Psychiatry, Munich, DE
60, MRC Centre for Neuropsychiatric Genetics and Genomics, Cardiff University, Cardiff, GB
61, Department of Psychological Medicine, University of Worcester, Worcester, GB
62, Division of Research, Kaiser Permanente Northern California, Oakland, CA, US
63, Psychiatry & The Behavioral Sciences, University of Southern California, Los Angeles, CA, US
64, Department of Biomedical Informatics, Harvard Medical School, Boston, MA, US
65, Department of Medicine, Brigham and Women's Hospital, Boston, MA, US
66, Informatics Program, Boston Children's Hospital, Boston, MA, US
67, Wellcome Trust Centre for Human Genetics, University of Oxford, Oxford, GB
68, Institute of Social and Preventive Medicine (IUMSP), University Hospital of Lausanne, Lausanne, VD, CH
69, Swiss Institute of Bioinformatics, Lausanne, VD, CH
70, Division of Psychiatry, Centre for Clinical Brain Sciences, University of Edinburgh, Edinburgh, GB
71, Mental Health, NHS 24, Glasgow, GB
72, Department of Psychiatry and Psychotherapy, University of Bonn, Bonn, DE
73, Statistics, University of Oxford, Oxford, GB
74, Psychiatry, Columbia University College of Physicians and Surgeons, New York, NY, US
75, School of Psychology and Counseling, Queensland University of Technology, Brisbane, QLD, AU
76, Child and Youth Mental Health Service, Children's Health Queensland Hospital and Health Service, South Brisbane, QLD, AU
77, Child Health Research Centre, University of Queensland, Brisbane, QLD, AU
78, Estonian Genome Center, University of Tartu, Tartu, EE
79, Medical Genetics, University of British Columbia, Vancouver, BC, CA
80, Statistics, University of British Columbia, Vancouver, BC, CA
81, DZHK (German Centre for Cardiovascular Research), Partner Site Greifswald, University Medicine, University Medicine Greifswald, Greifswald, Mecklenburg-Vorpommern, DE
82, Institute of Clinical Chemistry and Laboratory Medicine, University Medicine Greifswald, Greifswald, Mecklenburg-Vorpommern, DE

83, Institute of Health and Biomedical Innovation, Queensland University of Technology, Brisbane, QLD, AU
84, Humus, Reykjavik, IS
85, Virginia Institute for Psychiatric & Behavioral Genetics, Virginia Commonwealth University, Richmond, VA, US
86, Clinical Genetics, Vrije Universiteit Medical Center, Amsterdam, NL
87, Complex Trait Genetics, Vrije Universiteit Amsterdam, Amsterdam, NL
88, Solid Biosciences, Boston, MA, US
89, Department of Psychiatry, Washington University in Saint Louis School of Medicine, Saint Louis, MO, US
90, Department of Biochemistry and Molecular Biology II, Institute of Neurosciences, Biomedical Research Centre (CIBM), University of Granada, Granada, ES
91, Department of Psychiatry, University of Groningen, University Medical Center Groningen, Groningen, NL
92, Department of Psychiatry and Psychotherapy, University Hospital, Ludwig Maximilian University Munich, Munich, DE
93, Institute of Psychiatric Phenomics and Genomics (IPPG), University Hospital, Ludwig Maximilian University Munich, Munich, DE
94, Division of Cancer Epidemiology and Genetics, National Cancer Institute, Bethesda, MD, US
95, Behavioral Health Services, Kaiser Permanente Washington, Seattle, WA, US
96, Faculty of Medicine, Department of Psychiatry, University of Iceland, Reykjavik, IS
97, School of Medicine and Dentistry, James Cook University, Townsville, QLD, AU
98, Institute of Health and Wellbeing, University of Glasgow, Glasgow, GB
99, deCODE Genetics / Amgen, Reykjavik, IS
100, College of Biomedical and Life Sciences, Cardiff University, Cardiff, GB
101, Institute of Epidemiology and Social Medicine, University of Münster, Münster, Nordrhein-Westfalen, DE
102, Institute for Community Medicine, University Medicine Greifswald, Greifswald, Mecklenburg-Vorpommern, DE
103, Department of Psychiatry, University of California, San Diego, San Diego, CA, US
104, KG Jebsen Centre for Psychosis Research, Norway Division of Mental Health and Addiction, Oslo University Hospital, Oslo, NO
105, Medical Genetics Section, CGEM, IGMM, University of Edinburgh, Edinburgh, GB
106, Clinical Neurosciences, University of Cambridge, Cambridge, GB
107, Internal Medicine, Erasmus MC, Rotterdam, Zuid-Holland, NL
108, Roche Pharmaceutical Research and Early Development, Neuroscience, Ophthalmology and Rare Diseases Discovery & Translational Medicine Area, Roche Innovation Center Basel, F. Hoffmann-La Roche Ltd, Basel, CH
109, Department of Psychiatry and Psychotherapy, University Medicine Greifswald, Greifswald, Mecklenburg-Vorpommern, DE
110, Department of Psychiatry, Leiden University Medical Center, Leiden, NL
111, Virginia Institute for Psychiatric & Behavioral Genetics, Virginia Commonwealth University, Richmond, VA, US
112, Computational Sciences Center of Emphasis, Pfizer Global Research and Development, Cambridge, MA, US
113, Institute for Molecular Bioscience; Queensland Brain Institute, The University of Queensland, Brisbane, QLD, AU
114, Department of Psychiatry, University of Münster, Münster, Nordrhein-Westfalen, DE
115, Department of Psychiatry, University of Münster, Münster, DE
116, Department of Psychiatry, Melbourne Medical School, University of Melbourne, Melbourne, AU
117, Florey Institute for Neuroscience and Mental Health, University of Melbourne, Melbourne, AU

118, Institute of Medical Genetics and Pathology, University Hospital Basel, University of Basel, Basel, CH
119, Institute of Neuroscience and Medicine (INM-1), Research Center Juelich, Juelich, DE
120, Amsterdam Public Health Institute, Vrije Universiteit Medical Center, Amsterdam, NL
121, Centre for Integrative Biology, Università degli Studi di Trento, Trento, Trentino-Alto Adige, IT
122, Department of Psychiatry and Psychotherapy, Medical Center - University of Freiburg, Faculty of Medicine, University of Freiburg, Freiburg, DE
123, Center for NeuroModulation, Faculty of Medicine, University of Freiburg, Freiburg, DE
124, Psychiatry, Kaiser Permanente Northern California, San Francisco, CA, US
125, Medical Research Council Human Genetics Unit, Institute of Genetics and Molecular Medicine, University of Edinburgh, Edinburgh, GB
126, Department of Psychiatry, University of Toronto, Toronto, ON, CA
127, Centre for Addiction and Mental Health, Toronto, ON, CA
128, Division of Psychiatry, University College London, London, GB
129, Neuroscience Therapeutic Area, Janssen Research and Development, LLC, Titusville, NJ, US
130, Institute of Molecular and Cell Biology, University of Tartu, Tartu, EE
131, Psychosis Research Unit, Aarhus University Hospital, Risskov, Aarhus, DK
132, Munich Cluster for Systems Neurology (SyNergy), Munich, DE
133, University of Liverpool, Liverpool, GB
134, Mental Health Center Copenhagen, Copenhagen Universtity Hospital, Copenhagen, DK
135, Human Genetics and Computational Biomedicine, Pfizer Global Research and Development, Groton, CT, US
136, Psychiatry, Harvard Medical School, Boston, MA, US
137, Psychiatry, University of Iowa, Iowa City, IA, US
138, Department of Psychiatry and Behavioral Sciences, Johns Hopkins University, Baltimore, MD, US
139, Department of Psychiatry and Psychotherapy, University Medical Center Göttingen, Goettingen, Niedersachsen, DE
140, Human Genetics Branch, NIMH Division of Intramural Research Programs, Bethesda, MD, US
141, Faculty of Medicine, University of Iceland, Reykjavik, IS
142, Child and Adolescent Psychiatry, Erasmus MC, Rotterdam, Zuid-Holland, NL
143, Psychiatry, Erasmus MC, Rotterdam, Zuid-Holland, NL
144, Psychiatry, Dalhousie University, Halifax, NS, CA
145, Division of Epidemiology, New York State Psychiatric Institute, New York, NY, US
146, Department of Clinical Medicine, University of Copenhagen, Copenhagen, DK
147, Department of Medical & Molecular Genetics, King's College London, London, GB
148, Psychiatry & Behavioral Sciences, Stanford University, Stanford, CA, US
149, NIHR Maudsley Biomedical Research Centre, King's College London, London, GB
150, Genetics, University of North Carolina at Chapel Hill, Chapel Hill, NC, US
151, Psychiatry, University of North Carolina at Chapel Hill, Chapel Hill, NC, US

Bipolar Disorder Working Group of the Psychiatric Genomics Consortium

Eli A Stahl1,2,3†, Gerome Breen4,5†, Andreas J Forstner6,7,8,9,10†, Andrew McQuillin11†, Stephan Ripke12,13,14†, Vassily Trubetskoy13, Manuel Mattheisen15,16,17,18,19, Yunpeng Wang20,21, Jonathan R I Coleman4,5, Héléna A Gaspar4,5, Christiaan A de Leeuw22, Stacy Steinberg23, Jennifer M Whitehead Pavlides24, Maciej Trzaskowski25, Enda M Byrne25, Tune H Pers3,26, Peter A Holmans27, Alexander L Richards27, Liam Abbott12, Esben Agerbo19,28,29, Huda Akil30, Diego Albani31, Ney Alliey-Rodriguez32, Thomas D Als15,16,19, Adebayo Anjorin33, Verneri Antilla14, Swapnil Awasthi13, Judith A Badner34, Marie Bækvad-Hansen19,35, Jack D Barchas36, Nicholas Bass11, Michael Bauer37, Richard Belliveau12, Sarah E Bergen38, Carsten Bøcker Pedersen19,28,29, Erlend Bøen39, Marco P. Boks40, James Boocock41, Monika Budde42, William Bunney43, Margit Burmeister44, Jonas Bybjerg-Grauholm19,35, William Byerley45, Miquel Casas46,47,48,49, Felecia Cerrato12, Pablo Cervantes50, Kimberly Chambert12, Alexander W Charney2, Danfeng Chen12, Claire Churchhouse12,14, Toni-Kim Clarke51, William Coryell52, David W Craig53, Cristiana Cruceanu50,54, David Curtis55,56, Piotr M Czerski57, Anders M Dale58,59,60,61, Simone de Jong4,5, Franziska Degenhardt8, Jurgen Del-Favero62, J Raymond DePaulo63, Srdjan Djurovic64,65, Amanda L Dobbyn1,2, Ashley Dumont12, Torbjørn Elvsåshagen66,67, Valentina Escott-Price27, Chun Chieh Fan61, Sascha B Fischer6,10, Matthew Flickinger68, Tatiana M Foroud69, Liz Forty27, Josef Frank70, Christine Fraser27, Nelson B Freimer71, Louise Frisén72,73,74, Katrin Gade42,75, Diane Gage12, Julie Garnham76, Claudia Giambartolomei206, Marianne Giørtz Pedersen19,28,29, Jaqueline Goldstein12, Scott D Gordon77, Katherine Gordon-Smith78, Elaine K Green79, Melissa J Green80,133, Tiffany A Greenwood60, Jakob Grove15,16,19,81, Weihua Guan82, José Guzman-Parra83, Marian L Hamshere27, Martin Hautzinger84, Urs Heilbronner42, Stefan Herms6,8,10, Maria Hipolito85, Per Hoffmann6,8,10, Dominic Holland58,86, Laura Huckins1,2, Stéphane Jamain87,88, Jessica S Johnson1,2, Radhika Kandaswamy4, Robert Karlsson38, James L Kennedy89,90,91,92, Sarah Kittel-Schneider93, James A Knowles94,95, Manolis Kogevinas96, Anna C Koller8, Ralph Kupka97,98,99, Catharina Lavebratt72, Jacob Lawrence100, William B Lawson85, Markus Leber101, Phil H Lee12,14,102, Shawn E Levy103, Jun Z Li104, Chunyu Liu105, Susanne Lucae106, Anna Maaser8, Donald J MacIntyre107,108, Pamela B Mahon63,109, Wolfgang Maier110, Lina Martinsson73, Steve McCarroll12,111, Peter McGuffin4, Melvin G McInnis112, James D McKay113, Helena Medeiros95, Sarah E Medland77, Fan Meng30,112, Lili Milani114, Grant W Montgomery25, Derek W Morris115,116, Thomas W Mühleisen6,117, Niamh Mullins4, Hoang Nguyen1,2, Caroline M Nievergelt60,118, Annelie Nordin Adolfsson119, Evaristus A Nwulia85, Claire O'Donovan76, Loes M Olde Loohuis71, Anil P S Ori71, Lilijana Oruc120, Urban Ösby121, Roy H Perlis122,123, Amy Perry78, Andrea Pfennig37, James B Potash63, Shaun M Purcell2,109, Eline J Regeer124, Andreas Reif93, Céline S Reinbold6,10, John P Rice125, Fabio Rivas83, Margarita Rivera4,126, Panos Roussos1,2,127, Douglas M Ruderfer128, Euijung Ryu129, Cristina Sánchez-Mora46,47,49, Alan F Schatzberg130, William A Scheftner131, Nicholas J Schork132, Cynthia Shannon Weickert80,133, Tatyana Shehktman60, Paul D Shilling60, Engilbert Sigurdsson134, Claire Slaney76, Olav B Smeland135,136, Janet L Sobell137, Christine Søholm Hansen19,35, Anne T Spijker138, David St Clair139, Michael Steffens140, John S Strauss91,141, Fabian Streit70, Jana Strohmaier70, Szabolcs Szelinger142, Robert C Thompson112, Thorgeir E Thorgeirsson23, Jens Treutlein70, Helmut Vedder143, Weiqing Wang1,2, Stanley J Watson112, Thomas W Weickert80,133, Stephanie H Witt70, Simon Xi144, Wei Xu145,146, Allan H Young147, Peter Zandi148, Peng Zhang149, Sebastian Zöllner112, eQTLGen Consortium, BIOS Consortium, Rolf Adolfsson119, Ingrid Agartz17,39,150, Martin Alda76,151, Lena Backlund73, Bernhard T Baune152,158, Frank Bellivier153,154,155,156, Wade H Berrettini157, Joanna M Biernacka129, Douglas H R Blackwood51, Michael Boehnke68, Anders D Børglum15,16,19, Aiden Corvin116, Nicholas Craddock27, Mark J Daly12,14, Udo Dannlowski158, Tõnu Esko3,111,114,159, Bruno Etain153,155,156,160, Mark Frye161, Janice M Fullerton133,162, Elliot S Gershon32,163, Michael Gill116, Fernando Goes63, Maria Grigoroiu-Serbanescu164, Joanna Hauser57, David M Hougaard19,35, Christina M Hultman38, Ian Jones27, Lisa A Jones78, René S Kahn2,40, George Kirov27, Mikael Landén38,165, Marion Leboyer88,153,166, Cathryn M Lewis4,5,167, Qingqin S Li168, Jolanta

Lissowska169, Nicholas G Martin77,170, Fermin Mayoral83, Susan L McElroy171, Andrew M McIntosh51,172, Francis J McMahon173, Ingrid Melle174,175, Andres Metspalu114,176, Philip B Mitchell80, Gunnar Morken177,178, Ole Mors19,179, Preben Bo Mortensen15,19,28,29, Bertram Müller-Myhsok54,180,181, Richard M Myers103, Benjamin M Neale3,12,14, Vishwajit Nimgaonkar182, Merete Nordentoft19,183, Markus M Nöthen8, Michael C O'Donovan27, Ketil J Oedegaard184,185, Michael J Owen27, Sara A Paciga186, Carlos Pato95,187, Michele T Pato95, Danielle Posthuma22,188, Josep Antoni Ramos-Quiroga46,47,48,49, Marta Ribasés46,47,49, Marcella Rietschel70, Guy A Rouleau189,190, Martin Schalling72, Peter R Schofield133,162, Thomas G Schulze42,63,70,75,173, Alessandro Serretti191, Jordan W Smoller12,192,193, Hreinn Stefansson23, Kari Stefansson23,194, Eystein Stordal195,196, Patrick F Sullivan38,197,198, Gustavo Turecki199, Arne E Vaaler200, Eduard Vieta201, John B Vincent141, Thomas Werge19,202,203, John I Nurnberger204, Naomi R Wray24,25, Arianna Di Florio27,198, Howard J Edenberg205, Sven Cichon6,8,10,117, Roel A Ophoff40,41,71, Laura J Scott68, Ole A Andreassen135,136, John Kelsoe60*, Pamela Sklar1,2*^

† Equal contribution * Co-last authors
^ deceased

Affiliations:

1 Department of Genetics and Genomic Sciences, Icahn School of Medicine at Mount Sinai, New York, NY, US
2 Department of Psychiatry, Icahn School of Medicine at Mount Sinai, New York, NY, US
3 Medical and Population Genetics, Broad Institute, Cambridge, MA, US
4 MRC Social, Genetic and Developmental Psychiatry Centre, King's College London, London, GB
5 NIHR BRC for Mental Health, King's College London, London, GB
6 Department of Biomedicine, University of Basel, Basel, CH
7 Department of Psychiatry (UPK), University of Basel, Basel, CH
8 Institute of Human Genetics, University of Bonn, School of Medicine & University Hospital Bonn, Bonn, DE
9 Centre for Human Genetics, University of Marburg, Marburg, DE
10 Institute of Medical Genetics and Pathology, University Hospital Basel, Basel, CH
11 Division of Psychiatry, University College London, London, GB
12 Stanley Center for Psychiatric Research, Broad Institute, Cambridge, MA, US
13 Department of Psychiatry and Psychotherapy, Charité - Universitätsmedizin, Berlin, DE
14 Analytic and Translational Genetics Unit, Massachusetts General Hospital, Boston, MA, US
15 iSEQ, Center for Integrative Sequencing, Aarhus University, Aarhus, DK
16 Department of Biomedicine - Human Genetics, Aarhus University, Aarhus, DK
17 Department of Clinical Neuroscience, Centre for Psychiatry Research, Karolinska Institutet, Stockholm, SE
18 Department of Psychiatry, Psychosomatics and Psychotherapy, Center of Mental Health, University Hospital Würzburg, Würzburg, DE
19 iPSYCH, The Lundbeck Foundation Initiative for Integrative Psychiatric Research, DK
20 Institute of Biological Psychiatry, Mental Health Centre Sct. Hans, Copenhagen, DK
21 Institute of Clinical Medicine, University of Oslo, Oslo, NO
22 Department of Complex Trait Genetics, Center for Neurogenomics and Cognitive Research, Amsterdam Neuroscience, Vrije Universiteit Amsterdam, Amsterdam, NL
23 deCODE Genetics / Amgen, Reykjavik, IS
24 Queensland Brain Institute, The University of Queensland, Brisbane, QLD, AU
25 Institute for Molecular Bioscience, The University of Queensland, Brisbane, QLD, AU
26 Division of Endocrinology and Center for Basic and Translational Obesity Research, Boston Children's Hospital, Boston, MA, US
27 Medical Research Council Centre for Neuropsychiatric Genetics and Genomics, Division of Psychological Medicine and Clinical Neurosciences, Cardiff University, Cardiff, GB
28 National Centre for Register-Based Research, Aarhus University, Aarhus, DK
29 Centre for Integrated Register-based Research, Aarhus University, Aarhus, DK
30 Molecular & Behavioral Neuroscience Institute, University of Michigan, Ann Arbor, MI, US
31 Department of Neuroscience, IRCCS - Istituto Di Ricerche Farmacologiche Mario Negri, Milan, IT
32 Department of Psychiatry and Behavioral Neuroscience, University of Chicago, Chicago, IL, US
33 Psychiatry, Berkshire Healthcare NHS Foundation Trust, Bracknell, GB
34 Psychiatry, Rush University Medical Center, Chicago, IL, US
35 Center for Neonatal Screening, Department for Congenital Disorders, Statens Serum Institut, Copenhagen, DK
36 Department of Psychiatry, Weill Cornell Medical College, New York, NY, US
37 Department of Psychiatry and Psychotherapy, University Hospital Carl Gustav Carus, Technische Universität Dresden, Dresden, DE
38 Department of Medical Epidemiology and Biostatistics, Karolinska Institutet, Stockholm, SE
39 Department of Psychiatric Research, Diakonhjemmet Hospital, Oslo, NO
40 Psychiatry, UMC Utrecht Brain Center Rudolf Magnus, Utrecht, NL

41 Human Genetics, University of California Los Angeles, Los Angeles, CA, US
42 Institute of Psychiatric Phenomics and Genomics (IPPG), University Hospital, LMU Munich, Munich, DE
43 Department of Psychiatry and Human Behavior, University of California, Irvine, Irvine, CA, US
44 Molecular & Behavioral Neuroscience Institute and Department of Computational Medicine & Bioinformatics, University of Michigan, Ann Arbor, MI, US
45 Psychiatry, University of California San Francisco, San Francisco, CA, US
46 Instituto de Salud Carlos III, Biomedical Network Research Centre on Mental Health (CIBERSAM), Madrid, ES
47 Department of Psychiatry, Hospital Universitari Vall d´Hebron, Barcelona, ES
48 Department of Psychiatry and Forensic Medicine, Universitat Autònoma de Barcelona, Barcelona, ES
49 Psychiatric Genetics Unit, Group of Psychiatry Mental Health and Addictions, Vall d´Hebron Research Institut (VHIR), Universitat Autònoma de Barcelona, Barcelona, ES
50 Department of Psychiatry, Mood Disorders Program, McGill University Health Center, Montreal, QC, CA
51 Division of Psychiatry, University of Edinburgh, Edinburgh, GB
52 University of Iowa Hospitals and Clinics, Iowa City, IA, US
53 Translational Genomics, USC, Phoenix, AZ, US
54 Department of Translational Research in Psychiatry, Max Planck Institute of Psychiatry, Munich, DE
55 Centre for Psychiatry, Queen Mary University of London, London, GB
56 UCL Genetics Institute, University College London, London, GB
57 Department of Psychiatry, Laboratory of Psychiatric Genetics, Poznan University of Medical Sciences, Poznan, PL
58 Department of Neurosciences, University of California San Diego, La Jolla, CA, US
59 Department of Radiology, University of California San Diego, La Jolla, CA, US
60 Department of Psychiatry, University of California San Diego, La Jolla, CA, US
61 Department of Cognitive Science, University of California San Diego, La Jolla, CA, US
62 Applied Molecular Genomics Unit, VIB Department of Molecular Genetics, University of Antwerp, Antwerp, Belgium
63 Department of Psychiatry and Behavioral Sciences, Johns Hopkins University School of Medicine, Baltimore, MD, US
64 Department of Medical Genetics, Oslo University Hospital Ullevål, Oslo, NO
65 NORMENT, KG Jebsen Centre for Psychosis Research, Department of Clinical Science, University of Bergen, Bergen, NO
66 Department of Neurology, Oslo University Hospital, Oslo, NO
67 NORMENT, KG Jebsen Centre for Psychosis Research, Oslo University Hospital, Oslo, NO
68 Center for Statistical Genetics and Department of Biostatistics, University of Michigan, Ann Arbor, MI, US
69 Department of Medical & Molecular Genetics, Indiana University, Indianapolis, IN, US
70 Department of Genetic Epidemiology in Psychiatry, Central Institute of Mental Health, Medical Faculty Mannheim, Heidelberg University, Mannheim, DE
71 Center for Neurobehavioral Genetics, University of California Los Angeles, Los Angeles, CA, US
72 Department of Molecular Medicine and Surgery, Karolinska Institutet and Center for Molecular Medicine, Karolinska University Hospital, Stockholm, SE
73 Department of Clinical Neuroscience, Karolinska Institutet and Center for Molecular Medicine, Karolinska University Hospital, Stockholm, SE
74 Child and Adolescent Psychiatry Research Center, Stockholm, SE
75 Department of Psychiatry and Psychotherapy, University Medical Center Göttingen, Göttingen, DE
76 Department of Psychiatry, Dalhousie University, Halifax, NS, CA
77 Genetics and Computational Biology, QIMR Berghofer Medical Research Institute, Brisbane, QLD, AU
78 Department of Psychological Medicine, University of Worcester, Worcester, GB

79 School of Biomedical Sciences, Plymouth University Peninsula Schools of Medicine and Dentistry, University of Plymouth, Plymouth, GB
80 School of Psychiatry, University of New South Wales, Sydney, NSW, AU
81 Bioinformatics Research Centre, Aarhus University, Aarhus, DK
82 Biostatistics, University of Minnesota System, Minneapolis, MN, US
83 Mental Health Department, University Regional Hospital, Biomedicine Institute (IBIMA), Málaga, ES
84 Department of Psychology, Eberhard Karls Universität Tübingen, Tubingen, DE
85 Department of Psychiatry and Behavioral Sciences, Howard University Hospital, Washington, DC, US
86 Center for Multimodal Imaging and Genetics, University of California San Diego, La Jolla, CA, US
87 Psychiatrie Translationnelle, Inserm U955, Créteil, FR
88 Faculté de Médecine, Université Paris Est, Créteil, FR
89 Campbell Family Mental Health Research Institute, Centre for Addiction and Mental Health, Toronto, ON, CA
90 Neurogenetics Section, Centre for Addiction and Mental Health, Toronto, ON, CA
91 Department of Psychiatry, University of Toronto, Toronto, ON, CA
92 Institute of Medical Sciences, University of Toronto, Toronto, ON, CA
93 Department of Psychiatry, Psychosomatic Medicine and Psychotherapy, University Hospital Frankfurt, Frankfurt am Main, DE
94 Cell Biology, SUNY Downstate Medical Center College of Medicine, Brooklyn, NY, US
95 Institute for Genomic Health, SUNY Downstate Medical Center College of Medicine, Brooklyn, NY, US
96 ISGlobal, Barcelona, ES
97 Psychiatry, Altrecht, Utrecht, NL
98 Psychiatry, GGZ inGeest, Amsterdam, NL
99 Psychiatry, VU medisch centrum, Amsterdam, NL
100 Psychiatry, North East London NHS Foundation Trust, Ilford, GB
101 Clinic for Psychiatry and Psychotherapy, University Hospital Cologne, Cologne, DE
102 Psychiatric and Neurodevelopmental Genetics Unit, Massachusetts General Hospital, Boston, MA, US
103 HudsonAlpha Institute for Biotechnology, Huntsville, AL, US
104 Department of Human Genetics, University of Michigan, Ann Arbor, MI, US
105 Psychiatry, University of Illinois at Chicago College of Medicine, Chicago, IL, US
106 Max Planck Institute of Psychiatry, Munich, DE
107 Mental Health, NHS 24, Glasgow, GB
108 Division of Psychiatry, Centre for Clinical Brain Sciences, University of Edinburgh, Edinburgh, GB
109 Psychiatry, Brigham and Women's Hospital, Boston, MA, US
110 Department of Psychiatry and Psychotherapy, University of Bonn, Bonn, DE
111 Department of Genetics, Harvard Medical School, Boston, MA, US
112 Department of Psychiatry, University of Michigan, Ann Arbor, MI, US
113 Genetic Cancer Susceptibility Group, International Agency for Research on Cancer, Lyon, FR
114 Estonian Genome Center, University of Tartu, Tartu, EE
115 Discipline of Biochemistry, Neuroimaging and Cognitive Genomics (NICOG) Centre, National University of Ireland, Galway, Galway, IE
116 Neuropsychiatric Genetics Research Group, Dept of Psychiatry and Trinity Translational Medicine Institute, Trinity College Dublin, Dublin, IE
117 Institute of Neuroscience and Medicine (INM-1), Research Centre Jülich, Jülich, DE
118 Research/Psychiatry, Veterans Affairs San Diego Healthcare System, San Diego, CA, US
119 Department of Clinical Sciences, Psychiatry, Umeå University Medical Faculty, Umeå, SE
120 Department of Clinical Psychiatry, Psychiatry Clinic, Clinical Center University of Sarajevo, Sarajevo, BA
121 Department of Neurobiology, Care sciences, and Society, Karolinska Institutet and Center for Molecular Medicine, Karolinska University Hospital, Stockholm, SE

122 Psychiatry, Harvard Medical School, Boston, MA, US
123 Division of Clinical Research, Massachusetts General Hospital, Boston, MA, US
124 Outpatient Clinic for Bipolar Disorder, Altrecht, Utrecht, NL
125 Department of Psychiatry, Washington University in Saint Louis, Saint Louis, MO, US
126 Department of Biochemistry and Molecular Biology II, Institute of Neurosciences, Center for Biomedical Research, University of Granada, Granada, ES
127 Department of Neuroscience, Icahn School of Medicine at Mount Sinai, New York, NY, US
128 Medicine, Psychiatry, Biomedical Informatics, Vanderbilt University Medical Center, Nashville, TN, US
129 Department of Health Sciences Research, Mayo Clinic, Rochester, MN, US
130 Psychiatry and Behavioral Sciences, Stanford University School of Medicine, Stanford, CA, US
131 Rush University Medical Center, Chicago, IL, US
132 Scripps Translational Science Institute, La Jolla, CA, US
133 Neuroscience Research Australia, Sydney, NSW, AU
134 Faculty of Medicine, Department of Psychiatry, School of Health Sciences, University of Iceland, Reykjavik, IS
135 Division of Mental Health and Addiction, Oslo University Hospital, Oslo, NO
136 NORMENT, University of Oslo, Oslo, NO
137 Psychiatry and the Behavioral Sciences, University of Southern California, Los Angeles, CA, US
138 Mood Disorders, PsyQ, Rotterdam, NL
139 Institute for Medical Sciences, University of Aberdeen, Aberdeen, UK
140 Research Division, Federal Institute for Drugs and Medical Devices (BfArM), Bonn, DE
141 Centre for Addiction and Mental Health, Toronto, ON, CA
142 Neurogenomics, TGen, Los Angeles, AZ, US
143 Psychiatry, Psychiatrisches Zentrum Nordbaden, Wiesloch, DE
144 Computational Sciences Center of Emphasis, Pfizer Global Research and Development, Cambridge, MA, US
145 Department of Biostatistics, Princess Margaret Cancer Centre, Toronto, ON, CA
146 Dalla Lana School of Public Health, University of Toronto, Toronto, ON, CA
147 Psychological Medicine, Institute of Psychiatry, Psychology & Neuroscience, King's College London, London, GB
148 Department of Mental Health, Johns Hopkins University Bloomberg School of Public Health, Baltimore, MD, US
149 Institute of Genetic Medicine, Johns Hopkins University School of Medicine, Baltimore, MD, US
150 NORMENT, KG Jebsen Centre for Psychosis Research, Division of Mental Health and Addiction, Institute of Clinical Medicine and Diakonhjemmet Hospital, University of Oslo, Oslo, NO
151 National Institute of Mental Health, Klecany, CZ
152 Department of Psychiatry, University of Melbourne, Melbourne, Victoria, AU
153 Department of Psychiatry and Addiction Medicine, Assistance Publique - Hôpitaux de Paris, Paris, FR
154 Paris Bipolar and TRD Expert Centres, FondaMental Foundation, Paris, FR
155 UMR-S1144 Team 1: Biomarkers of relapse and therapeutic response in addiction and mood disorders, INSERM, Paris, FR
156 Psychiatry, Université Paris Diderot, Paris, FR
157 Psychiatry, University of Pennsylvania, Philadelphia, PA, US
158 Department of Psychiatry, University of Münster, Münster, DE
159 Division of Endocrinology, Children's Hospital Boston, Boston, MA, US
160 Centre for Affective Disorders, Institute of Psychiatry, Psychology and Neuroscience, London, GB
161 Department of Psychiatry & Psychology, Mayo Clinic, Rochester, MN, US
162 School of Medical Sciences, University of New South Wales, Sydney, NSW, AU
163 Department of Human Genetics, University of Chicago, Chicago, IL, US

164 Biometric Psychiatric Genetics Research Unit, Alexandru Obregia Clinical Psychiatric Hospital, Bucharest, RO
165 Institute of Neuroscience and Physiology, University of Gothenburg, Gothenburg, SE
166 INSERM, Paris, FR
167 Department of Medical & Molecular Genetics, King's College London, London, GB
168 Neuroscience Therapeutic Area, Janssen Research and Development, LLC, Titusville, NJ, US
169 Cancer Epidemiology and Prevention, M. Sklodowska-Curie Cancer Center and Institute of Oncology, Warsaw, PL
170 School of Psychology, The University of Queensland, Brisbane, QLD, AU
171 Research Institute, Lindner Center of HOPE, Mason, OH, US
172 Centre for Cognitive Ageing and Cognitive Epidemiology, University of Edinburgh, Edinburgh, GB
173 Human Genetics Branch, Intramural Research Program, National Institute of Mental Health, Bethesda, MD, US
174 Division of Mental Health and Addiction, Oslo University Hospital, Oslo, NO
175 Division of Mental Health and Addiction, University of Oslo, Institute of Clinical Medicine, Oslo, NO
176 Institute of Molecular and Cell Biology, University of Tartu, Tartu, EE
177 Mental Health, Faculty of Medicine and Health Sciences, Norwegian University of Science and Technology - NTNU, Trondheim, NO
178 Psychiatry, St Olavs University Hospital, Trondheim, NO
179 Psychosis Research Unit, Aarhus University Hospital, Risskov, DK
180 Munich Cluster for Systems Neurology (SyNergy), Munich, DE
181 University of Liverpool, Liverpool, GB
182 Psychiatry and Human Genetics, University of Pittsburgh, Pittsburgh, PA, US
183 Mental Health Services in the Capital Region of Denmark, Mental Health Center Copenhagen, University of Copenhagen, Copenhagen, DK
184 Division of Psychiatry, Haukeland Universitetssjukehus, Bergen, NO
185 Faculty of Medicine and Dentistry, University of Bergen, Bergen, NO
186 Human Genetics and Computational Biomedicine, Pfizer Global Research and Development, Groton, CT, US
187 College of Medicine Institute for Genomic Health, SUNY Downstate Medical Center College of Medicine, Brooklyn, NY, US
188 Department of Clinical Genetics, Amsterdam Neuroscience, Vrije Universiteit Medical Center, Amsterdam, NL
189 Department of Neurology and Neurosurgery, McGill University, Faculty of Medicine, Montreal, QC, CA
190 Montreal Neurological Institute and Hospital, Montreal, QC, CA
191 Department of Biomedical and NeuroMotor Sciences, University of Bologna, Bologna, IT
192 Department of Psychiatry, Massachusetts General Hospital, Boston, MA, US
193 Psychiatric and Neurodevelopmental Genetics Unit (PNGU), Massachusetts General Hospital, Boston, MA, US
194 Faculty of Medicine, University of Iceland, Reykjavik, IS
195 Department of Psychiatry, Hospital Namsos, Namsos, NO
196 Department of Neuroscience, Norges Teknisk Naturvitenskapelige Universitet Fakultet for naturvitenskap og teknologi, Trondheim, NO
197 Department of Genetics, University of North Carolina at Chapel Hill, Chapel Hill, NC, US
198 Department of Psychiatry, University of North Carolina at Chapel Hill, Chapel Hill, NC, US
199 Department of Psychiatry, McGill University, Montreal, QC, CA
200 Dept of Psychiatry, Sankt Olavs Hospital Universitetssykehuset i Trondheim, Trondheim, NO
201 Clinical Institute of Neuroscience, Hospital Clinic, University of Barcelona, IDIBAPS, CIBERSAM, Barcelona, ES
202 Institute of Biological Psychiatry, MHC Sct. Hans, Mental Health Services Copenhagen, Roskilde, DK

203 Department of Clinical Medicine, University of Copenhagen, Copenhagen, DK
204 Psychiatry, Indiana University School of Medicine, Indianapolis, IN, US
205 Biochemistry and Molecular Biology, Indiana University School of Medicine, Indianapolis, IN, US
206 Department of Pathology and Laboratory Medicine, University of California Los Angeles, Los Angeles, CA, US

Schizophrenia Working Group of the Psychiatric Genomics Consortium

Stephan Ripke[1,2], Benjamin M. Neale[1,2,3,4], Aiden Corvin[5], James T. R. Walters[6], Kai-How Farh[1], Peter A. Holmans[6,7], Phil Lee[1,2,4], Brendan Bulik-Sullivan[1,2], David A. Collier[8,9], Hailiang Huang[1,3], Tune H. Pers[3,10,11], Ingrid Agartz[12,13,14], Esben Agerbo[15,16,17], Margot Albus[18], Madeline Alexander[19], Farooq Amin[20,21], Silviu A. Bacanu[22], Martin Begemann[23], Richard A Belliveau Jr[2], Judit Bene[24,25], Sarah E. Bergen [2,26], Elizabeth Bevilacqua[2], Tim B Bigdeli [22], Donald W. Black[27], Richard Bruggeman[28], Nancy G. Buccola[29], Randy L. Buckner[30,31,32], William Byerley[33], Wiepke Cahn[34], Guiqing Cai[35,36], Murray J. Cairns[39,120,170], Dominique Campion[37], Rita M. Cantor[38], Vaughan J. Carr[39,40], Noa Carrera[6], Stanley V. Catts[39,41], Kimberly D. Chambert[2], Raymond C. K. Chan[42], Ronald Y. L. Chen[43], Eric Y. H. Chen[43,44], Wei Cheng[45], Eric F. C. Cheung[46], Siow Ann Chong[47], C. Robert Cloninger[48], David Cohen[49], Nadine Cohen[50], Paul Cormican[5], Nick Craddock[6,7], Benedicto Crespo-Facorro[210], James J. Crowley[51], David Curtis[52,53], Michael Davidson[54], Kenneth L. Davis[36], Franziska Degenhardt[55,56], Jurgen Del Favero[57], Lynn E. DeLisi[128,129] , Ditte Demontis[17,58,59], Dimitris Dikeos[60], Timothy Dinan[61], Srdjan Djurovic[14,62], Gary Donohoe[5,63], Elodie Drapeau[36], Jubao Duan[64,65], Frank Dudbridge[66], Naser Durmishi[67], Peter Eichhammer[68], Johan Eriksson[69,70,71], Valentina Escott-Price[6], Laurent Essioux[72], Ayman H. Fanous[73,74,75,76], Martilias S. Farrell[51], Josef Frank[77], Lude Franke[78], Robert Freedman[79], Nelson B. Freimer[80], Marion Friedl[81], Joseph I. Friedman[36], Menachem Fromer[1,2,4,82], Giulio Genovese[2], Lyudmila Georgieva[6], Elliot S. Gershon[209], Ina Giegling[81,83], Paola Giusti-Rodríguez[51], Stephanie Godard[84], Jacqueline I. Goldstein[1,3], Vera Golimbet[85], Srihari Gopal[86], Jacob Gratten[87], Lieuwe de Haan[88], Christian Hammer[23], Marian L. Hamshere[6], Mark Hansen[89], Thomas Hansen[17,90], Vahram Haroutunian[36,91,92], Annette M. Hartmann[81], Frans A. Henskens[39,93,94], Stefan Herms[55,56,95], Joel N. Hirschhorn[3,11,96], Per Hoffmann[55,56,95], Andrea Hofman[55,56], Mads V. Hollegaard[97], David M. Hougaard[97], Masashi Ikeda[98], Inge Joa[99], Antonio Julià[100], René S. Kahn[34], Luba Kalaydjieva[101,102], Sena Karachanak-Yankova[103], Juha Karjalainen[78], David Kavanagh[6], Matthew C. Keller[104], Brian J. Kelly[120], James L. Kennedy[105,106,107], Andrey Khrunin[108], Yunjung Kim[51], Janis Klovins[109], James A. Knowles[110], Bettina Konte[81], Vaidutis Kucinskas[111], Zita Ausrele Kucinskiene[111], Hana Kuzelova-Ptackova[112], Anna K. Kähler[26], Claudine Laurent[19,113], Jimmy Lee Chee Keong[47,114], S. Hong Lee[87], Sophie E. Legge[6], Bernard Lerer[115], Miaoxin Li[43,44,116] Tao Li[117], Kung-Yee Liang[118], Jeffrey Lieberman[119], Svetlana Limborska[108], Carmel M. Loughland[39,120], Jan Lubinski[121], Jouko Lönnqvist[122], Milan Macek Jr[112], Patrik K. E. Magnusson[26], Brion S. Maher[123], Wolfgang Maier[124], Jacques Mallet[125], Sara Marsal[100], Manuel Mattheisen[17,58,59,126], Morten Mattingsdal[14,127], Robert W. McCarley[128,129], Colm McDonald[130], Andrew M. McIntosh[131,132], Sandra Meier[77], Carin J. Meijer[88], Bela Melegh[24,25], Ingrid Melle[14,133], Raquelle I. Mesholam-Gately[128,134], Andres Metspalu[135], Patricia T. Michie[39,136], Lili Milani[135], Vihra Milanova[137], Younes Mokrab[8], Derek W. Morris[5,63], Ole Mors[17,58,138], Kieran C. Murphy[139], Robin M. Murray[140], Inez Myin-Germeys[141], Bertram Müller-Myhsok[142,143,144], Mari Nelis[135], Igor Nenadic[145], Deborah A. Nertney[146], Gerald Nestadt[147], Kristin K. Nicodemus[148], Liene Nikitina-Zake[109], Laura Nisenbaum[149], Annelie Nordin[150], Eadbhard O'Callaghan[151], Colm O'Dushlaine[2], F. Anthony O'Neill[152], Sang-Yun Oh[153], Ann Olincy[79], Line Olsen[17,90], Jim Van Os[141,154], Psychosis Endophenotypes International Consortium[155], Christos Pantelis[39,156], George N. Papadimitriou[60], Sergi Papiol[23], Elena Parkhomenko[36], Michele T. Pato[110], Tiina Paunio[157,158], Milica Pejovic-Milovancevic[159], Diana O. Perkins[160], Olli Pietiläinen[158,161], Jonathan Pimm[53], Andrew J. Pocklington[6], John Powell[140], Alkes Price[3,162], Ann E. Pulver[147], Shaun M. Purcell[82], Digby Quested[163], Henrik B. Rasmussen[17,90], Abraham Reichenberg[36], Mark A. Reimers[164], Alexander L. Richards[6], Joshua L. Roffman[30,32], Panos Roussos[82,165], Douglas M. Ruderfer[6,82], Veikko Salomaa[71], Alan R. Sanders[64,65], Ulrich Schall[39,120], Christian R. Schubert[166], Thomas G. Schulze[77,167], Sibylle G. Schwab[168], Edward M. Scolnick[2], Rodney J. Scott[39,169,170], Larry J. Seidman[128,134], Jianxin Shi[171], Engilbert Sigurdsson[172], Teimuraz Silagadze[173], Jeremy M. Silverman[36,174], Kang Sim[47], Petr Slominsky[108], Jordan W. Smoller[2,4], Hon-Cheong So[43], Chris C. A. Spencer[175], Eli A. Stahl[3,82], Hreinn Stefansson[176], Stacy Steinberg[176], Elisabeth Stogmann[177], Richard E. Straub[178], Eric Strengman[179,34], Jana Strohmaier[77], T. Scott Stroup[119], Mythily Subramaniam[47], Jaana Suvisaari[122], Dragan M. Svrakic[48], Jin P. Szatkiewicz[51], Erik Söderman[12], Srinivas Thirumalai[180], Draga Toncheva[103], Paul A. Tooney[39,120,170] , Sarah Tosato[181],

Juha Veijola[182,183], John Waddington[184], Dermot Walsh[185], Dai Wang[86], Qiang Wang[117], Bradley T. Webb[22], Mark Weiser[54], Dieter B. Wildenauer[186], Nigel M. Williams[6], Stephanie Williams[51], Stephanie H. Witt[77], Aaron R. Wolen[164], Emily H. M. Wong[43], Brandon K. Wormley[22], Jing Qin Wu[39,170], Hualin Simon Xi[187], Clement C. Zai[105,106], Xuebin Zheng[188], Fritz Zimprich[177], Naomi R. Wray[87], Kari Stefansson[176], Peter M. Visscher[87], Wellcome Trust Case-Control Consortium 2[189], Rolf Adolfsson[150], Ole A. Andreassen[14,133], Douglas H. R. Blackwood[132], Elvira Bramon[190], Joseph D. Buxbaum[35,36,91,191], Anders D. Børglum[17,58,59,138], Sven Cichon[55,56,95,192], Ariel Darvasi[193], Enrico Domenici[194], Hannelore Ehrenreich[23], Tõnu Esko[3,11,96,135], Pablo V. Gejman[64,65], Michael Gill[5], Hugh Gurling[53], Christina M. Hultman[26], Nakao Iwata[98], Assen V. Jablensky[39,102,186,195], Erik G. Jönsson[12,14], Kenneth S. Kendler[196], George Kirov[6], Jo Knight[105,106,107], Todd Lencz[197,198,199], Douglas F. Levinson[19], Qingqin S. Li[86], Jianjun Liu[188,200], Anil K. Malhotra[197,198,199], Steven A. McCarroll[2,96], Andrew McQuillin[53], Jennifer L. Moran[2], Preben B. Mortensen[15,16,17], Bryan J. Mowry[87,201], Markus M. Nöthen[55,56], Roel A. Ophoff[38,80,34], Michael J. Owen[6,7], Aarno Palotie[2,4,161], Carlos N. Pato[110], Tracey L. Petryshen[2,128,202], Danielle Posthuma[203,204,205], Marcella Rietschel[77], Brien P. Riley[196], Dan Rujescu[81,83], Pak C. Sham[43,44,116] Pamela Sklar[82,91,165], David St Clair[206], Daniel R. Weinberger[178,207], Jens R. Wendland[166], Thomas Werge[17,90,208], Mark J. Daly[1,2,3], Patrick F. Sullivan[26,51,160] & Michael C. O'Donovan[6,7]

[1]Analytic and Translational Genetics Unit, Massachusetts General Hospital, Boston, Massachusetts 02114, USA.

[2]Stanley Center for Psychiatric Research, Broad Institute of MIT and Harvard, Cambridge, Massachusetts 02142, USA.

[3]Medical and Population Genetics Program, Broad Institute of MIT and Harvard, Cambridge, Massachusetts 02142, USA.

[4]Psychiatric and Neurodevelopmental Genetics Unit, Massachusetts General Hospital, Boston, Massachusetts 02114, USA.

[5]Neuropsychiatric Genetics Research Group, Department of Psychiatry, Trinity College Dublin, Dublin 8, Ireland.

[6]MRC Centre for Neuropsychiatric Genetics and Genomics, Institute of Psychological Medicine and Clinical Neurosciences, School of Medicine, Cardiff University, Cardiff, CF24 4HQ, UK.

[7]National Centre for Mental Health, Cardiff University, Cardiff, CF24 4HQ, UK.

[8]Eli Lilly and Company Limited, Erl Wood Manor, Sunninghill Road, Windlesham, Surrey, GU20 6PH, UK. [9]Social, Genetic and Developmental Psychiatry Centre, Institute of Psychiatry, King's College London, London, SE5 8AF, UK.

[10]Center for Biological Sequence Analysis, Department of Systems Biology, Technical University of Denmark, DK-2800, Denmark.

[11]Division of Endocrinology and Center for Basic and Translational Obesity Research, Boston Children's Hospital, Boston, Massachusetts, 02115USA.

[12]Department of Clinical Neuroscience, Psychiatry Section, Karolinska Institutet, SE-17176 Stockholm, Sweden. [13]Department of Psychiatry, Diakonhjemmet Hospital, 0319 Oslo, Norway.
[14]NORMENT, KG Jebsen Centre for Psychosis Research, Institute of Clinical Medicine, University of Oslo, 0424 Oslo, Norway.

[15]Centre for Integrative Register-based Research, CIRRAU, Aarhus University, DK-8210 Aarhus, Denmark.

[16]National Centre for Register-based Research, Aarhus University, DK-8210 Aarhus, Denmark.

[17]The Lundbeck Foundation Initiative for Integrative Psychiatric Research, iPSYCH, Denmark.

[18]State Mental Hospital, 85540 Haar, Germany.

[19]Department of Psychiatry and Behavioral Sciences, Stanford University, Stanford, California 94305, USA.

[20]Department of Psychiatry and Behavioral Sciences, Atlanta Veterans Affairs Medical Center, Atlanta, Georgia 30033, USA.

[21]Department of Psychiatry and Behavioral Sciences, Emory University, Atlanta Georgia 30322, USA.

[22]Virginia Institute for Psychiatric and Behavioral Genetics, Department of Psychiatry, Virginia Commonwealth University, Richmond, Virginia 23298, USA.

[23]Clinical Neuroscience, Max Planck Institute of Experimental Medicine, Göttingen 37075, Germany.

[24]Department of Medical Genetics, University of Pécs, Pécs H-7624, Hungary.

[25]Szentagothai Research Center, University of Pécs, Pécs H-7624, Hungary.

[26]Department of Medical Epidemiology and Biostatistics, Karolinska Institutet, Stockholm SE-17177, Sweden.

[27]Department of Psychiatry, University of Iowa Carver College of Medicine, Iowa City, Iowa 52242, USA.

[28]University Medical Center Groningen, Department of Psychiatry, University of Groningen NL-9700 RB, The Netherlands.

[29]School of Nursing, Louisiana State University Health Sciences Center, New Orleans, Louisiana 70112, USA.

[30]Athinoula A. Martinos Center, Massachusetts General Hospital, Boston, Massachusetts 02129, USA.

[31]Center for Brain Science, Harvard University, Cambridge, Massachusetts, 02138 USA.

[32]Department of Psychiatry, Massachusetts General Hospital, Boston, Massachusetts, 02114 USA.

[33]Department of Psychiatry, University of California at San Francisco, San Francisco, California, 94143 USA.

[34]University Medical Center Utrecht, Department of Psychiatry, Rudolf Magnus Institute of Neuroscience, 3584 Utrecht, The Netherlands.

[35]Department of Human Genetics, Icahn School of Medicine at Mount Sinai, New York, New York 10029 USA.

[36]Department of Psychiatry, Icahn School of Medicine at Mount Sinai, New York, New York 10029 USA.

[37]Centre Hospitalier du Rouvray and INSERM U1079 Faculty of Medicine, 76301 Rouen, France.

[38]Department of Human Genetics, David Geffen School of Medicine, University of California, Los Angeles, California 90095, USA.

[39]Schizophrenia Research Institute, Sydney NSW 2010, Australia.

[40]School of Psychiatry, University of New South Wales, Sydney NSW 2031, Australia.

[41]Royal Brisbane and Women's Hospital, University of Queensland, Brisbane, St Lucia QLD 4072, Australia.

[42]Institute of Psychology, Chinese Academy of Science, Beijing 100101, China.

[43]Department of Psychiatry, Li Ka Shing Faculty of Medicine, The University of Hong Kong, Hong Kong, China.

[44]State Key Laboratory for Brain and Cognitive Sciences, Li Ka Shing Faculty of Medicine, The University of Hong Kong, Hong Kong, China.

[45]Department of Computer Science, University of North Carolina, Chapel Hill, North Carolina 27514, USA.

[46]Castle Peak Hospital, Hong Kong, China.

[47]Institute of Mental Health, Singapore 539747, Singapore.

[48]Department of Psychiatry, Washington University, St. Louis, Missouri 63110, USA.

[49]Department of Child and Adolescent Psychiatry, Assistance Publique Hopitaux de Paris, Pierre and Marie Curie Faculty of Medicine and Institute for Intelligent Systems and Robotics, Paris, 75013, France.

[50] Blue Note Biosciences, Princeton, New Jersey 08540, USA

[51]Department of Genetics, University of North Carolina, Chapel Hill, North Carolina 27599-7264, USA.

[52]Department of Psychological Medicine, Queen Mary University of London, London E1 1BB, UK.

[53]Molecular Psychiatry Laboratory, Division of Psychiatry, University College London, London WC1E 6JJ, UK.

[54]Sheba Medical Center, Tel Hashomer 52621, Israel.

[55]Department of Genomics, Life and Brain Center, D-53127 Bonn, Germany.

[56]Institute of Human Genetics, University of Bonn, D-53127 Bonn, Germany.

[57]Applied Molecular Genomics Unit, VIB Department of Molecular Genetics, University of Antwerp, B-2610 Antwerp, Belgium.

[58]Centre for Integrative Sequencing, iSEQ, Aarhus University, DK-8000 Aarhus C, Denmark.

[59]Department of Biomedicine, Aarhus University, DK-8000 Aarhus C, Denmark.

[60]First Department of Psychiatry, University of Athens Medical School, Athens 11528, Greece.

[61]Department of Psychiatry, University College Cork, Co. Cork, Ireland.

[62]Department of Medical Genetics, Oslo University Hospital, 0424 Oslo, Norway.

[63]Cognitive Genetics and Therapy Group, School of Psychology and Discipline of Biochemistry, National University of Ireland Galway, Co. Galway, Ireland.

[64]Department of Psychiatry and Behavioral Neuroscience, University of Chicago, Chicago, Illinois 60637, USA.

[65]Department of Psychiatry and Behavioral Sciences, NorthShore University HealthSystem, Evanston, Illinois 60201, USA.

[66]Department of Non-Communicable Disease Epidemiology, London School of Hygiene and Tropical Medicine, London WC1E 7HT, UK.

[67]Department of Child and Adolescent Psychiatry, University Clinic of Psychiatry, Skopje 1000, Republic of Macedonia.

[68]Department of Psychiatry, University of Regensburg, 93053 Regensburg, Germany.

[69]Department of General Practice, Helsinki University Central Hospital, University of Helsinki P.O. Box 20, Tukholmankatu 8 B, FI-00014, Helsinki, Finland

[70]Folkhälsan Research Center, Helsinki, Finland, Biomedicum Helsinki 1, Haartmaninkatu 8, FI-00290, Helsinki, Finland.

[71]National Institute for Health and Welfare, P.O. BOX 30, FI-00271 Helsinki, Finland.

[72]Translational Technologies and Bioinformatics, Pharma Research and Early Development, F. Hoffman-La Roche, CH-4070 Basel, Switzerland.

[73]Department of Psychiatry, Georgetown University School of Medicine, Washington DC 20057, USA.

[74]Department of Psychiatry, Keck School of Medicine of the University of Southern California, Los Angeles, California 90033, USA.

[75]Department of Psychiatry, Virginia Commonwealth University School of Medicine, Richmond, Virginia 23298, USA.

[76]Mental Health Service Line, Washington VA Medical Center, Washington DC 20422, USA.

[77]Department of Genetic Epidemiology in Psychiatry, Central Institute of Mental Health, Medical Faculty Mannheim, University of Heidelberg, Heidelberg , D-68159 Mannheim, Germany.

[78]Department of Genetics, University of Groningen, University Medical Centre Groningen, 9700 RB Groningen, The Netherlands.

[79]Department of Psychiatry, University of Colorado Denver, Aurora, Colorado 80045, USA.

[80]Center for Neurobehavioral Genetics, Semel Institute for Neuroscience and Human Behavior, University of California, Los Angeles, California 90095, USA.

[81]Department of Psychiatry, University of Halle, 06112 Halle, Germany.

[82]Division of Psychiatric Genomics, Department of Psychiatry, Icahn School of Medicine at Mount Sinai, New York, New York 10029, USA.

[83]Department of Psychiatry, University of Munich, 80336, Munich, Germany.

[84]Departments of Psychiatry and Human and Molecular Genetics, INSERM, Institut de Myologie, Hôpital de la Pitiè-Salpêtrière, Paris, 75013, France.

[85]Mental Health Research Centre, Russian Academy of Medical Sciences, 115522 Moscow, Russia.

[86]Neuroscience Therapeutic Area, Janssen Research and Development, Raritan, New Jersey 08869, USA.

[87]Queensland Brain Institute, The University of Queensland, Brisbane, Queensland, QLD 4072, Australia.

[88]Academic Medical Centre University of Amsterdam, Department of Psychiatry, 1105 AZ Amsterdam, The Netherlands.

[89]Illumina, La Jolla, California, California 92122, USA.

[90]Institute of Biological Psychiatry, Mental Health Centre Sct. Hans, Mental Health Services Copenhagen, DK-4000, Denmark.

[91]Friedman Brain Institute, Icahn School of Medicine at Mount Sinai, New York, New York 10029, USA.

[92]J. J. Peters VA Medical Center, Bronx, New York, New York 10468, USA.

[93]Priority Research Centre for Health Behaviour, University of Newcastle, Newcastle NSW 2308, Australia.

[94]School of Electrical Engineering and Computer Science, University of Newcastle, Newcastle NSW 2308, Australia.

[95]Division of Medical Genetics, Department of Biomedicine, University of Basel, Basel, CH-4058, Switzerland.

[96]Department of Genetics, Harvard Medical School, Boston, Massachusetts 02115, USA.

[97]Section of Neonatal Screening and Hormones, Department of Clinical Biochemistry, Immunology and Genetics, Statens Serum Institut, Copenhagen, DK-2300, Denmark.

[98]Department of Psychiatry, Fujita Health University School of Medicine, Toyoake, Aichi, 470-1192, Japan.

[99]Regional Centre for Clinical Research in Psychosis, Department of Psychiatry, Stavanger University Hospital, 4011 Stavanger, Norway.

[100]Rheumatology Research Group, Vall d'Hebron Research Institute, Barcelona, 08035, Spain.

[101]Centre for Medical Research, The University of Western Australia, Perth, WA 6009, Australia.

[102]The Perkins Institute for Medical Research, The University of Western Australia, Perth, WA 6009, Australia.

[103]Department of Medical Genetics, Medical University, Sofia1431, Bulgaria.

[104]Department of Psychology, University of Colorado Boulder, Boulder, Colorado 80309, USA.

[105]Campbell Family Mental Health Research Institute, Centre for Addiction and Mental Health, Toronto, Ontario, M5T 1R8, Canada.

[106]Department of Psychiatry, University of Toronto, Toronto, Ontario, M5T 1R8, Canada.

[107]Institute of Medical Science, University of Toronto, Toronto, Ontario, M5S 1A8, Canada.

[108]Institute of Molecular Genetics, Russian Academy of Sciences, Moscow123182, Russia.

[109]Latvian Biomedical Research and Study Centre, Riga, LV-1067, Latvia.

[110]Department of Psychiatry and Zilkha Neurogenetics Institute, Keck School of Medicine at University of Southern California, Los Angeles, California 90089, USA.

[111]Faculty of Medicine, Vilnius University, LT-01513 Vilnius, Lithuania.

[112] Department of Biology and Medical Genetics, 2nd Faculty of Medicine and University Hospital Motol, 150 06 Prague, Czech Republic.

[113] Department of Child and Adolescent Psychiatry, Pierre and Marie Curie Faculty of Medicine, Paris 75013, France.

[114]Duke-NUS Graduate Medical School, Singapore 169857, Singapore.

[115]Department of Psychiatry, Hadassah-Hebrew University Medical Center, Jerusalem 91120, Israel.

[116]Centre for Genomic Sciences, The University of Hong Kong, Hong Kong, China.

[117]Mental Health Centre and Psychiatric Laboratory, West China Hospital, Sichuan University, Chengdu, 610041, Sichuan, China.

[118]Department of Biostatistics, Johns Hopkins University Bloomberg School of Public Health, Baltimore, Maryland 21205, USA.

[119]Department of Psychiatry, Columbia University, New York, New York 10032, USA.

[120]Priority Centre for Translational Neuroscience and Mental Health, University of Newcastle, Newcastle NSW 2300, Australia.

[121]Department of Genetics and Pathology, International Hereditary Cancer Center, Pomeranian Medical University in Szczecin, 70-453 Szczecin, Poland.

[122]Department of Mental Health and Substance Abuse Services; National Institute for Health and Welfare, P.O. BOX 30, FI-00271 Helsinki, Finland

[123]Department of Mental Health, Bloomberg School of Public Health, Johns Hopkins University, Baltimore, Maryland 21205, USA.

[124]Department of Psychiatry, University of Bonn, D-53127 Bonn, Germany.

[125]Centre National de la Recherche Scientifique, Laboratoire de Génétique Moléculaire de la Neurotransmission et des Processus Neurodégénératifs, Hôpital de la Pitié Salpêtrière, 75013, Paris, France.

[126]Department of Genomics Mathematics, University of Bonn, D-53127 Bonn, Germany.

[127]Research Unit, Sørlandet Hospital, 4604 Kristiansand, Norway.

[128]Department of Psychiatry, Harvard Medical School, Boston, Massachusetts 02115, USA.

[129]VA Boston Health Care System, Brockton, Massachusetts 02301, USA.

[130]Department of Psychiatry, National University of Ireland Galway, Co. Galway, Ireland.

[131]Centre for Cognitive Ageing and Cognitive Epidemiology, University of Edinburgh, Edinburgh EH16 4SB, UK.

[132]Division of Psychiatry, University of Edinburgh, Edinburgh EH16 4SB, UK.

[133]Division of Mental Health and Addiction, Oslo University Hospital, 0424 Oslo, Norway.

[134]Massachusetts Mental Health Center Public Psychiatry Division of the Beth Israel Deaconess Medical Center, Boston, Massachusetts 02114, USA.

[135]Estonian Genome Center, University of Tartu, Tartu 50090, Estonia.

[136]School of Psychology, University of Newcastle, Newcastle NSW 2308, Australia.

[137]First Psychiatric Clinic, Medical University, Sofia 1431, Bulgaria.

[138]Department P, Aarhus University Hospital, DK-8240 Risskov, Denmark.

[139]Department of Psychiatry, Royal College of Surgeons in Ireland, Dublin 2, Ireland.

[140]King's College London, London SE5 8AF, UK.

[141]Maastricht University Medical Centre, South Limburg Mental Health Research and Teaching Network, EURON, 6229 HX Maastricht, The Netherlands.

[142]Institute of Translational Medicine, University of Liverpool, Liverpool L69 3BX, UK.

[143]Max Planck Institute of Psychiatry, 80336 Munich, Germany.

[144]Munich Cluster for Systems Neurology (SyNergy), 80336 Munich, Germany.

[145]Department of Psychiatry and Psychotherapy, Jena University Hospital, 07743 Jena, Germany.

[146]Department of Psychiatry, Queensland Brain Institute and Queensland Centre for Mental Health Research, University of Queensland, Brisbane, Queensland, St Lucia QLD 4072, Australia.

[147]Department of Psychiatry and Behavioral Sciences, Johns Hopkins University School of Medicine, Baltimore, Maryland 21205, USA.

[148]Department of Psychiatry, Trinity College Dublin, Dublin 2, Ireland.

[149]Eli Lilly and Company, Lilly Corporate Center, Indianapolis, 46285 Indiana, USA.

[150]Department of Clinical Sciences, Psychiatry, Umeå University, SE-901 87 Umeå, Sweden.

[151]DETECT Early Intervention Service for Psychosis, Blackrock, Co. Dublin, Ireland.

[152]Centre for Public Health, Institute of Clinical Sciences, Queen's University Belfast, Belfast BT12 6AB, UK.

[153]Lawrence Berkeley National Laboratory, University of California at Berkeley, Berkeley, California 94720, USA.

[154]Institute of Psychiatry, King's College London, London SE5 8AF, UK.

[155]A list of authors and affiliations appear in the Supplementary Information.

[156]Melbourne Neuropsychiatry Centre, University of Melbourne & Melbourne Health, Melbourne, Vic 3053, Australia.

[157]Department of Psychiatry, University of Helsinki, P.O. Box 590, FI-00029 HUS, Helsinki, Finland.

[158]Public Health Genomics Unit, National Institute for Health and Welfare, P.O. BOX 30, FI-00271 Helsinki, Finland.

[159]Medical Faculty, University of Belgrade, 11000 Belgrade, Serbia.

[160]Department of Psychiatry, University of North Carolina, Chapel Hill, North Carolina 27599-7160, USA.

[161]Institute for Molecular Medicine Finland, FIMM, University of Helsinki, P.O. Box 20

FI-00014, Helsinki, Finland.

[162]Department of Epidemiology, Harvard School of Public Health, Boston, Massachusetts 02115, USA.

[163]Department of Psychiatry, University of Oxford, Oxford, OX3 7JX, UK.

[164]Virginia Institute for Psychiatric and Behavioral Genetics, Virginia Commonwealth University, Richmond, Virginia 23298, USA.

[165]Institute for Multiscale Biology, Icahn School of Medicine at Mount Sinai, New York, New York 10029, USA.

[166]PharmaTherapeutics Clinical Research, Pfizer Worldwide Research and Development, Cambridge, Massachusetts 02139, USA.

[167]Department of Psychiatry and Psychotherapy, University of Gottingen, 37073 Göttingen, Germany.

[168]Psychiatry and Psychotherapy Clinic, University of Erlangen, 91054 Erlangen, Germany.

[169]Hunter New England Health Service, Newcastle NSW 2308, Australia.

[170]School of Biomedical Sciences and Pharmacy, University of Newcastle, Callaghan NSW 2308, Australia.

[171]Division of Cancer Epidemiology and Genetics, National Cancer Institute, Bethesda, Maryland 20892, USA.

[172]University of Iceland, Landspitali, National University Hospital, 101 Reykjavik, Iceland.

[173]Department of Psychiatry and Drug Addiction, Tbilisi State Medical University (TSMU), **N33, 0177** Tbilisi, Georgia.

[174]Research and Development, Bronx Veterans Affairs Medical Center, New York, New York 10468, USA.

[175]Wellcome Trust Centre for Human Genetics, Oxford, OX3 7BN, UK.

[176]deCODE Genetics, 101 Reykjavik, Iceland.

[177]Department of Clinical Neurology, Medical University of Vienna, 1090 Wien, Austria.

[178]Lieber Institute for Brain Development, Baltimore, Maryland 21205, USA.

[179]Department of Medical Genetics, University Medical Centre Utrecht, Universiteitsweg 100, 3584 CG, Utrecht, The Netherlands.

[180]Berkshire Healthcare NHS Foundation Trust, Bracknell RG12 1BQ, UK.

[181]Section of Psychiatry, University of Verona, 37134 Verona, Italy.

[182]Department of Psychiatry, University of Oulu, P.O. BOX 5000, 90014, Finland

[183]University Hospital of Oulu, P.O.BOX 20, 90029 OYS, Finland.

[184]Molecular and Cellular Therapeutics, Royal College of Surgeons in Ireland, Dublin 2, Ireland.

[185]Health Research Board, Dublin 2, Ireland.

[186]School of Psychiatry and Clinical Neurosciences, The University of Western Australia, Perth WA6009, Australia.

[187]Computational Sciences CoE, Pfizer Worldwide Research and Development, Cambridge, Massachusetts 02139, USA.

[188]Human Genetics, Genome Institute of Singapore, A*STAR, Singapore 138672, Singapore.

[189]A list of authors and affiliations appear in the Supplementary Information.

[190]University College London, London WC1E 6BT, UK.

[191]Department of Neuroscience, Icahn School of Medicine at Mount Sinai, New York, New York 10029, USA.

[192]Institute of Neuroscience and Medicine (INM-1), Research Center Juelich, 52428 Juelich, Germany.

[193]Department of Genetics, The Hebrew University of Jerusalem, 91905 Jerusalem, Israel.

[194]Neuroscience Discovery and Translational Area, Pharma Research and Early Development, F. Hoffman-La Roche, CH-4070 Basel, Switzerland.

[195]Centre for Clinical Research in Neuropsychiatry, School of Psychiatry and Clinical Neurosciences, The University of Western Australia, Medical Research Foundation Building, Perth WA 6000, Australia.

[196]Virginia Institute for Psychiatric and Behavioral Genetics, Departments of Psychiatry and Human and Molecular Genetics, Virginia Commonwealth University, Richmond, Virginia 23298, USA.

[197]The Feinstein Institute for Medical Research, Manhasset, New York, 11030 USA.

[198]The Hofstra NS-LIJ School of Medicine, Hempstead, New York, 11549 USA.

[199]The Zucker Hillside Hospital, Glen Oaks, New York,11004 USA.

[200]Saw Swee Hock School of Public Health, National University of Singapore, Singapore 117597, Singapore.

[201]Queensland Centre for Mental Health Research, University of Queensland, Brisbane 4076, Queensland, Australia.

[202]Center for Human Genetic Research and Department of Psychiatry, Massachusetts General Hospital, Boston, Massachusetts 02114, USA.

[203]Department of Child and Adolescent Psychiatry, Erasmus University Medical Centre, Rotterdam 3000, The Netherlands.

[204]Department of Complex Trait Genetics, Neuroscience Campus Amsterdam, VU University Medical Center Amsterdam, Amsterdam 1081, The Netherlands.

[205]Department of Functional Genomics, Center for Neurogenomics and Cognitive Research, Neuroscience Campus Amsterdam, VU University, Amsterdam 1081, The Netherlands.

[206]University of Aberdeen, Institute of Medical Sciences, Aberdeen, AB25 2ZD, UK.

[207]Departments of Psychiatry, Neurology, Neuroscience and Institute of Genetic Medicine, Johns Hopkins School of Medicine, Baltimore, Maryland 21205, USA.

[208]Department of Clinical Medicine, University of Copenhagen, Copenhagen 2200, Denmark.

[209]Departments of Psychiatry and Human Genetics, University of Chicago, Chicago, Illinois 60637, USA.

[210]University Hospital Marqués de Valdecilla, Instituto de Formación e Investigación Marqués de Valdecilla, University of Cantabria, E-39008 Santander, Spain.

Tourette Syndrome and Obsessive Compulsive Disorder Working Group of the Psychiatric Genomics Consortium

Harald Aschauer[1], Gil Atzmon[2], Cathy Barr[3,4], Nir Barzilai[2], Robert Batterson[5,6], Fortu Benarroch[7,8], Cheston Berlin[9], Lawrence W. Brown[10], Cathy Budman[11], Danielle Cath[12,13], Keun-Ah Cheon[14], Barbara J. Coffey[15,16], Christel Depienne[17,18], Andrea Dietrich[19], Valsamma Eapen[20], Peter Falkai[21], Thomas V. Fernandez[22], Blanca Garcia-Delgar[23,24], Donald L. Gilbert[25], Hans J. Grabe[26], Marco Grados[27], Erica Greenberg[28], Dorothy E. Grice[15], Andreas Hartmann[30,31], Johannes Hebebrand[32], Tammy Hedderly[33], Gary A. Heiman[34], Isobel Heyman[35], Pieter J. Hoekstra[36], Hyun Ju Hong[37,38], Alden Huang[39], Chaim Huyser[40,41], Cornelia Illmann[28], Young-Shin Kim[42], Robert A. King[22], Yun-Joo Koh[43,44], Sodahm Kook[45,46,47], Samuel Kuperman[48], James Leckman[49], Bennett L. Leventhal[50], Jurjen Luykx[51,52], Gholson Lyon[53], Marcos Madruga-Garrido[54], Peter Malaty[55], Athanasios Maras[56,57], Carol A. Mathews[58], Manuel Mattheisen[59,60,61], Pablo Mir[62,63], Astrid Morer[64,65,66], Kirsten Müller-Vahl[67], Alexander Münchau[68], Tara L. Murphy[35], Peter Nagy[69], Benjamin Neale[70], Markus Nöthen[71], Erika Nurmi[72], Michael S. Okun[55], Peristera Paschou[73], Christopher Pittenger[74], Kerstin J. Plessen[75], Yehuda Pollak[76], Victor Reus[77], Renata Rizzo[78], Mary Robertson[79], Veit Roessner[80], Joshua Roffman[28], Guy Rouleau[81], Jack Samuels[27], Paul Sandor[82,83,84], Jeremiah M. Scharf[70,85], Eun-Young Shin[86], Harvey Singer[87], Jan Smit[88], Jungeun Song[89], Dong-Ho Song[47,90,91], Manfred Stuhrmann[92], Jae Hoon Sul[72], Zsanett Tarnok[93], Jay A. Tischfield[94], Fotis Tsetsos[95], Michael Wagner[96], Sheng Wang[97], Arthur J. Willsey[98], Yulia Worbe[99,100,102], Dongmei Yu[70,102,103], Samuel H. Zinner[104]

[1] Biopsychosocial Corporation, Vienna, Austria

[2] Department of Genetics and the Department of Medicine, Albert Einstein College of Medicine, Bronx, NY

[3] Krembil Research Institute, University Health Network, Toronto, ON, Canada

[4] Hospital for Sick Children, Toronto, ON, Canada

[5] Children's Mercy Kansas City, Dvision of Developmental and Behavioral Health, Kansas City, MO

[6] Clinical Professor, Department of Pediatrics, University of Missouri, Kansas City School of Medicine

[7] Herman Dana Child and Adolescent Psychiatry Division, Hadassah Medical Center, Jerusalem, Israel

[8] Faculty of Medicine, Hebrew University, Jerusalem, Israel

[9] Pennsylvania State University College of Medicine, Hershey

[10] Division of Neurology, Children's Hospital of Philadelphia, The University of Pennsylvania Perelman School of Medicine, Philadelphia, PA, USA

[11] Clinical Professor, Zucker School of Medicine, Hofstra/Northwell Health

[12] Rijksuniversiteit Groningen & University Medical Center Groningen, Department of Psychiatry, the Netherlands

[13] Drenthe Mental Health Institute, Department of Specialist Training

[14] Yonsei University College of Medicine, Seodaemun-gu, Seoul, KR

[15] Department of Psychiatry, Icahn School of Medicine at Mount Sinai, New York, NY, USA

[16] University of Miami Health System, Miami, FL, USA

[17] Institute of Human Genetics, University Hospital Essen, University of Duisburg-Essen, Hufelandstraße 55, 45147 Essen, Germany

[18] Institut du Cerveau et de la Moelle épinière (ICM), Sorbonne Université, UMR S 1127, Inserm U1127, CNRS UMR 7225, F-75013 Paris, France

[19] Department of Child and Adolescent Psychiatry, University Medical Center Groningen, University of Groningen, Groningen, NL

[20] University of New South Wales, Sydney, AU

[21] Department of Psychiatry, University Hospital of Munich, Munich, Germany

[22] Yale University School of Medicine, New Haven, CT, USA

[23] Servei de Psiquiatria i Psicologia Infantil i Juvenil Hospital Clinic Barcelona (Spain)

[24] Farmacology Department, Faculty of Medicine , University of Barcelona , Spain.

[25] Division of Neurology, Cincinnati Children's Hospital Medical Center; Department of Pediatrics, University of Cincinnati College of Medicine, Cincinnati, OH, USA

[26] Department of Psychiatry and Psychotherapy, University Medicine Greifswald, Greifswald, Mecklenburg-Vorpommern, DE

[27] Department of Psychiatry and Behavioral Sciences, Johns Hopkins University, Baltimore, MD, USA

[28] Massachusetts General Hospital, Boston, MA, USA

[29] Child and Adolescent Mental Health Center, Mental Health Services – Capital Region of Denmark, DK

[30] National Reference Center for Tourette syndrome, Assistance Publique des Hôpitaux de Paris, Groupe Hospitalier Pitié-Salpêtrière, F-75013, Paris, France

[31] Sorbonne University, 75005 Paris, Inserm U1127, CNRS UMR7225, UM75, ICM, F-75013, Paris, France. Movement Investigation and Therapeutics Team, Paris, France.

[32] Department of Child and Adolescent Psychiatry, Psychosomatics and Psychtherapy, University Hospital Essen (AöR), University of Duisburg-Essen, Essen, Germany

[33] Guy's and Saint Thomas' NHS Foundation Trust, King's College London, London, GB

[34] Department of Genetics and Human Genetics Institute, Rutgers University, Piscataway, NJ, USA

[35] Psychological Medicine, UCL Great Ormond Street Institute of Child Health, London, UK

[36] Department of Child and Adolescent Psychiatry, University Medical Center Groningen, University of Groningen, Groningen, NL

[37] Department of Psychiatry, Hallym University Sacred Heart Hospital, Anyang, Gyeonggido, South Korea

[38] Suicide and School Mental Health Institute, Hallym University, Anyang, Gyeonggido, South Korea

[39] Institute for Precision Health, University of California, Los Angeles

[40] Levvel, Specialists in Youth and Family, Amsterdam, The Netherlands.

[41] Department of child and adolescent psychiatry, Amsterdam UMC, Amsterdam The Netherlands.

[42] University of California Medical Center, San Francisco, CA, USA

[43] Korea Institute for Children's Social Development, Seoul, KR

[44] University of Cologne, Cologne, DE

[45] Yonsei University College of Medicine, Seodaemun-gu, Seoul, KR

[46] Kangbuk Samsung Medical Center, Seoul, KR

[47] Severance Hospital, Seoul, KR

[48] Carver College of Medicine, University of Iowa, Iowa City, IA, USA

[49] Child Study Center, Departments of Pediatrics, Psychiatry and Psychology, Yale University

[50] University of California, San Francisco, CA, USA

[51] Brain Center Rudolf Magnus, Department of Translational Neuroscience, University Medical Center Utrecht, Utrecht, NL
[52] Department of Psychiatry, Brain Center Rudolf Magnus, University Medical Center Utrecht, Utrecht, CG, NL
[53] Jervis Clinic, NYS Institute for Basic Research in Developmental Disabilities (IBR), Staten Island, NY, 10314, USA.
[54] Sección de Neuropediatría, Instituto de Biomedicina de Sevilla, Hospital Universitario Virgen del Rocío/CSIC/Universidad de Sevilla, Seville, ES
[55] Department of Neurology, University of Florida Norman Fixel Institute for Neurological Diseases
[56] Yulius Academy, Yulius Mental Health Organization, Dordrecht, The Netherlands
[57] Mondriaan Mental Health Organization, Heerlen, The Netherlands
[58] Department of Psychiatry, Genetics Institute, Center for OCD, Anxiety and Related Disorders, University of Florida
[59] Department of Psychiatry, Psychosomatics and Psychotherapy, Center of Mental Health, University Hospital Wuerzburg, Wuerzburg, DE
[60] Department of Biomedicine, Aarhus University, Aarhus, DK
[61] Department of Clinical Neuroscience, Centre for Psychiatry Research, Karolinska Institutet, Stockholm, SE
[62] Unidad de Trastornos del Movimiento, Servicio de Neurología y Neurofisiología Clínica, Instituto de Biomedicina de Sevilla, Hospital Universitario Virgen del Rocío/CSIC/Universidad de Sevilla, Seville, Spain
[63] Centro de Investigación Biomédica en Red sobre Enfermedades Neurodegenerativas (CIBERNED), Madrid, Spain.
[64] Instituto de Salud Carlos III, Biomedical Network Research Centre on Mental Health (CIBERSAM), Barcelona, ES
[65] Universitat de Barcelona Facultat de Medicina, Barcelona, ES
[66] Servei de Psiquiatria i Psicologia Infantil i Juvenil Hospital Clinic Barcelona (Spain) . Institut d'Investigacions Biomédiques (IDIBAPS)
[67] Department of Psychiatry, Socialpsychiatry and Psychotherapy, Hannover Medical School, Hannover, Germany
[68] Institute of Systems Motor Science, University of Lübeck, Germany
[69] Vadaskert Child Psychiatric Hospital and Outpatient Clinic, Budapest, HU
[70] Stanley Center for Psychiatric Research, Broad Institute of Harvard and MIT, Cambridge, MA, USA
[71] Institute of Human Genetics, University of Bonn School of Medicine & University Hospital Bonn, Bonn, Germany
[72] Department of Psychiatry and Biobehavioral Sciences, University of California at Los Angeles, Los Angeles, CA, USA
[73] Department of Biological Sciences, Purdue University
[74] Department of Psychiatry and Yale Child Study Center, Yale University School of Medicine
[75] Capital Region Psychiatry, University of Lausanne, Child and Adolescent Mental Health Centre Capital, Region, University of Copenhagen, Copenhagen, DK
[76] Neuropediatric Unit, Shaare Zedek Medical Center, Jerusalem, Israel
[77] Department of Psychiatry, University of California San Francisco, San Francisco, CA, USA
[78] Department of Clinical and Experimental Medicine, Catania University, IT
[79] Division of Neuropsychiatry, University College London, London, UK

[80] Department of Child and Adolescent Psychiatry, Faculty of Medicine, Technischen Universität Dresden, Dresden, DE
[81] Montreal Neurological Institute, Department of Neurology and Neurosurgery, McGill University, Montreal, QC, CA
[82] Department of Psychiatry, University of Toronto, Toronto, CA
[83] University Health Network, University of Toronto, Toronto, CA
[84] Youthdale Treatment Centers, Toronto, CA
[85] Center for Genomic Medicine, Departments of Neurology and Psychiatry, Massachusetts General Hospital, Harvard Medical School, Boston, MA
[86] Yonsei Yoo&Kim Mental health clinic, Seoul, South Korea
[87] Johns Hopkins University School of Medicine, Baltimore, MD, USA
[88] Department of Psychiatry, Amsterdam Public Health Research Institute, Amsterdam UMC, Vrije Universiteit, Amsterdam, The Netherlands
[89] Department of Psychiatry, National Health Insurance Service Ilsan Hospital, Goyang, South Korea
[90] Yonsei University College of Medicine, Seoul, KR
[91] Catholic University of Korea, Seoul, KR
[92] The Institute of Human Genetics, Hannover Medical School, Hannover, Germany
[93] Vadaskert Child and Adolescent Psychiatry, Budapest, HU
[94] Deptartment of Genetics and the Human Genetics Institute, Rutgers, the State University Of New Jersey, Piscataway NJ 08854, USA
[95] Department of Molecular Biology and Genetics, Democritus University of Thrace, Alexandroupolis, Greece
[96] Department of Psychiatry and Psychotherapy, University Hospital Bonn, Bonn, Germany
[97] Institute for Neurodegenerative Diseases, UCSF Weill Institute for Neurosciences, University of California, San Francisco, San Francisco, CA, USA
[98] Department of Psychiatry and Behavioral Sciences, University of California San Francisco, San Francisco, CA
[99] Université Pierre et Marie Curie Paris, FR
[100] Hôpital Saint-Antoine, Paris, FR
[101] Hopital Pitie-Salpetriere, Paris, FR
[102] Center for Genomic Medicine, Massachusetts General Hospital, Boston, MA, USA
[103] Department of Neurology, Massachusetts General Hospital, Harvard Medical School, Boston, MA, USA
[104] Department of Pediatrics, University of Washington, Seattle, WA 98195, USA

iPSYCH, The Lundbeck Foundation Initiative for Integrative Psychiatric Research, Denmark

Anders D. Børglum[1-3], Thomas D. Als[1-3], Manuel Mattheisen[1-3], Jakob Grove[1-4], Ditte Demontis[1-3], Thomas Werge[1,7,8], Preben Bo Mortensen[1,2,9,10], Esben Agerbo[1,9,10], Ole Mors[1,6], Merete Nordentoft[1,11], David M. Hougaard[1,5], Jonas Bybjerg-Grauholm[1,5]

[1]iPSYCH, The Lundbeck Foundation Initiative for Integrative Psychiatric Research, Denmark

[2] Center for Genomics and Personalized Medicine, Aarhus, Denmark

[3] Department of Biomedicine - Human Genetics and the iSEQ Center, Aarhus University, Aarhus, Denmark

[4] Bioinformatics Research Centre, Aarhus University, Aarhus, Denmark

[5]Center for Neonatal Screening, Department for Congenital Disorders, Statens Serum Institut, Copenhagen, Denmark

[6] Psychosis Research Unit, Aarhus University Hospital, Aarhus, Denmark

[7] Institute of Biological Psychiatry, MHC Sct. Hans, Mental Health Services Copenhagen, Roskilde, Denmark

[8] Department of Clinical Medicine, University of Copenhagen, Copenhagen, Denmark

[9] National Centre for Register-Based Research, Aarhus University, Aarhus, Denmark

[10] Centre for Integrated Register-based Research, Aarhus University, Aarhus, Denmark

[11] Mental Health Services in the Capital Region of Denmark, Mental Health Center Copenhagen, University of Copenhagen, Copenhagen, Denmark